"Force nanoscopy of staphylococcal adhesion"

Herman, Philippe

ABSTRACT

Staphylococcus aureus and Staphylococcus epidermidis are two nosocomial pathogens. They are the leading cause of biofilm-associated infections in healthcare facilities. Understanding the molecular interactions lying behind the biofilm formation is essential for preventing nosocomial infections. The objective of this PhD thesis is to gain insights into the forces involved in staphylococcal adhesion, the first step of biofilm formation. The strategy involved the development and use of atomic force microscopy (AFM) techniques for characterizing adhesion forces at the single-molecule and single-cell levels. We investigated two serine-aspartate repeat proteins, SdrG and SdrF involved in fibrinogen (Fg) and collagen (Cn) binding respectively. The SdrG-Fg interaction involves strong forces and low dissociation rates leading to stable complexes. SdrG forms nanodomains at the cell surface highlighting how this bacterium might withstand shear forces on indwelling medical devices. Our next study shows that SdrF binds Cn through two types of molecular bonds involving two subdomains of the protein. Next, we studied the S. aureus fibronectin-binding protein A (FnBPA), which mediates cell-cell interactions during biofilm accumulation. FnBPA mediates low affinity, Zn-dependent homophilic bonds of moderate strength. This might be the basis for cell dissemination and participate to the biofilm dynamics. Lastly, we examined the forces at play in the interaction between S. epidermidis and Candida albicans. We highlighted the importance of the yeast-to-hyphae transition and the crucial role o...

CITE THIS VERSION

Université catholique de Louvain
Faculté des bioingénieurs
Institut des Sciences de la Vie

Thesis submitted to fulfil the requirements for the degree of *Philosophae Doctor* in Bio-engineering of the Université catholique de Louvain

Force nanoscopy of staphylococcal adhesion

Philippe Herman-Bausier

Supervisor:
Prof. Yves F. Dufrêne, Université catholique de Louvain

Members of the examination Committee:
Prof. Bernard Hallet, Université catholique de Louvain
Prof. Pascal Hols, Université catholique de Louvain
Prof. Jacques Mahillon, Université catholique de Louvain
Dr. Gregory Francius, Université de Lorraine, France
Prof. Timothy J. Foster, Trinity College Dublin, Ireland

April 2016

Acknowledgments

Au terme de 3 années et un peu plus, je conclus une thèse de doctorat dans laquelle je me suis épanoui tout au long de sa durée. Je voudrais au terme de ce travail remercier les personnes autour de moi qui ont contribué directement ou indirectement à sa réalisation.

Mes premiers remerciements vont au Professeur Yves Dufrêne pour son flair et sa confiance. Je m'explique : à la fin de mon mémoire, j'avais émis l'idée de faire une thèse. Je me souviens avoir été apostrophé par le Professeur Dufrêne, à la cafétéria au moment où il lavait sa tasse de café. Yves était pour nous les étudiants peu connu de par nos cours. Qu'importe, l'info n'était pas tombée dans l'oreille d'un sourd, et en novembre 2012 après deux interviews, j'étais lancé. Mettre sa confiance dans un thésard est certainement un coup de poker, on mise sur un cheval dans une course qui dure plusieurs années. Je suis arrivé dans une petite équipe extrêmement dynamique et motivée, réunie autour d'un même appareil. Yves insuffle cette énergie et cet enthousiasme qui nous fait nous échanger tous les jours et nous fait partager entre nous une « niaque » autour des différentes thématiques et projets du groupe. Ce qui m'amène à parler de Sofiane et Audrey et à les remercier plus que chaleureusement. Ils ont été à eux deux très importants pour moi durant ma thèse. J'ai été poussé par leur détermination et leur abnégation et j'ai véritablement profité de leur expérience pour apprendre un maximum sur le monde de la recherche. Humainement, ce sont deux personnes extraordinaires sur lesquelles j'ai pu compter tous les jours de la semaine. Je les remercie aussi énormément pour tous les magnifiques moments partagés ensemble au labo et évidemment en dehors. Sylvie fait aussi partie du dynamisme de cette équipe et je la remercie pour son rôle prépondérant, son investissement et son enthousiasme. Sylvie est le ciment du laboratoire, sans elle, rien ne tient !

Je remercie spécialement les membres du jury de ma thèse et du comité d'accompagnement pour leur évaluation, leur apport et remarques nécessaires et extrêmement judicieux à la réalisation de ce travail. I wish to specially thank Professor Tim Foster for his special support and input which contributed to improve my thesis. Merci aussi à David qui a pris du temps pour m'aider et chez qui je peux toujours aller chercher des conseils et de l'aide au laboratoire.

Je veux aussi dire un petit mot sur les collègues qui rendent la vie plus facile et ont contribué et contribuent à la vie du labo : Françoise, Rose-Anne,

l'équipe de Christine, Cécile et Claire qui nous rejoint récemment ainsi que Martin (*aka* G.L.).

Ma famille est pour moi très importante et tout au long de ma thèse, j'ai pu compter sur leur support inconditionnel et ce même si parfois les concepts sont abstraits. Entre nous, les discussions sont toujours riches et productives que ce soit pour parler de choses importantes ou de sujets plus légers. Un petit mot aussi pour mes amis, qui sans le savoir directement participent fortement à mon équilibre personnel. C'est aussi grâce à eux que j'y suis arrivé.

Table of contents

Abstract i
List of abbreviations iii
Outline vii

Part I

Thesis overview 1

I. General introduction 3

I.1. Microbial biofilms 3

I.1.1. Generalities 3
I.1.2. Importance 4
I.1.3. Mechanisms of biofilm formation 6
I.1.4. Resistance mechanisms 8

I.2. *Staphylococcus aureus* and *Staphylococcus epidermidis* 9

I.2.1. Biology 9
I.2.2. Pathogenicity 12
I.2.3. Molecular determinants in staphylococcal biofilms 22

I.3. Atomic force microscopy 27

I.3.1. Introduction 27
I.3.2. The atomic force microscope set-up 29
I.3.3. AFM imaging 30
I.3.4. Force spectroscopy 33
I.3.5. Single-molecule force spectroscopy 36
I.3.6. Single-cell force spectroscopy 40

I.4. Objective and strategy 42

II. Short presentation of the thesis 45

II.1. Tool development: single-bacterial cell force spectroscopy 45

II.1.1. A new single-cell assay 45
II.1.2. Application to staphylococcal adhesion 47

II.2. Understanding ligand-binding mechanisms in Sdr proteins 49

II.2.1. Strength of the SdrG-fibrinogen bond 49
II.2.2. The density of SdrG controls staphylococcal adhesion to fibrinogen 51

II.2.3. SdrF displays a dual collagen-binding activity 51
II.3. Deciphering homophilic interactions in fibronectin-binding proteins 53
II.4. Unravelling the forces in staphylococcal-fungal co-adhesion 55
III. Conclusions and perspectives 57
III.1. Force nanoscopy, a powerful platform for biofilm research 57
III.2. From molecular forces to cellular function 58
III.2.1. Ligand-binding mechanisms of Sdr proteins 58
III.2.2. FnBP-mediated homophilic binding 60
III.2.3. Forces driving staphylococcal-fungal adhesion 62
III.3. Challenges ahead 63
IV. References 68

Part II

Detailed presentation of the thesis 85

Chapter I 87
The binding force of the staphylococcal adhesin SdrG is remarkably strong
Chapter II 117
***Staphylococcus epidermidis* affinity for fibrinogen-coated surfaces correlates with the abundance of the SdrG adhesin on the cell surface**
Chapter III 139
Atomic force microscopy reveals a dual collagen-binding activity for the staphylococcal surface protein SdrF
Chapter IV 161
***Staphylococcus aureus* fibronectin-binding protein A mediates cell-cell adhesion through low affinity homophilic bonds**

Chapter V **189**
Single-cell force spectroscopy of the medically important *Staphylococcus epidermidis*-*Candida albicans* interaction
Chapter VI **205**
Forces guiding staphylococcal adhesion

Part III
Appendices **223**
Appendix I **225**
Single-cell force spectroscopy of probiotic bacteria
Appendix II **235**
Quantifying the forces guiding microbial cell adhesion using single-cell force spectroscopy
Appendix III **245**
Forces driving the attachment of *Staphylococcus epidermidis* to fibrinogen-coatded surfaces

Abstract

Staphylococcus aureus and *Staphylococcus epidermidis* are two important nosocomial pathogens, together they represent the leading cause of bacterial biofilm-associated infections in healthcare facilities. Understanding and unravelling the molecular interactions lying behind the biofilm formation is essential for controlling and preventing nosocomial infections.

The objective of this PhD thesis is to gain insights into the forces involved in staphylococcal adhesion, the first step of biofilm formation. The strategy involved the development and use of advanced atomic force microscopy (AFM) techniques for characterizing cell adhesion forces at the single-molecule and single-cell levels.

We first investigated two important serine-aspartate repeat proteins, SdrG and SdrF involved in fibrinogen (Fg) binding and collagen (Cn) binding respectively. We showed that SdrG-Fg interaction involves strong forces and low dissociation rates leading to greatly stabilized complexes. We found that SdrG forms nanodomains at the cell surface, and that the surface density of SdrG dictates the ability of different strains to adhere on Fg-coated surfaces, highlighting how this bacterium might withstand shear forces on indwelling medical devices. Our next study demonstrates that SdrF binds Cn through two different types of molecular bonds that involves two subdomains of the protein.

Next, we investigated the *S. aureus* fibronectin-binding protein A (FnBPA), which mediates cell-cell interactions during biofilm accumulation. FnBPA was found to mediate low affinity, zinc-dependent homophilic bonds of moderate strength, which might be the basis for cell dissemination from the biofilm and participate to the biofilm dynamics.

Lastly, we studied the forces at play in mixed biofilms, focusing on the interaction between *S. epidermidis* and the fungal pathogen *Candida albicans*. The results highlighted the importance of the yeast-to hyphae transition in mediating adhesion to bacterial cells, and the crucial role of Als adhesins and *O*-mannosylations in co-adhesion.

In summary, this thesis sheds new light into the molecular forces at play during staphylococcal adhesion. In the future, AFM should contribute to the identification of novel binding partners and binding mechanisms in staphylococcal adhesins, and may contribute to the development of novel anti-adhesion therapies.

List of abbreviations

Aaa	Autolysin/adhesin from *S. aureus*
Aae	Autolysin/adhesin from *S. epidermidis*
Aap	Accumulation-associated protein
AdsA	Adenosine synthase A
AFM	Atomic Force Microscope
AIDS	Aquired Immune Defficiency Syndrome
Als	Agglutinin-like sequence
AMP	Antimicrobial peptide
APTES	3-AminoPropyl TriEthoxySilane
AtlE	Autolysin E protein
ATCC	American True Culture Collection
Bap	Biofilm-associated protein
Bhp	Bap-homologous protein
CHIPS	Chemotaxis inhibitory protein of *S. aureus*
Clf	Clumping factor protein
Cn	Collagen
Cna	Collagen adhesin
CWA	Cell Wall-Anchored
DLL	Dock, Lock and Latch mechanism
DNA	Deoxyribonucleic Acid
Eap	Extracellular adherence protein
ECM	Extra-Cellular Matrix
EDC	1-Ethyl-3-(3-dimethylaminopropyl) Carbodiimide
eDNA	Extracellular Deoxyribonucleic Acid
Efb	Extracellular fibrinogen binding
Embp	Extracellular matrix binding protein
EPS	Exo-Polymeric Substances
Fab	Fragment-antigen binding
Fc	Fragment crystallisable region
Fg	Fibrinogen
Fn	Fibronectin
FnBP	Fibronectin Binding Protein
HS-AFM	High-speed Atomic Force Microscope
Ig	Immunoglobulin
Isd	Iron surface determinant protein

LPXTG	Leucine-Proline-Any-Threonine-Glycine sequence
MGE	Mobile Genetic Element
MRSA	Methiciline-Resistant *Staphylococcus aureus*
MSCRAMMs	Microbial Surface Components Recognizing Adhesive Matrix Molecules
NEAT	Near-iron transporter
NHS	N-hydroxysuccinimide
NTA	Nitrilotriacetate
PBP	Penicilin-Binding Protein
PEG	PolyEthylene Glycol
PFT	PeakForce Tapping
PGA	Poly-γ-glutamic acid
pH	Potential of Hydrogen
PI	Propidium Iodide
PIA	Polysaccharide Intercellular Adhesin
pN	Pico-Newton
PSM	Phenol-Soluble Modulin
PVL	Panton-Valentine Leucocidin
QI	Quantitative Imaging
QS	Quorum-Sensing
ROS	Reactive Oxygen Species
SAM	Self-Assembled Monolayer
SasG	*S. aureus* surface protein G
Sbi	Second immunoglobulin-binding protein
Sbp	Small basic protein
SCFS	Single-Cell Force Spectroscopy
SCC	Staphylococcal Cassette Chromosome
SD	Serine-aspartate
Sdr	Serine-aspartate repeat protein
SdrF	Serine-aspartate repeat protein F
SdrG	Serine-aspartate repeat protein G
SERAMs	Secretable expanded repertoire adhesive molecules
SMFS	Single-Molecule Force Spectroscopy
SpA	*Staphylococcus* protein A

SS	Sorting-signal sequence
SSL	Staphylococcal superantigen-like
STM	Scanning Tunnelling Microscope
TSST	Toxic Shock Syndrome Toxin
W	Wall-spanning
WTAs	Wall Teichoic Acids

Outline

This thesis is divided in three main parts and three appendices.
Part I deals with a comprehensive introduction about microbial biofilms, depicting their general features. This section includes a state of the art concerning the two well-known human pathogens *Staphylococcus aureus* and *Staphylococcus epidermidis*, which are the focus of the present work. More precisely the molecular determinants involved in the biofilm formation cycle of these two staphylococcal species are discussed. A comprehensive overview of the atomic force microscope and its associated techniques is elaborated to understand how we used these tools to study these bacteria. A short presentation of the thesis is included describing the main achievements of this work.

Part II is a detailed presentation of the thesis, describing the main results in the form of six chapters and published as papers.

Chapter I: Herman P., El-Kirat-Chatel S., Beaussart A., Geoghegan J.A., Foster T.J., and Dufrêne Y.F. The binding force of the staphylococcal adhesin SdrG is remarkably strong. *Molecular Microbiology*, **2014**, 93, 356-368.

Chapter II: Vanzieleghem T., Herman P., Dufrêne Y.F., Mahillon J. *Staphylococcus epidermidis* affinity for Fibrinogen-coated surfaces correlates with the abundance of the SdrG adhesin on the cell surface. *Langmuir*, **2015**, 31(16), 4713.

Chapter III: Herman-Bausier P. and Dufrêne Y.F. Atomic force microscopy reveals a dual collagen-binding activity for the staphylococcal surface protein SdrF. *Molecular Microbiology*, **2015**, DOI: 10.1111mmi.13254.

Chapter IV: Herman-Bausier P., El-Kirat-Chatel S., Foster T. J., Geoghegan J.A., and Dufrêne Y.F. *Staphylococcus aureus* fibronectin-binding protein A mediates cell-cell adhesion through low affinity homophilic bonds. *mBio*, **2015**, e00413.

Chapter V: Beaussart A., Herman P., El-Kirat-Chatel S., Lipke P. N., Kucharíková S., Van Dijck P. and Dufrêne Y. F. Single-cell force

spectroscopy of the medically important *Staphylococcus epidermidis-Candida albicans* interaction. *Nanoscale*, **2013**, 3, 10894.

Chapter VI: Herman-Bausier P., Formosa-Dague C., Feuillie C., Valotteau C., and Dufrêne Y.F. Forces guiding staphylococcal adhesion. *Journal of Structural Biology,* **2015**, DOI:10.1016/j.jsb.2015.12.009.

The third and last part of this work, **Part III**, consists in three appendices in the form of published papers.

Appendix I: Beaussart A., El-Kirat-Chatel S., Herman P., Alsteens D., Mahillon J., Hols P. and Dufrêne Y.F. Single-cell force spectroscopy of probiotic bacteria. *Biophysical Journal*, **2013**, 104, 1886.

Appendix II: Beaussart A., El-Kirat-Chatel S. , Sullan R.M., Alsteens D., Herman P. , Derclaye S. & Dufrêne Y.F. Quantifying the forces guiding microbial cell adhesion using single-cell force spectroscopy. *Nature Protocols*, **2014**, 9, 1049

Appendix III: Herman P., El-Kirat-Chatel S., Beaussart A., Geoghegan J.A., Vanzieleghem T., Foster T.J., Hols P., Mahillon J., and Yves F. Dufrêne Y.F. Forces driving the attachment of *Staphylococcus epidermidis* to fibrinogen-coated surfaces. *Langmuir*, **2013**, 29, 13018.

Part I

Thesis overview

I. General introduction

I.1. Microbial biofilms

I.1.1. Generalities

The notion of biofilm was first described by Zobell and Mathews (Zobell & Mathews, 1936). However, the roots of the word "biofilm" are associated with the discovery of the Legionnaire's disease in 1976, where 4,400 veterans participated in the American Legion congress. During this event, 182 people declared a severe pneumonia of which 34 died. The organism responsible for the disease is *Legionella pneumophila* which is an intracellular bacterium and was found in the water tanks used for air humidification. *Legionella pneumophila* interacts with amoebae and ciliated protozoa, and this interaction plays a central role in bacterial infectivity. The bacteria formed structured colonies and biofilms on the walls of the tanks. The use of air conditioning systems generated aerosols as a vehicle to transmit *Legionella* from aquatic sources. Following an increase in temperature, a rapid multiplication of *L. pneumophila* inside the amoeba increases the chance of transmission (Richards *et al.*, 2013). Upon transmission to humans, *L. pneumophila* infects and replicate within alveolar macrophages causing pneumonia. A few years later, Costerton defined the notion of biofilm in his early work (Costerton *et al.*, 1978). He also realized that biofilms are the normal way of life for bacteria (Costerton *et al.*, 1999).

A biofilm defines microbial aggregates embedded in hydrated extracellular polymeric substances and accumulated at an interface (Costerton *et al.*, 1999, Flemming & Wingender, 2010). Biofilms in nature are usually multi-species, self-producing the extracellular material that accounts for 90% of the mass of the biofilm (Flemming & Wingender, 2010). Biofilms allow bacteria to survive, adapt and colonize hostile environments. Mature biofilms are formed of complex three-dimensional structures and heterogeneous differentiated cells. Cell-cell signalling and communication, *i.e.* the quorum sensing (QS) system inside the biofilm, make possible coordinated behaviour and the co-existence of several cell phenotypes, having areas specialized and differentiated in terms of molecules expressed (Hall-Stoodley & Stoodley, 2009, Fux *et al.*, 2005).

Adaptation is a fundamental component of life. Bacteria face adverse conditions, fluctuating nutrient supply or even host defences. These elements constitute stress factors that will affect bacterial cells and trigger a response.

These stress factors can induce global changes in gene expression and initiate a switch in the physiological state of bacteria into a biofilm mode of growth. Recently, biofilm gained attention due to their important role in gene regulation, bacterial physiology and ecology. (Thompson & Jefferson, 2009). The ability of bacteria to form biofilms confers undoubtedly a selective advantage over planktonic cells. Bacteria that are surface-bound outnumber the organisms in suspension (Dunne, 2002). From archaeological researches, it has been concluded that the ability to form biofilms is the key to provide stability and equilibrium to face fluctuating and harsh conditions in the first ages of Earth. These conditions include physical radiations such as exposure to UV-radiations, dessiccation or chemical agents (Hall-Stoodley *et al.*, 2004). Biofilms confer resistance to a large variety of mechanical, physical, nutritional chemical threats and represent a protected mode of growth.

I.1.2. Importance

Virtually any type of material that enters into contact with fluid containing bacteria is potentially a substrate for biofilm formation. The surface chemistry, the roughness or the presence of a conditioning film influence bacterial attachment dramatically (Goller & Romeo, 2008). In general, hydrophobic surfaces promote faster cell attachment inducing biofilm formation, and rougher surfaces are preferred because they offer protection against shear stress (Donlan, 2002). Surfaces adsorb small molecules and particles including bacterial cells. When a surface is in contact with proteins, a conditioning film forms and alters the surface properties thus the cell attachment (Goller & Romeo, 2008). A striking example is central venous catheters in which blood proteins coat the catheter surface and constitute a conditioning film. This proteinaceous film acts as a backdoor for staphylococcal species via specific receptors (Goller & Romeo, 2008). As a consequence of this ability to colonize surfaces, biofilms have either beneficial or detrimental effects in terms of human health and cost.

From a beneficial point of view, we can think of biofilms in geochemical processes, where biofilms have a large role in plant association. From nutrient-rich rhizospheres to poor soil deficient in key components, they induce plant growth and protection against pathogens (Bogino *et al.*, 2013). The association between bacteria and animals are also of prime importance. For instance, the symbiotic relationship between bacteria and ruminants allows them to recycle and degrade insoluble materials (Dunne, 2002). The human intestinal tract is also largely colonized by microbial biofilms since over 1,000 species have been discovered. Beneficial effects on humans include assimilation of non-digestible food components, degradation of toxic compounds or even the production of

vitamins (de Vos *et al.*, 2015). Bacterial biofilms are widely used in wastewater treatment for water purification (Andersson *et al.*, 2008) or to perform bioremediation of polluted soils (Kang, 2014). Bioremediation is a strategy where bacteria use exogenous toxic components as a food source. Bacterial biofilms are also used in mines to perform ore leaching by oxidation of metal sulphide to soluble metal sulfates (Mishra & Rhee, 2014).

Biofilms can also have terrible effects on human activities and economy. As an example, the biofouling process has tremendous effects in terms of industrial costs. Biofouling is the unwanted deposition and growth of biofilms on surfaces. Depending on the industrial process, biofouling leads to heat transfer resistance and thus energy losses, early replacement of equipment, intense cleaning equipment and finally quality and/or security problems (Flemming, 2002). Another severe issue is the biofilm-associated infections of indwelling devices and implants. Nosocomial biofilm infections have become a recurring and a growing problem over the years for health-care systems. Bacterial biofilms are more resistant to chemical and physical agents than planktonic bacteria. Biofilms tolerate higher concentrations of antibiotics and disinfectants and act as a protective barrier against host defences (Thompson & Jefferson, 2009). Biofilm-forming species are one of the first causes for nosocomial diseases associated with indwelling medical devices. About 250,000 to 500,000 bloodstream infections result each year from the 150 million intravascular devices implanted only in the United States of America (Darouiche, 2004, Uckay *et al.*, 2009). Common devices implicated in these infections are catheters (central venous, urethral), heart valves, ventricular assist devices, coronary stents, orthopaedic prostheses, and various implants (Lynch & Robertson, 2008, Wu *et al.*, 2015). It was estimated that *Staphylococcus aureus* and *Staphylococcus epidermidis* are responsible for 40-50% of prosthetic heart valve infections and 50-70% of catheter biofilm infections (Chen *et al.*, 2013). The reasons probably lie in the fact that staphylococci are natural human skin colonizers and their relative abundance. *Pseudomonas aeruginosa* is also a serious pathogen causing severe chronic infections in patients with cystic fibrosis (Joo & Otto, 2012).

I.1.3. Mechanisms of biofilm formation

Biofilms can form on abiotic surfaces like polymeric substrates and on biotic surfaces such as living tissues or implanted devices that readily become covered by host proteins (fibrinogen, fibronectin, etc.) (Costerton *et al.*, 1999, Kolter & Greenberg, 2006). **Figure 1** depicts the typical biofilm formation process of pathogens.

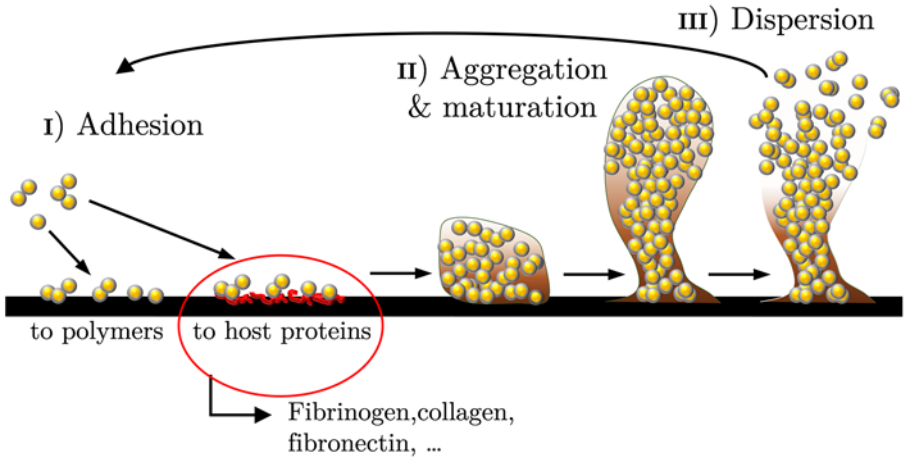

Figure 1: Biofilm formation process in bacterial pathogens such as staphylococcal species. Adapted from (Costerton *et al.*, 1999, Otto, 2009).

Biofilm formation is a cycle and proceeds as a regulated development sequence (Costerton *et al.*, 1999, Otto, 2009). It is widely accepted that biofilm formation occurs in three steps; I) adhesion is the initial step (**Figure 1**, I); II) cells aggregate and mature into characteristic biofilm structures (**Figure 1**, II); III) finally the cells detach to colonize new places (**Figure 1**, III) (Costerton *et al.*, 1999).

The process of bacterial adhesion on abiotic surfaces is often non-specific and driven by different types of interactions (Heilmann, 2011, Joo & Otto, 2012):

(i) Electrostatic interactions, which can be attractive or repulsive and depend on the medium (pH, salt concentration, etc.).

(ii) Hydrophobic interactions mainly mediated by the overall hydrophobicity of the bacterial cell as well as specific molecules expressed by the bacteria (Joo & Otto, 2012).

(iii) Other factors such as motility or chemotaxy, which can be of prime importance in species like *Pseudomonas. aeruginosa* and *Escherichia coli*, respectively (Kostakioti *et al.*, 2013).

Bacterial adhesion on biotic substrates such as tissues or protein-coated medical devices will more likely depend on the interactions with a conditioning

film. In aquatic or terrestrial environments, this layer is composed of complex polysaccharides, glycoproteins and humic substances (Percival *et al.*, 2011). In the human context, medical indwelling devices are conditioned by plasma proteins that dramatically influence bacterial adhesion. The conditioning film affects the physico-chemical properties of the surface, enables specific biomolecular interactions and provides a localized concentrated reservoir of nutrients. While, the conditioning film generally inhibits bacterial adhesion (Patel, 2006, Linnes, 2012, Abusalim, 2013), the presence of specific bioligands enables specific adhesion (Dunne, 2002, Percival *et al.*, 2011). Some bacterial species express specific cell adhesion molecules (adhesins) that recognize adhesive matrix molecules (Otto, 2009, Foster *et al.*, 2014), whereas in other biofilm-forming species, several surface-associated appendages (flagella, pili and fimbriae) and molecules (lipopolysaccharides) are known to promote adhesion (Laverty *et al.*, 2014, Beaussart *et al.*, 2014a).

In the second step, bacteria divide and form multicellular structures called microcolonies. Bacteria produce extracellular polymeric substances (EPS) that act as a cement between the cells. EPS fulfil essential functions such as cohesion of the biofilm, water retention, a protective barrier, accumulation of nutrients, retention of enzymes, etc. In the aggregation phase, EPS allow close contact between cells, the immobilization of the cell population, and high cell density conditions that are necessary for cell-cell signalling and coaggregation of the cells. EPS are composed of highly hydrated exopolysaccharides, proteins and extracellular DNA (mostly from lysed cells) (Flemming & Wingender, 2010). At the end of maturation, the biofilm acquires characteristic structures essential for providing all cells with nutrients and cell detachment or dispersal will become an option. Once the bacterial population reaches a certain cell density, the cells start to secrete several exoproteins, including proteases, hemolysins, and super-antigens, and simultaneously, the cell wall-associated molecules are downregulated (Wang *et al.,* 2016). This process which separates the colonization phase of the invasion phase is coordinated by an intercellular communication mechanism called the quorum-sensing which plays on gene expression patterns (Joo & Otto, 2012, Otto, 2013, Le *et al.*, 2014, Wang *et al.*, 2016).

The last stage of biofilm development is the cell dispersion into the environment where clusters of bacteria detach. The process is mediated by external mechanical forces such as shear stress when under flow, and surfactants and enzymes degrading the exopolymeric matrix. Cell detachment

and dispersal lead to a planktonic state in which bacteria can initiate a new cycle and colonize new places (Joo & Otto, 2012, Le *et al.*, 2014).

I.1.4. Resistance mechanisms

The formation of a biofilm is recognized as a key mechanism against host defences and resistance towards antibiotics. While shielded from the host immune system, biofilm cells produce a subpopulation of dormant persister cells which are highly tolerant to killing by antibiotics (Lewis, 2012). After antibiotic treatment, surviving persister cells will re-establish the bacterial population leading to chronic infection (Lewis, 2012). Biofilm is probably a protective shelter for persister cells limiting the diffusion and reducing the efficiency of bactericidal agents. Depending on the location of the cells inside the biofilm the cells are exposed to different gradients (pH, oxygen, nutrients, etc.), and are surrounded by different cell densities. Therefore, zones of different metabolic activities are created. Cells that are defective in nutrients can get into slow growing or dormant states. Persister cells inside a biofilm form a subpopulation that enters into a dormant, non-dividing state. Antibiotics require active targets to kill the cells. Bactericidal antibiotics cause the cells to produce corrupted products leading to cell death. Persister cells survive by blocking the target avoiding the corrupted product. The presence of persister cells inside a biofilm is another mechanism adding to classical resistance mechanisms that prevent the binding of the antibiotic to the target and leading to antibiotic tolerance (Lewis, 2012). The presence of persister cells in a chronic infection explains why the infection becomes untreatable even if the pathogen is not resistant to antibiotics (Costerton *et al.*, 1999, Jefferson, 2004, Fux *et al.*, 2005, Lewis, 2012)

It has recently been shown that the acyldepsipeptide (ADEP4) antibiotic activates a protease, ClpP, resulting in the killing of persister cells by the degradation of intracellular targets (Conlon *et al.*, 2013). ADEP4, a derivative of the natural product acyldepsipeptide factor A showed efficacy in a lethal murine infection of *Enterococcus faecalis* and *S. aureus* against growing cells with active protein synthesis and persisters cells. This study showed that ADEP4 is remarkable in its ability to kill dormant cells by activating a protease, a general approach to kill persister cells (Conlon *et al.*, 2013)

I.2. *Staphylococcus aureus* and *Staphylococcus epidermidis*

I.2.1. Biology

The genus *Staphylococcus* comprises bacteria that are Gram-positive spherical cocci. They belong to the order of Bacillales, and the family of Staphylococcacae. *Staphylococococcus* comes from the greek word *staphyle* translated as a "bunch of grapes" and the latin word "*coccus*" meaning grain. Around 40 species belong to the staphylococci genus. They are classified by their ability to endanger human or animal health (Rosenstein & Gotz, 2013). As understood from the etymology, staphylococci form grape-like clusters and have a diameter for single cells of 0.5-1.7 µm (Somerville & Proctor, 2009) (**Figure 2**).

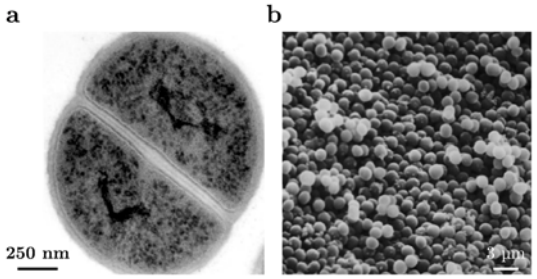

Figure 2: *Staphylococcus aureus* cells at high and low magnification.
a. Transmission electron microscopy of single *S. aureus* cell displaying cell separation.
b. Scanning electron microscopy of *S. aureus* cells in grapes.
Adapted from (Kahl *et al.*, 2003).

Staphylococci can grow in various environments, they are facultative anaerobes but grow best in aerobic conditions and in the presence of CO_2. Most staphylococci can grow in a wide range of pH, resist desiccation and survive for a limited time in hot environments. Their cell wall peptidoglycan is sensitive to lysostaphin but resistant to lysozyme. *S. aureus* is rapidly identified from the other less-virulent staphylococci species by the coagulase test in which a colony inoculated into plasma causes clotting. *S. aureus* is easily identified on blood agar plates by the gold pigmentation of the colonies, due to its ability to ferment mannitol (Somerville & Proctor, 2009, Foster & Geoghegan, 2015). It can eventually cause life-threatening infections and has become the leading cause of human bacterial infections in the hospital environment and in the community (Lowy, 1998, Foster *et al.*, 2014). *S. aureus* develops biofilm-associated infections that require intensive care, since these infections are difficult to treat and eradicate with antibiotics. These infections represent a reservoir of dissemination of *S. aureus* cells to other sites in the body (Otto, 2008). It can cause a broad range of human diseases including

deep skin abscesses, wound infections, meningitis, septicaemia, endocarditis or food poisoning (Somerville & Proctor, 2009).

The human microflora is a natural host for 16 species of staphylococci and are in that sense well-equipped with genes providing protection against harsh conditions on human epithelia (Otto, 2009). For instance, *Staphylococcus aureus* tolerates medium to high salt content (up to 10% NaCl) by producing osmoprotectants (Graham & Wilkinson, 1992, Somerville & Proctor, 2009). It is suggested that mammals are vectors of *S. aureus* since people having frequent contacts with cats, dogs or horses have more chance to be colonized (Somerville & Proctor, 2009). In humans, *S. aureus* colonizes the anterior nares, being persistently present in 20% of the population and found transiently in 80% of the people (Foster & Geoghegan, 2015). The organism is transmitted to skin and healthcare workers who have high nasal carriage rates. In healthcare facilities, the medical staff forms a reservoir for hand carriage and transmission of invasive infections (Somerville & Proctor, 2009, Foster & Geoghegan 2015). *S. epidermidis* is a permanent resident of the skin because it is better equipped to withstand the salt and low pH conditions of the skin.

S. aureus has a genome composed of 2.8 mega base pairs containing 2600 genes. About 80 % of the genome constitute the core genomic backbone with a highly conserved structure and organization. The genes in this part of the genome code for essential metabolic and regulatory functions. Some virulence factors are also encoded in the core genome such as surface proteins, toxins and enzymes. The other 20% of the genome constitute the accessory genome and are located on mobile genetic elements (MGEs) that comprise 50 % of the virulence factors expressed by *S. aureus.* MGEs have a prominent role in the emergence and evolution of new *S. aureus* strains with clinical implications (Gill, 2009). Five different types of genetic elements compose the MGEs, including pathogenicity islands, plasmids, bacteriophages and the staphylococcal cassette chromosome. Ten different *S. aureus* pathogenicity islands have been identified. They encode for enterotoxins that cause symptoms food poisoning and toxic shock syndrome (Gill, 2009). The plasmids are grouped depending on their size, ranging from 5kb to 60kb. They code for antibiotic determinants, metal tolerance and detergent resistance genes (Foster & Geoghegan, 2015). *S. aureus* hosts bacteriophages that play key roles in mobility of virulence factors. Some bacteriophages were shown to induce the replication of pathogenicity islands (Gill, 2009, Foster & Geoghegan 2015). They represent a source of genetic diversity and are clearly a mechanism leading to the emergence of virulent *S. aureus* clinical isolates (Gill, 2009). MRSA strains possess the staphylococcal cassette chromosome (SCC), a multifunctional MGE, carrying multiple genes involved in virulence or

antimicrobial resistance. The most common SCC is the SCC*mec* that harbours the *mecA* gene coding for the penicillin-binding protein (PBP). PBP is a protein that confers resistance to β-lactam antibiotics (Foster & Geoghegan, 2015). SCC*mec* also contains site-specific recombinase genes mediating its integration and excision from the genome (Foster & Geoghegan, 2015). There are other types of SCC including the SCC*far* responsible for fusidic acid resistance, or the SCC*pbp4* in *Staphylococcus epidermidis*, coding for another penicillin-binding protein and a cell-wall associated teichoic acid (Gill, 2009, Foster & Geoghegan, 2015).

S. epidermidis is considered to be a less virulent species in the staphylococci, yet it is associated with nosocomial diseases and biofilm-device associated infections. The core genomes of both *S. aureus* and *S. epidermidis* correspond well in terms of localisation. The structure and organisation of their core genomes are well-conserved (Gill, 2009). The differences are located in the MGEs *i.e.* genomic islands, bacteriophages and plasmids. The acquisition of virulence factors in *S. epidermidis* is the result of plasmid-mediated transfer of genes between staphylococci and other Gram-positive pathogens (Gill, 2009). Several virulence factors and surface proteins are shared by both *S. aureus* and *S. epidermidis*. These include phenol-soluble modulins or serine-aspartate repeat proteins.

S. epidermidis is usually non-pathogenic and adopts a commensal relationship with its host (Gomes *et al.*, 2014, Joo & Otto, 2012). *S. epidermidis* is an opportunistic pathogen because it infects mainly immune-compromised individuals such as AIDS patients, patients receiving immune suppressive therapies, premature new-borns and intravenous drug abusers (Otto, 2008). In healthy patients, *S. epidermidis* causes infections only after penetration of the skin barrier which happens by trauma, inoculation or implantation of medical devices. As a normal inhabitant of the human bacterial flora, *S. epidermidis* is probably introduced as a contaminant during surgical implantation of the indwelling medical device (Otto, 2008). Consequently, *S. epidermidis* is nowadays considered as a major causative agent of nosocomial infections as it is the most common source of infections of medical indwelling devices such as catheters and prostheses (Otto, 2009).

S. aureus and *S. epidermidis* are two staphylococci intensively studied because of their involvement in life-threatening infections. Other staphylococci maintain benign relationships with their host and will develop as opportunistic pathogens when the skin barrier is damaged. Some staphylococci are less present on the human skin and they lack the virulence factors to induce frequent biofilm-associated infections (Otto, 2008). Besides *S.aureus* and *S. epidermidis*, other *Staphylococcus* species can cause infections: *S. saprophyticus*

can cause urinary tract infections in humans whereas *S. anaerobius* is a pathogen of sheep causing skin infections (Somerville & Proctor, 2009). Non-coagulase producing species are usually found on the skin and mucuous membranes (Somerville & Proctor, 2009). Non-pathogenic staphylococci such as *S. carnosus* or *S. xylosus* are also used in the food industry, in meat and cheese fermentation (Rosenstein & Gotz, 2013).

I.2.2. Pathogenicity

S. aureus and *S. epidermidis* are two wide-spread human pathogens that can lead to life-threatening diseases. Both species exhibit two lifestyles. They can switch from being commensal inhabitants of mammals to pathogens as soon as they cross the skin barrier. Skin is a formidable barrier against pathogens and other physical dangers. The ability to become a dangerous pathogen causing various infections depends on the capability to modulate the production of a diverse array of virulence factors corresponding to an adaptation to the newly encountered environment (lack of nutrients and host immune response) (Smeltzer *et al.*, 2009). Virulence factors have been categorized following several considerations: i) the cellular localisation, ii) the temporal pattern of production and iii) the primary contribution to the disease process (toxins or colonization and evasion of host defenses) (Smeltzer *et al.*, 2009). This arsenal of virulence factors is completed by diverse genes responsible for antibiotics and antibacterial resistance. This makes *S. aureus* an outstanding pathogen within the staphylococcal genus, benchmarking the pathogenicity of *S. epidermidis* (Rosenstein & Götz, 2013).

Virulence factors include: i) surface-associated factors such as adhesins, ii) the ability to form a biofilm, iii) factors that help escape from the immune system, iv) internalization factors and v) finally toxins that exert damaging effects to the host. Fitness factors are also involved in infection as they support survival under hostile conditions in the host. They are subdivided into exoenzymes (nucleases, proteases and lipases) and iron uptake systems. Exoenzymes are secreted to retrieve nutrients and components for biosynthetic purposes while iron uptake systems are crucial since in the host iron is restricted (Rosenstein & Gotz, 2013). Here, we discuss and describe the main colonization factors as well as the other virulence factors. The molecular determinants of biofilm formation in staphylococci are covered in the next section.

Surface-associated virulence factors

S. aureus and *S. epidermidis* are the most versatile and adaptive species of staphylococci. They both express a rich assortment of surface-associated molecules. The surface-associated factors of *S. aureus* include structural

components of the cell wall such as teichoic acids, surface-exposed proteins and extracellular polysaccharides (Smeltzer *et al.*, 2009). Teichoic acids may have a role in nasal colonization and adherence to endothelial cells. Additionally, lipoteichoic acids and peptidoglycan induce inflammatory response and may have synergistic effects leading to the recruitment of neutrophils (Smeltzer *et al.*, 2009).

The cellular surfaces of *S. aureus* and *S. epidermidis* are coated with a variety of adhesins which are responsible for cellular adhesion. Three main categories of molecules coexist: the cell wall-anchored (CWA) surface proteins, the autolysins/adhesins and the molecules responsible for intercellular adhesion. CWA proteins are covalently attached to the peptidoglycan and they allow interactions with several structural component of the host extracellular matrix (ECM) and many plasma proteins (Rosenstein & Gotz, 2013). All CWA proteins contain a secretory signal sequence at the N-terminus directing the translation product to the secretory machinery in the cytoplasmic membrane (Geoghegan & Foster, 2015). This sequence is removed upon secretion. A sorting signal is present at the C-terminus composed of a LPXTG amino acid sequence, a hydrophobic domain and a positively charged tail. The LPXTG sequence is recognized and used by sortase A that covalently anchors the protein to the peptidoglycan (Geoghegan & Foster, 2015). Two sortases exist in *S. aureus*, sortase A and sortase B. Sortase A is responsible for anchoring the adhesins to the cell-wall peptidoglycan while sortase B processes only the iron-regulated surface determinant protein C (IsdC). During infection, the bacterium needs iron to perform metabolic activities. The cells of the human body accumulate large quantities of iron. *S. aureus* retrieves iron from haem groups that are released from erythrocytes by the action of microbial haemolysins. IsdC plays a key role in scavenging heme groups and transferring them into the cytoplasm where they are degraded to liberate iron (Villareal *et al.*, 2008). Due to their major roles in infection, sortase A and B are regarded indirectly as virulence factors.

S. aureus can express up to 24 distinct CWA proteins. Recently, the definition of CWA proteins was extended to include both structural and functional features but also proteins where structural details had not been elucidated (adenosine synthase AdsA) or proteins having a biological function located in an intrinsically disordered region (fibronectin-binding proteins (FnBPs), Geoghegan & Foster, 2015). Five different groups of proteins belong to CWA proteins depending on their function and structural organisation (Foster *et al.*, 2014, Geoghegan & Foster 2015): i) the "Microbial Surface Components Recognizing Adhesive Matrix Molecules (MSCRAMMs), ii) the G5-E repeat family, iii) the Near-iron transporter (NEAT) motif protein

family, iv) the three-helical bundle motif and v) the legume lectin domain protein family.

The principal group comprises the MSCRAMMs, which recognize and mediate attachment to components of the ECM such as fibrinogen (Fg), fibronectin (Fn), elastin or collagen (Cn). It is now known that these proteins are multifunctional, some having roles other than promoting initial adhesion for instance promoting intercellular adhesion during the accumulation phase in biofilm formation. (Foster *et al.*, 2014, Dufrêne, 2014, Geoghegan & Foster, 2015). The MSCRAMMs group is restricted to proteins sharing structural and functional similarities and a common ligand binding mechanism. Three subdivisions coexist in the MSCRAMM family based on the presence of different motifs (**Figure 3**).

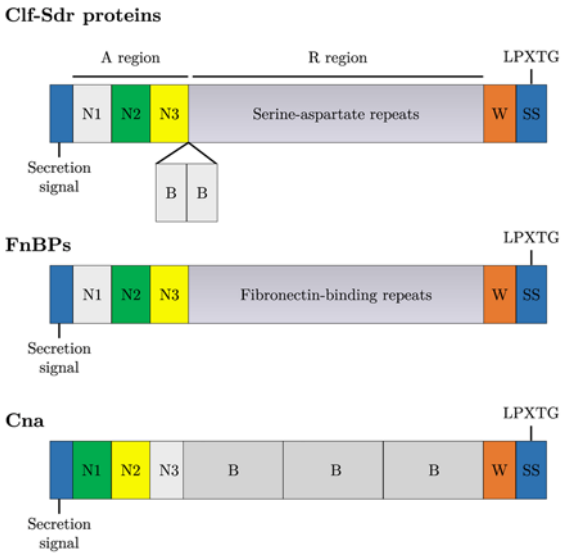

Figure 3: The MSCRAMMs protein family is subdivided in three main groups based on their structural motifs.

All cell wall-anchored (CWA) proteins contain a sorting sequence (SS) at the C-terminus followed by a proline-rich wall-spanning region (W). The A region is connected to the wall-spanning region by variable numbers of B domains constituting the R region.

The members of Clf-Sdr proteins are related to ClfA from *S. aureus*. The A region is composed of the three separately folded subdomains N1, N2 and N3. N2 and N3 bind ligands by the DLL mechanism. Additional B subdomains containing serine-aspartate repeats (Sdr) can flank the Sdr region located between the N3 subdomain and the W region.

Fibronectin binding proteins (FnBPs) have A domains structurally and functionally similar to the A domain of Clf-Sdr proteins. Tandem fibronectin-binding repeats replace the Sdr region between the A region and the wall-spanning region.
The collagen-adhesin (Cna) protein is organised differently having the ligand-binding activity located in the N1 and N2 subdomains, performing the collagen hug mechanism. The A region is connected to the wall-spanning region by variable numbers of B domains.
Adapted from (Foster *et al.*, 2014).

The G5-E tandem repeat family comprises the *S. aureus* surface protein G (SasG) which is very similar to the accumulation-associated protein (Aap) from *S. epidermidis*. Both contain repeats composed of 128 amino acid. These repeats fold tandemly into two domains that are structurally related: the domain E (50 residues) and the domain G5 (78 residues). Each domain folds in triple stranded β-sheets framing a central Cn-like triple helical region. In solution, the repeat regions of SasG form a monomeric and highly extended conformation that is resistant to mechanical stress allowing the protein to

maintain its length and stability. The E domains form mechanical clamps that bind non-adjacent G5 domains by forming hydrogen bonds between β-strands in flanking G5 domains. (Gruszka *et al.*, 2015). SasG was shown to promote cell-cell adhesion *via* Zn^{2+} homophilic bonds between β-sheet rich G5-E domains (Formosa-Dague *et al.*, 2016).

Four NEAT motif containing proteins (IsdA, IsdB, IsdC and IsdH) are cell wall-anchored proteins responsible for haem capture and transport from the host where iron is restricted to the bacterium. Iron-regulated surface determinants (Isd) proteins transport haem to a membrane transporter that transfers haem into the cytoplasm where haemoxygenase break down the haem and iron is released. The conserved NEAT domain comprises height β-strands folded in an immunoglobulin-like manner (Grigg *et al.*, 2010). Isd proteins have also key roles in adhesion: IsdA mediates adhesion to epithelial cells and promotes nasal colonization. IsdB binds to certain type of integrins and have a role in platelet activation and invasion of mammalian cells. IsdH participates to the evasion of host immune system by avoiding phagocytosis (Geoghegan & Foster, 2015).

Protein A (SpA), the only representative member of the three-helical bundles protein family is a well-known surface protein from *S. aureus*. SpA inhibits antibody-mediated opsonisation and therefore the phagocytosis (Smeltzer *et al.*, 2009). Five separately folded three-helical bundles compose the N-terminal region of Spa. Each three-helical bundle is able to bind several ligands: von Willebrand factor, TNFR1 a receptor for tumor necrosis factor and the Fab region of IgM, allowing SpA to play the role of a superantigen (Geoghegan & Foster 2015).

The last member of the CWA proteins is a family of glycoproteins. The N-terminal domain of serine-rich adhesin of platelet SraP is complex. It is composed of a short subdomain that is rich in serine repeats followed by a ligand-binding B domain divided into four subdomains: a legume-like lectin subdomain projected by two cadherin-like domains and a β-grasp fold domain. The lectin domain of SraP binds to glycoproteins of mammalian cells containing N-acetylneuraminic acid (Siboo *et al.*, 2005, Speziale *et al.*, 2014, Geoghegan & Foster, 2015).

Proteins with the N-terminal IgG-like folds characteristic of the MSCRAMM family bind their ligand through the dock, lock and latch (DLL) mechanism (Ponnuraj *et al.*, 2003, Foster *et al.*, 2014). This group includes the clumping factors of *S. aureus* (ClfA and ClfB) and several Sdr proteins of *S. epidermidis*, such as SdrG and SdrF. Sdr proteins contain five distinct regions: a secretion signal sequence, the A region containing a ligand binding activity, the B region of unknown function, the R region containing serine-aspartate

repeats sequences and at the C-terminal region, the sorting signal implicated in the anchorage of the protein to cell wall peptidoglycan (Hartford *et al.*, 2001, Foster *et al.*, 2014). SdrG, ClfA and ClfB proteins share Fg as a common ligand and bind different regions of the ligand by the DLL mechanism. The A region comprises three subdomains, N1, N2 and N3, with N2 and N3 being the minimum required for ligand binding (Geoghegan & Foster, 2015).

The DLL mechanism has been intensively studied through the SdrG-Fg interaction (Nilsson *et al.*, 1998, Hartford *et al.*, 2001, Ponnuraj *et al.*, 2003, Bowden *et al.*, 2008). In the A region of the adhesin, the N2 and N3 subdomains are folded separately into separate IgG-like folds and comprise 2 β-sheets. N2 and N3 are oriented in a specific way providing a hydrophobic trench of approximately 30 Å that allows ligand docking. The ligand inserts into the trench triggering a conformational change at the C-terminus of the N3 subdomain, resulting in a peptide folding over the bound ligand to lock it in place and latching it by the formation of an additional β-strand in one of the β-sheets of N2 (Ponnuraj *et al.*, 2003, Bowden *et al.*, 2008, Foster *et al.*, 2014, Herman *et al.*, 2014, Geoghegan & Foster 2015)(**Figure 4a**).The link between the A region and the wall-spanning region is the role of a domain either composed of repeats of the dipeptide Ser-Asp (SD repeats) or of Fn-binding repeats (in FnBPs). This domain acts as a flexible stalk, projecting the N-terminal ligand-biding region from the cell surface.

S. aureus is also able to bind to Cn-modified surfaces using another MSCRAMM called Cna through the "collagen hug" mechanism (Zong *et al.*, 2005). The mechanism differs from DLL since N1 and N2 are the A region subdomains with the ligand binding activity. In Cna, variable B repeated domains differing in sequence from SD repeats link the A region to the wall-spanning region. Collagens are formed from three separate polypeptide chains associated in a triple helix. The N1 and N2 subdomains are separated by an extended linker region forming a hole (the lock) between the subdomains. The hole can receive a rod-like Cn triple-helix in such a manner that the ligand docks into a trench in the N2 domain. The Cn is hugged by the N1N2 subdomains after which the latching complementation of a β-strand occurs to stabilize the complex (Zong *et al.*, 2005, Foster *et al.*, 2014)(**Figure 4b**).

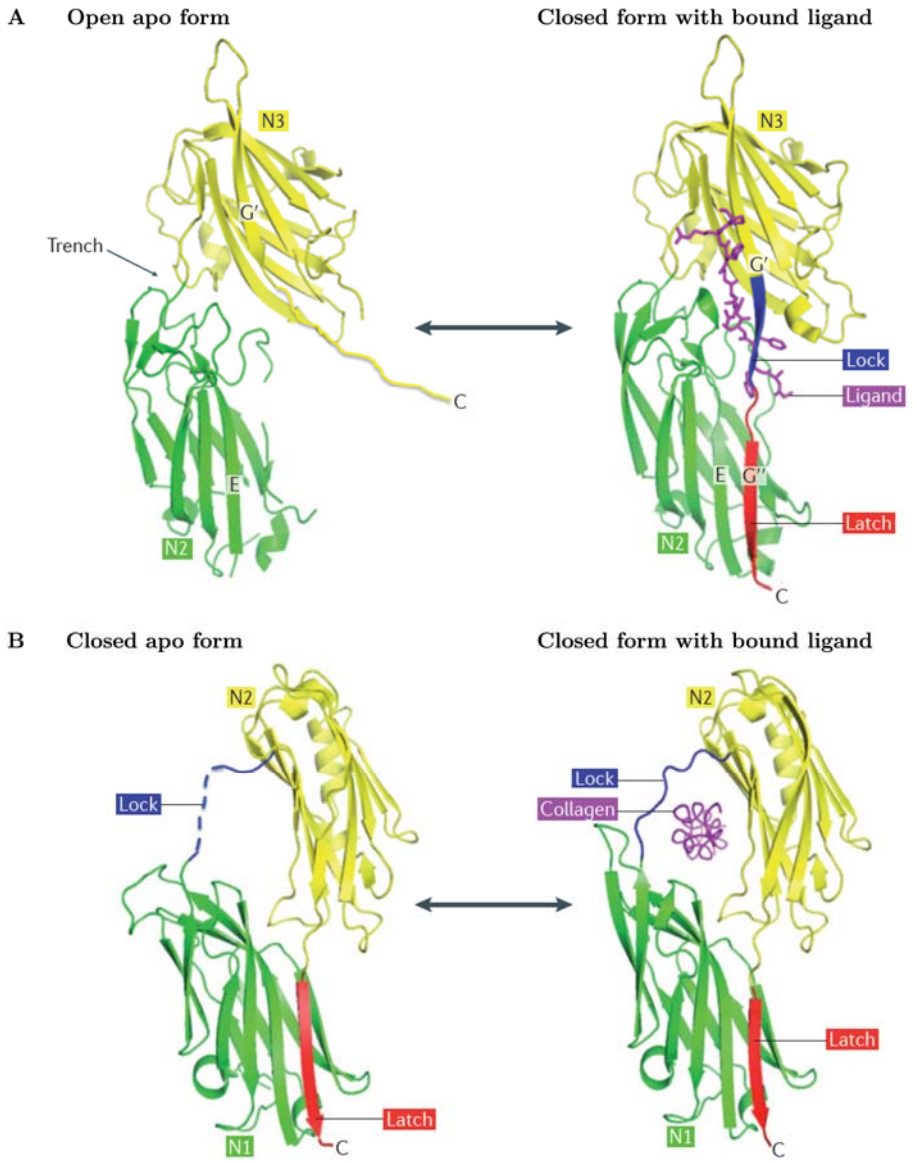

Figure 4: Mechanisms of ligand-binding by MSCRAMMs proteins.
A. The dock, lock and latch (DLL) mechanism. A wide hydrophobic trench is formed between the N2 and N3 subdomains of the A region of the MSCRAMM (open apo form). The ligand peptide (purple) inserts into the trench and the C-terminus end of the N3 subdomain undergoes conformational changes to a closed form and locks the ligand. After binding, the carboxy-terminus residues align *via* β-strand complementation forming the lock (in blue) and the latch (in red).
B. The collagen hug mechanism. (left) The closed apo form of the MSCRAMM shows the empty ligand-binding trench between the N1 and N2 subdomains that forms the lock (in blue). In red, the latch peptide is complemented by a β-strand to the N1 subdomain. The rope-like collagen triple helix docks into the trench between the N1 and N2 subdomains. The closed form shows the ligand (in purple) captured using residues in the lock region.
Adapted from (Foster *et al.*, 2014).

Apart from the MSCRAMMs, staphylococci also express secretable expanded repertoire adhesive molecules (SERAMs). This group is composed of several Fn and Fg binding proteins and other anchorless proteins (Rosenstein & Gotz, 2013). Recently, a novel protein, the small basic protein (Sbp) was discovered which promotes important steps of biofilm formation in *S. epidermidis* (Decker *et al.*, 2015). Sbp accumulates within the biofilm and is deposited at the biofilm-substrate interface. Sbp was shown to have a role in abiotic substrate colonization and adhesion to epithelial cells. Sbp influences the interactions between the adhesins responsible for intercellular adhesion which contributes to the stability of the biofilm and cell-cell aggregation. Interactions between Sbp and the B-domains of the accumulation-associated protein (Aap), a protein responsible for intercellular adhesion, were recently shown to be essential to mediate specific molecular interactions between *S. epidermidis* and matrix components (Decker *et al.*, 2015).

Autolysins are another class of bifunctional proteins for which adhesive properties have been described. (Rosenstein & Gotz, 2013). Autolysins are non-covalently bound surface associated enzymes that are in charge of peptidoglycan reorganisation. In general, autolysins are thought to play important roles in cell-wall turnover, cell division, cell separation, and antibiotic-induced lysis of bacteria (Heilmann, 2011). The autolysin/adhesin from *S. aureus* (Aaa) has adhesive properties towards immobilized Fg and Fn (Heilmann *et al.*, 2005). Earlier, the same team showed the dual role of an autolysin from *S. epidermidis* (AtlE) first by affecting the cell surface hydrophobicity enhancing its capability to adhere to hydrophobic substrates and second by mediating adhesion to vitronectin covered substrates (Heilmann *et al.*, 1997).

Evasion of immune responses

The ability to escape from the immune system is a strong virulence factor in staphylococci. *S. aureus* as well as *S. epidermidis* must cope with various mechanisms of the host defences after the penetration of the epithelial barrier. The innate immune system constitutes the first line of defence providing a fast response to invading microorganisms. Neutrophils, the most abundant leukocytes in blood, are the main cells responsible for killing the invading pathogens. Neutrophils are not carried by blood similarly to normal blood cells, but they can roll along the surface of endothelial cells. At an area of inflammation, neutrophils need to extravasate (the movement of the neutrophil from the circulatory system into the surrounding tissue), be activated and migrate to the site of inflammation. *S. aureus* expresses factors that are able to interfere with each step of neutrophil recruitment. SSL5 and SSL11, two secreted proteins interfere with neutrophil rolling and block the

endothelial P selectin which is a cell adhesion molecule that interacts with the surface the neutrophils to initiate the extravasation (Foster & Geoghegan, 2015). The Eap/Map protein of *S. aureus* directly inhibits the extravasation by binding a pro-inflammatory surface adhesin on endothelial cells (Foster & Geoghegan, 2015). At the site of infection, a gradient of molecules arises to recruit and inform neutrophils about the location of the inflammation. The C5a peptide is part of the complement system that fixes on the bacterial cell surface. Growing bacteria release formylated peptides that are neutrophil chemoattractants. The C5a peptide and formylated peptides have high affinities for specific receptors on the neutrophil surface. A secreted protein from *S. aureus* called CHIPS binds to the C5a receptor and the formyl peptide receptor to block the activation of the neutrophil (Foster & Geoghegan, 2015). Several *S. aureus* secreted and surface associated factors are known to interfere with the complement system which is required to enhance the capabilities of the phagocytic cells to clear the invasion of pathogens. The extracellular fibrinogen-binding protein (Efb) interacts with the bound complement factor C3b that leads to an antiphagocytic function. SdrE participates in immune evasion by binding to complement regulatory factor H (Rosenstein & Gotz, 2013). In *S. epidermidis*, SdrG has been shown to interfere with the release of fibrinopeptide B. SdrG binds Fg avoiding the clotting induced by thrombin, disturbing the flux of neutrophils (Rosenstein & Gotz, 2013). Additionally, *S. epidermidis* produces exopolymers such as poly- γ-glutamic acid (PGA) and the polysaccharide intercellular adhesin (PIA) that protects the bacterium form innate host defence. PGA is crucial in resistance to phagocytosis by neutrophils and to antimicrobial peptides (AMPs). *S. epidermidis* is also protected from neutrophil killing by PIA which has a role in interfering with complement deposition and protection from immunoglobulins and AMPs. Positively charged PIA is active against anionic and cationic AMPs, the explanation could be that PIA sequesters the oppositely charged AMPs and repulses AMPs of the same charge by electrostatic interactions (Otto, 2009).

Staphylococci also interfere with adaptive immunity. SpA is a CWA protein that inhibits phagocytosis mediated by opsonins by binding to the fragment crystallisable (Fc) region of IgG. Additionally, Spa binds to the fragment antigen region of the membrane-associated immunoglobulin IgM on B cells. SpA acts as a superantigen toxin that induces the apoptosis of B cells. Spa is thus able to modulate both the innate immune and the adaptive immune responses (Kobayashi & DeLeo, 2013). SpA also binds pathogen-specific antibodies by their Fc-gamma portion. This binding activity of SpA is shared by the staphylococcal binder of immonoglobulin (Sbi), which also associates with complement factors 3d and factor H to promote degradation of

complement (Kim *et al.*, 2012). Sbi is secreted protein that is also associated with the bactericidal envelope. Adenosine synthase A (AdsA) is an immune evasion factor that synthesizes the immune signalling molecule adenosine. AdsA is responsible for an overall increase in the content of extracellular adenosine thereby dampening innate and adaptive immune responses during infection. Adenosine is a powerful immunosuppressive signalling molecule that causes the inhibition of platelet aggregation and blocks the oxidative burst of neutrophils. Adenosine is believed to control excessive inflammation within mammalian organisms (Kim *et al.*, 2012). Staphylococci expressing AdsA and therefore extracellular adenosine during infection escape innate and adaptive defences mechanisms (Kim *et al.*,2012).

Internalization

Staphylococci are extracellular pathogens but they are able to evade the immune system by internalization into host cells. Neutrophils are the first line of defence against infection but they can also act as a Trojan horse to promote and disseminate the bacterial infection around the body (Foster & Geoghegan, 2015). The phagocytosis of *S. aureus* triggers the oxidative burst consisting of the generation of reactive oxygen species (ROS). *S. aureus* can resist ROS inside the phagosome by expressing superoxide dismutase. Additionally, AdsA produces extracellular adenosine resulting in the inhibition of production of superoxides and nitric oxide that allows bacterial survival inside the phagosome. Furthermore, antimicrobial peptides are neutralized by the metalloprotease aureolysin and staphylokinase, both responsible for binding and sequestering the peptides. The bacterium is able to increase the positive charge of its cell surface, resulting in the repulsion of cationic antimicrobial peptides (Foster & Geoghegan, 2015). Apart from internalization by neutrophils, it has been shown that *S. aureus* has the ability to invade and persist within non-professional phagocytes such as epithelial, endothelial or osteoblast cells (Alva-Murillo *et al.*, 2014). Intracellularly*, S. aureus* persists in a semi-dormant state called small colony variants which make it resistant to antibiotics. The role of CWA proteins is crucial for invading host cells. FnBPs bind Fn through their long intrinsically disordered binding region located in C-terminus of the A region (Foster *et al.*, 2014). This binding region is composed of up to 11 Fn binding domains each of which forms an extra β-strand with a short β-sheet in type I modules of Fn. Altogether, the tandem array of β-strands form a β-zipper mechanism of binding (Foster & Geoghegan, 2015). In the host, Fn is a plasma protein that binds to the integrin α5β1. Initially, integrins were known to be cell adhesion molecules and receptors for ECM molecules, but integrins are now seen as receptors able to regulate intracellular signalling and cellular responses (Schaffner *et al.*, 2013). Fn is

recognized by integrin α5β1 and binds to FnBPs. This results in Fn playing the role of a bridge between the host cell and the bacterium leading to internalization of the pathogen. This mode of invasion by FnBPs is the most efficient and dominant mechanism of internalization (Geoghegan & Foster, 2015). Other proteins are involved in the internalization of *S. aureus* such as the legume lectin SraP that mediates binding to glycoproteins on the surface of mammalian cells or the autolysins that contribute to internalization *via* heat shock proteins (Rosenstein & Götz, 2013). Internalization is not a strategy devoted to *S. aureus* since *S. epidermidis* is also able to internalize into bone cells. Khalil *et al.*, showed that internalization into bone cells does not involve the binding to Fn and is not dependent on an interaction with integrin α5β1 (Khalil *et al.*, 2007). Another mechanism involves the interaction between the heat shock protein Hsc70 and autolysins from both *S. aureus* and *S. epidermidis*. (Hirschhausen *et al.*, 2010, Rosenstein & Gotz, 2013).

Toxins

S. aureus has the ability to express a large array of extracellular proteins considered as toxins, since they mediate disease when administered in purified preparations (Smeltzer *et al.*, 2009). Three different types of toxins are expressed by *S. aureus*: the exfoliative or epidermolytic toxins, the enterotoxins which are also staphylococcal superantigens and the cytolytic toxins. Epidermolytic toxins induce a skin disorder known as staphylococcal scalded skin syndrome. Basically, four antigenically different toxins cause the exfoliation of the outer layers of the epidermis leading to characteristic skins lesions. Some staphylococcal exotoxins have superantigenic properties, meaning that they are able to overstimulate the immune system especially T lymphocytes, causing a variety of human diseases such as a toxic shock syndrome (Krakauer *et al.*, 2016). They include the toxic shock syndrome toxin (TSST-1), and many enterotoxins (Rosenstein & Götz, 2013). These superantigen toxins are also pyrogenic but not all cause emetic effects which is the sign of staphylococcal food poisoning. TSST-1 causes a toxic shock syndrome characterized by high fever, hypotension, skin desquamation, an erythematous rash and multi-organ failure ultimately leading to death (Smeltzer *et al.*, 2009). Cytolytic toxins are able to disrupt the membrane of various host cells leading to cell content leakage and cell death. These toxins are subdivided into single-component and bicomponent toxins. The most prominent example of the first category is the archetypal α-toxin. While β-toxin and δ-toxin also belong to this category, the latter is part of the PSMs family, produced by both *S. aureus* and *S. epidermidis*. They all are haemolytic toxins involved in the erythrocyte lysis necessary for iron uptake. The bicomponent toxins include Panton-Valentine leucocidin (PVL) and γ-toxin

that are produced by the association of two separate subunits. They exhibit cytolytic activity on leukocytes and therefore they participate to the evasion of the immune system (Rosenstein & Götz, 2013).

On the other hand, *S. epidermidis* and other coagulase negative species have low aggressive activity and they are not known to produce superantigen toxins (Becker *et al.*, 2014). However, *S. epidermidis* expresses phenol-soluble molecules that can be considered as cytolytic toxins (Rosenstein & Götz, 2013). For instance, production of δ-toxin, known as the PSM γ, induces the formation of pores in the membrane of host cells leading to the lysis of erythrocytes. *S. epidermidis* produces other PSMs that have cytolytic activities but the level of expression of these cytotoxic molecules is low (Becker *et al.*, 2014).

I.2.3. Molecular determinants in staphylococcal biofilms

As already discussed in section **I.1.3**, biofilm formation occurs in three steps: attachment of the bacteria to the substrate, accumulation in microcolonies and maturation in colonies, and lastly biofilm detachment. These steps are physiologically different from each other and require phase-specific factors (Otto, 2008). The formation of a biofilm is recognized as a virulence factor and a key mechanism against host defences and resistance towards antibiotics. Here, we describe the main molecular determinants affecting staphylococcal biofilm formation (see **Figure 5** for a general overview).

Staphylococcal adhesion to abiotic surfaces originates from the characteristics of both the bacterial cell surface and the substrate, involving physicochemical forces (Becker *et al.*, 2014). These forces such as electrostatic interactions, hydrophobic forces or van der Waals forces are mediated by the surface-associated molecules of staphylococci. CWA proteins, non-covalently-anchored proteins, and teichoic acids have been reported to alter the physicochemical properties of the cell surface in staphylococci (Otto, 2009, Otto, 2013, Becker *et al.*, 2014). AtlE, a major autolysin of *S. epidermidis* was shown to mediate attachment to polystyrene and to have a specific activity towards the host prote*in vitro*nectin, via repeated sequences (Heilmann *et al.*, 1997, Kohler *et al.*, 2014). It has been suggested that Atl mediates the release of extracellular DNA in biofilm formation and that eDNA would be the key for adhesion onto plastic surfaces (Becker *et al.*, 2014). Additionnally, Gross *et al.*, showed that teichoic acids influence bacterial adhesion via the cell surface charge (Gross *et al.*, 2001). These cell surface molecules are believed to modify the overall charge and hydrophobicity of the cell surface (Joo & Otto, 2012). Staphylococci stick very well to plastic surfaces. This ability was for a long time the basis for most *in vitro* research about biofilms in staphylococci and

also other biofilm-forming species. The role of direct attachment to plastic surfaces is not clear in the pathogenesis of infections associated with indwelling devices. Host matrix proteins readily cover the foreign material soon after insertion in the body, consequently, the interaction of this proteinaceous conditioning film is thought to play a more important role in bacterial colonization (Otto, 2008).

Besides adhesion to abiotic substrates, the interactions of *S. aureus* and *S. epidermidis* with surfaces modified with host extracellular matrix components –such as indwelling devices and other biomaterials– play a key role in initiating a biofilm-associated infection. As already explained, both species express a large panel of MSCRAMMs that have the capacity to bind proteins such as Fg, Fn or Cn. The roles of MSCRAMMs are of great importance for bacterial colonization (Otto, 2008). While many MSCRAMMs have not yet been assigned a function, a few of them have been intensively studied. *S. epidermidis* binds Cn and Fg *via* SdrF and SdrG respectively (McCrea *et al.*, 2000, Bowden *et al.*, 2005). SdrG-Fg binding occurs *via* the well-documented DLL mechanism. (Nilsson *et al.*, 1998, Hartford *et al.*, 2001, Ponnuraj *et al.*, 2003, Bowden *et al.*, 2008). The mechanism was originally discovered for SdrG, but it has been shown to apply to other proteins such as ClfA, ClfB or FnBPA from *S. aureus* (Ganesh *et al.*, 2011, Foster *et al.*, 2014). *S. aureus* has developed a more complex armada of surface proteins and has added functional redundancy to some MSCRAMMs. For example, at least 3 different proteins bind Fg. Two closely-related proteins that bind Fn, FnBPA and FnBPB also have a Fg/elastin binding activity at their N-terminus (Lower *et al.*, 2011).

During the phase of biofilm accumulation and maturation, cell-cell interactions occur and cells aggregate. Additionally, forces operate on biofilms that lead to the typical 3-dimensional appearance of mature biofilms (Otto, 2008). In staphylococci the major molecule responsible for intercellular adhesion is PIA sometimes called poly-*N*-acetylglucosamine (PNAG) due to its chemical composition (Mack *et al.*, 1996). PIA is an amphiphilic partially de-acetylated polymer of 130 β-1,6-linked N-acetylglucosamines, with 15 to 20% of the residues being deacetylated (Arciola *et al.*, 2015) Deacetylation is important to develop a biofilm based on exopolysaccharides, since it allows the fixation of positively charged deacetylated residues to the bacterial cell surface (Arciola *et al.*, 2015). PIA is a major determinant of the staphylococcal biofilm matrix (Otto, 2008, Arciola *et al.*, 2015). PIA together with teichoic acids, extracellular DNA and proteins, forms the extracellular matrix of the biofilm. The amphiphilic character of PIA is essential for resistance mechanisms against antimicrobial peptides or for acting as a diffusion barrier against

antibiotics (Otto, 2008.) PIA is important but not essential in the accumulation phase since some *S. aureus* and *S. epidermidis* strains have biofilm formation mechanisms that are independent of PIA production (Kogan *et al.*, 2006). Several proteins mediate cell-cell interactions, thus promoting maturation of the biofilm. For example, for *S. epidermidis*, the biofilm-associated protein (Bap) and the Bap-homologous protein (Bhp) were found to mediate proteinaceous biofilms independently from the production of PIA (Tormo *et al.*, 2005). *S. aureus* and *S. epidermidis* express two structurally and functionally related proteins, the *S. aureus* surface protein SasG and the accumulation-associated protein Aap, respectively (Speziale *et al.*, 2014). Aap was shown to be essential for biofilm accumulation on polymeric substrates (Becker *et al.*, 2014). Accumulation mediated by Aap is independent from the production of PIA, and this determinant was found in highly prevalent in clinical strains of *S. epidermidis* (Becker *et al.*, 2014). These proteins belong to the G5-E family proteins of the CWA proteins, having their B domains interacting to form homophilic interactions and promote biofilm accumulation (Speziale *et al.*, 2014). The G5-E repeats form Zn^{2+} dependent homophilic interactions and Aap and SasG are implicated in cell-cell interactions during biofilm formation by dimerization in a Zn^{2+}-dependent manner (Rohde *et al.*, 2005, Conrady *et al.*, 2013, Formosa-Dague & Dufrêne, 2015). Other proteins from *S. aureus* promote intercellular adhesion. SraP is thought to form homophilic interactions between the cadherin-like domains during biofilm formation (Speziale *et al.*, 2014). Several CWA proteins promote biofilm accumulation. The A domain of FnBPs were shown to be responsible for biofilm accumulation (O'Neill *et al.*, 2008, Geoghegan *et al.*, 2010, Geoghegan *et al.*, 2013, Herman-Bausier *et al.*, 2015). In the case of SdrC, the binding activity was localized to subdomain N2 (Barbu *et al.*, 2014). Other surface-associated proteins are involved in cell-cell adhesion (Speziale *et al.*, 2014) *e.g.* the non-covalently anchored extracellular matrix binding protein (Embp) from *S. epidermidis* and the *S. aureus* surface protein C (SasC). The Embp gene was found in more than 90 % of *S. epidermidis* clinical isolates (Rohde *et al.*, 2004, Arciola *et al.*, 2015). Embp was firstly attributed a role in primary attachment due to its Fn-binding activity, but it is now clear that Embp is a functional intercellular adhesin (Buttner *et al.*, 2015).

Additionally to intercellular adhesive factors during accumulation phase, the biofilm endures structuring forces and cell-cell disruptive factors leading to the last stage of biofilm formation, the dispersion of the cells (Joo & Otto, 2012). Although several molecules might contribute to the structure of the biofilm, to date, only the phenol-soluble modulins (PSMs) have been consistently demonstrated to have this role in *in vitro* and *in vivo* studies in

both *S. aureus* and *S. epidermidis* (Le *et al.*, 2014). PSMs are regulated directly in a cell-density-dependent manner by the accessory gene regulator (*agr*) locus. *Agr* locus is part of the QS system, regulating gene expression during cell dispersal. The QS promotes the upregulation of proteases and toxins and the downregulation of surface adhesion molecules such as MSCRAMMs (Joo & Otto, 2012). PSMs are surfactant peptides, they disrupt the non-covalent forces holding the biofilm extracellular matrix together. This step is essential for the formation of channels, to deliver nutrients to deeper biofilm layers, and for dispersal/dissemination of clusters of biofilm to distal organs in acute infections. Besides PSMs, *S. aureus* expresses proteases and nucleases that are responsible for the digestion of the protease-based biofilm and DNA-based biofilm matrix respectively (Joo & Otto, 2012, Le *et al.*, 2014).

Biofilm detachment and cell dispersal are crucial to colonization of new sites. Cells can detach in single cells or in clusters due to i) mechanical forces exerted in blood vessels, ii) a diminution in production of EPS or iii) by functional detachment factors, such as PSMs, enzymes, proteases (Otto, 2008). The biological significance of biofilm dispersal lies in the fact that cells will disseminate from the infection site to other sites via the bloodstream or the lymph. Detached cells can thus initiate a new biofilm formation cycle elsewhere and may cause severe diseases such as sepsis or endocarditis.

In summary, there is a wealth of molecular determinants leading to biofilm formation in staphylococci, as depicted in **Figure 5**.

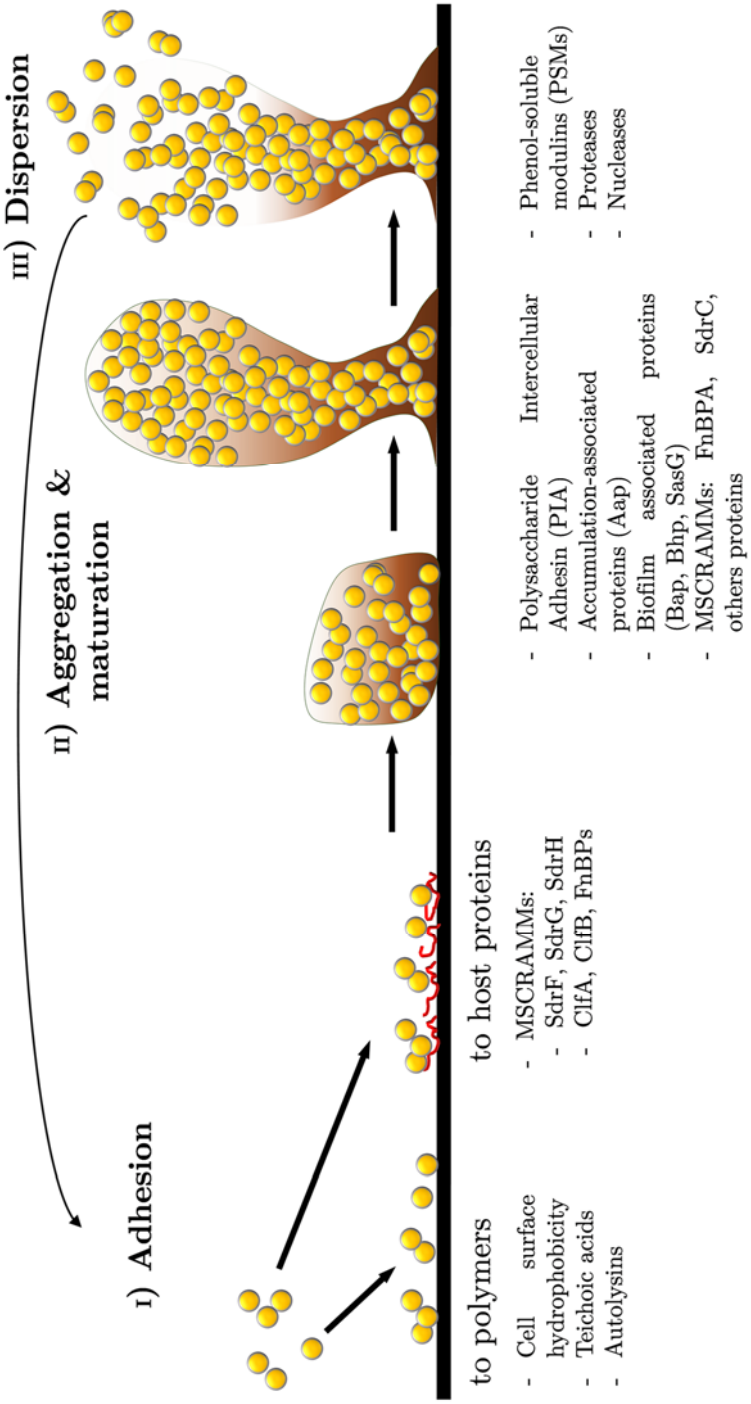

Figure 5: Principal molecular determinants during biofilm formation in staphylococci. Adapted from (Otto, 2008, Joo & Otto, 2012, Buttner *et al*, 2015).

I.3. Atomic force microscopy

I.3.1. Introduction

When we think of a microscope, we visualise a binocular system that uses light to produce a magnification of the object to analyse. Although optical microscopes are crucial in biology, they only produce flat images in two-dimensions and their resolution is limited by the wavelength of light. To overcome the resolution limitation, Binnig and Rohrer invented the scanning tunnelling microscope (STM) in 1982 (Binning *et al.*, 1982). STM uses a nanometric probe to scan the sample surface while measuring an electrical current, resulting from a quantum effect. When a sharp metallic tip is brought to a close distance (< 1 nm) from a conductive substrate, electrons can jump between the two surfaces. This flow of electrons is measurable and called the tunnelling current. Because of the strong dependence of the electric signal and the distance between the tip and the surface, STM allows high precision topographic and electronic maps of scanned substrates. STM allowed for the first time to see atoms on a surface. However, the system works only in ultra-high vacuum conditions using conductive substrates, making it not appropriate for biological systems (de Pablo & Carrion-Vazquez, 2014, Eaton *et al.*, 2010).

In 1986, another scanning probe microscope, the atomic force microscope (AFM) was invented (Binnig *et al.*, 1986). Here, interaction forces are measured while the tip is scanned across the surface. As the analysis can be performed in liquid, this technique is ideally suited for biology (de Pablo & Carrion-Vazquez, 2014, Dufrêne, 2015, Kilpatrick *et al.*, 2015). Today, contact mode is the most widely used imaging mode. A sharp tip attached at the end of a cantilever is brought into contact with the surface (Binnig *et al.*, 1986). The sample surface is scanned line by line with a piezoelectric scanner and each line is recorded as a 2-dimensions profile. The cantilever is able to deflect as the tip interacts with the surface, reproducing the sample topography. In other words, AFM is a mechanical imaging instrument that is able to reconstruct the surface topography of the sample with unprecedented spatial resolution and sensitivity (Eaton *et al.*, 2010, Ducheyne, 2011) (**Figure 6**).

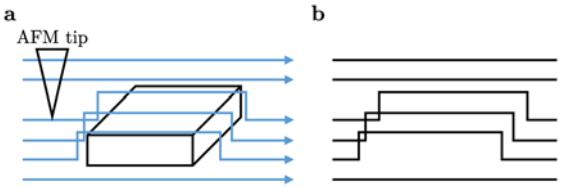

Figure 6: Contact mode AFM. **a.** A sharp tip is scanned over a surface from left to right. **b.** As a result, the topography of the surface is generated line by line. Adapted from (Eaton *et al.*, 2010).

Besides topographic imaging, AFM provides information on intra-and intermolecular forces, a method known as force spectroscopy (Cappella & Dietler, 1999). Forces are measured down to the picoNewton (pN) level through the recording of the cantilever deflection while the sample is moved up and down (**Figure 7a**). The forces can be repulsive or attractive depending on the nature of the surface. Examples of forces at play include van der Waals forces, electrostatic forces, or friction forces (Dufrêne, 2001, Gerber & Lang, 2006). The cantilever obeys Hook's law: $F = -kx$, where F is the interaction force (N), k is the spring constant of the cantilever (N/m) and x is the vertical deflection of the cantilever (m). For some applications, the tip is replaced by a living cell in order to measure single-cell adhesion forces (**Figure 7b**).

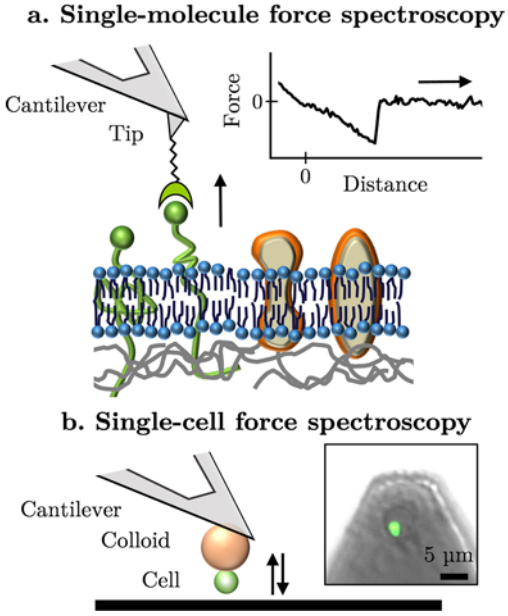

Figure 7: Atomic force microscopy modalities. AFM senses the forces acting between the tip and the sample surface.
a. In single-molecule force spectroscopy, the tip is functionalized to perform force-distance curves and retrieve information at the single-molecule level.
b. Single-cell force spectroscopy involves sticking a single live cell to the colloidal cantilever and recording of force-distance curves to measure detachment force towards a given substrate. The viability of the cell is checked by fluorescent staining (green means that cell membrane integrity is preserved).
Adapted from (Dufrêne, 2014).

I.3.2. The atomic force microscope set-up

The AFM is composed of a soft cantilever terminated by a sharp tip, a piezoelectric scanner on which the sample is mounted, a laser focused at the end of the cantilever and reflected in a photodiode (**Figure 8**). The laser and photodiode are a detection system used to monitor the movement of the cantilever and consequently, the physical interactions between the sample and the sharp tip.

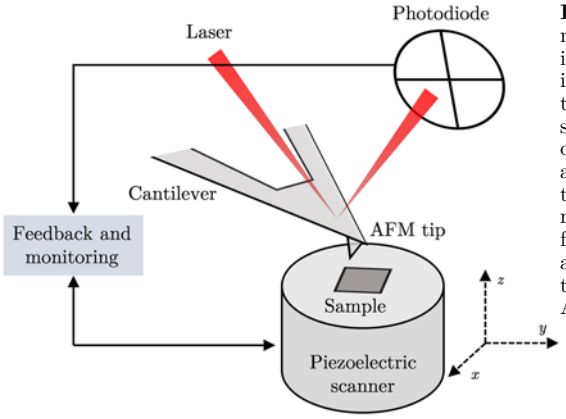

Figure 8: The atomic force microscope setup. The AFM generates images by measuring the physical interactions between a sharp tip and the sample mounted on a piezoelectric scanner able to move in the three dimensions. The cantilever deflection and consequently the forces acting on the tip is quantified by a laser reflected into a photodiode. The feedback loop allows monitoring and adjustments in the applied force on the sample.
Adapted from (Dufrene, 2004).

AFM cantilevers are usually made of silicon or silicon nitride (Si_3N_4). Two geometries are used, traditional rectangular shape and "V-shaped" cantilevers. The cantilever is usually coated with a thin layer of gold to enhance the reflectivity (Cappella *et al.*, 1997). The reflectivity of the laser beam on a cantilever made of Si_3N_4 is 0.3 for a non-polarized light while the totality of the light beam is reflected while using a gold coating on the cantilever (Rakić *et al.*, 1998). The appropriate choice of cantilever depends on the stiffness of the sample. In general, the cantilever stiffness should be as low as possible for biological samples to avoid sample damage while scanning. However, in some advanced modes, stiffer cantilevers might be used to reduce noise and instabilities (Cappella & Dietler, 1999). In imaging modes, the shape and sharpness of the cantilever decide the ultimate reachable resolution of the image. For some precise applications such as structural imaging, ultrasharp ($<$ 2 nm radius) carbon-nanotubes AFM tips were developed (Hafner *et al.*, 2001).

The AFM piezoscanner is usually made of ceramic material $PdBaTiO_3$. A piezoelectric material is a transducer able to convert an electrical potential to a mechanical deformation. When a voltage is applied across two opposite sides of a piezoelectric material, it is able to deform according to the magnitude of the voltage, the geometry of the device and the nature of the material (Eaton *et al.*, 2010). The deformation is not ideal and induces defects and inaccuracies in images (Eaton *et al.*, 2010). Typically, the piezoelectric scanner

allows the sample to move in the three dimensions of space (x, y, z) with high precision and accuracy. Commercial piezoelectric scanners are able to scan 100 µm in (x, y) and a few µm in (z) with a precision of 0.1 nm.

The detection system usually consists in a laser focused at the end of the cantilever, reflected in a photodiode. The forces acting between the probe and the surface are measured by a change in the amount of reflected light in the photodetector that translates the received light as a voltage. The bending of the cantilever induces a change in the amount of reflected light in the photodiode (**Figure 9**).

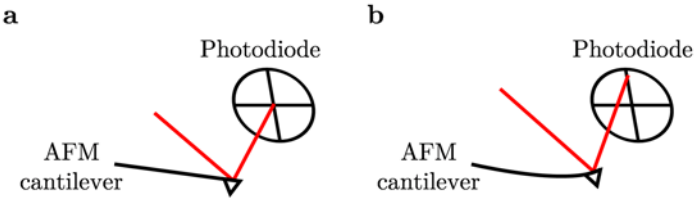

Figure 9: The AFM detection system uses a laser beam focused at the end of the cantilever. The laser beam is reflected in the photodiode. A voltage is measured from the photodiode and translated in a force using the sensitivity and the Hook's law.
a. Far away from the surface.
b. At contact with the sample surface.

I.3.3. AFM Imaging

As discussed in section I.3.1, in contact mode, the AFM tip scans the sample surface line by line and reconstructs the topography of the sample. There are two different options in contact mode: either the applied force is fixed, called the constant force mode or the height of the sample is kept constant, called the constant height mode. In the first mode, the result is a constant force applied on the sample and the measured height of the piezoelectric scanner gives the topography of the sample. This mode allows relatively low constraints on the sample while scanning, making it well-suited for biological imaging. In the constant height mode, the piezoelectric scanner does not move in (z), but the topography is directly red by the photodetector. The constant-height mode is used to ensure high precision in (z), but requires flat samples.

In contact mode, the tip remains in contact with the sample surface, sensing and feeling the forces while scanning. Two different images are generated: the height image and the deflection image. The height image provides accurate measurements on sample roughness. The deflection image is the error of the feedback loop used to maintain the force constant while scanning. Real-time adjustment is not perfect, leading to an error signal. This error signal is used to compute a deflection image, more sensitive to fine surface

details (Dorobantu *et al.*, 2012). Besides the contact mode, several dynamic modes have been developed to avoid shear forces between the tip and the sample in contact mode. These dynamic modes were introduced to limit the problem of friction forces acting on the sample. While dynamic modes are well-suited for applications in ultra-high vacuum, in liquids, oscillating and AFM cantilever is challenging. Due to lower van der Waals forces and high damping effects of the medium, the ratio signal over noise is strongly reduced leading to poor sensitivity (Moreno-Herrero *et al.*, 2004). Consequently, new modes for AFM applications in liquids were developed such as Peak Force Tapping (PFT) or Quantitative Imaging (QI). PFT and QI modes are often called multi-parametric imaging modes since in one image, several parameters are recorded such as the adhesion force, the rigidity of the sample and its topography (Dufrêne *et al.*, 2013).

Owing to the generation of high resolution images and the ability to observe living cells at nanoscale resolution, AFM has been widely used in biology, providing novel insights into the structure-function relationships of cell surfaces (Dorobantu *et al.*, 2012, Dufrêne, 2014). In microbiology, AFM has revealed the nanoscale organisation of cell wall components, directly on live cells (**Figure 10**, Dufrêne, 2014). Imaging single *L. rhamnosus* in buffer revealed a rough morphology with nanoscale waves reflecting polysaccharides at the cell surface. The mutant impaired in the production of exopolysaccharides showed a smoother surface (Francius *et al.*, 2008, **Figure 10a**). Correlating topographic imaging and AFM-modified tips, Andre *et al.*, found on *L. lactis* cells lacking cell wall exopolysaccharides that peptidoglycan is organised in periodic cables running parallel to the short axis of the cell (**Figure 10b**, Andre *et al.,* 2010). Teichoic acids are important molecules for cell elongation and cell division. AFM was used to map the distribution of wall teichoic acids (WTAs) in *L. plantarum.* Topographic imaging allowed a comparison between the wild type strain and a mutant deficient in WTA production. This revealed that the expression of WTAs is limited to the poles of the cell since they show a smoother surface than the side walls (Andre *et al.*, 2011). AFM used in air to gain insights into the nanoscale properties of strains of *Bacillus thuringiensis* revealed that the amount of flagella observed at the nanoscale correlates well with their microscopic swarming motility (**Figure 10d**, Gillis *et al.*, 2012). AFM Topographic images of dormant spores of *Aspergillus fumigatus* revealed the presence of nanoscale layered rodlets composed of hydrophobins (**Figure 10e**, Dague *et al.*, 2008). Crystalline bacterial cell surface layers (S-layers) are composed of glycoproteins. AFM was used to image S-layers on live bacterial cells of *Corynebacterium glutamicum.*

The high resolution of produced images shows the presence of highly organized surface layers (**Figure 10f**, Dupres (Dupres *et al.*, 2009)).

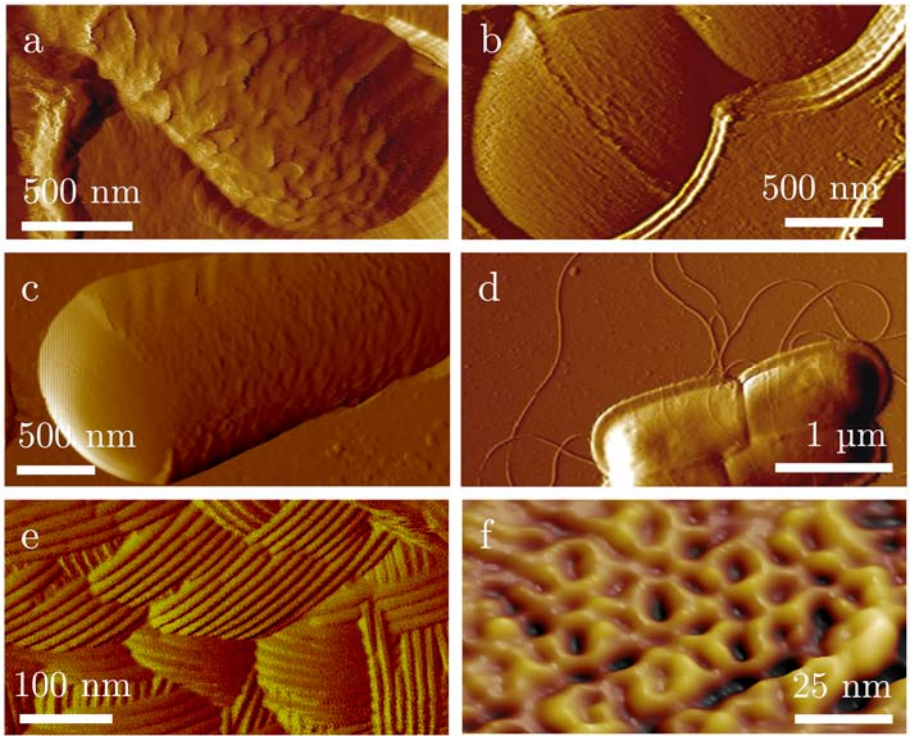

Figure 10: AFM unravels key cell wall components of microbial surfaces.
a to f. High-resolution AFM images of individual cells from
a. *Lactobacillus rhamnosus* GG
b. *Lactococcus lactis*
c. *Lactobacillus plantarum*
d. *Bacillus thuringiensis*
e. *Aspergillus fumigatus*
f. *Corynebacterium glutamicum*
Adapted from (Dufrêne, 2014)

Currently, conventional AFM is limited by its poor temporal resolution. Recent advances in instrumental AFM have enabled to track biomolecular dynamics with high-speed AFM (HS-AFM) (Eghiaian *et al.*, 2014). HS-AFM is now able to record images in a timeframe of hundred milliseconds (100ms), sufficient to visualize dynamic biological processes. Striking examples are the visualization of single-molecule myosin-5 walking on an actin filaments (Kodera *et al.*, 2010), or the degradation of cellulose by the enzyme cellulase (Igarashi *et al.*, 2011). High-speed AFM is still a complex and young technique allowing only experts to take advantage of the technique. While HS-AFM has been applied to various samples, from purified membranes to live cells, efforts are still needed to broaden its use in biology (Eghiaian *et al.*, 2014).

I.3.4. Force spectroscopy

Besides imaging, AFM also provides a wealth of information on molecular interactions and biophysical properties. In single-molecule force spectroscopy (SMFS), an AFM tip is modified with a bioligand of interest to manipulate individual receptors, while in single-cell force spectroscopy (SCFS), the tip is replaced by a living cell in order to measure single-cell adhesion forces (Hinterdorfer & Dufrêne, 2006, Müller & Dufrêne, 2008, Dufrêne, 2015). These two techniques have provided new challenges in nanomicrobiology (Dufrêne, 2015, Dufrêne, 2014).

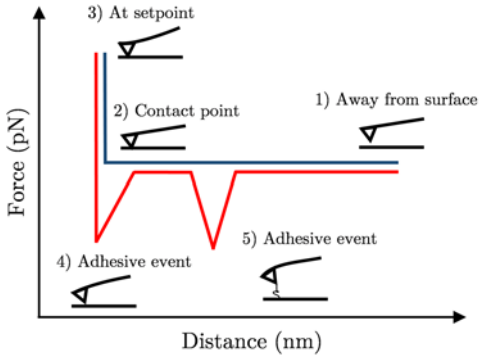

Figure 11: Schematic of an AFM force-distance curve associated with typical bending events. The approach is in blue, the retraction is in red.

The general principle of force spectroscopy is to acquire force-distance curves with high lateral (25 nm), vertical (0.2 nm) and force resolution (up to 10 pN) (Cappella & Dietler, 1999). A typical force-distance curve is presented in **Figure 11**, showing two traces, the first in blue is the approach curve, the second in red is the retraction of the tip from the sample surface.

The approach is a in three step process: 1) away from the surface, the tip does not sense any force, the cantilever is not deflected; 2) at the contact point, the cantilever bends until a defined setpoint is reached in 3); the retraction of the tip occurs from the setpoint in 3); until the situation the tip

reaches again step 1). During retraction, the tip can interact with the surface and show short distance adhesion events in 4) or, further away, long distance adhesion events in 5). In 4), at short distance the tip can sense non-specific adhesion linked with surface energy or binding forces of small molecules. At long distance, in 5), stretching and/or unfolding of biomolecules can occur. The raw curve recorded is the cantilever vertical deflection (in volts) versus the vertical displacement of the piezoelectric scanner (in nm). This curve is corrected in two steps. First, using the deflection sensitivity that links the voltage to the cantilever deflection and second using the spring constant of the cantilever in the Hook's law.

Force-distance curves can be acquired in all (x,y) spots of a scanned area to locally probe the sample properties and interactions (Cappella & Dietler, 1999). This mode is called spatially-resolved force imaging or force-volume imaging (**Figure 12**). The physico-chemical properties are gathered from individual force curves and represented in a two dimensional map. By post-processing the acquired data, each force curve is analysed and the quantity of interest (e.g., adhesion force) is recovered and displayed as a black or coloured pixel. The colour intensity is related to the quantity of interest.

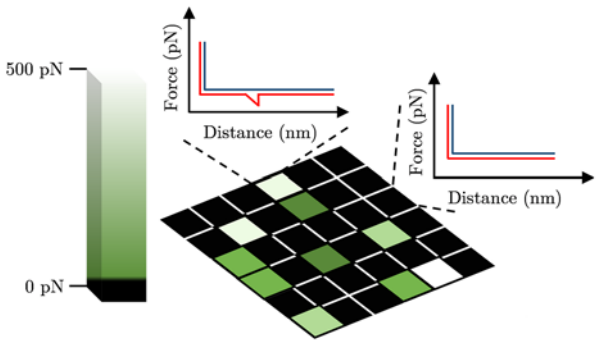

Figure 12: Spatially-resolved force –distance curves that allows reconstruction of the adhesion force map. From each force curve the adhesion force is recovered (color scale). The whiter the pixel, the stronger the force.
A pre-defined cut-off value is set depending on the experiment that brings the non-adhesive and aberrant force curves to non-adhesive events. (black).

Various properties can be extracted from the force curves. In the retraction curves, the adhesion force (F_{adh}) is the most obvious parameter, defined as the force needed to break the bond between the AFM probe and the surface. The rupture length also provides valuable information about the distance at which the interaction breaks and the cantilever returns to initial position. The separation energy (E_s) can be computed by integration of the area below the curve defined by F_{adh} and the distance needed to separate the tip from the surface (**Figure 13**).

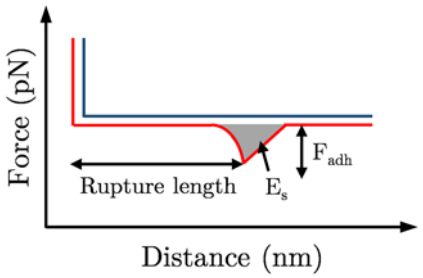

Figure 13: The retraction of force-distance curve brings valuable information on adhesion processes.
The adhesion force (F_{adh}), the separation energy (E_s) and rupture length are key parameters of the interaction probed.

In the contact area, the shape of the curve provides information on sample elasticity. When the tip compresses the material, the indentation (δ) [nm] can be computed by subtracting the cantilever deflection (x) [nm] from the measured displacement of piezo (Z) [nm]: $Z = \delta + x$. By measuring the indentation at a given force, the local modulus of elasticity can be assessed using fitting models that depend on the geometry of the AFM probe (Cappella & Dietler, 1999). In biology, AFM has proved useful for measuring the nano-mechanical properties of cells and biomolecules in physiological conditions (Kurland *et al.*, 2012, Kilpatrick *et al.*, 2015). There is an interest in studying the cell elasticity since it plays crucial roles in cellular functions including migration, division and shape (Müller & Dufrêne, 2008), and changes in the mechanical properties of cells may alter the biological and mechanical responses of tissues and organs (Sokolov *et al.*, 2013). Mechanical characterization at the nanoscale of biomolecules provides insights on how they are involved in biological complexes and tissues allowing us to describe their contribution to macroscale properties (Kurland *et al.*, 2012).

I.3.5. Single-molecule force spectroscopy

In single-molecule force spectroscopy (SMFS), the tip is generally functionalized with biomolecules of interest such as proteins, carbohydrates or even viruses to detect, localize and manipulate individual receptors (Müller & Dufrêne, 2008). The binding force measured during tip retraction is the key parameter providing information of the intra- and intermolecular forces, and mechanical properties of individual biomolecules (Müller & Dufrêne, 2011). In doing so, the interactions between antigen-antibody, double strands of DNA, lectin carbohydrate and various protein-ligands have been measured (Hinterdorfer & Dufrêne, 2006).

To ensure reliable experiments in SMFS, proper functionalization is required. The method should meet key requirements (Hinterdorfer & Dufrêne, 2006, Carvalho & Santos, 2012):

i) The strength of the bond linking the molecule to the tip should be stronger than the interaction probed
ii) The grafting density has to be tuned and sufficiently low to ensure single-molecule interactions
iii) The grafted molecules should keep mobility on the tip allowing interactions with complementary molecules
iv) Unspecific adsorption of irrelevant molecules should be minimized to avoid unspecific contributions to adhesion.
v) For oriented systems, proper methods with defined molecular orientation on the tip might be required.

To meet these key points, a first strategy is based on the immobilization by chemisorption of thiol-based self-assembled monolayers (SAMs) on gold. Thiols groups have a strong affinity for gold, leading to quasi-covalent bonds (Carvalho & Santos, 2012, Frisbie *et al.*, 1994). The SAM is obtained by immersion of gold surfaces in ethanol solutions containing the selected alkanethiols (Hinterdorfer & Dufrêne, 2006). Chosen molecules are usually a mixture of two different alkanethiols: one terminated by a reactive group, and the other used to passivate the rest of the reactive sites on the surface and to avoid aspecific contributions to the force signature. Alkanethiols terminated with carboxyl functions can react with amino groups of proteins using 1-ethyl-3(3-dimethylaminopropyl) carbodiimide (EDC) and *N*-hydroxysuccinimide (NHS) in aqueous solution, to form an amide bond (Hinterdorfer & Dufrêne, 2006). For some studies, it can be important to orient the protein on the tip. Here, Histidine-tagged proteins are attached on the tip using a mixture of alkanethiols terminated with nitrilotriacetate combined with nickel (Ni^{2+}-NTA) and alkanethiols terminated by polyethylene glycol groups (PEG). This

strategy allows site-specific interactions and offers an optimal exposure of the domains responsible for the interaction probed (Dupres *et al.*, 2005, Kienberger *et al.*, 2000, Hinterdorfer & Dufrêne, 2006).

The second strategy uses direct amination by covalent attachment of silanes (Hinterdorfer & Dufrêne, 2006, Carvalho & Santos, 2012). While different methods are available, they share common key steps: generation of reactive sites on the silicon substrate, grafting of a bifunctional linear polymer, the cross-linker, which is attached *via* one of its reactive ends, the other end being used to attach the biomolecule of interest. In the first step, amino groups are generated on the AFM tip surface. Two ways are possible for direct amino-functionalisation: using ethanolamine in dimethylsulfoxide as a solvent or aminopropyltriethoxysilane (APTES) in a gas phase. The first method is simpler and less demanding whereas the second one produces better AFM data (Wildling *et al.*, 2011). For biomolecules with amino groups, typically proteins, different types of cross-linkers are available. The simplest approach to link a protein to an amino-functionalized AFM tip is to use a cross-linker able to react firstly with the amino groups located on the AFM tip and secondly, to use the amino groups of the protein of interest (Wildling *et al.*, 2011, Ebner *et al.*, 2007). The heterobifunctional cross-linker is a molecule bearing a NHS group (**Figure 14a**) spaced by a PEG chain (**Figure 14b**) and terminated with an acetal group (**Figure 14c**) (acetal-PEG-NHS).

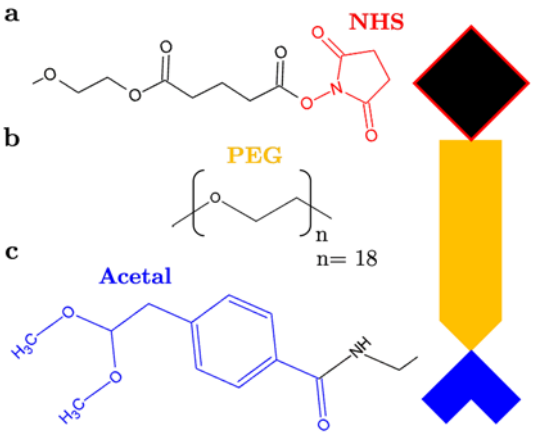

Figure 14: The heterobifunctional cross-linker used for protein grafting on AFM tips.
a to c. The NHS molecule (**a**) linked to the PEG spacer chain (**b**) attached to the acetal terminated chemical group (**c**).

After amino-functionalization of the AFM-tip, the cross-linker is attached by reaction of the NHS group with the amino groups on the AFM tip, forming a covalent amide bond with elimination of water and the NHS molecule. Proteins usually bear lysin residues having a primary amine function. The acetal group is converted into an aldehyde function, more reactive towards primary amines. The conversion is achieved by citric acid and the final coupling of the protein is possible in presence of $NaCNBH_3$, used as a reductive chemical to form an irreversible bond between the protein and the cross-linker (**Figure 15**, Ebner *et al.*, 2007, Wildling *et al.*, 2011).

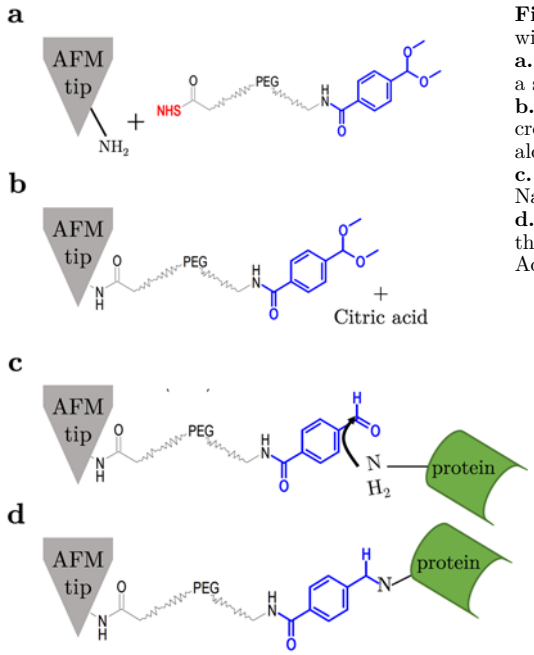

Figure 15: AFM tip functionalization with an acetal-PEG-NHS cross-linker.
a. An amino-silanized tip is immersed in a solution of acetal-PEG-NHS.
b. The acetal functions of the attached cross-linker is converted in reactive aldehyde functions.
c. Add the protein in presence of $NaCNBH_3$.
d. The protein is coupled covalently to the AFM tip.
Adapted from (Wilding *et al.*, 2011).

PEG is a flexible molecule allowing the attached biomolecule to freely orient avoiding the compression of the molecules between the tip and the probed surface. The length and elasticity of PEG is important to differentiate unspecific contributions from receptor-ligand binding (Carvalho & Santos, 2012).

Other chemistries than the process of conversion of acetal to aldehyde for protein-coupling are also possible. The straightforward alternative is to directly use reactive aldehyde functions avoiding the conversion step with citric acid. The advantages of the acetal-PEG-NHS chemistry resides in a simpler synthesis, lower cross-linker concentration and effective tip functionalization avoiding adjacent self-cross-linking (Wildling *et al.*, 2011).

For probing purified molecules on surfaces, the receptors or ligands to be analysed need to be strongly attached to a solid support using non-

destructive conditions. Muscovite mica, glass and silicon are well-known supports for immobilizing purified bio-ligands and receptors (Hinterdorfer & Dufrêne, 2006). Negatively charged surfaces allow simple physical adsorption, usually sufficient to withstand the pulling forces exerted on immobilized molecules (Hinterdorfer & Dufrêne, 2006). However, for most biomolecules, immobilization *via* the formation of covalent bonds is necessary. This can be achieved using the previously described NHS-EDC protocol, following gold deposition on a smooth surface (mica, glass or silicium surfaces) (Hinterdorfer & Dufrêne, 2006).

When applying SMFS to cell surfaces, the main issue to solve is cell immobilization. The key requirement is to maintain the cell viability and integrity to ensure the biological relevance of the experiment. For animal cells, the preparation is rather simple due to their ability of spreading on solid substrates (Heinisch *et al.*, 2012). However, for microbial cells that have defined shape and usually do not spread on substrates, other types of immobilization had to be developed (Heinisch *et al.*, 2012, Hinterdorfer & Dufrêne, 2006). Methods such as drying the cells on the surface, pre-treating the surface with polycations or binding covalently the cells onto the support are available. Such strategies are far from ideal as they induce cell denaturation. On the other hand, mechanical trapping of cells into porous membranes is a method of choice, allowing repetitive imaging, easy localization of single cells in pores and various cell shapes to be analysed. Furthermore, it allows high resolution live cell imaging and observation of dynamic processes (Francius *et al.*, 2008, Alsteens *et al.*, 2008, Dague *et al.*, 2008). However, there are disadvantages of the method. These include the relatively low cell surface exposed, the mechanical pressure induced on the cell that could affect AFM measurements and finally, the selection of a cell population *via* the pore size.

In the past years, SMFS has provided new insights into the molecular basis of microbial adhesion, the first and crucial step leading to biofilm formation. Probing single Als adhesins from *Candida albicans* with specific antibodies triggered the formation and propagation of adhesive nanodomains on the cell surface (Alsteens *et al.*, 2010, Garcia *et al.*, 2011). In the staphylococcal context, the Lower team used Fn-modified AFM tips to map the localisation of FnBPs across the cell surface and measure their binding forces. They were able to measure parallel bonding between FnBPs and Fn, and to show that the binding was consistent with a zipper-like binding mechanism (Buck *et al.*, 2010). They also showed that *S.aureus* cells bind more strongly to Fn-modified tips when they are deposited onto Fn-coated glass, suggesting that *S. aureus* is able to recognize Fn at the interface (Lower *et al.*, 2010). Another example deals with the protein Acm2 from the Gram positive

bacteria *Lactobacillus plantarum* (Beaussart *et al.*, 2013c). Acm2 is a peptidoglycan hydrolase, therefore playing a major role in cell division and growth. SMFS showed that Acm2 has a broad specificity and is able to bind to glucosamine residues in the peptidoglycan chain, but also binds to mucin, a protein secreted in to mucosal layer of the intestine.

I.3.6. Single-cell force spectroscopy

A variation of SMFS is single-cell force spectroscopy (SCFS) in which a living cell is attached on the cantilever to probe cell-substrate adhesion forces or cell-cell interactions. Several techniques are available to quantify cellular adhesion forces on a single-cell basis, including the surface probe apparatus, microneedles, optical and magnetic tweezers and AFM (Helenius *et al.*, 2008). In microbiology, AFM appears to be the most powerful tool to study single-microbial cell adhesion forces.

Central to SCFS is the attachment of single cells to the cantilever. For animal cells, protocols are generally based on receptor-ligands interactions and their ability to spread and adhere on welcoming substrates. Other strategies have been used which are based on different interactions such as electrostatic or hydrophobic interactions or chemical fixation (Dufrêne, 2008). However, critical requirements for AFM experiments have to be met to keep the biological significance and reliability of the method. First, the technique used has to ensure the metabolic activity and surface architecture of the cell after immobilization and second, the number of interacting cells has to be controlled (Dufrêne, 2015, Beaussart *et al.*, 2013a, Beaussart *et al.*, 2014b). In microbiology, an elegant way to reach these key points is FluidFM which uses microfluidics with nano-sized channelled cantilevers to manipulate single-cells (Guillaume-Gentil *et al.*, 2014, Potthoff *et al.*, 2015).

While the SCFS methodology has provided direct quantitative information on the specific and non-specific forces of microbial adhesins (Dufrêne, 2015), this technique has several drawbacks. SCFS has a low throughput, meaning that to obtain statistically relevant data, SCFS measurements take several days. In addition, only short contact times are possible using AFM (< 5 min) due to drift and software issues. Also, there are some difficulties to demonstrate the specificity of the probed interactions and the interpretation of the force-distance curves can be very delicate and need to be carefully considered. They result from the cell elasticity, membrane

properties, cell geometry and receptor properties such as binding strength, cooperativity and repartition on the cell surface (Helenius *et al.*, 2008).

Recently, SCFS has enabled researchers to understand the forces guiding the adhesion of medically-important microbes (**Figure 16**, Dufrêne, 2015). These analyses have greatly contributed to our understanding of the binding mechanisms (strength, specificity) of bacterial adhesins, of the role of hydrophobic forces in the adhesion of microbes to solid substrates, of the adhesion and nanomechanics of bacterial pili (extension, nanosprings), and of the forces driving microbe–microbe and microbe–host interactions. The results revealed that cell adhesion components exhibit remarkable adhesive and mechanical properties that have a strong impact on cell adhesion function.

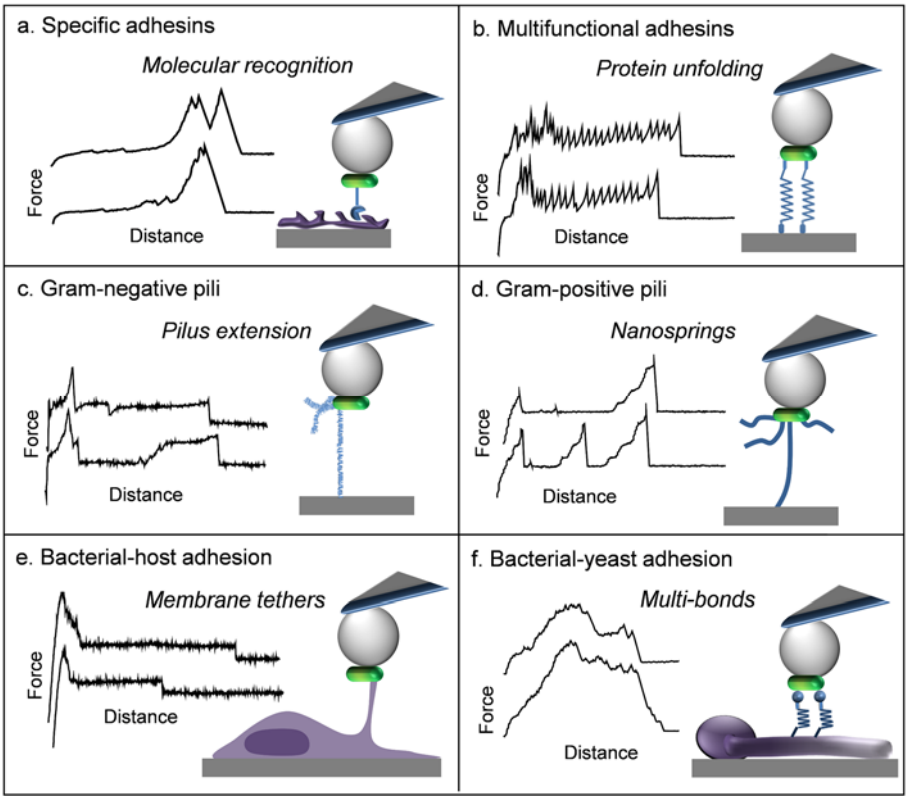

Figure 16: Cell adhesion components display a variety of mechanical properties that are important for cell surface interaction.
a. Ligand binding of specific adhesins.
b. Protein unfolding of multipurpose adhesins.
c. Elongation of Gram-negative pili.
d. Spring behaviour of Gram-positive pili.
e. Membrane tethers in microbe–host interactions.
f. Multiple macromolecular bonds in bacterium–yeast co-adhesion.
Adapted from (Dufrene, 2015).

I.4. Objective and strategy

S. aureus and *S. epidermidis* are two important bacterial pathogens which represent a leading cause of biofilm-associated infections on indwelling medical devices such as central venous catheters and prosthetic joints. These infections are difficult to eradicate because bacteria in biofilms are in a semi-dormant state and show increased resistance towards antibiotics. Host defences are also less effective against biofilm infections since the cells are resistant to phagocytosis by neutrophils or macrophages. In staphylococcal biofilms the situation is compounded by the prevalence of strains that are resistant to multiple antibiotics, such as methicillin-resistant *S. aureus* (MRSA). Consequently, understanding the molecular mechanisms underlying the formation of staphylococcal biofilms is an important topic in current microbiology. Because cell surface proteins play key roles in biofilm formation, studying their molecular interactions is highly relevant and may ultimately contribute to the development of novel therapeutic approaches (*e.g.* anti-adhesion molecules).

The general objective of this thesis is to gain insight into the binding mechanisms (binding strength, specificity, affinity and mechanics) of staphylococcal adhesins using the new tools of nanotechnology. Although much is known about the molecular biology of these proteins, the different molecular forces at play during cellular adhesion are poorly understood.

The strategy involved developing atomic force microscopy (AFM) techniques for localizing and manipulating single molecules on living bacteria, and for quantifying the forces driving the adhesion of whole bacterial cells. These nanoscale analyses were applied to a series of bacterial strains expressing specific adhesins, and complemented by traditional microscopic adhesion assays. Much of these experiments relied on close collaborations with Profs. T. Foster and J. Geoghegan (Trinity College, Dublin) and to some extent with Prof. J. Mahillon.

We initially aimed at developing a novel force spectroscopy assay for measuring single-bacterial cell adhesion forces (**Part III**, **Appendix I, II and III**). Although various single-cell force spectroscopy (SCFS) protocols have been developed in microbiology, none of them enabled true, reliable single-bacterial cell analysis. We therefore established a simple, non-destructive method that combines colloidal probe cantilevers and polydopamine and allows us to measure the adhesion of bacteria towards various substrates or other cells. The method was initially developed with probiotic bacteria (**Appendix I and III**), and then further validated with *S*

epidermidis (**Appendix II**). As in the later study we used the strain ATCC 12228, it is presented as an Appendix.

With this new method, we first explored the ligand binding mechanisms of the (Sdr) proteins SdrG and SdrF (**Part II, Chapter I, II and III**). SdrG is abundantly present in *S. epidermidis* clinical strains and is a well-known protein that binds to Fg through the multistep 'dock, lock and latch' (DLL) mechanism. Until now, the molecular forces involved and the dynamics of the SdrG-Fg interaction were not known. Single-molecule force spectroscopy (SMFS) and SCFS were therefore used to study the binding strength and cell surface localization of SdrG, both in *S. epidermidis* HB and in a *Lactococcus lactis* strain expressing SdrG. This latter organism enabled us to study SdrG-Fg interactions in the absence of other staphylococcal components. The adhesin was shown to mediate strong attachment of the bacteria to Fg coated surfaces, and to accumulate at the cell surface in the form of nanoscale domains, thus contributing to strengthening adhesion of the pathogen. We combined whole population and AFM assays to investigate the extent to which the surface density of SdrG determines the ability of *S. epidermidis* clinical strains HB, ATCC 35984 and ATCC 12228 to bind to Fg-coated surfaces (**Chapter II**). *S. epidermidis* strains that display a higher density of SdrG on their cell surface showed enhanced adhesion to Fg-coated substrates. We then focused on SdrF (**Chapter III**), another protein from *S. epidermidis* that mediates adherence to Cn substrates. Based on sequence identity, topology and secondary structure prediction, the A domain of SdrF was predicted to contain the ligand binding activity. However, another team demonstrated the key role of B domains in SdrF-promoted adherence to Cn-modified surfaces. So the relative contributions of the A and B regions in Cn binding were not completely clear, which prompted us to study the ligand-binding activity of the two SdrF domains expressed in *L. lactis* strains. Comparative analysis of strains producing either full-length proteins or only the A or B regions enabled us to assess the relative roles of these regions in the binding activity of type I Cn. SdrF mediated ligand binding by strong and weak bonds involving both the A and B regions of the protein, thus highlighting an unanticipated dual Cn-binding activity for this protein.

Next, we investigated Fn-binding protein A (FnBPA), which plays an important role in cell-cell adhesion during biofilm formation by MRSA (**Chapter IV**), with the goal to answer the following questions: how strong are intercellular bonds, how many FnBPA proteins do they involve, and is FnBPA-mediated intercellular adhesion achieved by means of homophilic interactions or ligand binding? Using SMFS and SCFS, we analysed the binding mechanism of full-length FnBPA expressed in *S. aureus* strain SH1000

defective in clumping factors (Clfs) A and B, and in FnBPA and B, as well as of the recombinant FnBPA A domain immobilized on model surfaces. FnBPA was shown to mediate specific cell-cell adhesion via multiple, low affinity homophilic bonds that depend on Zn^{2+} ions and involve the A domain.

Given the medical significance of mixed staphylococcal-fungal biofilms, we also explored the forces driving the adhesion between *S. epidermidis* and *C. albicans* using SCFS (**Chapter V**). As the yeast-to-hyphae transition is important for *C. albicans* adhesion and biofilm formation, we measured the forces between single bacterial cells and fungal hyphae, revealing the important role played by fungal Als proteins and O-mannosylations in controlling co-adhesion.

Finally, we summarized the main fundamental achievements of this thesis and discussed them in light of the existing literature (**Chapter VI**). While this is not a "result Chapter" per se, we feel that this discussion adequately concludes the detailed presentation of the thesis.

II. Short presentation of the thesis

II.1. Tool development: single-bacterial cell force spectroscopy

II.1.1. A new single-cell assay

Central to our thesis was the measurement of bacterial adhesion forces at the single-cell and single-molecule levels, using advanced AFM techniques. While there are well-established protocols for SMFS analysis on microbial cells (Dupres *et al.*, 2005, Andre *et al.*, 2010, Alsteens *et al.*, 2010), there was a strong need to improve current SCFS protocols for bacterial adhesion studies. None of the existing methods enabled true, reliable single-bacterial cell analysis for at least one of the following reasons: i) the cell-cantilever bond is too weak, leading to cell detachment; ii) the use of chemicals or drying leads to cell surface denaturation and/or cell death; iii) multiple cells are attached and probed together, meaning single cell analysis is not accessible.

Together with Drs A. Beaussart and S. El-Kirat-Chatel, we developed a generic AFM-based method to quantify the adhesion forces between single bacteria and solid substrates (**Appendix I**, **Figure 17**, Beaussart *et al.*, 2013a). In early work, Kang and co-workers (Kang & Elimelech, 2009) used polydopamine to coat tip-less cantilevers. This method does not provide a clear control over the cell-substrate contact area. As the cantilever is tilted by few degrees inside the holder, individual bacteria need to be attached on the very end of the cantilever, which is difficult to achieve.

Our single-cell force spectroscopy (SCFS) method combines colloidal probe cantilevers and polydopamine to allow precise and reproducible single-cell attachment. Living cell probes are prepared by three main steps. First, the colloidal cantilevers are assembled using AFM tip-less cantilevers on which silica beads are glued using a UV-curable glue (**Figure 17a**). Then, colloidal probes are coated with a thin film of wet adhesive by immersion in a polydopamine solution (**Figure 17b**). Surface-adherent polydopamine thin films form on a wide variety of surfaces upon slightly alkaline conditions and promote reactions with inorganic as well as organic surfaces (Lee *et al.*, 2007, Kang & Elimelech, 2009, Dreyer *et al.*, 2012). The last step consists in attaching a single living bacterium on the colloidal cantilever (**Figure 17c**). To confirm that the cells are alive and precisely attached on the cantilevers, they can be labelled with the *Bac*light LIVE/DEAD stain. This kit uses two

different fluorescent probes: the first is propium iodide (PI) which binds nucleic acids. PI is excluded from the cytosol by the selective permeability of cell membrane when the membrane is intact. By contrast, when the cell dies, the membrane becomes permeable to PI and stains the cell in red. The second dye, is the Syto9, which is permeable to the cell membrane and stains nucleic acids residues in green.

We applied the method to the probiotic bacterium *Lactobacillus plantarum*. We found that *L. plantarum* cells show strong adhesive properties towards biotic and abiotic surfaces. Binding to hydrophobic surfaces does not depend on interaction time and gives rise to multiple force peaks and extended rupture lengths that may be attributed to the stretching and unfolding of cell surface proteins. Binding to lectin surfaces is strongly-time dependent and is associated with the stretching of long, flexible glucose (mannose)-based macromolecules. The measured specific and non-specific adhesive forces are of biological relevance as they are likely to play important roles in mediating *L. plantarum* adhesive interactions towards inert and living surfaces. So SCFS with polydopamine-coated colloidal probes provides a novel powerful platform for quantifying bacterial cell adhesion forces on a single-cell basis. Unlike other existing assays, our methodology is simple, versatile, non-destructive (cells remain alive even after 1 h measurements), and affords much better control of the cell positioning and of the cell-substrate contact area.

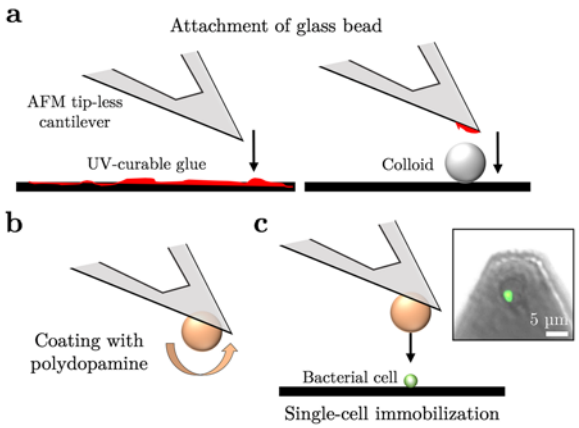

Figure 17: Single-bacterial cell force spectroscopy using a combination of colloidal probe and polydopamine. The method involves three steps (**a-c**):
a. attachment of the colloid on the cantilever.
b. The immersion of cantilever in polydopamine
c. Controlled immobilization of a single bacterium for force-distance measurements.
Adapted from (Beaussart *et al.*, 2013a).

II.1.2. Application to staphylococcal adhesion

Using this SCFS methodology, we measured the forces driving the adhesion of *S. epidermidis* ATCC 12 228 to fibrinogen (Fg) (**Appendix III**, **Figure 18**, Herman *et al.*, 2013). We found that the adhesion force and adhesion probability strongly increased with interaction time, suggesting that the adhesion process involves time-dependent conformational changes. SdrG targets a short sequence region composed of amino-acids residues 6 to 20 localized in the β-chain region of the Fg molecule. Therefore, we used the synthetic peptide $\beta_{6\text{-}20}$ (NEEGFFSARGHRPLD) for control experiments, revealing that the force signatures that we measured originate from the rupture of specific bonds between SdrG and this peptide ligand.

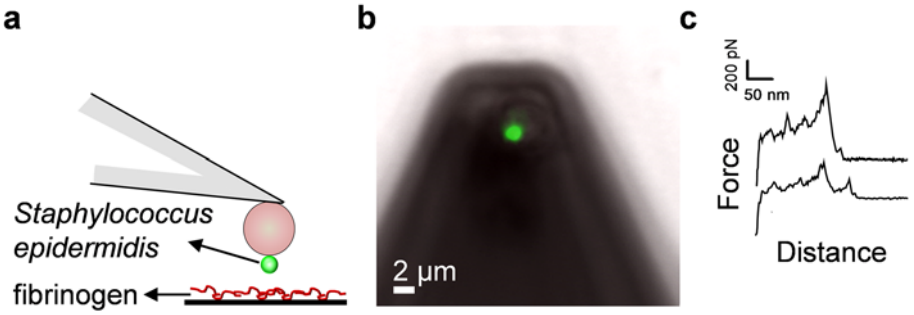

Figure 18: A novel single-bacterial cell force spectroscopy assay: application to the *S. epidermidis*-fibrinogen interaction.
a. Living bacteria are picked up with a polydopamine-coated colloidal probe, and the forces between individual bacteria and fibrinogen-coated substrates are measured.
b. Use of an integrated AFM-inverted optical microscope shows that single bacteria attached to the cantilever probes are properly located and alive (green color).
c. Typical force-distance curves document adhesion forces reflecting the rupture of specific bonds between SdrG and its peptide ligand. Adapted from (Herman *et al.*, 2013).

II.2. Understanding ligand-binding mechanisms in Sdr proteins

The Sdr protein family is a widely investigated group of MSCRAMMs (Josefsson *et al.*, 1998, McCrea *et al.*, 2000, Foster *et al.*, 2014). A hallmark of such adhesins is the *S. epidermidis* SdrG protein which binds with high affinity to the blood plasma protein Fg via the DLL mechanism involving dynamic conformational changes (**Part I, I.2.2**, Ponnuraj *et al.*, 2003, Otto, 2009). Because this interaction promotes bacterial attachment to Fg-coated biomaterials, it is thought to play an important role in infections. SdrF is another Sdr protein from *S. epidermidis* that binds Cn, thereby helping the bacteria to attach to transcutaneous drivelines from explanted ventricular assist devices from patients (Arrecubieta *et al.*, 2007). Despite the important role that these MSCRAMMs play in controlling staphylococcal adhesion, the forces driving their interaction with target proteins remain poorly understood. We therefore explored the strength and dynamics of the SdrG-Fg and SdrF-Cn interactions, as well as the impact of SdrG cell surface localization on bacterial adhesion.

II.2.1. Strength of the SdrG-Fg bond

SdrG contains five distinct regions: a secretion signal sequence, the A region containing the Fg binding activity, the B region of unknown function, the R region containing serine-aspartate repeats sequences, and at the C-terminal region, the sorting signal that is implicated in the anchorage of the protein to cell wall peptidoglycan (Hartford *et al.*, 2001, Foster *et al.*, 2014). The SdrG binding site is a cleft of approximately 30 Å in length between the N2 and N3 subdomains located in the A region of the protein. During the DLL binding process, once the ligand peptide is docked and stabilized by hydrophobic interactions and hydrogen bonds, a C-terminus extension of N3 subdomain folds over the ligand to insert and complement a β-sheet in the N2 subdomain (Ponnuraj *et al.*, 2003, Bowden *et al.*, 2008, Foster *et al.*, 2014).

Together with Professors. T. Foster and J. Geoghegan (Trinity College, Dublin), we used single-cell and single-molecule AFM to investigate the binding strength of SdrG, both in *S. epidermidis* HB and in a *Lactococcus lactis* strain expressing SdrG (*L. lactis* SdrG$^{(+)}$ cells) (**Part II**, **Chapter I**; **Figure 19**, Herman *et al.*, 2014). SCFS revealed that SdrG mediates time-dependent single bacterial cell adhesion to Fg-coated surfaces, with a mean adhesion force of ~2.1 nN, that we attribute to SdrG-Fg adhesive interactions (**Figure 19a**). *L. lactis* bacteria expressing SdrG show the same behaviour as *S. epidermidis* HB except that cell adhesion properties are more pronounced,

presumably due to the better exposure/orientation or accessibility of the adhesins. The adhesion strengthened with time, consistent with the dynamic, multistep nature of the DLL mechanism. This model involves the docking of the ligand in a binding trench formed between two SdrG subdomains followed by the movement of a C-terminal extension of one subdomain to cover the ligand and to insert and complement a β-sheet in a neighbouring subdomain. These structural changes are believed to increase greatly the stability of the closed conformation of the adhesin-ligand complex. So the increased contact time will favour optimal fitting of the interacting molecules, leading to stabilized closed conformations.

SMFS measurements revealed that the ~2 nN binding force corresponds to single SdrG-Fg bonds, which is similar to the strength of a covalent bond, thus much larger than that of other cell adhesion proteins, which is typically in the 50-400 pN range depending on the protein and on the loading rate (**Figure 19b**). Dynamic SMFS revealed a low dissociation rate and suggested that the SdrG-Fg bond is stable. These findings favour a dynamic, multistep DLL binding mechanism in which SdrG undergoes conformational changes to form greatly stabilized complexes. Such a strong bond is of biological relevance as it rationalizes the ability of *S. epidermidis* to colonize protein-coated biomaterials and to withstand physiological shear forces.

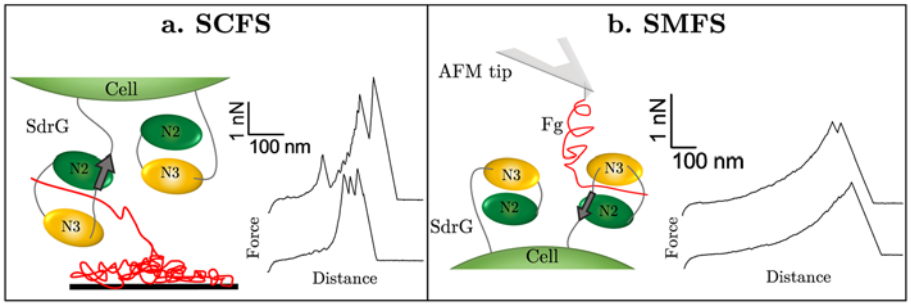

Figure 19: The binding force of the staphylococcal adhesin SdrG is equivalent to the strength of a covalent bond.
a. SCFS unravels adhesion forces between single *S. epidermidis* bacteria and fibrinogen (Fg) on solid substrates.
b. SMFS quantifies the binding strength of single SdrG adhesins on living bacteria. The left panels are cartoons of the experimental set-ups and the right panels show representative force profiles. Adapted from (Herman *et al.*, 2014).

II.2.2. The density of SdrG controls staphylococcal adhesion to Fg

Fg-coated tips were used to capture the localization of single SdrG proteins, demonstrating that they form nanoscale domains on the *S. epidermidis* cell surface (**Part II**, **Chapter I**; **Figure 20**; Herman *et al.*, 2014). Similar to multivalency, a ligand that dissociates from a cluster of adhesins is much more likely to rebind, thus largely contributing to stabilize adhesive interactions. This behaviour is similar to that observed for mycobacterial (Dupres *et al.*, 2005) and fungal adhesins (Alsteens *et al.*, 2010).

In a collaborative study with the Mahillon team, we used a combination of AFM and microscopic adhesion assays to investigate and correlate the amount of SdrG at the cell surface in controlling the ability of various *S. epidermidis* clinical strains (HB, ATCC 35984, and ATCC 12228) to bind to Fg-coated surfaces (**Part II, Chapter II**, Vanzieleghem *et al.*, 2015). Strains that showed enhanced adhesion towards Fg displayed increased amounts of SdrG adhesins, suggesting that the abundance of SdrG on the cell surface dramatically improves the ability of the cells to bind to Fg-coated implanted medical devices.

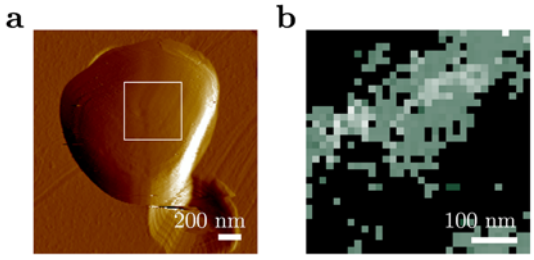

Figure 20: SMFS reveals that SdrG forms nanoscale domains on the *S. epidermidis* cell surface.
a. Deflection image showing single *S. epidermidis* cell trapped into porous membrane; the white square indicates the localization of the recorded force maps.
b. Adhesion force map recorded in buffer on a live *S. epidermidis* cell
Adapted from Herman *et al.*, 2014.

II.2.3. SdrF displays a dual Cn-binding activity

SdrF binds to Cn through mechanisms that are still poorly understood. Sequence similarity analysis and secondary structure prediction have suggested that the A region is the ligand binding domain, while the B region would help projecting the A region on the cell surface (Bowden *et al.*, 2005). However, a study using *Lactococcus lactis* expressing SdrF (SdrF^{+}), a protein-protein interaction assay and Western ligand blot analysis revealed that Cn binding involves the B region (Arrecubieta *et al.*, 2007). So the relative contributions of the A and B regions in Cn binding are not completely clear. Also, the specific forces engaged in ligand binding are not known.

We investigated the mechanical strength and binding mechanisms of SdrF using recombinant *L. lactis* strains expressing SdrF (kindly supplied by Prof. F. Lowy, Columbia University; Arrecubieta *et al.*, 2007). Single-cell analysis showed that SdrF mediates bacterial adhesion to Cn-coated substrates through both weak and strong bonds (**Part II, Chapter III**; **Figure 21,** Herman-Bausier and Dufrêne, 2015). By using the *S. epidermidis* 9142 strain (McCrea *et al.*, 2000), which shows a strong capacity to bind Cn, we demonstrated that the SdrF-Cn binding forces measured in *L. lactis* are relevant to those occurring in *S. epidermidis*, and that the use of *L. lactis* as a surface display model to study SdrF is appropriate. SMFS revealed that the protein is capable of dual ligand-binding involving both the A and B regions of SdrF and that both the weak and strong molecular bonds have high dissociation rates. These results indicate that the weak and strong bonds involved in the SdrF-Cn binding are less stable than the bonds formed by the DLL mechanism in the SdrG-Fg interaction. Collectively our experiments showed that MSCRAMMs can bind to ligands by other mechanisms than the well-known DLL mechanism. We anticipate that AFM will contribute to the identification of novel binding mechanisms and novel binding partners in staphylococcal CWA proteins.

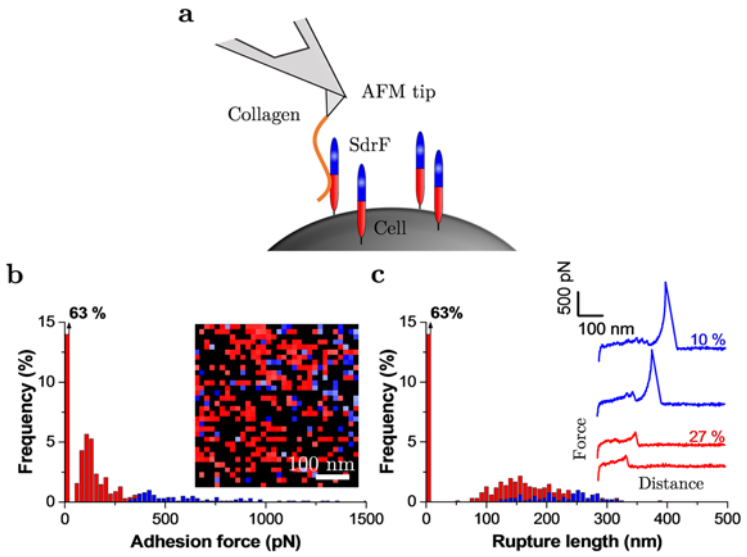

Figure 21: Localization and binding strength of single SdrF proteins on *L. lactis* SdrF$^{(+)}$ cells.
a. To probe the distribution and binding forces of single SdrF proteins on living bacteria with SMFS, we used Cn-modified AFM tips.
b. Adhesion force histogram together with adhesion force map.
c. Rupture length histogram with representative force curves (inset). The red and blue colours highlight dual detection of weak and strong binding events.
Adapted from (Herman-Bausier and Dufrêne, 2016).

II.3. Deciphering homophilic interactions in FnBPs

The *S. aureus* Fn-binding proteins FnBPA and FnBPB promote biofilm formation by clinically-relevant MRSA, both community-associated and hospital-associated strains (O'Neill *et al.*, 2008, Geoghegan *et al.*, 2013, McCourt *et al.*, 2014). Both FnBPA and FnBPB have N-terminal A domains that are structurally and functionally-related to the clumping factor A and the *S. epidermidis* SdrG proteins and bind to Fg by a variation of the DLL mechanism whereby conformational changes in subdomains N2N3 within the A region result in highly stabilized complexes (Ponnuraj *et al.*, 2003). The biofilm forming region of FnBPA was localized to subdomains N2N3 of the N-terminal A region but accumulation was shown not to involve a DLL mechanism (Geoghegan *et al.*, 2013). The molecular interactions leading to FnBP-promoted biofilms are poorly understood. In particular, it was unclear whether they involve direct homophilic bonds or binding of the proteins to surface-located receptors on adjacent cells (Foster *et al.*, 2014).

In collaboration with Profs. T. Foster and J. Geoghegan (Trinity College, Dublin), we studied the molecular mechanism of FnBPA-dependent cell-cell adhesion (**Part II**, **Chapter IV**; **Figure 22**, Herman-Bausier *et al.*, 2015).

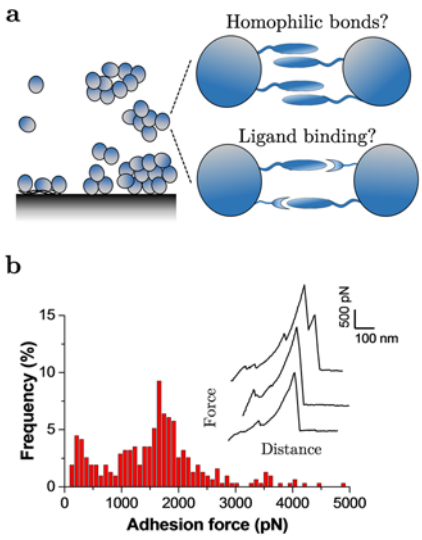

Figure 22: FnBPA mediates cell-cell adhesion trough low affinity, zinc-dependent homophilic bonds.
a. Whether it is achieved by homophilic interactions or by ligand binding on adjacent cells is not yet established.
b. SCFS demonstrates homophilic bonds between FnBPA proteins on opposing cells.
Adapted (from Herman *et al.*, 2015).

We analysed the binding forces of *S. aureus* SH1000 bacteria expressing FnBPA as well as of the recombinant FnBPA A domain immobilized on model surfaces. FnBPA-dependent cell-cell adhesion forces were found to be ~1000 pN and to involve about 10 cumulative homophilic bonds between A domains of FnBPA. Although the structural details of FnBPA homophilic interactions are unclear, we speculate that they occur between residues on the surface of

the N2 or N3 subdomains. Homophilic binding required the presence of zinc, in agreement with earlier studies showing that FnBPs and other staphylococcal adhesins mediate zinc-dependent adhesion (Conrady *et al.*, 2008, Geoghegan *et al.*, 2010, Conrady *et al.*, 2013, Geoghegan *et al.*, 2013). Dynamic SMFS data revealed low affinity homophilic bonds between FnBPA proteins. So, unlike the very strong and stable DLL bonds, homophilic bonds show moderate strength and fast dissociation, a trait which may be important for biofilm dissemination. Low affinity binding by means of FnBPA may represent the primary step in biofilm accumulation, enabling dynamic cell behaviours to occur, while subsequent higher affinity binding would lead to firm cell-cell adhesion

II.4. Unravelling the forces in staphylococcal-fungal co-adhesion

Polymicrobial infections are now recognized with increasing frequency. In these type of infections, the presence of one microbe creates a niche favourable for other microorganisms to generate infections. Polymicrobial infections generally involve the formation of mixed biofilms, *i.e.* attachment of various microbial species to a substrate and to each other (Elias & Banin, 2012). The interactions between bacterial and fungal pathogens are of high clinical importance as they may lead to higher morbidity and mortality (Peleg *et al.*, 2010, Morales & Hogan, 2010). Both species are found in catheter-associated infections and are known to interact when grown together. (Adam *et al.*, 2002). Therefore, knowledge of the molecular mechanisms behind bacterial-fungal co-adhesion is critical to our understanding of mixed infections.

SCFS was used to quantify the forces driving the co-adhesion between *S. epidermidis* and the fungal pathogen *Candida albicans* (**Part II**, **Chapter V**, **Figure 23**, Beaussart *et al.*, 2013b). Using an integrated AFM-inverted optical microscope, a bacterial probe was positioned on top of a fungal cell. Force curves recorded between single bacterial and fungal germ tubes showed large adhesion forces (~5 nN) with extended rupture lengths (up to 500 nm). By contrast, bacteria poorly adhered to yeast cells, emphasizing the important role of the yeast-to-hyphae transition in mediating adhesion to bacterial cells. Analysis of mutant strains altered in cell wall composition showed that bacterial-fungal adhesion involved two types of highly adhesive fungal macromolecules, *i.e.*, Als adhesins and O-mannosylations, which presumably recognize Als ligands and lectins on the bacterial surface. When subjected to mechanical force, the interacting cell surfaces will detach but the cells will remain bridged through these extended polymers.

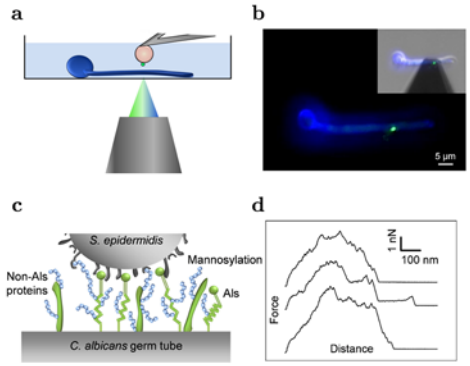

Figure 23: Quantification of the specific forces engaged in bacterial-fungal interactions. **a.** Schematic of the set-up. We used an integrated AFM inverted microscope. **b.** A single *S. epidermidis* cell attached on a colloidal cantilever (green color) is approached toward single *C. albicans* hyphae immobilized on a hydrophobic substrate (blue color). **c.** Key players in the adhesion process are the *C. albicans* cell surface glycoproteins (green) and mannose-rich glycoconjugates (blue). **d.** Typical force-distance curves recorded in buffer between *S. epidermidis* and *C. albicans* hyphae. Adapted from (Beaussart *et al.*, 2013b).

III. Conclusions and perspectives

III.1. Force nanoscopy, a powerful platform in biofilm research

Traditionally, biofilms are studied using molecular biology and genetic approaches, optical and electron microscopy, and microscopic adhesion or biofilm assays. These methods generally probe large ensembles of cells and molecules, and do not provide information on cellular interaction forces. This thesis shows that AFM offers unprecedented opportunities for studying the forces involved in cell adhesion and biofilm formation, down to molecular resolution. In SMFS, force-distance curves are acquired between AFM tips labelled with ligands and cell surfaces in order to detect, localize, and force probe individual receptors (Hinterdorfer and Dufrêne, 2006). Using these single-molecule analyses, we have provided novel molecular insights into the binding strength, affinity and specificity of staphylococcal adhesins. In SCFS, a living cell is attached on the AFM probe and force curves are obtained between the cell probe and a solid substrate or another cell. We implemented a novel, non-destructive SCFS assay enabling the reliable and reproducible analysis of single-bacterial cell adhesion forces (**Appendix I** and **II**). A colloidal silica particle is attached to the end of a tip-less cantilever and coated with a bioinspired polydopamine wet adhesive. The sticky colloidal probe is used to pick up a single live cell. A key asset of the procedure is that it provides excellent control of the cell positioning, thus of the cell-substrate contact area, meaning reliable single-cell analysis is guaranteed. This SCFS assay has enabled the quantification of cell-substrate and cell-cell adhesive forces of staphylococci at the whole cell level. In the future, the AFM toolbox should contribute to the identification of novel binding partners and binding mechanisms in staphylococcal adhesins. It is also hoped that AFM will help design new anti-adhesion drugs to treat microbial infections, including those caused by multidrug-resistant organisms.

III.2. From molecular forces to cellular function

Studying the fundamental interactions involved in staphylococcal adhesion and biofilm formation is an important challenge in current microbiological and medical research. We applied SMFS and SCFS to a variety of bacterial strains, to show the central role of the molecular forces at the cell surface and how they guide cell adhesive functions in staphylococci. Here after we survey the main fundamental achievements of this thesis (see also **Part II, Chapter VI** for a minireview).

III.2.1. Ligand-binding mechanisms of Sdr proteins

We showed that SdrG mediates strong specific binding to Fg, therefore explaining the ability of *S. epidermidis* to firmly attach to Fg-coated surfaces (**Part II**, **Chapter I**, Herman *et al.*, 2014). The adhesion probability increases with interaction time, suggesting that stable cell adhesion requires time-dependent conformational changes. This time dependency is consistent with earlier AFM studies on staphylococcal adhesion. Xu *et al.* showed that the binding strength between FnBPs of *S. aureus* and Fn increases when increasing the interaction to 2 s (Xu *et al.*, 2008). Boks *et al.* reported that adhesion of *S. epidermidis* to hydrophobic and hydrophilic surfaces was time-dependent (Boks *et al.*, 2008).

The strength of single SdrG-Fg bonds, as measured by SMFS, is ~2 nN, thus much larger than that of other cell adhesion proteins, including other MSCRAMMs. Using optical tweezers, Simpson *et al.* showed that the binding forces between *S. aureus* FnBPs and Fn occur as an integer multiple of 20-25 pN (Simpson *et al.*, 2003). Using AFM, the Lower team extensively studied the binding forces of FnBPs from *S. aureus* laboratory strains and clinical isolates (Yongsunthon *et al.*, 2007, Buck *et al.*, 2010, Lower *et al.*, 2011, Casillas-Ituarte *et al.*, 2012) showing that they range between 0.25 and 2.5 nN. However, the 2.5 nN force was attributed to the rupture of 10 parallel Fn-FnBP bonds, consistent with the notion that FnBPs can bind up to nine Fn molecules, and that Fn was attached on the tip at high density. We note that the SdrG-Fg bond is also much stronger than other Fg binding systems. For instance, laser tweezer experiments revealed that the specific binding force between integrin αIIbβ3 and Fg ranges from ~20 to 150 pN (Litvinov *et al.*, 2012).

Dynamic SMFS revealed a low dissociation rate and suggested that the SdrG-Fg bond is stable, thus favouring a dynamic, multistep DLL binding mechanism in which SdrG undergoes conformational changes to form greatly stabilized complexes. Our findings are of biological relevance as they

rationalize the ability of staphylococci to colonize protein-coated biomaterials and to withstand physiological shear forces while being engaged in bacterial-biomaterial interactions.

We also mapped the localization of single SdrG proteins, demonstrating that they form nanoscale domains on the *S. epidermidis* cell surface that are likely to enhance cell adhesive interactions (**Part II**: **Chapter I**, Herman *et al.*, 2014). The heterogeneous distribution of SdrG is also reminiscent of that reported for FnBPs on *S. aureus*. Mapping the surface of *S. aureus* cells attached on solid substrates, revealed that the regions of greatest Fn activity were always along the cell perimeter, suggesting localization of binding proteins between the cells and the substrate (Lower *et al.*, 2010). We expect that clustering of densely packed SdrG adhesins will result in the physical equivalent of multivalency. In a related study, the surface density of SdrG was shown to control the ability of various *S. epidermidis* clinical strains HB, ATCC 35984, and ATCC 12228 to bind to Fg-coated surfaces (**Part II**, **Chapter II**, Vanzieleghem *et al.*, 2015). Strains that show enhanced adhesion towards Fg display increased amounts of SdrG adhesins, suggesting that the abundance of SdrG on the cell surface dramatically improves the ability of the cells to bind to Fg-coated implanted medical devices. These data suggest that *S. epidermidis* has developed a strategy to crowd its surface with SdrG when the bacteria are inside their host. Sellman *et al.*, detected an increase of the transcripts the *sdrG* gene in four methicillin-resistant *S. epidermidis* clinical strains within 60min of a murine infection. The expression of SdrG at the cell surface was confirmed and showed a concomitant increase in protein levels as detected by immunofluorescence microscopy (Sellman *et al.*, 2008). Taken together with the results of this work, it suggests that *S. epidermidis* responds to uncharacterized host environmental signals in order to improve its adhesiveness to surfaces partially coated by Fg, such as indwelling medical devices and host tissues. It is generally admitted that increased adhesion to biomaterials is a key step for *S. epidermidis* to establish in the host in the form of a biofilm, therefore causing chronic infections.

Lastly, we found that SdrF mediates bacterial adhesion to Cn-coated substrates through both weak and strong bonds (**Part II**, **Chapter III**, Herman-Bausier & Dufrêne, 2015). These bonds involve the A and B regions of SdrF, thus revealing that the protein is capable of dual ligand-binding activity. Both weak and strong bonds show high dissociation rates, indicating they are much less stable than those which are formed by the well-characterized DLL mechanism. Collectively, these results show that MSCRAMMs can bind to ligands by mechanisms other that the well-established ones. Staphylococci have the capacity to express a limited

repertoire of CWA surface proteins (Foster *et al.*, 2014). *S. aureus* can express up to 24 CWA proteins but in *S. epidermidis* this is much less (~8). These proteins are exposed to the host and are under strong pressure to support adhesion to the extracellular matrix and to host cells, as well as to help evade innate immune responses. Therefore a single protein may have evolved to bind to more than one ligand and to have more than one function. Different binding mechanisms are also likely. Thus FnBPA and FnBPB A domains can bind to Fg and elastin by the DLL mechanism (Keane *et al.*, 2007). In addition, the A domains can form dimers by homophilic interactions that do not involve DLL. Mutants of FnBPA that lacked the ability to bind Fg by DLL could still form biofilm. Similarly the A domain of SdrC can form dimers and promote biofilm aggregation while N2N3 subdomains of the same A domain are involved in the ligand-binding of the β-neurexin by the DLL mechanism (Barbu *et al.*, 2010, Barbu *et al.*, 2014). So we conclude that SdrF A region binds Cn by a novel mechanism. Hopefully, AFM will greatly contribute to the identification of novel binding partners and binding mechanisms in staphylococcal CWA proteins.

III.2.2.FnBP-mediated homophilic binding

Next, we unravelled the mechanism by which FnBPA mediates *S. aureus* intercellular during biofilm formation (**Part II, Chapter IV**, Herman-Bausier *et al.*, 2015). FnBPA is shown to be responsible for specific cell-cell interactions that involve the FnBPA A domain and cause microscale cell aggregation. The strength of FnBPA-mediated adhesion originates from multiple low-affinity homophilic interactions between FnBPA A domains on neighbouring cells. Although the structural details of FnBPA homophilic interactions are unclear, we speculate that they occur between residues on the surface of the N2 or N3 subdomains. The N2N3 subdomains have also been shown to promote cell-cell interactions (O'Neill *et al.*, 2008, Geoghegan *et al.*, 2013). This suggests that homophilic interactions by these domains could be a general mechanism to promote the accumulation phase in *S. aureus* biofilms. In the case of the serine-aspartate protein SdrC, two amino acid sequences located within the N2 subdomain were found to act cooperatively to promote SdrC dimerization and, as a result, intercellular interactions (Barbu *et al.*, 2014). Whether a similar mechanism applies to FnBPA remains to be determined.

Unlike the very strong and stable DLL bonds, homophilic bonds show moderate strength and fast dissociation, a trait which may be important for biofilm dissemination. Several factors can lead to biofilm detachment, including mechanical stress like fluid flow, and detachment agents like enzymes

or surfactants (Otto, 2008, Otto, 2014). Together with these factors, the fast dissociation of the FnBPA bonds may contribute to cell detachment (isolated cells or cell clusters) therefore favouring colonization of new sites.

Our finding that zinc is required to form homophilic bonds is consistent with earlier reports showing that FnBPA (Geoghegan *et al.*, 2013), but also other staphylococcal adhesins like SasG (Geoghegan *et al.*, 2010) and Aap (Conrady *et al.*, 2008, Conrady *et al.*, 2013) promote zinc-dependent biofilm accumulation. It is therefore tempting to speculate that *S. aureus* has evolved these subdomains to promote homophilic cellular interactions, thus providing a general mechanism to favour biofilm accumulation. The biological significance of the Zn^{2+} dependent cell-cell interactions promoted by FnBPA can be called into question since the concentration of the cation is limiting *in vivo*. The mammalian host restricts access to cations such as Zn^{2+} and Mn^{2+} that bacteria need for growth and proliferation *in vivo*, a phenomenon called nutritional immunity (Becker & Skaar, 2014). An important host factor that contributes to this phenomenon is calprotectin, a Zn^{2+}-binding protein that can reach high levels in infected tissue (Kehl-Fie & Skaar, 2010). However, successful pathogens such as *S. aureus* produce dedicated uptake machinery for cations (Becker & Skaar, 2014). It should be noted that Zn^{2+} is present in the cytosol of mammalian cells and bacteria (Zalewski *et al.*, 2006). *S. aureus* lyses host cells by secreting cytolytic toxins which releases cytoplasmic contents. In addition during biofilm development some of the bacterial cells undergo autolysis to release DNA which is an important component of the biofilm matrix (Rice *et al.*, 2007). This altruistic action will also release bacterial cytoplasmic contents including Zn^{2+}. More than 3% of *E. coli* proteins contain Zn^{2+} (Katayama *et al.*, 2002). The extracellular zinc-dependent metalloprotease aureolysin of *S. aureus* contributes to virulence in mice indicating that it is active *in vivo* and presumably acquires its Zn^{2+} co-factor following secretion (Cassat *et al.*, 2013). We thus argue that the local concentration of Zn^{2+} at the early stages of biofilm development will be sufficient to support FnBP-mediated aggregation. Finally, the expression of FnBPs has been shown to support biofilm formation on subcutaneous catheters during an experimental infections of mice, arguing that adequate Zn^{2+} is likely to be present *in vivo* (Vergara-Irigaray *et al.*, 2009). Overall, our results provide compelling evidence that homophilic interactions play key roles in intercellular interactions during biofilm formation.

III.2.3. Forces driving staphylococcal-fungal adhesion

Co-adhesion between different species is of medical relevance as this leads to mixed biofilm infections with increased mortality and antibiotic resistance. The association of *S. epidermidis* and *C. albicans* is found in catheter-associated infections, but is poorly investigated. We quantified the forces driving the co-adhesion between *S. epidermidis* and the fungal pathogen *C. albicans*. Bacterial-fungal adhesion involved two types of highly adhesive fungal macromolecules, *i.e.*, Als adhesins and O-mannosylations, which presumably recognize Als ligands and lectins on the bacterial surface. Bacterial lectins have roles in mediating interactions with host cells (Lizcano *et al.*, 2012). SraP, a protein with a lectin-like module from *S. aureus* and a family member of glycoproteins found in Gram-positive, interacts with a trisaccharide ligand to mediate adhesion to epithelial cells (Yang *et al.*, 2014). Our finding of strong *S. epidermidis*-*C. albicans* adhesion forces is reminiscent of the well-known *S. aureus*-*C. albicans* interaction (Shirtliff *et al.*, 2009, Peters *et al.*, 2010), thus suggesting that the *S. epidermidis*-*C. albicans* co-adhesion quantified here will favour the formation of mixed biofilms, and in turn promote polymicrobial infections. This study indicates that AFM may become an important tool to understand the molecular bases of polymicrobial interactions. In the bacterial co-adhesion context, Younes *et al.*, measured strong adhesion forces between lactobacilli and virulent *S. aureus* strains, explaining how co-aggregation could eliminate these pathogens (Younes *et al.*, 2012).

III.3. Challenges ahead

Although valuable, our novel SCFS method is rather slow and demanding: AFM cantilever coating to ensure cell stickiness and liveliness on the tip is time-consuming and needs rigorous protocols. To ensure correct positioning of the cell on the tip, a combination of epifluorescence and optical controls are performed. Moreover, during the experiment, the cell can sometimes roll on the bead, leading to force signatures changing and finally the replacement of the cantilever.

Therefore, a major challenge in future biofilm research will be to increase the throughput of single-cell analyses. Classical SCFS methods like ours are based on attaching single cells to AFM cantilever. Consequently, each cell needs a separate cantilever which limits high throughput experiments and statistically significant number of probed cells. A promising approach is the recent fluidic force microscopy (FluidFM) technology which combines with microfluidics (Guillaume-Gentil *et al.*, 2014, Potthoff *et al.*, 2015). Microchanneled cantilevers with nano-sized apertures are used for the fast manipulation of single living cells under physiological conditions. The bacterial immobilization is reversible since it is achieved by underpressure (Potthoff *et al.*, 2015). The hollow cantilever is connected to a pressure controller, enabling its operation in liquid as a force-controlled nanopipette under optical control (**Figure 24,** Guillaume-Gentil *et al.*, 2014**)**.

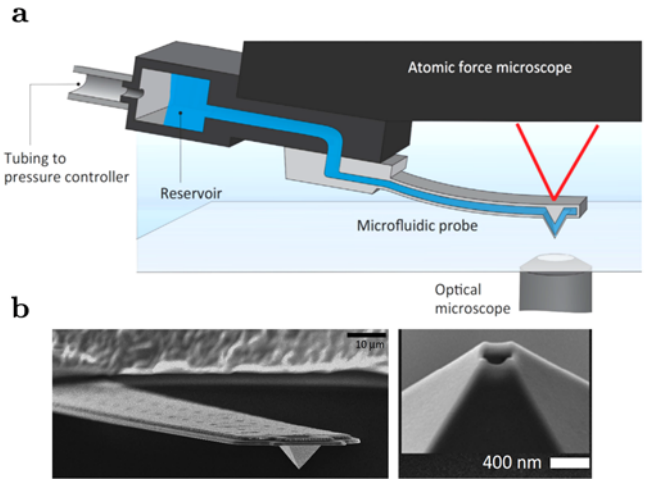

Figure 24: The fluidic force microscopy (FluidFM) technology is a combination of the atomic force microscope and microfluidics.
a. The FluidFM setup. A hollow cantilever is connected to a pressure controller that allows reversible bacterial cell immobilization. The cell targeting is achieved by optical microscopy.
b. Scanning electron microscopy images of microchanneled cantilevers for FluidFM. (Right) Zoomed-in image of the 300 nm aperture of the hollow cantilever. Adapted from (Guillaume-Gentil *et al.*, 2014).

The FluidFM technology do not use chemical agents for cell immobilization. Many cells can be probed in a short time, meaning statistically relevant data sets are obtained within hours (up to 200 cells in a day)(Guillaume-Gentil *et al.*, 2014). Recently, the technique has been applied to bacterial cells and cell-substrate and cell-cell interactions were probed revealing a great potential in biofilms and infection biology studies (Potthoff *et al.*, 2015). However, the possible consequences of the suction force caused by underpressure on the cell are not clear and need to be assessed.

With this novel technique, we could think of new ways to study the adhesion process of bacterial pathogens to substrates and cells. For example, it is known that not every cell will adhere on a substrate (Unpublished observations). Based on this observation made in flow cell experiments, we could combine single-cell force spectroscopy and modified substrates that promote bacterial adherence. Thus, we could study bacteria that are already in a biofilm state, not just in the initial adhesion stage.

The low speed and poor spatial resolution of SMFS-based imaging have limited its use in microbiology. In the future, multiparametric imaging should enable the mapping of the biophysical properties of single bacteria at unprecedented spatiotemporal resolution, and to localize their individual adhesins (Alsteens *et al.*, 2012, Heu *et al.*, 2012, Alsteens *et al.*, 2013, Chopinet *et al.*, 2013, Dufrêne *et al.*, 2013, Formosa-Dague *et al.*, 2015). Force-distance curves are recorded across the cell surface at high frequency, enabling the acquisition of correlated images of the structure, adhesion and mechanics of cells, at much higher speed and spatial resolution than before. In the staphylococcal context, multiparametric imaging was applied to *S. aureus* bacteria expressing the surface protein SasG (Formosa-Dague *et al.*, 2015). Zn^{2+} strongly altered the structural, mechanical and adhesive properties of the cell surface, in that the surface morphology was much smoother, stiffer and stickier when this ion was present. Together with SCFS results, these findings favoured a new model for the zinc-dependent activation of SasG-mediated adhesion: adsorption of zinc ions to cell wall components increases the cohesion of the cell surface, thereby favouring the projection of highly elongated SasG proteins beyond other surface components and making them fully functional for zinc-dependent homophilic interactions.

Clearly, the potential of AFM could be amplified by combining it with optical imaging. Correlated AFM-fluorescence imaging has already been used to study cell surface dynamics during cellular morphogenesis. El-Kirat-Chatel *et al.* followed the various steps of the interaction between fungal pathogens and macrophages (El-Kirat-Chatel & Dufrene, 2012). Using AFM-fluorescence microscopy, Andre *et al.*, studied the distribution of wall teichoic acids (WTAs)

during the cell cycle of *Lactobacillus plantarum* (Andre *et al.,* 2011). Cells showed a heterogeneous distribution of WTAs, important for control of cell shape, elongation and division. An exciting direction is to combine AFM with super-resolution microscopy. In the first such study, correlated single molecule fluorescence and AFM was recently developed for localizing specific proteins within high-resolution AFM images of bacteria (Odermatt *et al.*, 2015).

Another research direction would be to study the role of protein mechanics in cellular adhesion using other-based methods. The mechanics of receptor-ligands interactions regulates molecular forces and have consequences on cellular functions. AFM is able to track protein folding and refolding pathways (Bujalowski & Oberhauser, 2013). By pulling the AFM tip, a stretching force is applied to the protein. At constant velocity, force-extension curves are recorded. For multi-domain proteins the forces curves show typical sawtooth patterns which represent the unfolding of individual domains (Bujalowski & Oberhauser, 2013). The force-clamping mode controls the force applied to the protein by correcting the distance between the tip and the sample allowing to control the end-to-end distance of the protein with a nanometer resolution. When a constant stretching force is applied to a multidomain protein, the domains unfold stochastically in an all-or-none fashion leading to a stepwise increase of the end-to-end length of the protein (Bujalowski & Oberhauser, 2013). Force-clamp AFM is currently used to tackle key problems in biology, linking protein mechanic stability and the kinetics of unfolding/refolding (Ott *et al.*, 2016, Bujalowski & Oberhauser, 2013). By combining our SCFS method with force-clamp we could gain new insights the role of molecular mechanics in bacterial adhesion and pathogenicity. Focusing on the role of major adhesins and using adequate bacterial strains expressing various levels of adhesins, we could investigate the behaviour of the whole bacterial cell towards different substrates such as host proteins, other bacterial cells or host mammalian cells.

From the biological perspective, we anticipate that AFM will greatly contribute to the identification of novel binding partners and binding mechanisms in staphylococcal proteins. As biofilm formation by MRSA strains depends on proteins, AFM offers exciting prospects for the design of drugs or vaccines to inhibit protein-dependent intercellular interactions in MRSA biofilms (Rindi *et al.*, 2006, Provenza *et al.*, 2010, Speziale *et al.*, 2014). Anti-adhesin antibodies are promising candidates since immunization with adhesins induces protection against biofilm development (Stranger-Jones *et al.*, 2006, Otto, 2010). The advantage of anti-adhesive compounds over antibiotics is that

they avoid bacterial adhesion, rather than try to kill bacteria, meaning the development of resistant mutants may be reduced.

Here, we used AFM to study the adhesion process, the first stage of biofilm formation, using planktonic cells grown in rich conditions. So the question arises: how close are we from actual biofilm forming conditions? As a matter of fact, cells in our *in vitro* assays were in the stationary phase, well-fed in rich growth media, centrifuged several times and analysed in buffer. These treatments have consequences on how the bacteria will perceive their surrounding environment and express their surface molecules. Planktonic cells and cells inside a biofilm are physiologically different. It is known that these two types of cells express different molecules from each other. To better mimic biofilm conditions, we could think of applying biofilm-inducing conditions to cells (nutrient depletion, increase of salt concentration, etc.). Then, with an AFM colloidal probe or with the FluidFM, we could pick-up one biofilm-forming cell to study the molecules expressed on its surface.

Another issue is the cell population heterogeneity. Are we sure that all the cells probed by AFM will end-up forming a biofilm, knowing that cells can vary from one population to another, even within a population? When we conducted the experiments with flow chambers, we were able to see that some cells stick on the modified surfaces while the others are flushed by the constant flow. By combining these flow experiments and AFM, we might be able to stick a bacterium that is more likely to form a biofilm, based on the fact that it already adhered on the relevant substrate (see **Part II**, **Chapter II**). This kind of combination could also lead to probe the dynamics of the biofilm. In **Chapter II**, we demonstrated that SdrG plays a key role in mediating staphylococcal adhesion on Fg-coated surfaces, both at the populational and the nanoscale scales. We believe that these kinds of studies are needed to pinpoint key molecular determinants and verify biological relevance of AFM studies.

Another question is the genetic aspects behind staphylococcal biofilms which were not assessed in our experiments. Gene expression patterns are influenced by numerous factors such as the oxygen concentration, the cell density or other chemical gradients. Proteins such as MSCRAMMs, but also toxins or PIA production are regulated by complex pathways. For instance, *fnbA*, the gene coding for FnBPA, or *sdrC*, coding for SdrC, are upregulated during the transition from colonization to early bacteraemia (Jenkins *et al.*, 2015). Moreover, in biofilms, most bacteria do not have a direct contact with the surface (Büttner *et al.*, 2015), meaning gene expression may vary. This

shows that in the future our nanoscale experiments should be combined with genetic studies to get a more realistic view of biofilms.

IV. References

Adam, B., Baillie, G.S. & Douglas, L.J., (2002) Mixed species biofilms of *Candida albicans* and *Staphylococcus epidermidis*. *J. Med. Microbiol.* **51**: 344-349.

Alsteens, D., Dupres, V., Mc Evoy, K., Wildling, L., Gruber, H.J. & Dufrêne, Y.F., (2008) Structure, cell wall elasticity and polysaccharide properties of living yeast cells, as probed by AFM. *Nanotechnology* **19**: 384005.

Alsteens, D., Dupres, V., Yunus, S., Latge, J.P., Heinisch, J.J. & Dufrêne, Y.F., (2012) High-resolution imaging of chemical and biological sites on living cells using peak force tapping atomic force microscopy. *Langmuir* **28**: 16738-16744.

Alsteens, D., Garcia, M.C., Lipke, P.N. & Dufrêne, Y.F., (2010) Force-induced formation and propagation of adhesion nanodomains in living fungal cells. *Proc. Natl. Acad. Sci. USA* **107**: 20744-20749.

Alsteens, D., Trabelsi, H., Soumillion, P. & Dufrêne, Y.F., (2013) Multiparametric atomic force microscopy imaging of single bacteriophages extruding from living bacteria. *Nat. Commun.* **4**: 2926.

Alva-Murillo, N., López-Meza, J.E. & Ochoa-Zarzosa, A., (2014) Nonprofessional Phagocytic Cell Receptors Involved in Staphylococcus aureus Internalization. *BioMed Res. Int.* **2014**: 9.

Andersson, S., Kuttuva Rajarao, G., Land, C.J. & Dalhammar, G., (2008) Biofilm formation and interactions of bacterial strains found in wastewater treatment systems. *FEMS Microbiol. Lett.* **283**: 83-90.

Andre, G., Kulakauskas, S., Chapot-Chartier, M.P., Navet, B., Deghorain, M., Bernard, E.*, et al.*, (2010) Imaging the nanoscale organization of peptidoglycan in living *Lactococcus lactis* cells. *Nat. Commun.* **1**: 27.

Arciola, C.R., Campoccia, D., Ravaioli, S. & Montanaro, L., (2015) Polysaccharide intercellular adhesin in biofilm: structural and regulatory aspects. *Front. Cell. Infect. Microbiol.* **5**: 7.

Arrecubieta, C., Lee, M.H., Macey, A., Foster, T.J. & Lowy, F.D., (2007) SdrF, a *Staphylococcus epidermidis* surface protein, binds type I collagen. *J. Biol. Chem.* **282**: 18767-18776.

Barbu, E.M., Mackenzie, C., Foster, T.J. & Hook, M., (2014) SdrC induces staphylococcal biofilm formation through a homophilic interaction. *Mol. Microbiol.* **94**: 172-185.

Barbu, E.M., Ganesh, V.K., Gurusiddappa, S., Mackenzie, R.C., Foster, T.J., Sudhof, T.C. & Hook, M., (2010) beta-Neurexin is a ligand for the *Staphylococcus aureus* MSCRAMM SdrC. *PLoS Pathog.* **6**: e1000726.

Beaussart, A., Baker, A.E., Kuchma, S.L., El-Kirat-Chatel, S., O'Toole, G.A. & Dufrêne, Y.F., (2014a) Nanoscale adhesion forces of *Pseudomonas aeruginosa* type IV Pili. *ACS Nano* **8**: 10723-10733.

Beaussart, A., El-Kirat-Chatel, S., Herman, P., Alsteens, D., Mahillon, J., Hols, P. & Dufrêne, Y.F., (2013a) Single-cell force spectroscopy of probiotic bacteria. *Biophys. J.* **104**: 1886-1892.

Beaussart, A., El-Kirat-Chatel, S., Sullan, R.M., Alsteens, D., Herman, P., Derclaye, S. & Dufrêne, Y.F., (2014b) Quantifying the forces guiding microbial cell adhesion using single-cell force spectroscopy. *Nat. Protoc.* **9**: 1049-1055.

Beaussart, A., Herman, P., El-Kirat-Chatel, S., Lipke, P.N., Kucharikova, S., Van Dijck, P. & Dufrêne, Y.F., (2013b) Single-cell force spectroscopy of the medically important *Staphylococcus epidermidis-Candida albicans* interaction. *Nanoscale* **5**: 10894-10900.

Beaussart, A., Rolain, T., Duchene, M.C., El-Kirat-Chatel, S., Andre, G., Hols, P. & Dufrêne, Y.F., (2013c) Binding mechanism of the peptidoglycan hydrolase Acm2: low affinity, broad specificity. *Biophys. J.* **105**: 620-629.

Becker, K.W. & Skaar, E.P., (2014) Metal limitation and toxicity at the interface between host and pathogen. *FEMS Microbiol Rev* **38**: 1235-1249.

Becker, K., Heilmann, C. & Peters, G., (2014) Coagulase-Negative Staphylococci. *Clinical microbiology reviews* **27**: 870-926.

Binnig, G., Quate, C.F. & Gerber, C., (1986) Atomic force microscope. *Phys. Rev. Lett.* **56**: 930-933.

Binning, G., Rohrer, H., Gerber, C. & Weibel, E., (1982) Surface studies by scanning tunneling microscopy. *Phys. Rev. Lett.* **49**: 57-61.

Bogino, P.C., Oliva Mde, L., Sorroche, F.G. & Giordano, W., (2013) The role of bacterial biofilms and surface components in plant-bacterial associations. *Int. J. Mol. Sci.* **14**: 15838-15859.

Boks, N.P., Busscher, H.J., van der Mei, H.C. & Norde, W., (2008) Bond-strengthening in staphylococcal adhesion to hydrophilic and hydrophobic surfaces using atomic force microscopy. *Langmuir* **24**: 12990-12994.

Bowden, M.G., Chen, W., Singvall, J., Xu, Y., Peacock, S.J., Valtulina, V., *et al.*, (2005) Identification and preliminary characterization of cell-wall-

anchored proteins of *Staphylococcus epidermidis*. *Microbiology* **151**: 1453-1464.

Bowden, M.G., Heuck, A.P., Ponnuraj, K., Kolosova, E., Choe, D., Gurusiddappa, S., *et al.*, (2008) Evidence for the "dock, lock, and latch" ligand binding mechanism of the staphylococcal microbial surface component recognizing adhesive matrix molecules (MSCRAMM) SdrG. *J. Biol. Chem.* **283**: 638-647.

Buck, A.W., Fowler, V.G., Jr., Yongsunthon, R., Liu, J., DiBartola, A.C., Que, Y.A., *et al.*, (2010) Bonds between fibronectin and fibronectin-binding proteins on *Staphylococcus aureus* and *Lactococcus lactis*. *Langmuir* **26**: 10764-10770.

Bujalowski, P.J. & Oberhauser, A.F., (2013) Tracking unfolding and refolding reactions of single proteins using atomic force microscopy methods. *Methods* **60**: 151-160.

Buttner, H., Mack, D. & Rohde, H., (2015) Structural basis of *Staphylococcus epidermidis* biofilm formation: mechanisms and molecular interactions. *Front. Cell. Infect. Microbiol.* **5**: 14.

Cappella, B., Baschieri, P., Frediani, C., Miccoli, P. & Ascoli, C., (1997) Force-distance curves by AFM. A powerful technique for studying surface interactions. *IEEE Eng Med Biol Mag* **16**: 58-65.

Cappella, B. & Dietler, G., (1999) Force-distance curves by atomic force microscopy. *Surf. Sci. Rep.* **34**: 1-104.

Carvalho, F.A. & Santos, N.C., (2012) Atomic force microscopy-based force spectroscopy--biological and biomedical applications. *IUBMB Life* **64**: 465-472.

Casillas-Ituarte, N.N., Lower, B.H., Lamlertthon, S., Fowler, V.G., Jr. & Lower, S.K., (2012) Dissociation rate constants of human fibronectin binding to fibronectin-binding proteins on living *Staphylococcus aureus* isolated from clinical patients. *J. Biol. Chem.* **287**: 6693-6701.

Cassat, J.E., Hammer, N.D., Campbell, J.P., Benson, M.A., Perrien, D.S., Mrak, L.N., *et al.*, (2013) A secreted bacterial protease tailors the *Staphylococcus aureus* virulence repertoire to modulate bone remodeling during osteomyelitis. *Cell Host Microbe* **13**: 759-772.

Chen, M., Yu, Q., & Sun, H. (2013). Novel strategies for the prevention and treatment of biofilm related infections. *Int. J. Mol. Sci.* **14(9)**, 18488-18501.

Chopinet, L., Formosa, C., Rols, M.P., Duval, R.E. & Dague, E., (2013) Imaging living cells surface and quantifying its properties at high resolution using AFM in QI mode. *Micron* **48**: 26-33.

Conlon, B.P., Nakayasu, E.S., Fleck, L.E., LaFleur, M.D., Isabella, V.M., Coleman, K.*, et al.*, (2013) Killing persister cells and eradicating a biofilm infection by activating the ClpP protease. *Nature* **503**: 365-370.

Conrady, D.G., Brescia, C.C., Horii, K., Weiss, A.A., Hassett, D.J. & Herr, A.B., (2008) A zinc-dependent adhesion module is responsible for intercellular adhesion in staphylococcal biofilms. *Proc. Natl Acad Sci USA* **105**: 19456-19461.

Conrady, D.G., Wilson, J.J. & Herr, A.B., (2013) Structural basis for Zn2+-dependent intercellular adhesion in staphylococcal biofilms. *Proc. Natl Acad Sci USA* **110**: E202-211.

Costerton, J.W., Geesey, G.G. & Cheng, K.J., (1978) How bacteria stick. *Scientific American* **238**: 86-95.

Costerton, J.W., Stewart, P.S. & Greenberg, E.P., (1999) Bacterial biofilms: a common cause of persistent infections. *Science* **284**: 1318-1322.

Dague, E., Alsteens, D., Latge, J.P. & Dufrêne, Y.F., (2008) High-resolution cell surface dynamics of germinating Aspergillus fumigatus conidia. *Biophys. J.* **94**: 656-660.

Darouiche, R.O., (2004) Treatment of infections associated with surgical implants. *N. Engl.J. Med.* **350**: 1422-1429.

de Pablo, P.J. & Carrion-Vazquez, M., (2014) Imaging biological samples with atomic force microscopy. *Cold Spring Harb. Protoc.* **2014**: 167-177.

Decker, R., Burdelski, C., Zobiak, M., Buttner, H., Franke, G., Christner, M.*, et al.*, (2015) An 18 kDa scaffold protein is critical for *Staphylococcus epidermidis* biofilm formation. *PLoS Pathog.* **11**: e1004735.

Donlan, R.M., (2002) Biofilms: microbial life on surfaces. *Emerging infectious diseases* **8**: 881-890.

Dorobantu, L.S., Goss, G.G. & Burrell, R.E., (2012) Atomic force microscopy: a nanoscopic view of microbial cell surfaces. *Micron* **43**: 1312-1322.

Dreyer, D.R., Miller, D.J., Freeman, B.D., Paul, D.R. & Bielawski, C.W., (2012) Elucidating the structure of poly(dopamine). *Langmuir* **28**: 6428-6435.

Ducheyne, P., (2011) *Comprehensive biomaterials.* Elsevier, Amsterdam ; London.

Dufrêne, Y.F., (2001) Application of atomic force microscopy to microbial surfaces: from reconstituted cell surface layers to living cells. *Micron* **32**: 153-165.

Dufrene, Y.F., (2004) Using nanotechniques to explore microbial surfaces. *Nat Rev Micro* **2**: 451-460.

Dufrêne, Y.F., (2008) Towards nanomicrobiology using atomic force microscopy. *Nat. Rev. Microbiol.* **6**: 674-680.

Dufrêne, Y.F., (2014) Atomic force microscopy in microbiology: new structural and functional insights into the microbial cell surface. *mBio* **5**: e01363-01314.

Dufrêne, Y.F., (2015) Sticky microbes: forces in microbial cell adhesion. *Trends Microbiol.* **23**: 376-382.

Dufrêne, Y.F., Martinez-Martin, D., Medalsy, I., Alsteens, D. & Müller, D.J., (2013) Multiparametric imaging of biological systems by force-distance curve-based AFM. *Nat. Methods* **10**: 847-854.

Dunne, W.M., Jr., (2002) Bacterial adhesion: seen any good biofilms lately? *Clin. Microbiol. Rev.* **15**: 155-166.

Dupres, V., Menozzi, F.D., Locht, C., Clare, B.H., Abbott, N.L., Cuenot, S., *et al.*, (2005) Nanoscale mapping and functional analysis of individual adhesins on living bacteria. *Nat. Methods* **2**: 515-520.

Dupres, V., Alsteens, D., Pauwels, K. & Dufrêne, Y.F., (2009) In Vivo Imaging of S-Layer Nanoarrays on *Corynebacterium glutamicum*. *Langmuir* **25**: 9653-9655.

Eaton, P., West, P. & Oxford University Press., (2010) Atomic force microscopy. In. Oxford: Oxford University Press,, pp. 1 online resource, 248 p.

Ebner, A., Wildling, L., Kamruzzahan, A.S., Rankl, C., Wruss, J., Hahn, C.D., *et al.*, (2007) A new, simple method for linking of antibodies to atomic force microscopy tips. *J. Bioconjug. Chem.* **18**: 1176-1184.

Eghiaian, F., Rico, F., Colom, A., Casuso, I. & Scheuring, S., (2014) High-speed atomic force microscopy: imaging and force spectroscopy. *FEBS letters* **588**: 3631-3638.

Elias, S. & Banin, E., (2012) Multi-species biofilms: living with friendly neighbors. *FEMS Microbiol. Rev.* **36**: 990-1004.

El-Kirat-Chatel, S. & Dufrene, Y.F., (2012) Nanoscale imaging of the *Candida*-macrophage interaction using correlated fluorescence-atomic force microscopy. *ACS nano* **6**: 10792-10799.

Flemming, H.C., (2002) Biofouling in water systems--cases, causes and countermeasures. *Appl. Microbiol. Technol.* **59**: 629-640.

Flemming, H.C. & Wingender, J., (2010) The biofilm matrix. *Nat. Rev. Microbiol.* **8**: 623-633.

Formosa-Dague, C., Speziale, P., Foster, T.J., Geoghegan, J.A. & Dufrêne, Y.F., (2015) Zinc-dependent mechanical properties of *Staphylococcus aureus* biofilm-forming surface protein SasG. *Proc. Natl Acad Sci USA* **113**: 410-415.

Foster, T.J., Geoghegan, J.A., Ganesh, V.K. & Hook, M., (2014) Adhesion, invasion and evasion: the many functions of the surface proteins of *Staphylococcus aureus*. *Nat. Rev. Microbiol.* **12**: 49-62.

Foster, T.J. & Geoghegan, J.A., (2015) Chapter 37 - *Staphylococcus aureus*, In: Molecular Medical Microbiology (Second Edition) edited by Tang, Y., Sussman, M., Dongyou, L., Powton, I. & Schwartzman, J. Boston: Academic Press, pp. 655-674.

Francius, G., Domenech, O., Mingeot-Leclercq, M.P. & Dufrêne, Y.F., (2008) Direct observation of *Staphylococcus aureus* cell wall digestion by lysostaphin. *J. Bact.* **190**: 7904-7909.

Frisbie, C.D., Rozsnyai, L.F., Noy, A., Wrighton, M.S. & Lieber, C.M., (1994) Functional group imaging by chemical force microscopy. *Science* **265**: 2071-2074.

Fux, C.A., Costerton, J.W., Stewart, P.S. & Stoodley, P., (2005) Survival strategies of infectious biofilms. *Trend Microbiol.* **13**: 34-40.

Ganesh, V.K., Barbu, E.M., Deivanayagam, C.C., Le, B., Anderson, A.S., Matsuka, Y.V., *et al.*, (2011) Structural and biochemical characterization of *Staphylococcus aureus* clumping factor B/ligand interactions. *J. Biol. Chem.* **286**: 25963-25972.

Garcia, M.C., Lee, J.T., Ramsook, C.B., Alsteens, D., Dufrêne, Y.F. & Lipke, P.N., (2011) A role for amyloid in cell aggregation and biofilm formation. *PloS one* **6**: e17632.

Geoghegan, J.A., Corrigan, R.M., Gruszka, D.T., Speziale, P., O'Gara, J.P., Potts, J.R. & Foster, T.J., (2010) Role of surface protein SasG in biofilm formation by *Staphylococcus aureus*. *J. Bact.* **192**: 5663-5673.

Geoghegan, J.A., Monk, I.R., O'Gara, J.P. & Foster, T.J., (2013) Subdomains N2N3 of fibronectin binding protein A mediate *Staphylococcus aureus* biofilm formation and adherence to fibrinogen using distinct mechanisms. *J. Bacteriol.* **195**: 2675-2683.

Geoghegan, J.A. & Foster, T.J., (2015) Cell Wall-Anchored Surface Proteins of *Staphylococcus aureus*: Many Proteins, Multiple Functions. In: Curr. Top. Microbiol. & Immun. Berlin, Heidelberg: Springer Berlin Heidelberg, pp. 1-26.

Gerber, C. & Lang, H.P., (2006) How the doors to the nanoworld were opened. *Nat. Nanotech.* **1**: 3-5.

Gill, S.R., (2009) Genomics of the staphylococci. In: Staphylococci in Human Disease. Wiley-Blackwell, pp. 19-30.

Goller, C.C. & Romeo, T., (2008) Environmental influences on biofilm development. *Curr. Top Microbiol Immun.* **322**: 37-66.

Gomes, F., Teixeira, P. & Oliveira, R., (2014) Mini-review: *Staphylococcus epidermidis* as the most frequent cause of nosocomial infections: old and new fighting strategies. *Biofouling* **30**: 131-141.

Graham, J.E. & Wilkinson, B.J., (1992) *Staphylococcus aureus* osmoregulation: roles for choline, glycine betaine, proline, and taurine. *J. Bacteriol.* **174**: 2711-2716.

Grigg, J.C., Ukpabi, G., Gaudin, C.F.M. & Murphy, M.E.P., (2010) Structural biology of heme binding in the *Staphylococcus aureus* Isd system. *J. Inorg. Biochem.* **104**: 341-348.

Gross, M., Cramton, S.E., Gotz, F. & Peschel, A., (2001) Key role of teichoic acid net charge in *Staphylococcus aureus* colonization of artificial surfaces. *Infect. Immun.* **69**: 3423-3426.

Gruszka, D.T., Whelan, F., Farrance, O.E., Fung, H.K.H., Paci, E., Jeffries, C.M.*, et al.*, (2015) Cooperative folding of intrinsically disordered domains drives assembly of a strong elongated protein. *Nat. Commun.* **6**.

Guggenberger, C., Wolz, C., Morrissey, J.A. & Heesemann, J., (2012) Two distinct coagulase-dependent barriers protect *Staphylococcus aureus* from neutrophils in a three dimensional *in vitro* infection model. *PLoS Pathog.* **8**: e1002434.

Guillaume-Gentil, O., Potthoff, E., Ossola, D., Franz, C.M., Zambelli, T. & Vorholt, J.A., (2014) Force-controlled manipulation of single cells: from AFM to FluidFM. *Trends Biotechnol.* **32**: 381-388.

Hafner, J.H., Cheung, C.L., Woolley, A.T. & Lieber, C.M., (2001) Structural and functional imaging with carbon nanotube AFM probes. *Prog. Biophys. Mol. Biol.* **77**: 73-110.

Hall-Stoodley, L., Costerton, J.W. & Stoodley, P., (2004) Bacterial biofilms: from the natural environment to infectious diseases. *Nat. Rev. Microbiol.* **2**: 95-108.

Hall-Stoodley, L. & Stoodley, P., (2009) Evolving concepts in biofilm infections. *Cell. Microbiol.* **11**: 1034-1043.

Hartford, O., O'Brien, L., Schofield, K., Wells, J. & Foster, T.J., (2001) The Fbe (SdrG) protein of *Staphylococcus epidermidis* HB promotes bacterial adherence to fibrinogen. *Microbiology* **147**: 2545-2552.

Heilmann, C., (2011) Adhesion mechanisms of staphylococci. *Adv. Exp. Med. Biol.* **715**: 105-123.

Heilmann, C., Hartleib, J., Hussain, M.S. & Peters, G., (2005) The multifunctional *Staphylococcus aureus* autolysin aaa mediates adherence to immobilized fibrinogen and fibronectin. *Infect. Immun.* **73**: 4793-4802.

Heilmann, C., Hussain, M., Peters, G. & Gotz, F., (1997) Evidence for autolysin-mediated primary attachment of *Staphylococcus epidermidis* to a polystyrene surface. *Mol. Mic.* **24**: 1013-1024.

Heinisch, J.J., Lipke, P.N., Beaussart, A., El Kirat Chatel, S., Dupres, V., Alsteens, D. & Dufrêne, Y.F., (2012) Atomic force microscopy - looking at mechanosensors on the cell surface. *J. Cell Sci.* **125**: 4189-4195.

Helenius, J., Heisenberg, C.P., Gaub, H.E. & Müller, D.J., (2008) Single-cell force spectroscopy. *J. Cell Sci.* **121**: 1785-1791.

Herman-Bausier, P. & Dufrêne, Y.F., (2015) Atomic force microscopy reveals a dual collagen-binding activity for the staphylococcal surface protein SdrF. *Mol. Microbiol.* **99**: 611-621.

Herman-Bausier, P., El-Kirat-Chatel, S., Foster, T.J., Geoghegan, J.A. & Dufrêne, Y.F., (2015) *Staphylococcus aureus* Fibronectin-Binding Protein A Mediates Cell-Cell Adhesion through Low-Affinity Homophilic Bonds. *mBio* **6**: e00413-00415.

Herman, P., El-Kirat-Chatel, S., Beaussart, A., Geoghegan, J.A., Foster, T.J. & Dufrêne, Y.F., (2014) The binding force of the staphylococcal adhesin SdrG is remarkably strong. *Mol. Microbiol.* **93**: 356-368.

Herman, P., El-Kirat-Chatel, S., Beaussart, A., Geoghegan, J.A., Vanzieleghem, T., Foster, T.J., *et al.*, (2013) Forces driving the attachment of *Staphylococcus epidermidis* to fibrinogen-coated surfaces. *Langmuir* **29**: 13018-13022.

Herron-Olson, L., Fitzgerald, J.R., Musser, J.M. & Kapur, V., (2007) Molecular correlates of host specialization in *Staphylococcus aureus*. *PloS one* **2**: e1120.

Heu, C., Berquand, A., Elie-Caille, C. & Nicod, L., (2012) Glyphosate-induced stiffening of HaCaT keratinocytes, a Peak Force Tapping study on living cells. *J. Struct. Biol* **178**: 1-7.

Hinterdorfer, P. & Dufrêne, Y.F., (2006) Detection and localization of single molecular recognition events using atomic force microscopy. *Nat Methods* **3**: 347-355.

Hirschhausen, N., Schlesier, T., Schmidt, M.A., Gotz, F., Peters, G. & Heilmann, C., (2010) A novel staphylococcal internalization mechanism involves the major autolysin Atl and heat shock cognate protein Hsc70 as host cell receptor. *Cell. Microbiol.* **12**: 1746-1764.

Igarashi, K., Uchihashi, T., Koivula, A., Wada, M., Kimura, S., Okamoto, T., *et al.*, (2011) Traffic jams reduce hydrolytic efficiency of cellulase on cellulose surface. *Science* **333**: 1279-1282.

Jefferson, K.K., (2004) What drives bacteria to produce a biofilm? *FEMS Microbiol. Lett.* **236**: 163-173.

Jenkins, A., Diep, B.A., Mai, T., Vo, N.H., Warrener, P., Suzich, J., Stover C.K., Sellman B.R., (2015) Differential expression and roles of *Staphylococcus aureus* virulence determinants during colonization and disease. *mBio* **6**: e02272.

Joo, H.S. & Otto, M., (2012) Molecular basis of *in vivo* biofilm formation by bacterial pathogens. *Chem. Biol.* **19**: 1503-1513.

Josefsson, E., McCrea, K.W., Ni Eidhin, D., O'Connell, D., Cox, J., Hook, M. & Foster, T.J., (1998) Three new members of the serine-aspartate repeat protein multigene family of *Staphylococcus aureus*. *Microbiology* **144 (Pt 12)**: 3387-3395.

Kahl, B.C., Belling, G., Reichelt, R., Herrmann, M., Proctor, R.A. & Peters, G., (2003) Thymidine-dependent small-colony variants of *Staphylococcus aureus* exhibit gross morphological and ultrastructural changes consistent with impaired cell separation. *J. Clin. Microbiol.* **41**: 410-413.

Kang, J.W., (2014) Removing environmental organic pollutants with bioremediation and phytoremediation. *Biotechnol. Lett.* **36**: 1129-1139.

Kang, S. & Elimelech, M., (2009) Bioinspired single bacterial cell force spectroscopy. *Langmuir* **25**: 9656-9659.

Katayama, A., Tsujii, A., Wada, A., Nishino, T. & Ishihama, A., (2002) Systematic search for zinc-binding proteins in *Escherichia coli*. *Eur. J. Biochem.* **269**: 2403-2413.

Keane, F.M., Loughman, A., Valtulina, V., Brennan, M., Speziale, P. & Foster, T.J., (2007) Fibrinogen and elastin bind to the same region within the A domain of fibronectin binding protein A, an MSCRAMM of *Staphylococcus aureus*. *Mol. Microbiol.* **63**: 711-723.

Kehl-Fie, T.E. & Skaar, E.P., (2010) Nutritional immunity beyond iron: a role for manganese and zinc. *Curr. Opin. Chem. Biol.* **14**: 218-224.

Kienberger, F., Kada, G., Gruber, H.J., Pastushenko, V.P., Riener, C., Trieb, M.*, et al.*, (2000) Recognition Force Spectroscopy Studies of the NTA-His6 Bond. *Single Molecules* **1**: 59-65.

Khalil, H., Williams, R.J., Stenbeck, G., Henderson, B., Meghji, S. & Nair, S.P., (2007) Invasion of bone cells by *Staphylococcus epidermidis*. *Microb. Infect.* **9**: 460-465.

Kilpatrick, J.I., Revenko, I. & Rodriguez, B.J., (2015) Nanomechanics of Cells and Biomaterials Studied by Atomic Force Microscopy. *Adv. Healthc. Mater.* **4**(16):2456-74.

Kim, H.K., Thammavongsa, V., Schneewind, O. & Missiakas, D., (2012) Recurrent infections and immune evasion strategies of *Staphylococcus aureus*. *Curr. Opin. Microbiol.* **15**: 92-99.

Kobayashi, S.D. & DeLeo, F.R., (2013) *Staphylococcus aureus* Protein A Promotes Immune Suppression. *mBio* **4**: e00764-00713.

Kodera, N., Yamamoto, D., Ishikawa, R. & Ando, T., (2010) Video imaging of walking myosin V by high-speed atomic force microscopy. *Nature* **468**: 72-76.

Kogan, G., Sadovskaya, I., Chaignon, P., Chokr, A. & Jabbouri, S., (2006) Biofilms of clinical strains of *Staphylococcus* that do not contain polysaccharide intercellular adhesin. *FEMS Microbiol. Lett.* **255**: 11-16.

Kohler, T.P., Gisch, N., Binsker, U., Schlag, M., Darm, K., Volker, U.*, et al.*, (2014) Repeating structures of the major staphylococcal autolysin are essential for the interaction with human thrombospondin 1 and vitronectin. *J. Biol. Chem.* **289**: 4070-4082.

Kolter, R. & Greenberg, E.P., (2006) Microbial sciences: the superficial life of microbes. *Nature* **441**: 300-302.

Kostakioti, M., Hadjifrangiskou, M. & Hultgren, S.J., (2013) Bacterial biofilms: development, dispersal, and therapeutic strategies in the dawn of the postantibiotic era. *Cold Spring Harb. Perspect. Med.* **3**: a010306.

Krakauer, T., Pradhan, K. & Stiles, B.G., (2016) Staphylococcal Superantigens Spark Host-Mediated Danger Signals. *Front. Immun.* **7**: 23.

Kurland, N.E., Drira, Z. & Yadavalli, V.K., (2012) Measurement of nanomechanical properties of biomolecules using atomic force microscopy. *Micron* **43**: 116-128.

Laverty, G., Gorman, S.P. & Gilmore, B.F., (2014) Biomolecular Mechanisms of *Pseudomonas aeruginosa* and *Escherichia coli* Biofilm Formation. *Pathogens* **3**: 596-632.

Le, K.Y., Dastgheyb, S., Ho, T.V. & Otto, M., (2014) Molecular determinants of staphylococcal biofilm dispersal and structuring. *Front. Cell. Infet. Immun.* **4**: 167.

Lee, H., Dellatore, S.M., Miller, W.M. & Messersmith, P.B., (2007) Mussel-inspired surface chemistry for multifunctional coatings. *Science* **318**: 426-430.

Lewis, K., (2012) Persister Cells: Molecular Mechanisms Related to Antibiotic Tolerance. In: Antibiotic Resistance. Edited by Coates, R.M.A., Berlin, Heidelberg: Springer Berlin Heidelberg, pp. 121-133.

Litvinov, R.I., Mekler, A., Shuman, H., Bennett, J.S., Barsegov, V. & Weisel, J.W., (2012) Resolving two-dimensional kinetics of the integrin IIβ3-fibrinogen interactions using binding-unbinding correlation spectroscopy. *J. Biol. Chem.* **287**: 35275-35285.

Lizcano, A., Sanchez, C.J. & Orihuela, C.J., (2012) A role for glycosylated serine-rich repeat proteins in Gram-positive bacterial pathogenesis. *Mol. Oral Microbiol.* **27**: 257-269.

Lower, S.K., Lamlertthon, S., Casillas-Ituarte, N.N., Lins, R.D., Yongsunthon, R., Taylor, E.S., *et al.*, (2011) Polymorphisms in fibronectin binding protein A of *Staphylococcus aureus* are associated with infection of cardiovascular devices. *Proc. Natl Acad. Sci. USA.* **108**: 18372-18377.

Lower, S.K., Yongsunthon, R., Casillas-Ituarte, N.N., Taylor, E.S., DiBartola, A.C., Lower, B.H., *et al.*, (2010) A tactile response in *Staphylococcus aureus*. *Biophys. J.* **99**: 2803-2811.

Lowy, F.D., (1998) *Staphylococcus aureus* infections. *N. Engl. J. Med.* **339**: 520-532.

Lynch, A.S. & Robertson, G.T., (2008) Bacterial and fungal biofilm infections. *Annu. Rev. Med.* **59**: 415-428.

Mack, D., Fischer, W., Krokotsch, A., Leopold, K., Hartmann, R., Egge, H. & Laufs, R., (1996) The intercellular adhesin involved in biofilm accumulation of *Staphylococcus epidermidis* is a linear beta-1,6-linked glucosaminoglycan: purification and structural analysis. *J. Bacteriol.* **178**: 175-183.

McCourt, J., O'Halloran, D.P., McCarthy, H., O'Gara, J.P. & Geoghegan, J.A., (2014) Fibronectin-binding proteins are required for biofilm formation by community-associated methicillin-resistant *Staphylococcus aureus* strain LAC. *FEMS Microbiol. Lett.* **353**: 157-164.

McCrea, K.W., Hartford, O., Davis, S., Eidhin, D.N., Lina, G., Speziale, P., *et al.*, (2000) The serine-aspartate repeat (Sdr) protein family in *Staphylococcus epidermidis*. *Microbiology* **146 (Pt 7)**: 1535-1546.

Mishra, D. & Rhee, Y.H., (2014) Microbial leaching of metals from solid industrial wastes. *J. Microbiol.* **52**: 1-7.

Morales, D.K. & Hogan, D.A., (2010) *Candida albicans* interactions with bacteria in the context of human health and disease. *PLoS Pathog.* **6**: e1000886.

Moreno-Herrero, F., Colchero, J., Gomez-Herrero, J. & Baro, A.M., (2004) Atomic force microscopy contact, tapping, and jumping modes for imaging biological samples in liquids. *Phys. Rev. E. Stat. Nonlin. Soft. Matter. Phys.* **69**: 031915.

Müller, D.J. & Dufrêne, Y.F., (2008) Atomic force microscopy as a multifunctional molecular toolbox in nanobiotechnology. *Nature Nanotech.* **3**: 261-269.

Müller, D.J. & Dufrêne, Y.F., (2011) Force nanoscopy of living cells. *Curr. Biol.* **21**: R212-216.

Nilsson, M., Frykberg, L., Flock, J.I., Pei, L., Lindberg, M. & Guss, B., (1998) A fibrinogen-binding protein of *Staphylococcus epidermidis*. *Infect. Immun.* **66**: 2666-2673.

Odermatt, P.D., Shivanandan, A., Deschout, H., Jankele, R., Nievergelt, A.P., Feletti, L.*, et al.*, (2015) High-Resolution Correlative Microscopy: Bridging the Gap between Single Molecule Localization Microscopy and Atomic Force Microscopy. *Nano Letters* **15**: 4896-4904.

O'Neill, E., Pozzi, C., Houston, P., Humphreys, H., Robinson, D.A., Loughman, A.*, et al.*, (2008) A novel *Staphylococcus aureus* biofilm phenotype mediated by the fibronectin-binding proteins, FnBPA and FnBPB. *J. Bacteriol.* **190**: 3835-3850.

Ott, W., Jobst, M.A., Schoeler, C., Gaub, H.E. & Nash, M.A., (2016) Single-molecule force spectroscopy on polyproteins and receptor–ligand complexes: The current toolbox. *J. Struct. Biol.* **In press**.

Otto, M., (2008) Staphylococcal biofilms. *Curr. Top. Microbiol. Immun.* **322**: 207-228.

Otto, M., (2009) *Staphylococcus epidermidis*--the 'accidental' pathogen. *Nat. Rev. Microbiol.* **7**: 555-567.

Otto, M., (2010) Novel targeted immunotherapy approaches for staphylococcal infection. *Expert. Opin. Biol. Ther.* **10**: 1049-1059.

Otto, M., (2013) Staphylococcal infections: mechanisms of biofilm maturation and detachment as critical determinants of pathogenicity. *Annu; Rev; Med.* **64**: 175-188.

Otto, M., (2014) Physical stress and bacterial colonization. *FEMS Microbiol. Rev.* **38**: 1250-1270.

Peleg, A.Y., Hogan, D.A. & Mylonakis, E., (2010) Medically important bacterial-fungal interactions. *Nat. Rev. Microbiol.* **8**: 340-349.

Percival, S., Malic, S., Cruz, H. & Williams, D., (2011) Introduction to Biofilms. In: Biofilms and Veterinary Medicine. S. Percival, D. Knottenbelt & C. Cochrane (eds). Springer Berlin Heidelberg, pp. 41-68.

Peters, B.M., Jabra-Rizk, M.A., Scheper, M.A., Leid, J.G., Costerton, J.W. & Shirtliff, M.E., (2010) Microbial interactions and differential protein expression in *Staphylococcus aureus -Candida albicans* dual-species biofilms. *FEMS Immun. Med. Microbiol.* **59**: 493-503.

Ponnuraj, K., Bowden, M.G., Davis, S., Gurusiddappa, S., Moore, D., Choe, D., *et al.*, (2003) A "dock, lock, and latch" structural model for a staphylococcal adhesin binding to fibrinogen. *Cell* **115**: 217-228.

Potthoff, E., Ossola, D., Zambelli, T. & Vorholt, J.A., (2015) Bacterial adhesion force quantification by fluidic force microscopy. *Nanoscale* **7**: 4070-4079.

Provenza, G., Provenzano, M., Visai, L., Burke, F.M., Geoghegan, J.A., Stravalaci, M., *et al.*, (2010) Functional analysis of a murine monoclonal antibody against the repetitive region of the fibronectin-binding adhesins fibronectin-binding protein A and fibronectin-binding protein B from *Staphylococcus aureus*. *FEBS J.* **277**: 4490-4505.

Rakić, A.D., Djurišić, A.B., Elazar, J.M. & Majewski, M.L., (1998) Optical properties of metallic films for vertical-cavity optoelectronic devices. *Appl. Opt.* **37**: 5271-5283.

Rice, K.C., Mann, E.E., Endres, J.L., Weiss, E.C., Cassat, J.E., Smeltzer, M.S. & Bayles, K.W., (2007) The cidA murein hydrolase regulator contributes to DNA release and biofilm development in *Staphylococcus aureus*. *Proc. Natl. Acad. Sci. USA.* **104**: 8113-8118.

Richards, A.M., Von Dwingelo, J.E., Price, C.T. & Abu Kwaik, Y., (2013) Cellular microbiology and molecular ecology of *Legionella*–amoeba interaction. *Virulence* **4**: 307-314.

Rindi, S., Cicalini, S., Pietrocola, G., Venditti, M., Festa, A., Foster, T.J., *et al.*, (2006) Antibody response in patients with endocarditis caused by *Staphylococcus aureus*. *Eur. J. Clin. Invest.* **36**: 536-543.

Rohde, H., Burdelski, C., Bartscht, K., Hussain, M., Buck, F., Horstkotte, M.A., *et al.*, (2005) Induction of *Staphylococcus epidermidis* biofilm formation via proteolytic processing of the accumulation-associated protein by staphylococcal and host proteases. *Mol. Microbiol.* **55**: 1883-1895.

Rohde, H., Kalitzky, M., Kroger, N., Scherpe, S., Horstkotte, M.A., Knobloch, J.K., *et al.*, (2004) Detection of virulence-associated genes not useful for discriminating between invasive and commensal *Staphylococcus epidermidis* strains from a bone marrow transplant unit. *J. Clin. Microbiol.* **42**: 5614-5619.

Rosenstein, R. & Gotz, F., (2013) What distinguishes highly pathogenic staphylococci from medium- and non-pathogenic? *Curr. Topics Microbiol. Immun.* **358**: 33-89.

Schaffner, F., Ray, A.M. & Dontenwill, M., (2013) Integrin α5β1, the Fibronectin Receptor, as a Pertinent Therapeutic Target in Solid Tumors. *Cancers* **5**: 27-47.

Schaeffer, C.R., Woods, K.M., Longo, G.M., Kiedrowski, M.R., Paharik, A.E., Buttner, H.*, et al.*, (2015) Accumulation-associated protein enhances *Staphylococcus epidermidis* biofilm formation under dynamic conditions and is required for infection in a rat catheter model. *Infect. Immun.* **83**: 214-226.

Sellman, B.R., Timofeyeva, Y., Nanra, J., Scott, A., Fulginiti, J.P., Matsuka, Y.V. & Baker, S.M., (2008) Expression of *Staphylococcus epidermidis* SdrG Increases following Exposure to an In Vivo Environment. *Infect Immun.* **76**: 2950-2957.

Shirtliff, M.E., Peters, B.M. & Jabra-Rizk, M.A., (2009) Cross-kingdom interactions: *Candida albicans* and bacteria. *FEMS Microbiol. Lett.* **299**: 1-8.

Simpson, K.H., Bowden, G., Hook, M. & Anvari, B., (2003) Measurement of adhesive forces between individual *Staphylococcus aureus* MSCRAMMs and protein-coated surfaces by use of optical tweezers. *J. Bact.* **185**: 2031-2035.

Smeltzer, M.S., Lee, C.Y., Harik, N. & Hart, M.E., (2009) Molecular Basis of Pathogenicity. In: Staphylococci in Human Disease. Wiley-Blackwell, pp. 65-108.

Sokolov, I., Dokukin, M.E. & Guz, N.V., (2013) Method for quantitative measurements of the elastic modulus of biological cells in AFM indentation experiments. *Methods* **60**: 202-213.

Somerville, G.A. & Proctor, R.A., (2009) The Biology of Staphylococci. In: Staphylococci in Human Disease. Wiley-Blackwell, pp. 1-18.

Speziale, P., Pietrocola, G., Foster, T.J. & Geoghegan, J.A., (2014) Protein-based biofilm matrices in Staphylococci. *Front. Cell. Infect. Microbiol.* **4**: 171.

Spiliopoulou, A.I., Krevvata, M.I., Kolonitsiou, F., Harris, L.G., Wilkinson, T.S., Davies, A.P.*, et al.*, (2012) An extracellular *Staphylococcus epidermidis* polysaccharide: relation to Polysaccharide Intercellular Adhesin and its implication in phagocytosis. *BMC Microbiol.* **12**: 76.

Stranger-Jones, Y.K., Bae, T. & Schneewind, O., (2006) Vaccine assembly from surface proteins of Staphylococcus aureus. *Proc. Natl. Acad. Sci. USA* **103**: 16942-16947.

Thompson, K. M., & Jefferson, K. K. (2009). Adaptation to stress: Biofilms and small-colony variants. Staphylococci *in human disease: Second edition* (pp. 109-124) doi:10.1002/9781444308464.ch5

Tormo, M.A., Knecht, E., Gotz, F., Lasa, I. & Penades, J.R., (2005) Bap-dependent biofilm formation by pathogenic species of *Staphylococcus*: evidence of horizontal gene transfer? *Microbiology* **151**: 2465-2475.

Uckay, I., Pittet, D., Vaudaux, P., Sax, H., Lew, D. & Waldvogel, F., (2009) Foreign body infections due to *Staphylococcus epidermidis*. *Ann. Med.* **41**: 109-119.

Vanzieleghem, T., Herman-Bausier, P., Dufrêne, Y.F. & Mahillon, J., (2015) *Staphylococcus epidermidis* Affinity for Fibrinogen-Coated Surfaces Correlates with the Abundance of the SdrG Adhesin on the Cell Surface. *Langmuir* **31**: 4713-4721.

Vergara-Irigaray, M., Valle, J., Merino, N., Latasa, C., Garcia, B., Ruiz de Los Mozos, I.*, et al.*, (2009) Relevant role of fibronectin-binding proteins in *Staphylococcus aureus* biofilm-associated foreign-body infections. *Infect. Immun.* **77**: 3978-3991.

Villareal, V.A., Pilpa, R.M., Robson, S.A., Fadeev, E.A. & Clubb, R.T., (2008) The IsdC Protein from Staphylococcus aureus Uses a Flexible Binding Pocket to Capture Heme. *J. Biol. Chem.* **283**: 31591-31600.

Wang, B. & Muir, Tom W., (2016) Regulation of Virulence in *Staphylococcus aureus:* Molecular Mechanisms and Remaining Puzzles. Cell Chemical Biology 23: 214-224.

Wildling, L., Unterauer, B., Zhu, R., Rupprecht, A., Haselgrubler, T., Rankl, C.*, et al.*, (2011) Linking of sensor molecules with amino groups to amino-functionalized AFM tips. *Bioconjug Chem* **22**: 1239-1248.

Wu, H., Moser, C., Wang, H.Z., Hoiby, N. & Song, Z.J., (2015) Strategies for combating bacterial biofilm infections. *Int. J. Oral Sci.* **7**: 1-7.

Yongsunthon, R., Fowler, V.G., Jr., Lower, B.H., Vellano, F.P., 3rd, Alexander, E., Reller, L.B.*, et al.*, (2007) Correlation between fundamental binding forces and clinical prognosis of *Staphylococcus aureus* infections of medical implants. *Langmuir* **23**: 2289-2292.

Younes, J.A., van der Mei, H.C., van den Heuvel, E., Busscher, H.J. & Reid, G., (2012) Adhesion forces and coaggregation between vaginal staphylococci and lactobacilli. *PloS one* **7**: e36917.

Yang, Y.H., Jiang, Y.L., Zhang, J., Wang, L., Bai, X.H., Zhang, S.J., et al., (2014) Structural insights into SraP-mediated *Staphylococcus aureus* adhesion to host cells. *PLoS Pathog.* **10**: e1004169.

Zalewski, P., Truong-Tran, A., Lincoln, S., Ward, D., Shankar, A., Coyle, P.*, et al.*, (2006) Use of a zinc fluorophore to measure labile pools of zinc in body fluids and cell-conditioned media. *Biotechniques* **40**: 509-520.

Zobell, C.E. & Mathews, H.M., (1936) A Qualitative Study of the Bacterial Flora of Sea and Land Breezes. *Proc. Natl. Acad. Sci. USA.* **22**: 567-572.

Zong, Y., Xu, Y., Liang, X., Keene, D.R., Hook, A., Gurusiddappa, S.*, et al.*, (2005) A 'Collagen Hug' model for *Staphylococcus aureus* CNA binding to collagen. *EMBO J.* **24**: 4224-4236.

Part II

Detailed presentation of the thesis

Chapter I

The binding force of the staphylococcal adhesin SdrG is remarkably strong

Philippe Herman, Sofiane El-Kirat-Chatel, Audrey Beaussart, Joan A. Geoghegan, Timothy J. Foster, and Yves F. Dufrêne
P.H. and S.E-K-C. contributed equally to this article

In *Molecular Microbiology,* **2014**, 93, 356-368.

My personal contribution to this work was to perform the research and wrote the paper.
S. E-K-C., helped with some experiments and biological interpretation.

Summary

SdrG is a cell surface adhesin from *Staphylococcus epidermidis* which binds to the blood plasma protein fibrinogen (Fg). Ligand binding follows a 'dock, lock and latch' model involving dynamic conformational changes of the adhesin that result in a greatly stabilized adhesin-ligand complex. To date, the force and dynamics of this multistep interaction are poorly understood. Here we use atomic force microscopy (AFM) to unravel the binding strength and cell surface localization of SdrG at molecular resolution. Single-cell force spectroscopy shows that SdrG mediates time-dependent attachment to Fg-coated surfaces. Single-molecule force spectroscopy with Fg-coated AFM tips demonstrates that the adhesin forms nanoscale domains on the cell surface, which we believe contribute to strengthen cell adhesion. Notably, we find that the rupture force of single SdrG-Fg bonds is very large, ~2 nN, equivalent to the strength of a covalent bond, and shows a low dissociation rate, suggesting that the bond is very stable. The strong binding force, slow dissociation and clustering of SdrG provide a molecular foundation for the ability of *S. epidermidis* to colonize implanted biomaterials and to withstand physiological shear forces.

Introduction

The Gram positive bacterium *Staphylococcus epidermidis* is a common colonizer of the human skin which represents the most common source of infection of medical indwelling devices such as catheters and prostheses (Otto, 2009, Mack, 1999). Survival of *S. epidermidis* in the host relies on its ability to attach to surfaces and form biofilms via a family of adhesion proteins, the Microbial Surface Components Recognizing Adhesive Matrix Molecules (MSCRAMMs) that target host extracellular proteins such as albumin, fibronectin and fibrinogen (Foster *et al.*, 2014, Otto, 2009) . Despite the vast amount of structural and biochemical data available on *S. epidermidis* adhesion molecules, little is known about the fundamental forces by which these adhesins drive bacterial adhesion.

The serine-aspartate repeat (Sdr) protein family is a widely investigated group of MSCRAMMs (Josefsson *et al.*, 1998, McCrea *et al.*, 2000, Foster *et al.*, 2014). Among these, SdrG is encoded by the *fbe* gene in the chromosomal DNA of *S. epidermidis* which specifically targets fibrinogen (Fg) (Nilsson *et al.*, 1998). SdrG contains five distinct regions: a secretion signal sequence, the A region containing the Fg binding activity, the B region of unknown function, the R region containing serine-aspartate repeats sequences, and at the C-terminal region, the sorting signal that is implicated in the anchorage of the protein to cell wall peptidoglycan (Hartford *et al.*, 2001, Foster *et al.*, 2014; **Figure 1A**). The adhesin specifically binds to a peptide sequence of 14 amino acids found in the N-terminus of the β-chain of Fg (Ponnuraj *et al.*, 2003). This interaction is believed to play an important role in *S. epidermidis* infections as it mediates attachment of the pathogen to Fg-coated biomaterials. The SdrG binding site is a cleft of approximately 30 Å in length between the N2 and N3 subdomains located in the A region of the protein. Once the ligand peptide is docked and stabilized by hydrophobic interactions and hydrogen bonds, a C-terminus extension of N3 subdomain folds over the ligand to insert and complement a β-sheet in the N2 subdomain (Ponnuraj *et al.*, 2003, Bowden *et al.*, 2008, Foster *et al.*, 2014; **Figure 2A**). This 'dock, lock and latch' mechanism thus greatly stabilizes the conformation of the SdrG-ligand complex.

Atomic force microscopy (AFM) is being increasingly used to explore the molecular mechanisms of cell adhesion (Fritz *et al.*, 1998, Baumgartner *et al.*, 2000, Dupres *et al.*, 2005, Helenius *et al.*, 2008, Müller *et al.*, 2009, Alsteens *et al.*, 2010) including staphylococcal adhesion (Emerson *et al.*, 2006, Boks *et al.*, 2008, Liu *et al.*, 2008, Xu *et al.*, 2008, Buck *et al.*, 2010, Lower *et al.*, 2010). Here, single-cell and single-molecule AFM techniques are used to investigate

the binding strength and cell surface localization of SdrG, both in *S. epidermidis* HB and in a *Lactococcus lactis* strain expressing SdrG (hereafter *L. lactis* SdrG$^{(+)}$; (Hartford *et al.*, 2001). This latter organism enables us to study SdrG-Fg interactions in the absence of other staphylococcal components. We show that the adhesin mediates strong attachment of the bacteria to Fg-coated surfaces. SdrG accumulates at the cell surface in the form of nanoscale domains, and shows strong binding strength and low dissociation rate, thus contributing to strengthen adhesion of the pathogen.

Results and Discussion

SdrG mediates bacterial adhesion to Fg-coated surfaces

We first studied the role of SdrG in the attachment of bacterial cells to Fg-coated surfaces using two complementary adhesion assays (**Figure 1**). We compared the behaviour of the wild-type (WT) *S. epidermidis* HB strain with that of a SdrG$^{(-)}$ mutant in which SdrG is lacking because of *fbe* gene disruption. Optical microscopy images revealed that SdrG promotes bacterial adhesion to Fg since *S. epidermidis* HB cells covered 22 ± 3 % of the surface (**Figure 1B**), whereas SdrG$^{(-)}$ mutant cells hardly adhered (<1 % coverage; **Figure 1C**). Strikingly, *L. lactis* SdrG$^{(+)}$ cells formed a dense monolayer covering 87 ± 0.6 % of the surface (**Figure 1D**), whereas cells from a *L. lactis* strain carrying an empty vector (EV) lacking the SdrG gene did not adhere (<1 %; **Figure 1E**). Similar adhesion phenotypes were observed using crystal violet assays (**Figure 1F**): *L. lactis* SdrG$^{(+)}$ adhered strongly to Fg, while the EV strain did not adhere at all. Adherence of wild type *S. epidermidis* HB was considerably weaker than for *L. lactis* SdrG$^{(+)}$. The *S. epidermidis* HB SdrG$^{(-)}$ mutant lacked the ability to adhere, indicating that the level of adherence observed for the wild type can be attributed entirely to SdrG. These observations demonstrate that SdrG mediates bacterial adhesion to Fg, and strongly suggest that *L. lactis* cells containing the *fbe* gene expresses higher levels of SdrG than *S. epidermidis* HB, and/or that the orientation/conformation of the adhesins is different.

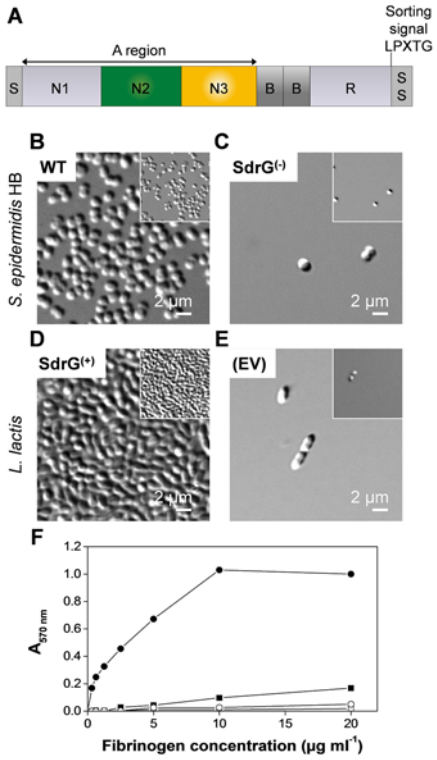

Figure 1: Bacterial adherence to fibrinogen.
A. Schematic representation of the *S. epidermidis* SdrG molecule: S, secretion signal sequence; A, N-terminal Fg-binding region; N1, subdomain frequently cleaved proteolytically; N2-N3, minimum Fg-binding region; B, repeat of unknown function; R, serine-aspartate repeat region; C-terminus region implicated in the anchorage of the protein.
B-E. Optical microscopy (DIC) images showing microscopic adhesion behaviours towards Fg-coated substrates for (B) *S. epidermidis* HB, (C) the *S. epidermidis* mutant impaired in SdrG expression (SdrG$^{(-)}$), (D) the *L. lactis* strain expressing SdrG (*L. lactis* SdrG$^{(+)}$), and (E) the *L. lactis* empty vector strain lacking SdrG (EV). Insets are representative images from a duplicate experiment.
F. Crystal violet assay. Cell suspensions of *S. epidermidis* HB (■), *S. epidermidis* SdrG$^{(-)}$ (□), *L. lactis* SdrG$^{(+)}$ (●) and *L. lactis* EV (○) were added to wells coated with Fg. Adherent cells were stained with crystal violet and the absorbance was read at 570 nm. Data shown are representative of two independent experiments.

Single-cell and single-molecule measurements

To investigate SdrG-Fg interactions, we used two complementary AFM modalities (**Figure 2**). Single-cell force spectroscopy (SCFS) (Helenius *et al.*, 2008, Müller *et al.*, 2009, Beaussart *et al.*, 2013a, Beaussart *et al.*, 2013b, Sullan *et al.*, 2013) enabled us to quantify the SdrG-Fg binding forces at the whole cell level. To this end, single-bacterial cells were picked up with colloidal probe cantilevers coated with polydopamine (**Figure 2A**). Labelling of the attached cells with the *Bac*light LIVE/DEAD stain demonstrated that the cell membrane was still intact, thus that the method is non-destructive (**Figure 2B**, green color). Force-distance curves were then recorded between the cellular probes and Fg-coated substrates to measure the SdrG-Fg binding forces. We note that force measurements using either stained or non-stained cells gave the same results, suggesting that labelling does not alter the properties of the outer cell surface. Using single-molecule force spectroscopy (SMFS) (Dupres *et al.*, 2005, Hinterdorfer & Dufrêne, 2006, Dupres *et al.*, 2009, Alsteens *et al.*, 2010, Andre *et al.*, 2010, El-Kirat-Chatel *et al.*, 2014) with AFM tips functionalized with Fg molecules, we also mapped and force probed single SdrG molecules on the surface of single bacterial cells (**Figure 2C**). To ensure single-adhesin detection, the tip was functionalized with a PEG-benzaldehyde

linker using a well-established protocol (Ebner *et al.*, 2007). Spatially-resolved SMFS of live cells immobilized on porous membranes (**Figure 2D**) allowed us to directly measure the localization and binding strength of single adhesins.

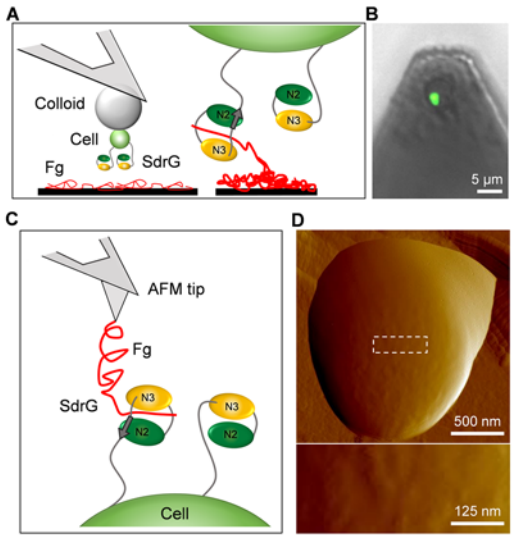

Figure 2: Single-cell and single-molecule analysis of the SdrG-Fg interaction.
A. For single-cell force spectroscopy, living bacteria were attached on polydopamine-coated colloidal probes, enabling us to measure the adhesion forces between an individual bacterium and Fg-coated substrates. The arrow across the N2 domain indicates the -strand complementation that has occurred after ligand binding. The cartoon is not to scale.
B. Optical microscope image of single bacteria attached to the colloidal cantilever probe showing that the cells were properly located and alive (green color).
C. For single-molecule force spectroscopy, AFM tips were functionalized with Fg molecules, enabling us to measure the localization and adhesion of single adhesins on the surface of living bacteria.
D. Low (top) and high (bottom) magnification AFM deflection images of a single *S. epidermidis* HB bacterium trapped into a pore of a porous polymer membrane.

Single-cell analysis demonstrates strong SdrG-Fg interactions

We measured the binding forces between *S. epidermidis* HB cells and Fg-surfaces using SCFS (**Figure 3** and **Figure S1**). **Figure 3A** and **S1A** show the adhesion force and rupture length histograms, together with representative force curves, obtained at short contact time (100 ms) for 10 different WT cells, including cells from independent cultures. A large fraction of the curves showed well-defined, single or multiple force peaks of 2098 ± 157 pN magnitude (mean value obtained from Gaussian fits of the force distributions of 10 different cells; total number of force curves n = 5123), and 50-500 nm rupture lengths that we attribute to SdrG-Fg adhesive interactions for reasons explained below. The characteristics of the curves did not substantially change when recording consecutive force curves on different spots of the substrate, meaning that force measurements did not alter the cell surface properties. Cells from different cultures generally yielded similar behaviour, with the same maximum adhesion force at ~2.1 nN, indicating homogeneity and reproducibility of the cell populations (**Figure S1A**). Yet, a few cells also showed greater adhesion

values in addition to these ~2.1 nN forces (**Figure S1A**), suggesting that multiple interactions were probed in parallel.

Control experiments were performed to assess whether the measured forces were specific to the SdrG-Fg interaction, *i.e.* blocking with free Fg and use of a the SdrG$^{(-)}$ mutant in which the *fbe* gene was disrupted. **Figure 3C** presents the results of a blocking experiment with free Fg, *i.e.* the classical control in AFM molecular recognition studies. As can be seen, this treatment led to a major reduction of adhesion frequency (from 86 % to 26 %; cell #3), indicating that a large fraction of the binding events indeed reflected rupture of SdrG-Fg bonds. Supporting further this view, **Figure 3E** shows that the SdrG$^{(-)}$ strain did not bind at all to Fg. Lastly, we also showed that the forces obtained with *S. epidermidis* HB cell probes were very different from those recorded with polydopamine-coated probes, the latter showing poorly defined force signatures with smaller adhesion forces (**Figure S2**). This indicates that bacteria were well-centred on the probe, thus enabling direct and reproducible cell-substrate contacts, and that they remained tightly immobilized on the probe through the force measurements. All together, these findings lead us to believe that the ~2.1 nN adhesion forces reflect specific SdrG-Fg bonds.

The adhesion of animal cells is known to strengthen with the interaction time due to the increase of receptor-ligand pairs anchoring the cell to the substrate (Helenius *et al.*, 2008). To demonstrate whether this applies to the SdrG-Fg interaction, we measured the adhesion forces between *S. epidermidis* HB and Fg surfaces using a contact time of 1 s. **Figure 3B** and **S1B** show that increasing the contact time generally increased the adhesion frequency (e.g. from ~50 to 85-95 % for cells #1 and #2 in **Figure 3B**), suggesting that the probability to form SdrG-Fg bonds increases with interaction time. Interestingly, the maximum adhesion force remained essentially unchanged, 2128 ± 149 pN magnitude (n = 6613 force curves from 10 different cells), but forces in the 2500-5000 pN range were observed more frequently, suggesting a slight increase in the number of multiple interactions with time. At 1 s interaction time, blocking with free Fg had only a moderate effect on the adhesion frequency (from 86 % to 68 %; cell #3; **Figure 3D**), compared to the strong effect seen at short contact time (from 86 % to 26 %; cell #3; **Figure 3C**). This suggests that with time, Fg molecules blocking the cell surface are being displaced by Fg molecules on the substrate. Use of the SdrG$^{(-)}$ mutant strain led to a substantial decrease of adhesion frequency, confirming the specificity of the measurements (**Figure 3F**). Our data are also consistent with earlier AFM studies on staphylococcal adhesion. Xu *et al.* showed that the binding strength between fibronectin-binding proteins (FnBPs) of *S. aureus* and fibronectin (Fn) increases when increasing the interaction to 2 s

(Xu *et al.*, 2008). Boks *et al.* reported that adhesion of *S. epidermidis* to hydrophobic and hydrophilic surfaces was time-dependent (Boks *et al.*, 2008). The time-dependency observed here for SdrG agrees well with the dynamic, multistep nature of the "dock, lock and latch model". This model involves the docking of the ligand in a binding trench formed between two SdrG subdomains followed by the movement of a C-terminal extension of one subdomain to cover the ligand and to insert and complement a β-sheet in a neighbouring subdomain (Bowden *et al.*, 2008; **Figure 2A**). These structural changes are believed to increase greatly the stability of the closed conformation of the adhesin-ligand complex. Hence, we expect that increased contact time will favour optimal fitting of the interacting molecules, leading to stabilized closed conformations.

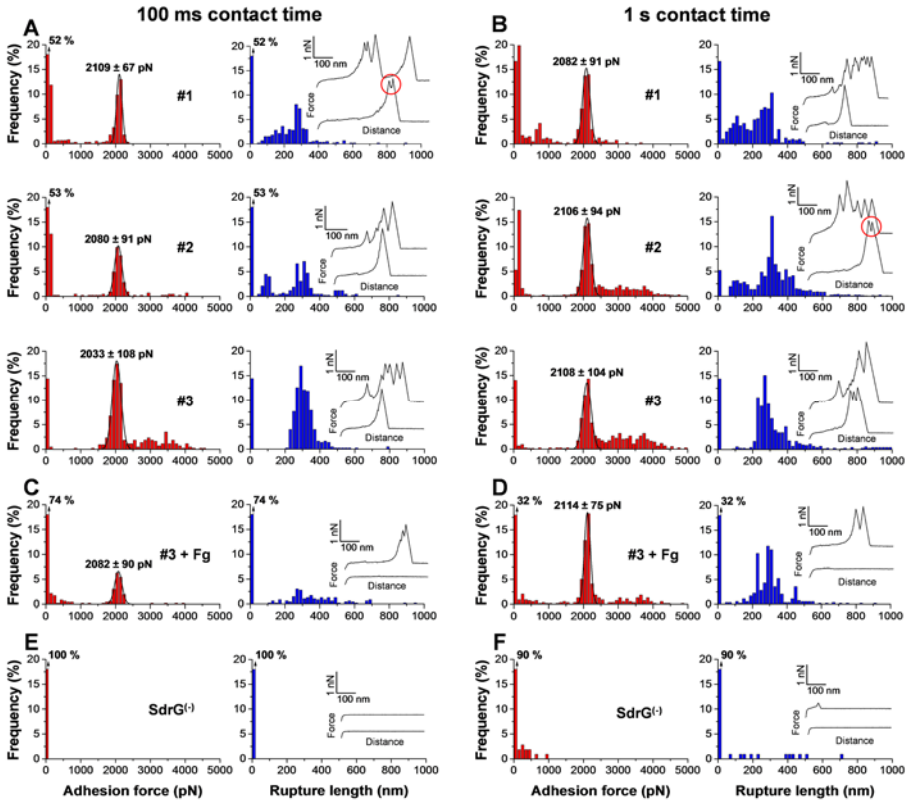

Figure 3: Single-cell analysis demonstrates that SdrG mediates attachment of *S. epidermidis* HB to Fg surfaces.
A and B. Adhesion force (red) and rupture length (blue) histograms, as well as representative retraction force curves (insets), obtained by recording multiple force curves in buffer at short contact time (100 ms, **A**) or prolonged contact time (1 s, **B**) between single *S. epidermidis* HB cells and Fg-substrates. Adhesion and rupture length histograms were generated by considering, for every force curve, the maximum adhesion force and the rupture length of the last peak, respectively. Red circles on the curves indicate double force peak signatures. Results from three cells from independent cultures are shown (n > 400 force-distances curves for each cell). All curves were obtained using a maximum applied force of 250 pN, and approach and retraction speeds of 1 µm s^{-1}. Data obtained for 10 different cells are shown in **Figure S1**.
C and D. Force data obtained by recording multiple force curves in buffer at short contact time (100 ms, C) or prolonged contact time (1 s, **D**) between a single *S. epidermidis* HB cell (cell 3) and Fg-substrates in the presence of free Fg (0.2 mg ml^{-1}). Similar data were obtained in at least two independent experiments (Figure S1).
E and F. Force data obtained by recording multiple force curves in buffer at short contact time (100 ms, **E**) or prolonged contact time (1 s, **F**) between a *S. epidermidis* mutant cell impaired in SdrG expression ($SdrG^{(-)}$) and Fg-substrates. Similar data were obtained in at least two independent experiments.

One may argue that the various constituents of the *S. epidermidis* HB cell wall, including other adhesins, may contribute to the measured forces. To investigate SdrG interactions in the absence of other staphylococcal components, we therefore probed the *L. lactis* SdrG$^{(+)}$ strain that expresses SdrG, an approach that has already been used for studying FnBPs-Fn binding forces (Buck *et al.*, 2010). As shown in **Figure 4A** and **S3A**, *L. lactis* SdrG$^{(+)}$ cells showed adhesive events with force signatures similar to those observed for *S. epidermidis* HB cells. Although adhesion force peaks of 2-2.5 nN magnitude similar to those of *S. epidermidis* HB were frequently observed, the maxima in the force distributions were difficult to fit with a Gaussian curve. Also, in *L. lactis* SdrG$^{(+)}$ more cells (~90 %; see cells #2 and #3 in **Figure 4A**) showed a very high adhesion frequency. Consistent with this, some of the cells investigated showed larger force values, up to ~15 nN, reflecting multiple SdrG interactions (**Figure S3A**). These observations, which correlate with the microscopic adhesion phenotypes of the strains (**Figure 1**), suggest that *L. lactis* can accumulate more SdrG molecules on its surface, or that the cell wall allows a better conformation and exposure of the binding sites. Again, the specificity of the measured interaction was confirmed by two control experiments, blocking with free Fg (**Figure 4C** and **D**) and use of a *L. lactis* strain transformed with an empty vector (EV) that does not contain the *fbe* gene and consequently does not express SdrG (**Figure 4E** and **F**). Finally, we also found an increase in adhesion frequency and/or adhesion force with contact time (1 s; **Figure 4B** and **S3B**), depending on the cell investigated. Accordingly, these results reveal that the *L. lactis* SdrG$^{(+)}$ strain shows the same behaviour as *S. epidermidis* HB except that cell adhesion properties are more pronounced, most likely due to increased adhesin exposure. The strong binding forces measured here for the two strains are not surprising for single-bacterial cell experiments. Using cell probes, the Camesano team found that the adhesion forces between *S. epidermidis* and Fn-coated surfaces is around 1 nN (Liu *et al.*, 2008). Using a micromanipulation technique, Tsang *et al.* showed that *Caulobacter crescentus* cells attach to borosilicate substrates through their adhesive holdfast with an adhesion strength in the micronewton range (Tsang *et al.*, 2006).

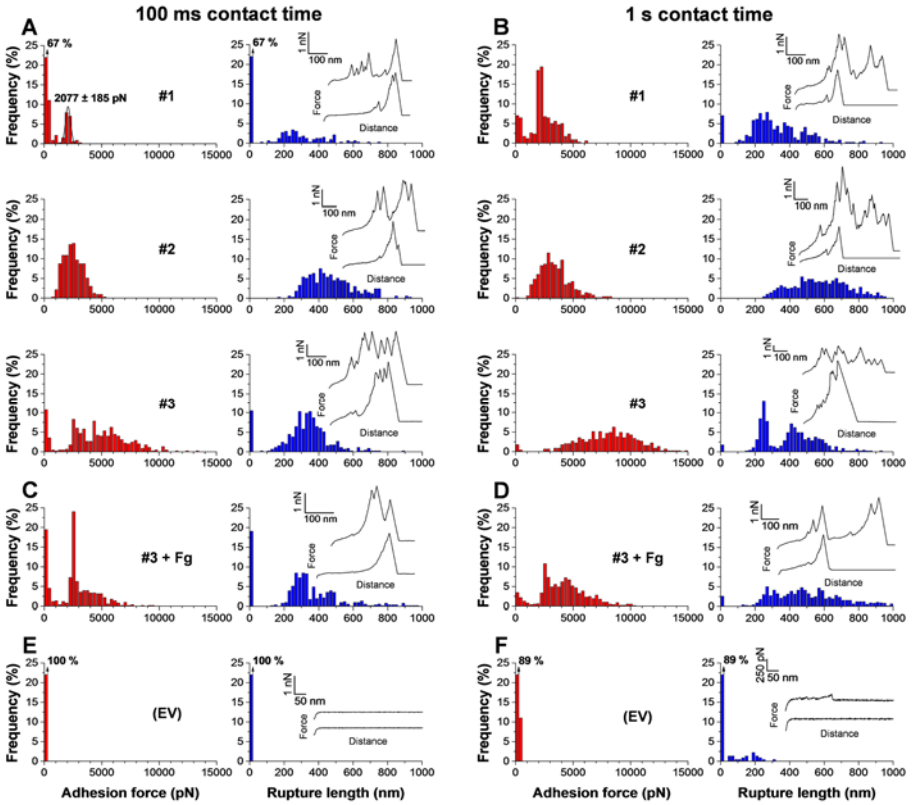

Figure 4: Single-cell analysis of the model *Lactococcus lactis* strain expressing SdrG.
A and B. Adhesion force (red) and rupture length (blue) histograms, as well as representative retraction force curves (insets), obtained by recording multiple force curves in buffer at short contact time (100 ms, **A**) or prolonged contact time (1 s, **B**) between single *L. lactis* SdrG$^{(+)}$ cells and Fg-substrates. Adhesion and rupture length histograms were generated by considering, for every force curve, the maximum adhesion force and the rupture length of the last peak, respectively. Results from three cells from independent cultures are shown (n > 330 force-distances curves for each cell). All curves were obtained using a maximum applied force of 250 pN, and approach and retraction speeds of 1 µm s^{-1}. Data obtained for 10 different cells are shown in Figure S3.
C and D. Force data obtained by recording multiple force curves in buffer at short contact time (100 ms, C) or prolonged contact time (1 s, **D**) between a single *L. lactis* SdrG$^{(+)}$ cell (cell #3) and Fg-substrates in the presence of free Fg (0.2 mg ml^{-1}). Similar data were obtained in at least two independent experiments (**Figure S3**).
E and F. Force data obtained by recording multiple force curves in buffer at short contact time (100 ms, **E**) or prolonged contact time (1 s, **F**) between a *L. lactis* empty vector cell lacking SdrG (EV) and Fg-substrates. Similar data were obtained in at least two independent experiments.

Single-molecule AFM shows that SdrG localizes into nanodomains and has a binding force in the nanonewton range

We then used SMFS with Fg-tips to map the distribution of single SdrG molecules on living bacteria and to quantify the strength of the SdrG-Fg bonds (**Figures 5, 6** and **7**). **Figure 5A-C** shows the adhesion force maps, as well as the adhesion force and rupture length histograms with representative force curves recorded between Fg-tips and the surface of 3 WT *S. epidermidis* HB cells (for data on 10 cells, see **Figure 6**). A substantial fraction of the curves were adhesive, with well-defined rupture peaks of 2082 ± 154 pN magnitude (n = 10240 force curves from 10 different cells) and 50-600 nm rupture lengths, thus very similar to the single-cell force signatures (**Figure 3**). Although the same results were generally obtained with cells from independent experiments (**Figure 6**), a few cells also showed larger adhesion forces and extensions, suggesting multiple adhesins were sometimes detected. We attribute the measured adhesion forces to the detection, stretching and rupture of SdrG-Fg complexes based on two controls, *i.e.* i) blocking with free Fg led to a major reduction of adhesion frequency (from 30 % to 16 %; cell #3 in **Figure 5D-F**), and ii) there was hardly no adhesion on the *S. epidermidis* SdrG$^{(-)}$ mutant strain (**Figure 5G-I**).

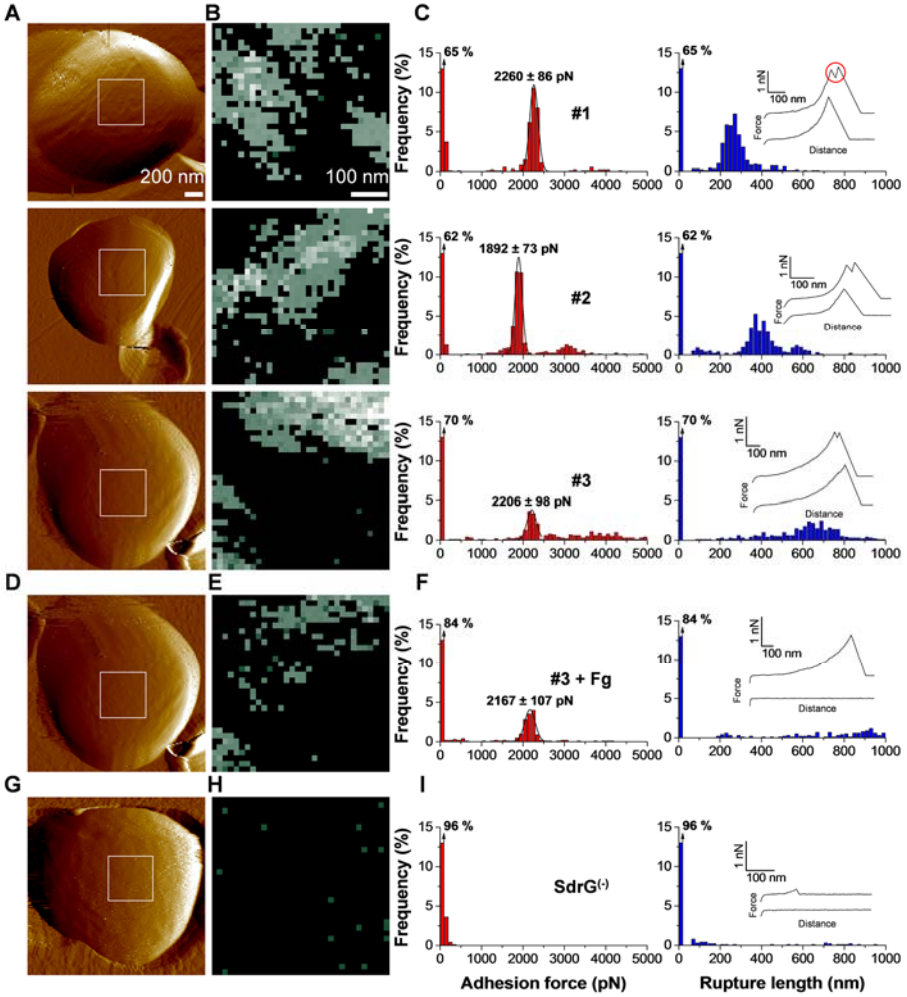

Figure 5: Single-molecule analysis deciphers the localization and binding force of SdrG.
A. Deflection images recorded in buffer with silicon nitride AFM tips showing single *S. epidermidis* HB cells trapped into porous membranes. The white squares indicate the regions where the force maps were recorded.
B. Adhesion force maps (500 nm x 500 nm; z range = 5000 pN; bright pixels correspond to the detection of single adhesins) recorded at 100 ms in buffer between AFM tips functionalized with Fg molecules and *S. epidermidis* HB cells (corresponding to the square areas in **A**). All curves were obtained using a maximum applied force of 250 pN, and approach and retraction speeds of 1 µm s^{-1}.
C. Adhesion force (red) and rupture length (blue) histograms, as well as representative retraction force curves (insets) corresponding to the maps shown in A. Adhesion and rupture length histograms were generated by considering, for every force curve, the adhesion force of the last peak and its rupture length. The red circle shown on the top curves indicates double force peak signatures.
D, E and F. Single-molecule force data recorded between a Fg-tip and the surface of a *S. epidermidis* HB cell in the presence of free Fg (0.1 mg ml^{-1}). Similar data were obtained in at least two independent experiments.
G, H and I. Single-molecule force data recorded between a Fg-tip and a *S. epidermidis* mutant cell impaired in SdrG expression. Similar data were obtained in at least two independent experiments.

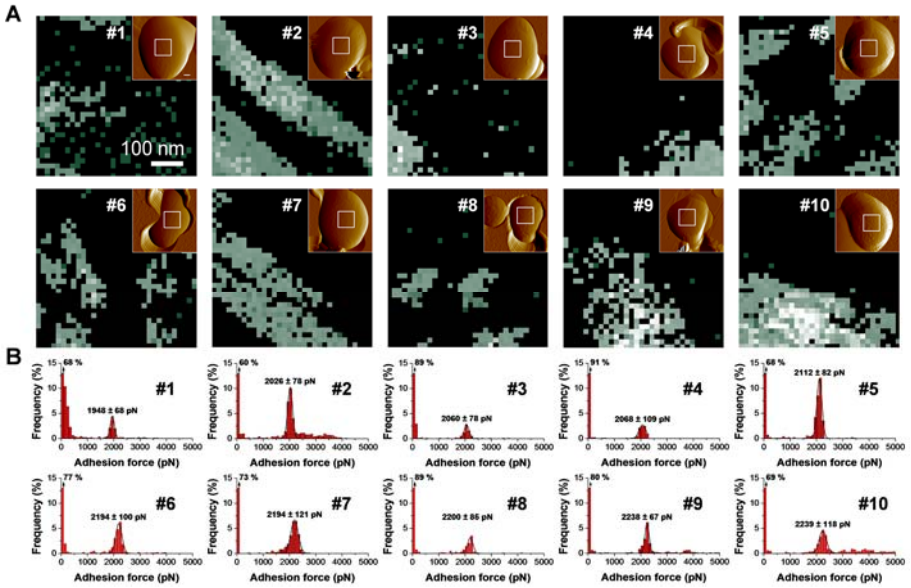

Figure 6: Distribution and binding force of SdrG on *S. epidermidis* HB, using different cell preparations and different tips.
A. Adhesion force maps (500 nm x 500 nm; z range = 5000 pN) recorded at 100 ms in buffer between AFM tips functionalized with Fg molecules and the surface of 10 different *S. epidermidis* HB cells. The insets show deflection images of the cells obtained with silicon nitride tips, square areas corresponding to the location of the force maps. Data obtained using 10 different tips on 10 bacteria from 6 independent samples.
B. Adhesion force histograms corresponding to the maps shown in **A**.

Several pieces of evidence suggest that the ~2.1 nN force represents the strength of a single SdrG-Fg bond. First, we used a well-established PEG chemistry to attach Fg molecules to the AFM tip at low density (Ebner *et al.*, 2007, Alsteens *et al.*, 2010), thus favoring single-molecule measurements. Second, SdrG is believed to only bind one Fg molecule while other staphylococcal adhesins like FnBPs can bind as many as nine molecules of Fn. Third, adhesion force values showed a well-defined Gaussian distribution with a single maximum at 2.1 nN for all cells investigated (**Figure 6**). Clearly, if multiple bonds were probed in parallel, we would expect to see some variations in the maximum adhesion forces when comparing different cells, reflecting variations in the number of bonds, which was not observed here. Fourth, blocking with free Fg decreased the adhesion frequency but did not decrease the mean adhesion force, which is expected if multiple molecules are probed. Fifth, we also probed the SdrG-Fg interaction by attaching Fg via a surface chemistry allowing to tune the Fg surface density (**Figure S4**). Fg was covalently immobilized onto gold-coated tips modified with 1 % or 0.1 % COOH groups using NHS/EDC. At 1 % density, a well-defined Gaussian distribution with a single maximum at 2270 ± 231 pN was observed, thus similar to the results obtained with the PEG chemistry (**Figure S4B**).

Diluting the Fg density by an order of magnitude dramatically decreased the adhesion frequency (from 50 % to 6 %), but without changing the maximum adhesion forces (**Figure S4C**). If multiple SdrG-Fg interactions were probed, we would expect that dilution of the Fg density would give rise to lower forces corresponding to the unit force of single bonds, an effect that was not observed. We note that our single-molecule rupture forces were similar to single-cell rupture forces, suggesting that single SdrG molecules were addressed in both experiments.

Adhesion force maps showed that SdrG is exposed at rather high density on the cell surface, although there were variations from one cell to another (**Figure 5** and **6**). The observed detection frequencies ranged from 9 % to 40 % corresponding to a maximum surface density of 376 to 1640 sites/μm^2, although this value may be an over-estimation if the same molecule is probed more than once. Variation in detection frequency may reflect differences in the surface density of SdrG molecules or in their orientation/conformation. Of note, the adhesins were not randomly distributed but seemed to form nanometer-scale clusters, as observed for mycobacterial (Dupres *et al.*, 2005) and fungal adhesins (Alsteens *et al.*, 2010). The heterogeneous distribution of SdrG is also reminiscent of that reported for FnBPs on *S. aureus*. Mapping the surface of *S. aureus* cells attached on solid substrates, revealed that the regions of greatest Fn activity were always along the cell perimeter, suggesting localization of binding proteins between the cells and the substrate (Lower *et al.*, 2010). We expect that clustering of densely packed SdrG adhesins will result in the physical equivalent of multivalency. Because the binding sites are close to each other, a ligand that dissociates from one adhesin molecule is much more likely to rebind to another, a phenomenon that will strengthen the bacterial-Fg interaction.

The SdrG-Fg complex: strong bond, slow dissociation

Our force measurements indicate that the binding force of the SdrG-Fg bond is remarkably strong, ~2 nN, which is similar to the strength of a covalent bond (Grandbois *et al.*, 1999). Such a binding force is much larger than that reported for other cell adhesion molecules, which is typically in the 50-400 pN range (Fritz *et al.*, 1998, Baumgartner *et al.*, 2000, Dupres *et al.*, 2005, Alsteens *et al.*, 2010). It is also much larger than that reported for other MSCRAMMs. Using optical tweezers, Simpson *et al.* showed that the binding forces between *S. aureus* FnBPs and Fn occur as an integer multiple of 20-25 pN (Simpson *et al.*, 2003). Using AFM, the Lower team extensively studied the binding forces of FnBPs from *S. aureus* laboratory strains and clinical isolates (Yongsunthon *et al.*, 2007, Buck *et al.*, 2010, Lower *et al.*, 2011, Casillas-Ituarte *et al.*, 2012) showing that they range between 0.25 and 2.5 nN. However, the 2.5 nN force was attributed to the rupture of 10 parallel Fn-FnBP bonds, consistent with the notion that FnBPs can bind up to nine Fn molecules, and that Fn was attached on the tip at high density. Lastly, we note that the SdrG-Fg bond is also much stronger than other Fg binding systems. For instance, laser tweezer experiments revealed that the specific binding force between integrin αIIbβ3 and fibrinogen ranges from ~20 to 150 pN (Litvinov *et al.*, 2012). We believe that the strength of the SdrG-Fg bond results from the 'dock, lock and latch' mechanism, which strongly stabilizes the interaction. Such a strong bond is of biological relevance as it explains the ability of staphylococci to colonize protein-coated biomaterials and to withstand physiological shear forces while being engaged in bacterial-biomaterial interactions.

Close inspection of the adhesion force peaks revealed several interesting features. Most peaks could not be fitted with the worm-like-chain (WLC) model which usually describes the unfolding of protein secondary structures (α-helices, β-sheets) (Oberhauser *et al.*, 1998, Rief *et al.*, 1997, Rief *et al.*, 1999). In fact, many curves showed a linear relationship between force and distance (**Figure 5C**), suggesting that the stretched complexes behaved as linear springs. Is this model consistent with our 50-600 nm rupture lengths? The length of a fully extended Fg molecule is 255 nm (Zhmurov *et al.*, 2011). As the peptide ligand is located in the central nodule, we expect that about half of the molecule can be stretched, yielding protein extensions of ~130 nm. On the other hand, the processed SdrG molecule is made of 1005 amino acids, giving rise to a fully extended length of ~362 nm if we consider that each amino acid contributes ~0.36 nm to the contour length of a fully extended polypeptide chain. Full unfolding of Fg and SdrG should therefore result in ~500 nm extensions. As we generally observed shorter extensions, this indicates that SdrG were not completely unfolded when subjected to force. Another

interesting finding is that many of the rupture events (cell #1: 49 %; cell #2: 31%; cell #3; 31 %) showed double force peak signatures separated by only 37.6 ± 5.4 nm (n = 150 force curves; 50 curves from each cell). The high reproducibility of these double force signatures when comparing different curves from different cells suggests they reflect an intrinsic property of the adhesin.

Finally, to assess the dissociation rate of the adhesin-ligand complex, we explored the dependence of the binding strength with the loading rate, *i.e.* the rate at which the force is applied to the complex (Fritz *et al.*, 1998, Baumgartner *et al.*, 2000) (**Figure 7**). To avoid the contribution of other staphylococcal cell wall molecules, these experiments were carried out on the model *L. lactis* SdrG$^{(+)}$ strain. Mapping the cell surface with Fg-tips revealed a detection frequency that ranged from 9 % to 52 %, thus corresponding to a maximum surface density of 376 to 2120 sites/µm^2 (**Figure 7A**). In view of this variability, *S. epidermidis* HB and *L. lactis* SdrG$^{(+)}$ strains do not show substantial differences in apparent protein density. Adhesive curves showed well-defined, single or double force peaks of 2056 ± 103 pN (n = 9216 force curves from 9 different cells) reflecting detection and stretching of single adhesins (**Figure 7B**). **Figure 7C** shows that the mean adhesion force (F) of SdrG increased linearly with the logarithm of the loading rate (r) as observed for other receptor-ligand systems (Hinterdorfer & Dufrêne, 2006, Merkel *et al.*, 1999). While the length scale of the energy barrier, x_β, was assessed from the slope f_β of the F versus $\ln(r)$ plot, extrapolation to zero forces yielded the kinetic off-rate constant of dissociation at zero force: $k_{off} = r_{F=0}\, x_\beta / k_B T = 0.9 \times 10^{-9}\ s^{-1}$. The slow off-rate means that the SdrG-Fg complex dissociates very slowly, thus that it is stable. This finding is qualitatively consistent with isothermal titration calorimetry measurements showing that recombinant SdrG binds its Fg ligand peptide with high affinity (K_d ~0.3 µM; (Ponnuraj *et al.*, 2003, Bowden *et al.*, 2008). Thus our measured dissociation rate is again in favour of the 'dock, lock and latch' model in which large conformational changes lead to greatly stabilized adhesin-ligand complexes.

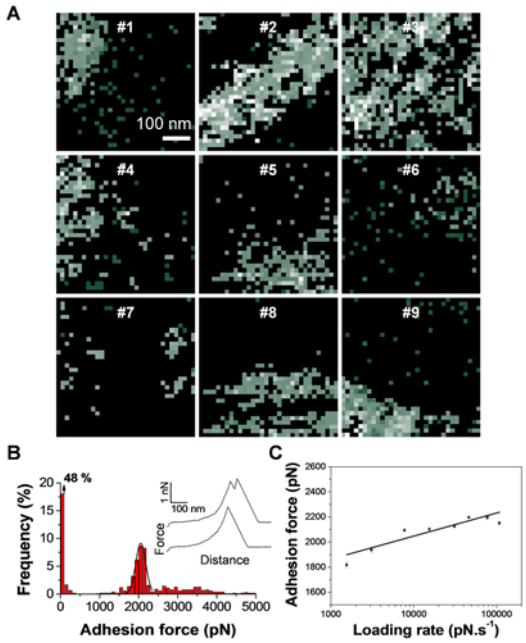

Figure 7: Measuring the dynamics of the SdrG-Fg interaction on *L. lactis* expressing SdrG.
A. Adhesion force maps (500 nm x 500 nm; z range = 5000 pN) recorded at short contact time (100 ms) in buffer between AFM tips functionalized with Fg molecules and the surface of nine different L. lactis SdrG$^{(+)}$ cells. All curves were obtained using a maximum applied force of 250 pN, and approach and retraction speeds of 1 µm s^{-1}. Data obtained using 9 different tips on 9 bacteria from 9 independent samples.
B. Adhesion force histogram as well as representative retraction force curves (insets) corresponding to one map shown in A.
C. Dependence of the adhesion force on the loading rate applied during retraction (mean ± s.e.m; n > 400 force curves for each data point). The mean adhesion force (F) increased linearly with the logarithm of the loading rate (r): $F = 8.0\ 10^{-11} \ln(r) + 3.5\ 10^{-9}$. The R^2 value obtained for the linear fit was 0.78.

Conclusions

Despite the important role that SdrG and other MSCRAMMs play in controlling staphylococcal adhesion, the forces driving their interaction with target proteins remain poorly understood. The experiments reported here demonstrate that SdrG mediates strong specific binding to Fg, therefore explaining the ability of *S. epidermidis* to firmly attach to Fg-coated surfaces. The adhesion probability increases with interaction time, suggesting that stable cell adhesion requires time-dependent conformational changes. *L. lactis* bacteria expressing SdrG show the same behaviour as *S. epidermidis* HB except that cell adhesion properties are more pronounced, presumably due to the better exposure/orientation of the adhesins. Single-molecule imaging reveals that SdrG proteins accumulate at the cell surface, and form nanoscale domains. As these clusters represent the physical equivalent of multivalency, they may largely contribute to stabilize cell adhesion. Single-molecule force measurements show that SdrG has a binding strength (~2 nN) that is equivalent to that of a covalent bond, thus much larger than that of other cell adhesion proteins investigated so far. Finally, dynamic force spectroscopy reveals a low dissociation rate, suggesting that the SdrG-Fg bond is rather stable. These results are in favour of a dynamic, multistep binding mechanism in which SdrG undergoes conformational changes upon ligand binding to form greatly stabilized complexes.

Experimental procedures

Bacterial strains and growth conditions

The WT *S. epidermidis* HB strain and the derivative strain SdrG$^{(-)}$ in which SdrG expression was impaired by gene disruption after pG^{+}Host9'*fbe* plasmid integration in the *fbe* (SdrG) gene (Hartford *et al.*, 2001) were grown at 37°C, 150 rpm, in Trypto-Caseine-Soy broth (TCS). For SdrG$^{(-)}$ erythromycin was added at 10 µg ml^{-1}. The *L. lactis* SdrG strain transformed with the pKS80 plasmid harbouring the WT *fbe* gene for heterologous expression of SdrG and the *L. lactis* (EV) strain transformed with the empty pKS80 plasmid were grown at 30°C in Brain Heart Infusion medium (BHI) supplemented with 10 µg ml^{-1} of erythromycin. For SCFS and SMFS experiments, cells from stationary growth phase (16-18 h) were harvested by centrifugation 10 min at 7500 x *g* and washed 3 times in PBS buffer.

Fibrinogen coated surfaces

To prepare Fg-coated substrates for single-cell probe experiments, glass coverslips coated with a thin layer of gold were immersed overnight in an ethanol solution containing 1 mM of 10 % 16-mercaptododecahexanoic

acid/90% 1-mercapto-1-undecanol (Sigma), rinsed with ethanol, and dried with N2. Substrates were then immersed for 30 min into a solution containing 10 mg ml^{-1} N-hydroxysuccinimide (NHS) and 25 mg ml^{-1} 1-ethyl-3-(3-dimethylaminopropyl)-carbodiimide (EDC) (Sigma), rinsed 5 times with Ultrapure water (ELGA LabWater), incubated with 0.2 mg ml^{-1} of Human Fg (Sigma) for 1 h, rinsed further with PBS buffer, and then immediately used without de-wetting.

Adhesion assays

Two complementary adhesion assays were performed to assess the adhesion phenotype of the bacterial strains. In the first assay, Fg-coated substrates were incubated at 37°C in 200 µl bacterial suspensions adjusted in PBS to an OD600 of 8.0. After 2 h, the substrates were gently rinsed by 3 consecutives washing in PBS and directly imaged using an inverted optical microscope (Zeiss axio Observer Z1) equipped with a Hamamatsu camera C10600. For the second assay, Microtitre plates (Sarstedt) were coated with doubling dilutions of a solution of human Fg (Enzyme Research Laboratories) in PBS overnight at 4 °C. Wells were blocked with 5% (w/v) bovine serum albumin for 2 h at 37 °C. Washed bacteria were adjusted to an OD600 of 2.0 in PBS, and 100 µl was added to each well and incubated for 2 h at 37 °C. Wells were washed with PBS, and adherent cells fixed with formaldehyde (25% v/v), stained with crystal violet and the absorbance at 570 nm (A570 nm) measured.

Single-cell force spectroscopy

Bacterial cell probes were obtained as previously described (Beaussart *et al.*, 2013a, Beaussart *et al.*, 2013b). Briefly, colloidal probes were obtained by attaching single silica microsphere (6.1 µm diameter, Bangs laboratories) with a thin layer of UV-curable glue (NOA 63, Norland Edmund Optics) on triangular shaped tipless cantilevers (NP-O10, Microlevers, Veeco Metrology Group) and using a Nanoscope VIII Multimode AFM (Bruker corporation, Santa Barbara, CA). The cantilever was then immersed for 1 h in a 10 mM TRIS Buffer + 150 mM NaCl solution (pH 8.5) containing 4 mg ml^{-1} dopamine hydrochloride (99%, Sigma). The probe was then rinsed in TRIS Buffer + 150 mM NaCl solution (pH 8.5) and used directly for cell probe preparation. The nominal spring constant of the colloidal probe cantilever was ~0.06 N m^{-1} as determined by the thermal noise method (Picoforce, Bruker).

For cell probe preparation, 50 µl of a suspension of ca. 1 x 10^6 cells were transferred into a glass petri dish in which Fg-coated substrates were attached. The cells were stained in the dark during 15 min using a Baclight viability kit (Invitrogen, kit L7012) following the manufacturer instructions to check the viability and positioning of the cell. After staining, 4 ml of PBS were added to immerse bacteria and Fg surfaces. The colloidal probe was brought into contact

with an isolated bacterium. Single bacteria were attached on the centre of the colloidal probes using a Bioscope Catalyst AFM (Bruker Corporation, Santa Barbara, CA) equipped with a Zeiss Axio Observer Z1 and a Hamamatsu camera C10600. When proper attachment of the cell was confirmed by fluorescence imaging, the cell probe was positioned over the Fg-substrates without de-wetting. Single-cell interaction forces with Fg-surfaces were measured at room temperature (20 °C) by recording multiple forces curves on three different spots, using a maximum applied force of 250 pN, short (<100 ms) or long (1 s) contact times, and constant approach and retraction speeds of 1000 nm s^{-1}. For each condition, at least three bacteria from independent cultures were probed. For blocking experiments, free human Fg was added to the sample at a final concentration of 0.2 mg ml^{-1}.

Single-molecule force spectroscopy

SMFS measurements were performed at room temperature (20 °C) in PBS buffer using a Nanoscope VIII Multimode AFM (Bruker corporation, Santa Barbara, CA) and oxide sharpened microfabricated Si3Ni4 cantilevers with a nominal spring constant of ~0.01 N m^{-1} (Microlevers, Bruker Corporation). The spring constants of the cantilevers were measured using the thermal noise method (Picoforce, Bruker). Bacterial cells were immobilized by mechanical trapping into porous polycarbonate membranes (Millipore, Billerica, MA) with a pore size similar to the cell size (Dufrêne *et al.*, 1999). After filtering a cell suspension, the filter was gently rinsed with PBS, carefully cut (1 cm x 1 cm), attached to a steel sample puck using a small piece of double face adhesive tape, and the mounted sample was transferred into the AFM liquid cell while avoiding de-wetting.

Unless stated otherwise, Fg functionalized tips were obtained using PEG-benzaldehyde linkers (Ebner *et al.*, 2007). Prior to functionalization, cantilevers were washed with chloroform and ethanol, placed in an UV-ozone-cleaner for 30 min, immersed overnight into an ethanolamine solution (3.3 g ethanolamine into 6 ml of DMSO), then washed 3 times with DMSO and 2 times with ethanol, and dried with N_2. The ethanolamine-coated cantilevers were immersed for two hours in a solution prepared by mixing 1 mg Acetal-PEG-NHS dissolved in 0.5 ml of chloroform with 10 µl triethylamine, then washed with chloroform and dried with N2. Cantilevers were further immersed for 5 min in a 1 % citric acid solution, washed in Ultrapure water (ELGA LabWater), and then covered with a 200 µl droplet of PBS solution containing human Fg (2 µM) to which 2 µl of a 1 M NaCNBH3 solution were added. After 50 min, cantilevers were incubated with 5 µl of a 1 M ethanolamine solution in order to passivate unreacted aldehyde groups, and then washed with and stored in buffer. For control experiments, we also attached Fg to the tips via

the N-hydroxysuccinimide (NHS) surface chemistry. To this end, gold-coated cantilevers (Olympus; nominal spring constant of 0.02 N m^{-1}) were immersed overnight in ethanol solutions containing 1 mM of (16-Mercaptohexadecanoic acid) (Sigma) and (11-Mercapto-1-undecanol) (Sigma) at a molar ration of either (1:99) or (0.1:99.9), and then rinsed with ethanol. Cantilevers were immersed for 30 minutes in a solution containing 10 mg ml^{-1} NHS (Sigma) and 25 mg ml-1 1-ethyl-3-(3-dimethylaminopropyl)-carbodiimide (EDC) (Sigma) and rinsed with water. The activated surfaces were then incubated with 0.2 mg ml^{-1} Fg in PBS for 1 hour, followed by rinsing with PBS and used immediately.

For single-molecule imaging, bare tips were first used to localize and image individual cells and then replaced by Fg-tips. Adhesion maps were obtained by recording 32 x 32 force-distance curves on areas of 500 x 500 nm, calculating the adhesion force for each force curve and displaying the adhesive events as grey pixels. Unless specified otherwise, all force curves were recorded at 100 ms contact time, with a maximum applied force of 250 pN and using a constant approach and retraction speed of 1000 nm s^{-1}. For blocking experiments, 0.1 mg ml^{-1} of free human Fg were added.

Acknowledgements

Work at the Université catholique de Louvain was supported by the National Fund for Scientific Research (FNRS), the Université catholique de Louvain (Fonds Spéciaux de Recherche), the Région Wallonne, the Federal Office for Scientific, Technical and Cultural Affairs (Interuniversity Poles of Attraction Programme), and the Research Department of the Communauté française de Belgique (Concerted Research Action). Y.F.D. is Research Director of the FNRS.

Supplementary figures

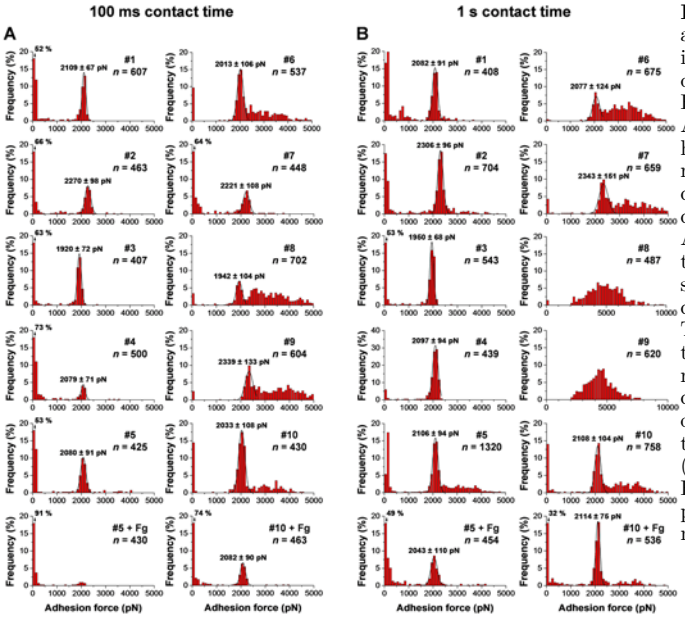

Figure S1. Single-cell analysis of the SdrG-Fg interaction on ten different *S. epidermidis* HB cells.
A and B. Adhesion force histograms obtained by recording multiple force curves in buffer at short contact time (100 ms, A) or prolonged contact time (1 s, B) between single *S. epidermidis* HB cells and Fg-substrates. The lowest line shows the data obtained by recording multiple force curves in buffer at short or prolonged contact time between two cells (cells #5 and #10) and Fg-substrates in the presence of free Fg (0.2 mg.mL^{-1}).

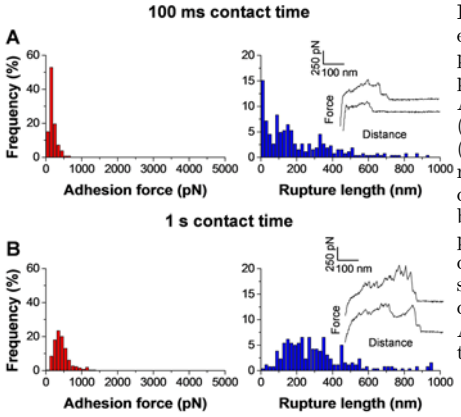

Figure S2. Control experiment with polydopamine-coated probes.
A and B. Adhesion force (red) and rupture length (blue) histograms with representative force curves recorded in buffer between a polydopamine-coated colloidal probe and Fg-substrates, at short contact time (100 ms, A) or prolonged contact time (1 s, B).

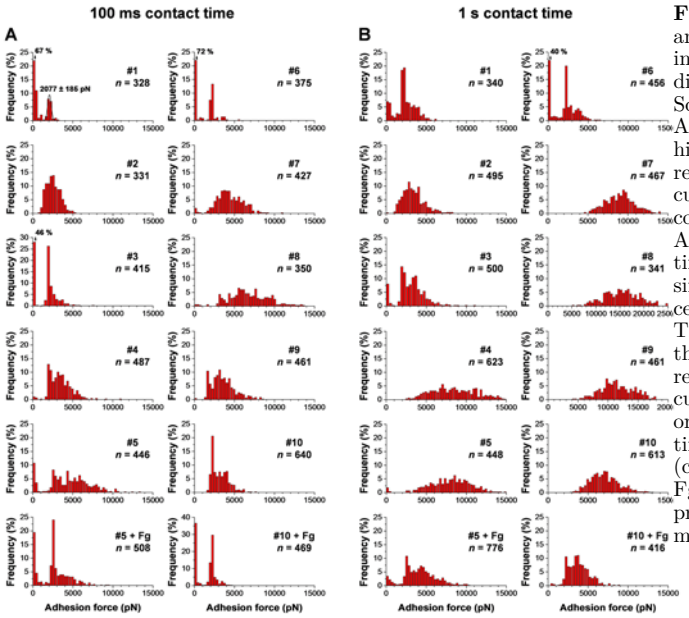

Figure S3. Single-cell analysis of the SdrG-Fg interaction on ten different *L. lactis* SdrG$^{(+)}$ cells.
A and B. Adhesion force histograms obtained by recording multiple force curves in buffer at short contact time (100 ms, A) or prolonged contact time (1 s, B) between single *L. lactis* SdrG$^{(+)}$ cells and Fg-substrates. The lowest line shows the data obtained by recording multiple force curves in buffer at short or prolonged contact time between two cells (cells #5 and #10) and Fg-substrates in the presence of free Fg (0.2 mg.mL^{-1}).

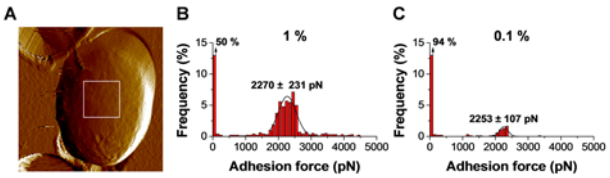

Figure S4. Single-molecule control experiment supporting the notion that single SdrG-Fg bonds are being measured.
A. Deflection image recorded in buffer with silicon nitride AFM tips showing a single *S. epidermidis* HB cell trapped into a porous membrane. The white squares indicate the region where the force maps were recorded.
B and C. Adhesion force histograms recorded at 100 ms in buffer between a *S. epidermidis* HB cell and AFM tips functionalized at 1 % NHS (B) or 0.1 % NHS with Fg molecules.

References

Alsteens, D., Garcia, M.C., Lipke, P.N. & Dufrêne, Y.F. (2010) Force-induced formation and propagation of adhesion nanodomains in living fungal cells. *Proc Natl Acad Sci USA* **107**: 20744-20749.

Andre, G., Kulakauskas, S., Chapot-Chartier, M.P., Navet, B., Deghorain, M., Bernard, E., *et al.* (2010) Imaging the nanoscale organization of peptidoglycan in living *Lactococcus lactis* cells. *Nat Commun* **1**: 27.

Baumgartner, W., Hinterdorfer, P., Ness, W., Raab, A., Vestweber, D., Schindler, H. & Drenckhahn, D. (2000) Cadherin interaction probed by atomic force microscopy. *Proc. Natl. Acad. Sci. USA*. 97: 4005-4010.

Beaussart, A., El-Kirat-Chatel, S., Herman, P., Alsteens, D., Mahillon, J., Hols, P. & Dufrêne, Y.F. (2013a) Single-cell force spectroscopy of probiotic bacteria. *Biophys J* **104**: 1886-1892.

Beaussart, A., Herman, P., El-Kirat-Chatel, S., Lipke, P.N., Kucharikova, S., Van Dijck, P. & Dufrêne, Y.F. (2013b) Single-cell force spectroscopy of the medically important *Staphylococcus epidermidis-Candida albicans* interaction. *Nanoscale* **5**: 10894-10900.

Boks, N.P., Busscher, H.J., van der Mei, H.C. & Norde, W. (2008) Bond-strengthening in staphylococcal adhesion to hydrophilic and hydrophobic surfaces using atomic force microscopy. *Langmuir* **24**: 12990-12994.

Bowden, M.G., Heuck, A.P., Ponnuraj, K., Kolosova, E., Choe, D., Gurusiddappa, S., *et al.* (2008) Evidence for the "dock, lock, and latch" ligand binding mechanism of the staphylococcal microbial surface component recognizing adhesive matrix molecules (MSCRAMM) SdrG. *J Biol Chem* **283**: 638-647.

Buck, A.W., Fowler, V.G., Jr., Yongsunthon, R., Liu, J., DiBartola, A.C., Que, Y.A., *et al.* (2010) Bonds between fibronectin and fibronectin-binding proteins on *Staphylococcus aureus* and *Lactococcus lactis*. *Langmuir* **26**: 10764-10770.

Casillas-Ituarte, N.N., Lower, B.H., Lamlertthon, S., Fowler, V.G., Jr. & Lower, S.K. (2012) Dissociation rate constants of human fibronectin binding to fibronectin-binding proteins on living *Staphylococcus aureus* isolated from clinical patients. *J Biol Chem* **287**: 6693-6701.

Dufrêne, Y.F., Boonaert, C.J., Gerin, P.A., Asther, M. & Rouxhet, P.G. (1999) Direct probing of the surface ultrastructure and molecular interactions

of dormant and germinating spores of *Phanerochaete chrysosporium*. *J Bacteriol* **181**: 5350-5354.

Dupres, V., Menozzi, F.D., Locht, C., Clare, B.H., Abbott, N.L., Cuenot, S., *et al.* (2005) Nanoscale mapping and functional analysis of individual adhesins on living bacteria. *Nat Methods* **2**: 515-520.

Dupres, V., Verbelen, C., Raze, D., Lafont, F. & Dufrêne, Y.F. (2009) Force spectroscopy of the interaction between mycobacterial adhesins and heparan sulphate proteoglycan receptors. *Chem phys chem* **10**: 1672-1675.

Ebner, A., Wildling, L., Kamruzzahan, A.S., Rankl, C., Wruss, J., Hahn, C.D., *et al.* (2007) A new, simple method for linking of antibodies to atomic force microscopy tips. *Bioconjug Chem* **18**: 1176-1184.

El-Kirat-Chatel, S., Boyd, C.D., O'Toole, G.A. & Dufrêne, Y.F. (2014) Single-Molecule Analysis of *Pseudomonas fluorescens* Footprints. *ACS Nano* **8**: 1690-1698.

Emerson, R.J.t., Bergstrom, T.S., Liu, Y., Soto, E.R., Brown, C.A., McGimpsey, W.G. & Camesano, T.A. (2006) Microscale correlation between surface chemistry, texture, and the adhesive strength of *Staphylococcus epidermidis*. *Langmuir* **22**: 11311-11321.

Foster, T.J., Geoghegan, J.A., Ganesh, V.K. & Hook, M. (2014) Adhesion, invasion and evasion: the many functions of the surface proteins of *Staphylococcus aureus*. *Nat. Rev. Microbiol.* **12**: 49-62.

Fritz, J., Katopodis, A.G., Kolbinger, F. & Anselmetti, D. (1998) Force-mediated kinetics of single P-selectin/ligand complexes observed by atomic force microscopy. *Proc. Natl. Acad. Sci. USA* **95**: 12283-12288.

Grandbois, M., Beyer, M., Rief, M., Clausen-Schaumann, H. & Gaub, H.E. (1999) How strong is a covalent bond? *Science* **283**: 1727-1730.

Hartford, O., O'Brien, L., Schofield, K., Wells, J. & Foster, T.J. (2001) The Fbe (SdrG) protein of *Staphylococcus epidermidis* HB promotes bacterial adherence to fibrinogen. *Microbiology* **147**: 2545-2552.

Helenius, J., Heisenberg, C.P., Gaub, H.E. & Müller, D.J. (2008) Single-cell force spectroscopy. *J. Cell. Sci.* **121**: 1785-1791.

Hinterdorfer, P. & Dufrêne, Y.F. (2006) Detection and localization of single molecular recognition events using atomic force microscopy. *Nat Methods* **3**: 347-355.

Josefsson, E., McCrea, K.W., Ni Eidhin, D., O'Connell, D., Cox, J., Hook, M. & Foster, T.J. (1998) Three new members of the serine-aspartate repeat

protein multigene family of *Staphylococcus aureus*. *Microbiology* **144**: 3387-3395.

Litvinov, R.I., Mekler, A., Shuman, H., Bennett, J.S., Barsegov, V. & Weisel, J.W. (2012) Resolving two-dimensional kinetics of the integrin alphaIIbeta3-fibrinogen interactions using binding-unbinding correlation spectroscopy. *J Biol Chem* **287**: 35275-35285.

Liu, Y., Strauss, J. & Camesano, T.A. (2008) Adhesion forces between *Staphylococcus epidermidis* and surfaces bearing self-assembled monolayers in the presence of model proteins. *Biomaterials* **29**: 4374-4382.

Lower, S.K., Lamlertthon, S., Casillas-Ituarte, N.N., Lins, R.D., Yongsunthon, R., Taylor, E.S., *et al.* (2011) Polymorphisms in fibronectin binding protein A of *Staphylococcus aureus* are associated with infection of cardiovascular devices. *Proc. Natl. Acad. Sci. USA.* 108: 18372-18377.

Lower, S.K., Yongsunthon, R., Casillas-Ituarte, N.N., Taylor, E.S., DiBartola, A.C., Lower, B.H., *et al.* (2010) A tactile response in *Staphylococcus aureus*. *Biophys. J.* 99: 2803-2811.

Mack, D. (1999) Molecular mechanisms of *Staphylococcus epidermidis* biofilm formation. *J Hosp Infect* **43** Suppl: S113-125.

McCrea, K.W., Hartford, O., Davis, S., Eidhin, D.N., Lina, G., Speziale, P., *et al.* (2000) The serine-aspartate repeat (Sdr) protein family in *Staphylococcus epidermidis*. *Microbiology* **146**: 1535-1546.

Merkel, R., Nassoy, P., Leung, A., Ritchie, K. & Evans, E. (1999) Energy landscapes of receptor-ligand bonds explored with dynamic force spectroscopy. *Nature* **397**: 50-53.

Müller, D.J., Helenius, J., Alsteens, D. & Dufrêne, Y.F. (2009) Force probing surfaces of living cells to molecular resolution. *Nat Chem Biol* **5**: 383-390.

Nilsson, M., Frykberg, L., Flock, J.I., Pei, L., Lindberg, M. & Guss, B. (1998) A fibrinogen-binding protein of *Staphylococcus epidermidis*. *Infect Immun* **66**: 2666-2673.

Oberhauser, A.F., Marszalek, P.E., Erickson, H.P. & Fernandez, J.M. (1998) The molecular elasticity of the extracellular matrix protein tenascin. *Nature* **393**: 181-185.

Otto, M., (2009) *Staphylococcus epidermidis*--the 'accidental' pathogen. *Nat Rev Microbiol* **7**: 555-567.

Ponnuraj, K., Bowden, M.G., Davis, S., Gurusiddappa, S., Moore, D., Choe, D., *et al.* (2003) A "dock, lock, and latch" structural model for a staphylococcal adhesin binding to fibrinogen. *Cell* **115**: 217-228.

Rief, M., Gautel, M., Oesterhelt, F., Fernandez, J.M. & Gaub, H.E. (1997) Reversible unfolding of individual titin immunoglobulin domains by AFM. *Science* **276**: 1109-1112.

Rief, M., Pascual, J., Saraste, M. & Gaub, H.E. (1999) Single molecule force spectroscopy of spectrin repeats: low unfolding forces in helix bundles. *J Mol Biol* **286**: 553-561.

Simpson, K.H., Bowden, G., Hook, M. & Anvari, B. (2003) Measurement of adhesive forces between individual *Staphylococcus aureus* MSCRAMMs and protein-coated surfaces by use of optical tweezers. *J Bacteriol* **185**: 2031-2035.

Sullan, R.M., Beaussart, A., Tripathi, P., Derclaye, S., El-Kirat-Chatel, S., Li, J.K., *et al.* (2013) Single-cell force spectroscopy of pili-mediated adhesion. *Nanoscale* **6**: 1134-1143.

Tsang, P.H., Li, G., Brun, Y.V., Freund, L.B. & Tang, J.X. (2006) Adhesion of single bacterial cells in the micronewton range. *Proc Natl Acad Sci USA* **103**: 5764-5768.

Xu, C.P., Boks, N.P., de Vries, J., Kaper, H.J., Norde, W., Busscher, H.J. & van der Mei, H.C. (2008) *Staphylococcus aureus*-fibronectin interactions with and without fibronectin-binding proteins and their role in adhesion and desorption. *Appl. Environ. Microbiol.* **74**: 7522-7528.

Yongsunthon, R., Fowler, V.G., Jr., Lower, B.H., Vellano, F.P., Alexander, E., Reller, L.B., *et al.* (2007) Correlation between fundamental binding forces and clinical prognosis of *Staphylococcus aureus* infections of medical implants. *Langmuir* **23**: 2289-2292.

Zhmurov, A., Brown, A.E., Litvinov, R.I., Dima, R.I., Weisel, J.W. & Barsegov, V. (2011) Mechanism of fibrin(ogen) forced unfolding. *Structure* **19**: 1615-1624.

Chapter II

Staphylococcus epidermidis affinity for Fibrinogen-coated surfaces correlates with the abundance of the SdrG adhesin on the cell surface

Thomas Vanzieleghem, Philippe Herman, Yves F. Dufrêne, Jacques Mahillon

In *Langmuir*, **2015**, 31(16), 4713.

I contributed by doing all AFM analyses, and by helping to write the paper.

Abstract

Staphylococcus epidermidis is a world leading pathogen in health-care facilities, mainly causing medical device-associated infections.

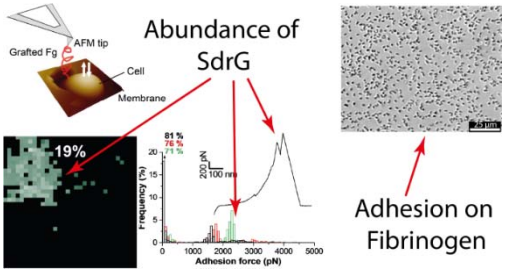

These nosocomial diseases often result in complications such as bacteremia, fibrosis or peritonitis. The virulence of *S. epidermidis* relies on its ability to colonize surfaces and develop thereupon in the form of biofilms. Bacterial adherence on biomaterials, usually covered with plasma proteins after implantation, is a critical step leading to biofilm infections. The cell surface protein SdrG mediates adhesion of *S. epidermidis* to Fibrinogen (Fg) through a specific 'dock, lock and latch' mechanism, which results in greatly stabilized protein-ligand complexes. Here, we combine single-molecule, single-cell and whole population assays to investigate the extent to which the surface density of SdrG determines the ability of *S. epidermidis* clinical strains HB, ATCC 35984 and ATCC 12228 to bind to Fg-coated surfaces. Strains that showed enhanced adhesion on Fg-coated PolyDiMethylSiloxane (PDMS) were characterized by increased amounts of SdrG proteins on the cell surface, as observed by single-molecule analysis. Consistent with previous reports showing increased expression of SdrG following *in vivo* exposure, this work provides direct evidence that abundance of SdrG on the cell surface of *S. epidermidis* strains dramatically improves their ability to bind to Fg-coated implanted medical devices.

Introduction

The opportunistic pathogen *Staphylococcus epidermidis* is the main etiological agent of infections associated with implanted medical devices, especially vascular and urinary catheters[1]. In the US, infections involving *S. epidermidis* are estimated to reach 200.000 cases per year[2]. Most often, these diseases occur in a chronic form owing to the development of a biofilm on the implanted material[3,4]. The treatment of chronic infections is complicated by the intrinsic resistance of bacteria or tolerance of biofilms to antibiotics, resulting in a significant burden for public health systems[5,6].

Bacterial contamination of implanted devices in patients can happen during surgery or while the device is being used to inject drugs to or withdraw biological fluids from patients[7]. Adhesion of bacteria on the surface of biomaterials will determine their ability to start an infection. In the human body, surfaces of medical devices tend to be readily coated by host factors upon contact with biological fluids. On its cell surface, *S. epidermidis* possesses a group of receptors, referred to as MSCRAMMs (Microbial Surface Components Recognizing Adhesive Matrix Molecules), that specifically bind to human proteins such as Fg, Fibronectin (Fn) and Collagen (Cn)[8–10]. One of these MSCRAMMs is SdrG, a protein belonging to the Serine Aspartate Repeat family (Sdr), anchored to the cell wall by a LPXTG motif. SdrG mediates binding to Fg with a high affinity[11]. A sequence of 14 amino acids at the N-terminus of Fg is specifically recognized by SdrG according to a specific 'dock, lock and latch' mechanism[12]. Recently, SdrG was found to bind to Fg with a force of 2 nN, which is remarkably strong[13]. It was also shown that contact time between the two protein influences the rate of efficient SdrG-Fg binding and consequently the fate of bacterial adhesion on Fg-coated surfaces[14]. While the molecular mechanism controlling the SdrG-Fg interaction is well established, little is known about the impact of SdrG surface density on the ability of various *S. epidermidis* strains to adhere on Fg-coated surfaces. By combining whole population, single-cell and single-molecule atomic force microscopy (AFM)[15,16] approaches, we show that *S. epidermidis* strains that display a higher density of SdrG on their cell surface show enhanced adhesion to Fg-coated substrates. In light of these data, a model is proposed in which the density of cell surface sites displaying high Fg affinity (*i.e.* active SdrG molecules) correlates with the proportion of bacteria from a population that effectively bind to Fg-coated substrates.

Experimental section

Bacterial strains and culture

Four *S. epidermidis* strains were used in this study: HB[17], HB SdrG$^{(-)}$ a mutant in which the *sdrG* gene is deleted, kindly provided by Prof. T. Foster[11], ATCC 12228 and ATCC 35984. Bacteria from -80°C frozen stocks were grown on Tryptic Soy Agar (TSA, Bio-Rad) for at least 16 h at 37°C. Single colonies were then used to inoculate Tryptic Soy Broth (TSB) and cultures were carried out under agitation at 120 RPM, 37°C for 16 h.

Preparation of bacterial suspensions

Bacterial suspensions were prepared according to the following procedure. Stationary phase cultures were centrifuged, the supernatant was removed and the pellet was re-suspended in PBS at pH 7.4 (Tablets, Sigma). Centrifugation were performed either once or three times, at either 1,000 *g* or 6,000 *g* for 15 min.

Whole population adhesion assays in 96-well plates

The adhesion assays in static conditions were carried out in 96-well plates coated with PolyDiMethylSiloxane (PDMS). The coating of the wells was performed by adding 10 µL of 1:2 (v:v) solution of PDMS (Sylgard 184, Dow Corning) in hexane (VWR), previously filtered on 0.22 µm. 96-well plates were then left to dry at 55°C for at least 1 h.

To coat the PDMS wells for whole population adhesion assays, they were first filled either with PBS or a 0.22 µm filtered solution of Human Fg (Sigma) 0.5 mg/ml in PBS or Bovine Serum Adult (BS, Sigma) diluted 1:10 in PBS, also previously filtered on 0.22 µm and left to incubate at 37°C for 1 h. Five rinsing steps were then applied to the wells by removing 150 µL of supernatant and adding 150 µL of PBS. 50 µL of liquid were left in the wells at each step to avoid un-wetting. In the last rinsing step, 100 µL of liquid was withdrawn and 100 µL of bacterial suspension was added. The content of each well was homogenized by pipetting up and down twice. Incubation was performed for 1 h at 37°C. The same rinsing procedure was applied to the plates to remove unbound bacteria. Each strain was tested at least in four wells for each PDMS surface type (bare, Fg or BS coated) and repeated three times with independent cultures.

To quantify bacterial adhesion at the bottom of the wells, two bright field micrographs were taken in each well using a 40x long working distance objective (numerical aperture 0.6, Fluotar, Leica) mounted on an inverted microscope (Leica, DMI 6000) equipped with a sensitive B/W cooled CCD camera (Leica, DFX 365). Surface bound bacteria were counted in ImageJ thanks to the particle analyzer function, after an appropriate thresholding was

performed. Results (number of bacteria per image (covering 75.600 µm²)) were converted into bacterial surface densities expressed as the number of bacterial cells/mm².

Single-molecule force spectroscopy

Single-molecule force spectroscopy (SMFS) measurements were performed at room temperature (20 °C) in PBS buffer using a Nanoscope VIII Multimode AFM (Bruker corporation, Santa Barbara, CA) and oxide sharpened micro-fabricated Si_3N_4 cantilevers with a nominal spring constant of ~0.01 N m^{-1} (Microlevers, Bruker Corporation). The spring constants of the cantilevers were measured using the thermal noise method (Picoforce, Bruker). Bacterial cells were immobilized by mechanical trapping into porous polycarbonate membranes (Millipore, Billerica, MA) with a pore size similar to the cell size[18]. After filtering a cell suspension, the filter was gently rinsed with PBS, carefully cut (1 cm x 1 cm), attached to a steel sample puck using a small piece of double face adhesive tape, and the mounted sample was transferred into the AFM liquid cell while avoiding de-wetting.

Unless stated otherwise, Fg-functionalized tips were obtained using PEG-benzaldehyde linkers[19]. Prior to functionalization, cantilevers were washed with chloroform and ethanol, placed in an UV-ozone-cleaner for 30 min, immersed overnight into an ethanolamine solution (3.3 g ethanolamine into 6 ml of DMSO), then washed 3 times with DMSO and twice with ethanol, and dried with N_2. The ethanolamine-coated cantilevers were immersed for two hours in a solution prepared by mixing 1 mg Acetal-PEG-NHS dissolved in 0.5 ml of chloroform with 10 µl triethylamine, then washed with chloroform and dried with N_2. Cantilevers were further immersed for 5 min in a 1 % citric acid solution, washed in Ultrapure water (ELGA LabWater), and covered with a 200 µl droplet of PBS solution containing human Fg (2 µM) to which 2 µl of a 1 M $NaCNBH_3$ solution were added. After 50 min, cantilevers were incubated with 5 µl of a 1 M ethanolamine solution in order to passivate unreacted aldehyde groups, and then washed three times with PBS and lastly with PBS + 0.01% NaN_3 for storage.

Bare tips were first used to localize and to image individual cells and then replaced by Fg-tips. Adhesion maps were obtained by recording 32 x 32 force-distance curves on areas of 500 x 500 nm, calculating the adhesion force for each force curve and displaying the adhesive events as grey pixels. Unless specified otherwise, all force curves were recorded at 100 ms contact time, with

a maximum applied force of 250 pN and using a constant approach and retraction speed of 1,000 nm s^{-1}.

Single-cell force spectroscopy

PDMS-coated surfaces

Round glass cover slips were spin coated with PDMS. Briefly, a 1:5 solution of PDMS (Sylgard 184) in hexane (VWR) was prepared and 0.2 ml of this solution was dropped onto the cover slips before they were spun at 3,000 rpm for 1 min in the spin-coater (Technologies, model: WS-400B-6NPP/Lite). Surfaces were then cured at 95°C for 1 h to allow to PDMS to polymerize. PDMS coated cover slips were stored at room temperature in sealed Petri dishes until use.

Fibrinogen and bovine serum-coated substrates

To prepare Fg-coated substrates, as well as bovine serum substrates, for single-cell probe experiments, glass cover slips coated with a thin layer of gold were immersed overnight in an ethanol solution containing 1 mM of 10 % 16-mercapto-dodecahexanoic acid, 90 % 1-mercapto-1-undecanol (Sigma), rinsed with ethanol, and dried with N_2. Substrates were then immersed for 30 min into a solution containing 10 mg ml^{-1} N-hydroxysuccinimide (NHS) and 25 mg ml^{-1} 1-ethyl-3-(3-dimethylaminopropyl)-carbodiimide (EDC) (Sigma), and rinsed five times with Ultrapure water (ELGA LabWater). For Fg-coated surfaces, substrates were incubated with 0.5 mg ml^{-1} of Human Fg (Sigma) for 1 h, rinsed with PBS buffer, and immediately used without de-wetting. For BS surfaces, substrates were incubated with bovine serum diluted 1:10 in PBS, rinsed with PBS buffer, and immediately used without de-wetting.

Single-cell force spectroscopy measurements

Bacterial cell probes were obtained as previously described[20]. Briefly, colloidal probes were obtained by attaching single silica microsphere (6.1 µm diameter, Bangs laboratories) with a thin layer of UV-curable glue (NOA 63, Norland Edmund Optics) on triangular-shaped tipless cantilevers (NP-O10, Microlevers, Veeco Metrology Group) and using a Nanoscope VIII Multimode AFM (Bruker corporation, Santa Barbara, CA). The cantilever was then immersed for 1 h in a 10 mM Tris Buffer, 150 mM NaCl solution (pH 8.5) containing 4 mg ml^{-1} dopamine hydrochloride (99%, Sigma). The probe was then rinsed in 10 mM Tris Buffer, 150 mM NaCl solution (pH 8.5) and used directly for cell probe preparation. The nominal spring constant of the colloidal probe cantilever was ~ 0.06 N m^{-1}, as determined by the thermal noise method (Picoforce, Bruker).

For cell probe preparation, 50 µl of a suspension of ca. 1×10^6 CFU were transferred into a glass Petri dish in which the different substrates were attached. The cells were stained in the dark during 15 min using a Baclight

viability kit (Invitrogen, kit L7012) following the manufacturer instructions to check the viability and positioning of the cell. After staining, 4 ml of PBS were added to immerse bacteria and the surfaces. The colloidal probe was brought into contact with an isolated bacterium. Single bacteria were attached on the centre of the colloidal probes using a Bioscope Catalyst AFM (Bruker Corporation, Santa Barbara, CA) equipped with a Zeiss Axio Observer Z1 and a Hamamatsu camera C10600. When proper attachment of the cell was confirmed by fluorescence imaging, the cell probe was positioned over the appropriate substrate without de-wetting. Single-cell interaction forces with surfaces were measured at room temperature (20°C) by recording multiple forces curves on three different spots, using a maximum applied force of 250 pN, 1 s contact time, and constant approach and retraction speeds of 1,000 nm s^{-1}. For each condition, at least three bacterial cells from independent cultures were probed, 150 times for BS surfaces, and at least 350 times with PDMS and Fg-coated substrates.

Statistical analysis

Results of whole population assays were treated with JMP© (SAS) to calculate the means, standard deviations and confidence intervals at 95 % of bacterial surface densities on coated or bare PDMS surfaces.

Results

Fg binding activity of SdrG is sensitive to repeated frictional forces

The impact of centrifugation on the preparation of bacterial suspensions was assessed by means of whole population adhesion assays to Fg-coated PDMS. In brief, the bacterial suspensions were removed after 1 h of incubation in contact with the surface and the wells were thoroughly rinsed with PBS. Adherent bacterial cells were numbered on microscopic pictures to determine the surface density in terms of cells per mm². **Figure 1A** presents the results for suspensions obtained by centrifuging the liquid cultures three times either at 1,000g or 6,000g for 10 min. Almost twice as many bacteria from the suspension centrifuged three times at 1,000g remained bound to the Fg-coated PDMS surface compared to the suspension centrifuged at 6,000g. These results strongly suggest a loss in SdrG activity in response to a higher centrifugation speed. The adherence to Fg-coated surfaces of bacterial cells that were centrifuged either once or three times at 6,000g was tested (**Figure 1B**). Strikingly, increasing the number of centrifugation steps decreases the ability of a population of *S. epidermidis* to attach to surface bound Fg. Repeated exposures of the cell surface to mechanical stresses partially inactivate SdrG and may lead to underestimate its role in bacterial adhesion. In the following experiments, the preparation of bacterial suspensions was performed with only one centrifugation step to preserve the activity of SdrG on the bacterial cell surface.

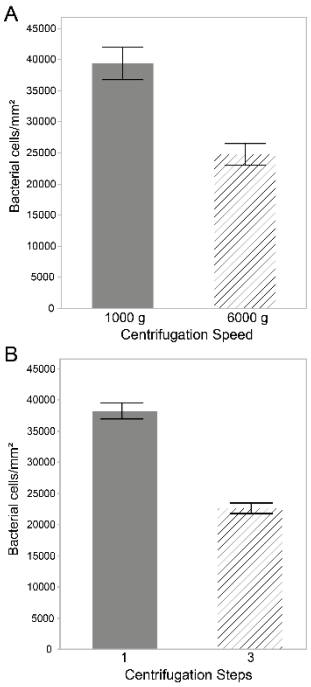

Figure 1: Influence of centrifugation on the adhesion of *S. epidermidis* strain HB to Fg-coated PDMS. Whole population adhesion assays performed with bacterial suspension of the HB strain. **A.** Centrifuged three times at 1,000 and 6,000*g* and **B.** Centrifuged once or three times at 6,000*g*. Error bars are confidence intervals at 95 %.

Whole population adhesion assay of four *S. epidermidis* strains on bare and coated PDMS substrates

Figure 2 presents the results of whole population adhesion assays of four *S. epidermidis* isolates: ATCC 12228, ATCC 35984, HB and HB SdrG$^{(-)}$, an

isogenic mutant in which *fbe* has been knocked out, to PDMS surfaces, either bare or coated with BS or Fg in modified multiwell plates (**Figure 2A**).
On bare PDMS, all strains tested in this study strongly adhered to cover the entire surface of the wells entirely as shown in **Figure 2B**. This situation is achieved when around 150.000 cells can be found per square mm. On PDMS coated with BS, bacterial adhesion was generally weak (at least two orders of magnitude less than on bare PDMS). Bacterial surface densities of all tested strains could not be statistically discriminated and remained just above or close to the limit of detection of our method, *i.e.* 500 bacteria/mm².
On Fg-coated PDMS, SdrG$^{(-)}$ behaved as for the reference BS-coated PDMS, with about 1,000 surface-bound bacteria/mm². This means that the mutant strain SdrG$^{(-)}$ interacts with the layer of adsorbed Fg in the same way as with a layer of other proteins, as expected given the absence of SdrG on its cell surface. For the other strains, WT HB strain (see **Figure 2C**) adhered significantly better than ATCC 12228 by 0.6 log, and the latter displayed a significantly higher affinity for Fg-coated surfaces than ATCC 35984, also marked by a 0.6 log difference in the bacterial surface density. The adhesion of ATCC 35984 on Fg could just be discriminated from its adhesion to the control BS-coated surface.

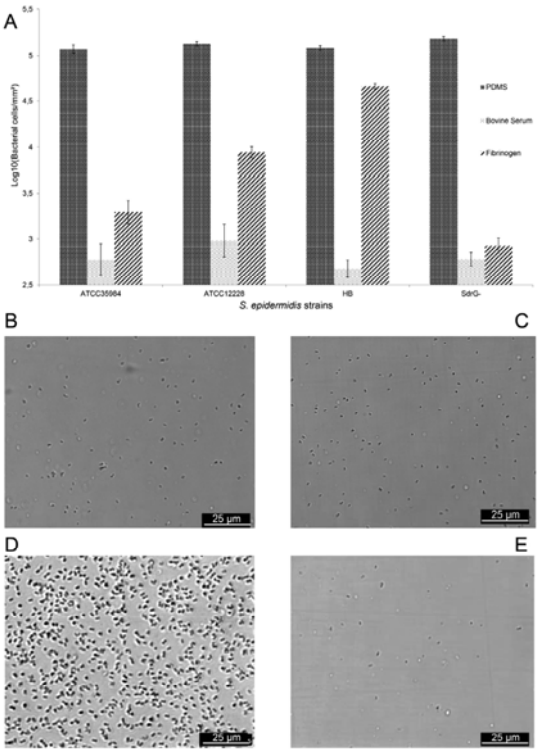

Figure 2: Whole population adhesion assays on bare and coated PDMS surfaces in 96-well plates.
A. Plot density of surface bound bacterial cells on the surface of the well. Adhesion of *S. epidermidis* strains ATCC 12228, ATCC35984, HB and HB SdrG$^{(-)}$ to PDMS either bare or coated with Fg or BS is represented. Error bars are confidence intervals at 95 %.
B—E. Micrographs of the surface of a well of Fg-coated PDMS at the end of the adhesion assay performed with suspensions of ATCC 35984, ATCC 12228, HB, and HB SdrG$^{(-)}$, respectively. The scale bar indicates 25 µm.

Single-cell adhesion forces

The binding forces between single *S. epidermidis* cells and PDMS, Fg-coated and BS-coated surfaces were then measured using SCFS[20]. As illustrated in **Figure 3A**, single-bacterial cells were picked up with colloidal probe cantilevers coated with polydopamine. Force-distance curves were then recorded between the cellular probes and the different substrates. **Figure 3B** shows the adhesion force histograms, as well as representative force curves, obtained between three different cells (black, red and green histograms) of ATCC 12228, ATCC 35984, HB and HB SdrG$^{(-)}$ strains and bare, BS-coated and Fg-coated PDMS surfaces.

On bare PDMS, all strains displayed 100 % of adhesive events, indicating strong binding to hydrophobic surfaces. The binding forces varied amongst the strains, from ~250 pN to 1,500 pN. These forces most probably result from hydrophobic interactions between the cell surfaces and PDMS. The surface hydrophobicity of *S. epidermidis* has been reported to be strain-dependent[21] and be essentially mediated by surface proteins such as AtlE and Aae[8]. By contrast, on BS-coated surfaces, ATCC 35984, HB and SdrG$^{(-)}$ cells showed hardly any binding, while ATCC 12228 featured adhesion forces of 50-100 pN in 20 % of the curves. On Fg-coated surfaces, the differences between the strains were more pronounced. While there was hardly any adhesion with ATCC 35984, one out of the three ATCC 12228 cells showed strong interactions towards the Fg-coated surface. This *intra*-strain variation reflects heterogeneity of the cell population. The force value (~2.1 nN), as well as the force signatures, were similar to those previously observed and associated with the Fg-SdrG 'dock, lock and latch' binding mechanism[13]. The adhesive ATCC 12228 cell presented a relatively low adhesion frequency of 30 % compared to what we found previously[13]. For strain HB, the adhesion frequency, the recorded force value and the force signatures were comparable to what was previously observed[13]. *S. epidermidis* HB however showed greater adhesion reflecting the possibility of probing multiple SdrG-Fg interactions in parallel. HB SdrG$^{(-)}$, in which the *fbe* gene has been disrupted, was then used to confirm the specificity of the SdrG-Fg interactions. As expected, HB SdrG$^{(-)}$ cells showed little to no adhesion.

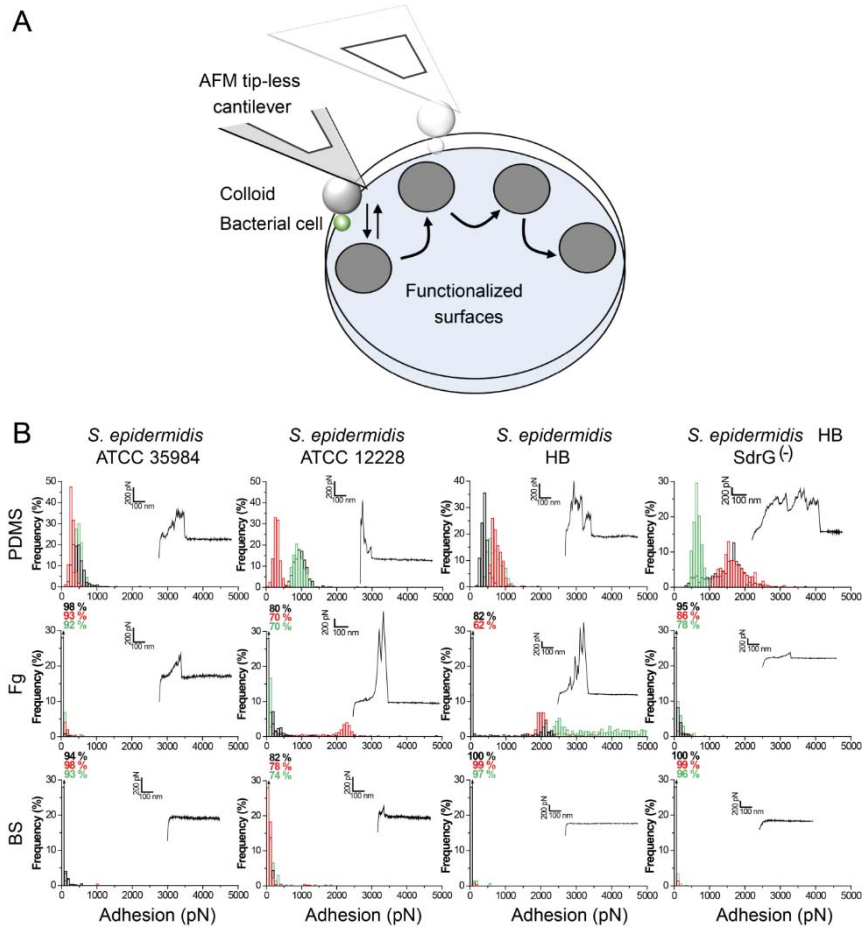

Figure 3: Single-cell force spectroscopy (SCFS) of the interaction between *S. epidermidis* strains and PDMS, Fg-, and BS-coated substrates.
A. Schematic representation of the SCFS protocol. The bacterial probe is composed of a bacterial cell, attached to a colloidal bead immobilized onto a tipless AFM cantilever. The same bacterial probe is brought into contact with PDMS, Fg, and BS-coated surfaces.
B. Adhesion force histograms, together with representative force curves (x axis represents the distance (in nm) while the y axis is the force (in pN), for the four *S. epidermidis* strains ATCC 12228, ATCC 35984, HB and HB SdrG$^{(-)}$ interacting with the three types of surfaces. The three colors (black, red and green) represent the results obtained with three independent bacterial cells.

Finally, BS-coated surfaces were tested to further control the specificity of binding on PDMS and Fg-coated substrates. ATCC 35984, HB and HB SdrG$^{(-)}$ cells showed hardly any adhesion reflecting the specific nature of the adhesion forces. ATCC 12228 however showed little adhesion characterized by weak adhesion forces (< 250 pN) with a low adhesion frequency (18 to 26 %).
In general, the trends observed in SCFS results are in line with those of whole population adhesion assays. Adhesion to Fg-coated surfaces occurring through the specific SdrG-Fg recognition is well documented in the SCFS data of the HB strain and still present but less marked in the strain ATCC 12228, whereas

ATCC 35984 and SdrG$^{(-)}$ showed no sign of affinity for Fg. Hydrophobic PDMS is very reactive towards *S. epidermidis* cell surfaces and the protein layer covering the BS-coated PDMS almost totally inhibits the cell-surface interactions resulting in very low adhesiveness.

Mapping single SdrG proteins on the *S. epidermidis* cell surface

AFM-based single molecule force spectroscopy (SMFS)[22,23] was used to map the distribution of single SdrG molecules on living bacteria. The cell surface of the ATCC 12228, ATCC 35984, HB and HB SdrG$^{(-)}$ strains was probed with a Fg-modified tip in order to detect the presence of SdrG (**Figure 4**). Spatially-resolved SMFS of live cells immobilized on porous membranes (**Figure 4A**) allowed us to directly measure the localization and binding strength of single adhesions. In this analysis, specific adhesive events were attributed to single SdrG molecules in the light of previous work[13]. The maps resulting from these experiments are shown in **Figure 4B**; they display the spatial distribution of single SdrG molecules of a 0.25 µm² area on the cell surface which represents about 1/10 of the total bacterial cell surface.

The highest density (between 19 and 29 %) of SdrG molecules was found on the HB strain. The strain ATCC 12228, ranked second as one of the tested cells, displayed 12 % of adhesive events, while the cell surfaces of the two others were almost non-adhesive. This behavior could reflect the natural heterogeneity of the bacterial population. Indeed, stochastic gene expression can generate diversity amongst the cells of a population[24,25]. For the mutant strain SdrG$^{(-)}$, two cells displayed 10 % of adhesive events but these interactions are likely to be non-specific since no typical SdrG-Fg force signatures were observed (**Figure 4C**). Finally, ATCC 35984 was essentially non-adhesive (99 % of non-adhesive events). This indicates that ATCC 35984 has the same reactivity towards Fg as the mutant strain in which the *fbe* gene coding for SdrG has been deleted. As this strain carries a copy of *fbe*, its lack of adhesion to Fg could be explained by a strain dependent genetic regulation, possibly cross-influenced by other regulatory/signaling pathways. The possibility to have a significant crowding by other cell surface polymers that would reduce the opportunity for SdrG to appropriately bind to Fg cannot be excluded.

These SMFS results provide direct indication as to the abundance of SdrG on the cell surface of *S. epidermidis* strains. These strains can be classified in the following order: HB > ATCC 12228 > ATCC35984 ≈ SdrG$^{(-)}$. This corresponds to the conclusions drawn from the whole population adhesion assays and the SCFS data on Fg-coated surfaces.

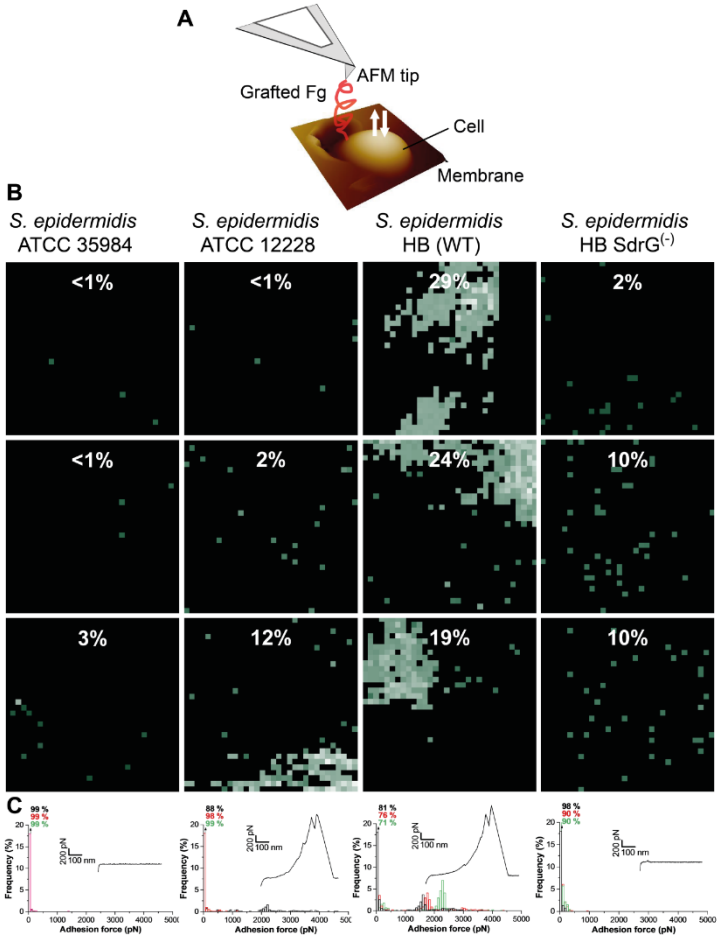

Figure 4: Imaging single SdrG proteins on the *S. epidermidis* cell surfaces using single-molecule force spectroscopy (SMFS) with Fg-modified AFM tips.
A. The surface of a bacterial cell trapped in a porous membrane is probed with a Fg-modified tip. Deflection image shows the emerging part of the trapped cell.
B. Adhesion forces maps (500 nm x 500 nm) recorded on the different strains using Fg-tips. Every bright pixel documents the detection of a single SdrG protein. Percentages indicated on top of the maps correspond to the detection frequency for every map. The data were obtained from three independent cells for each strain.
C. Adhesion force histograms (x-axis represents the magnitude of the binding forces while y-axis represents the percentage of events) together with representative force curves. For HB and ATCC 12228 strain, the large forces (~ 2 nN) are attributed to the binding of SdrG to Fg. The three colors (black, red and green) represent the results obtained with the three independent bacterial cells of each strain.

Discussion

Adhesion of bacteria on implanted biomaterials determines their fate in the host. Bacterial anchorage on surfaces paves the way to the development of biofilms and determines the ability to cause chronic infections[7]. In *S. epidermidis*, SdrG mediates strong and specific binding to Fg, a molecule most often present in the conditioning film of proteins that forms upon implantation

of devices [26]. In this paper, we present pieces of evidence that underline the importance of the cell surface abundance of SdrG in the ability of single cells and whole populations to efficiently adhere to surface bound Fg.

First, it was observed that the Fg binding activity of SdrG on the cell surface is influenced by strong frictional forces. Adhesion assays performed with bacterial suspensions from the same culture prepared using distinct centrifugation parameters resulted in decrease bacterial surface density on Fg-coated PDMS for the suspension submitted to repeated centrifugation steps or to a higher centrifugation speed. Centrifugation has recently been reported to cause damages at the bacterial cell surface, notably causing a decrease in *Staphylococcus aureus* adhesion to glass substrates[27]. It is likely that the quaternary structure of SdrG is altered by excessive frictional forces occurring between two cells surfaces, therefore impairing its ability to specifically recognize Fg. As a consequence, reducing manipulations that involve frictional forces as much as possible is highly recommended when studying the Fg-binding function of SdrG.

Using complementary population- and single cell-based approaches, the adhesion of *S. epidermidis* to Fg-coated surfaces was found to be strongly strain dependent. Indeed, SCFS showed that the affinity of HB strain for surface bound Fg was high, ATCC 12228 affinity was less marked whereas ATCC 35984 and SdrG$^{(-)}$ did not display any specific recognition of Fg. In line with these conclusions, the adhesion of whole population assays resulted in high surface bacterial density of the HB strain, moderate adhesion of ATCC 12228 and the two other strains displayed the same level of adhesion as on the control BS-coated PDMS, indicating the absence of specific SdrG-Fg recognition.

Based on these results, it was postulated that the differences between strains could originate from variations in the abundance of SdrG on the cell surface. To get more insights on the distribution of active SdrG molecules on the *S. epidermidis* surface, SMFS with a Fg-modified AFM tip was used to probe the surface of the strains. The proportion of sites that specifically recognized Fg were numerous for HB strain, with about 20 % of the surface of three independent HB cells that interacted with Fg according to the 'dock, lock and latch' mechanism. For ATCC 12228, 12 % of the surface of one ATCC 12228 cell did recognize Fg, but no SdrG could be detected on the other two cells tested. On the last two strains ATCC 35984 and HB SdrG$^{(-)}$, the SdrG adhesin was not detected on the cell surface. Our interpretation is that the abundance

of SdrG on the cell surface determines the ability of single cells and whole bacterial population to remain bound on a surface conditioned with Fg.
The results of bacterial adhesion on bare and BS-coated PDMS lead us to argue on the ecological role of SdrG in *S. epidermidis*. Indeed, since the attractive hydrophobic surfaces become repelling as they are conditioned with serum proteins[28,29], SdrG provides bacteria with the ability to counterbalance the effect of the adhesion-inhibiting layer of proteins and mediate adhesion to the surface.
The expression of *fbe*, at both mRNA and protein levels, has already been shown to be rather low in *in vitro* culture and to significantly increase following exposure to *in vivo* environments, *i.e.* in a murine model[30]. In *S. aureus*, the expression of many virulence factors, including the fibrinogen binding protein, is significantly higher in human blood as confirmed by transcriptome analysis[31]. In the same vein, the expression of MSCRAMMs in *S. aureus* has recently been reported to strongly increase in the presence of human plasma *in vitro*[32]. Even though the regulatory pathway involved in *fbe* expression has not yet been elucidated, it is clear that *S. epidermidis* has developed a strategy to crowd its surface with SdrG when the bacteria are inside their host. Taken together with the results of this work, this suggests that *S. epidermidis* responds to environmental changes in order to improve its adhesiveness to surfaces partially coated by Fg, such as indwelling medical devices and host tissues. It is generally admitted that increased adhesion to biomaterials is a key step for *S. epidermidis* to establish in the host in the form of a biofilm, therefore causing chronic infections.
In conclusion, this paper establishes a link between the abundance of SdrG on the cell surface of *S. epidermidis* and the adherence of this species to the surface of materials coated with Fg, *i.e.* vascular catheters and prostheses. Future works identifying the molecular regulation pathways that control *fbe* expression and surface density of SdrG and, hence, the adherence to Fg-coated surfaces would help to understand the critical factors that govern the onset of a chronic nosocomial infection involving biofilms of *S. epidermidis*.

Acknowledgements

We thank Prof. T. Foster for kindly providing the HB SdrG$^{(-)}$ *S. epidermidis* strain. This work was supported by the National Foundation for Scientific Research (FNRS), the *Université catholique de Louvain* and the Research Department of the *Communauté française de Belgique* (Concerted Research Action, ARC12-17-046), the Federal Office for Scientific, Technical and Cultural Affairs (Interuniversity Poles of Attraction Programme). T. Vanzieleghem is a FNRS research fellow, Y.F.D. is a Research Director of the FNRS.

References

(1) McCann, M. T.; Gilmore, B. F.; Gorman, S. P. *Staphylococcus epidermidis* Device-Related Infections: Pathogenesis and Clinical Management. *J. Pharm. Pharmacol.* 2008, 60, 1551–1571.

(2) Otto, M. Molecular basis of *Staphylococcus epidermidis* Infections. *Semin Immunopathol.* 2012, 34, 201–214.

(3) Raad, I.; Hanna, H.; Maki, D. Intravascular Catheter-Related Infections: Advances in Diagnosis, Prevention, and Management. *Lancet. Infect. Dis.* 2007, 7, 645–657.

(4) O'Grady, N. P.; Alexander, M.; Dellinger, E. P.; Gerberding, J. L.; Heard, S. O.; Maki, D. G.; Masur, H.; McCormick, R. D.; Mermel, L. A.; Pearson, M. L.; *et al.* Guidelines for the Prevention of Intravascular Catheter-Related Infections. Centers for Disease Control and Prevention. Recomm. reports Morb. Mortal. Wkly. report. *Recomm. reports / Centers Dis. Control* 2002, 51, 1–29.

(5) Dantes, R.; Mu, Y.; Belflower, R.; Aragon, D.; Dumyati, G.; Harrison, L. H.; Lessa, F. C.; Lynfield, R.; Nadle, J.; Petit, S.; *et al.* National Burden of Invasive Methicillin-Resistant *Staphylococcus aureus* Infections, United States, 2011. *JAMA Intern. Med.* 2013, 173, 1970–1978.

(6) Boles, B. R.; Horswill, A. R. Staphylococcal Biofilm Disassembly. *Trends Microbiol.* 2011, 19, 449–455.

(7) Pavithra, D.; Doble, M. Biofilm Formation, Bacterial Adhesion and Host Response on Polymeric Implants--Issues and Prevention. *Biomed. Mater.* 2008, 3, 034003.

(8) Heilmann, C. Bacterial Adhesion. In Advances in Experimental Medicine and Biology; Linke, D.; Goldman, A., Eds.; *Adv. Exp. Med. Biol.* Springer Netherlands: Dordrecht, 2011; Vol. 715, pp. 105–123.

(9) Mack, D.; Davies, A. P.; Harris, L. G.; Rohde, H.; Horstkotte, M. a; Knobloch, J. K.-M. Microbial Interactions in *Staphylococcus epidermidis* Biofilms. *Anal. Bioanal. Chem.* 2007, 387, 399–408.

(10) Arrecubieta, C.; Lee, M.-H.; Macey, A.; Foster, T. J.; Lowy, F. D. SdrF, a *Staphylococcus epidermidis* Surface Protein, Binds Type I Collagen. *J. Biol. Chem.* 2007, 282, 18767–18776.

(11) Hartford, O.; O'Brien, L.; Schofield, K.; Wells, J.; Foster, T. J. The Fbe (SdrG) Protein of *Staphylococcus epidermidis* HB Promotes Bacterial Adherence to Fibrinogen. *Microbiology* 2001, 147, 2545–2552.

(12) Ponnuraj, K.; Bowden, M. G.; Davis, S.; Gurusiddappa, S.; Moore, D.; Choe, D.; Xu, Y.; Hook, M.; Narayana, S. V. L. A "Dock, Lock, and

Latch" Structural Model for a Staphylococcal Adhesin Binding to Fibrinogen. *Cell* 2003, 115, 217–228.

(13) Herman, P.; El-Kirat-Chatel, S.; Beaussart, A.; Geoghegan, J. A.; Foster, T. J.; Dufrêne, Y. F. The Binding Force of the Staphylococcal Adhesin SdrG Is Remarkably Strong. *Mol. Microbiol.* 2014, 93, 356–368.

(14) Herman, P.; El-Kirat-Chatel, S.; Beaussart, A.; Geoghegan, J. A.; Vanzieleghem, T.; Foster, T. J.; Hols, P.; Mahillon, J.; Dufrêne, Y. F. Forces Driving the Attachment of *Staphylococcus epidermidis* to Fibrinogen-Coated Surfaces. *Langmuir* 2013, 29, 13018–13022.

(15) Alsteens, D.; Beaussart, A.; El-Kirat-Chatel, S.; Sullan, R. M. A.; Dufrêne, Y. F. Atomic Force Microscopy: A New Look at Pathogens. *PLoS Pathog.* 2013, 9, e1003516.

(16) Dufrêne, Y. F. Atomic Force Microscopy in Microbiology: New Structural and Functional Insights into the Microbial Cell Surface. *MBio* 2014, 5, e01363–14.

(17) Nilsson, M.; Frykberg, L.; Flock, J.; Pei, L.; Guss, B.; Pei, L. E. I.; Lindberg, M. A Fibrinogen-Binding Protein of *Staphylococcus epidermidis*. *Infect. Immun.* 1998, 66, 2666–2673.

(18) Dufrêne, Y. F. Towards Nanomicrobiology Using Atomic Force Microscopy. *Nat. Rev. Microbiol.* 2008, 6, 674–680.

(19) Ebner, A.; Wildling, L.; Kamruzzahan, A. S. M.; Rankl, C.; Wruss, J.; Hahn, C. D.; Hölzl, M.; Zhu, R.; Kienberger, F.; Blaas, D.; *et al.* A New, Simple Method for Linking of Antibodies to Atomic Force Microscopy Tips. *Bioconjug. Chem.* 2007, 18, 1176–1184.

(20) Beaussart, A.; El-Kirat-Chatel, S.; Sullan, R. M. A.; Alsteens, D.; Herman, P.; Derclaye, S.; Dufrêne, Y. F. Quantifying the Forces Guiding Microbial Cell Adhesion Using Single-Cell Force Spectroscopy. *Nat. Protoc.* 2014, 9, 1049–1055.

(21) Krepsky, N.; Rocha Ferreira, R. B.; Ferreira Nunes, A. P.; Casado Lins, U. G.; Costa e Silva Filho, F.; de Mattos-Guaraldi, A. L.; Netto-dosSantos, K. R. Cell Surface Hydrophobicity and Slime Production of *Staphylococcus epidermidis* Brazilian Isolates. *Curr. Microbiol.* 2003, 46, 280–286.

(22) Alsteens, D.; Garcia, M. C.; Lipke, P. N.; Dufrêne, Y. F. Force-Induced Formation and Propagation of Adhesion Nanodomains in Living Fungal Cells. *Proc. Natl. Acad. Sci. U. S. A.* 2010, 107, 20744–20749.

(23) Andre, G.; Kulakauskas, S.; Chapot-Chartier, M.-P.; Navet, B.; Deghorain, M.; Bernard, E.; Hols, P.; Dufrêne, Y. F. Imaging the

Nanoscale Organization of Peptidoglycan in Living *Lactococcus lactis* Cells. *Nat. Commun.* 2010, 1, 27.

(24) Thattai, M.; van Oudenaarden, A. Stochastic Gene Expression in Fluctuating Environments. *Genetics* 2004, 167, 523–530.

(25) Kaern, M.; Elston, T. C.; Blake, W. J.; Collins, J. J. Stochasticity in Gene Expression: From Theories to Phenotypes. *Nat. Rev. Genet.* 2005, 6, 451–464.

(26) Canales, B. K.; Higgins, L.; Markowski, T.; Anderson, L.; Li, Q. a; Monga, M. Presence of Five Conditioning Film Proteins Are Highly Associated with Early Stent Encrustation. *J. Endourol.* 2009, 23, 1437–1442.

(27) Peterson, B. W.; Sharma, P. K.; van der Mei, H. C.; Busscher, H. J. Bacterial Cell Surface Damage due to Centrifugal Compaction. *Appl. Environ. Microbiol.* 2012, 78, 120–125.

(28) Linnes, J. C.; Mikhova, K.; Bryers, J. D. Adhesion of *Staphylococcus epidermidis* to Biomaterials Is Inhibited by Fibronectin and Albumin. *J. Biomed. Mater. Res.* A 2012, 100, 1990–1997.

(29) Xu, L.-C.; Siedlecki, C. A. Effects of Plasma Proteins on *Staphylococcus epidermidis* RP62A Adhesion and Interaction with Platelets on Polyurethane Biomaterial Surfaces. *J. Biomater. Nanobiotechnol.* 2012, 03, 487–498.

(30) Sellman, B. R.; Timofeyeva, Y.; Nanra, J.; Scott, A.; Fulginiti, J. P.; Matsuka, Y. V; Baker, S. M. Expression of *Staphylococcus epidermidis* SdrG Increases Following Exposure to an *in vivo* Environment. *Infect. Immun.* 2008, 76, 2950–2957.

(31) Malachowa, N.; Whitney, A. R.; Kobayashi, S. D.; Sturdevant, D. E.; Kennedy, A. D.; Braughton, K. R.; Shabb, D. W.; Diep, B. A.; Chambers, H. F.; Otto, M.; *et al.* Global Changes in *Staphylococcus aureus* Gene Expression in Human Blood. *PLoS One* 2011, 6, e18617.

(32) Cardile, A. P.; Sanchez, C. J.; Samberg, M. E.; Romano, D. R.; Hardy, S. K.; Wenke, J. C.; Murray, C. K.; Akers, K. S. Human Plasma Enhances the Expression of Staphylococcal Microbial Surface Components Recognizing Adhesive Matrix Molecules Promoting Biofilm Formation and Increases Antimicrobial Tolerance *In vitro*. *BMC Res. Notes* 2014, 7, 457.

Chapter III

Atomic force microscopy reveals a dual collagen-binding activity for the staphylococcal surface protein SdrF

Philippe Herman-Bausier and Yves F. Dufrêne

In *Molecular Microbiology*, **2015**, DOI: 10.1111mmi.13254

I performed the research and wrote the paper.

Summary

Staphylococcus epidermidis causes nosocomial infections by colonizing and forming biofilms on indwelling medical devices. This process involves specific interactions between cell wall-anchored (CWA) proteins and host proteins adsorbed onto the biomaterial. Here, we have explored the molecular forces by which the *S. epidermidis* CWA protein SdrF binds to type I collagen, by means of advanced atomic force microscopy (AFM) techniques. Using single-cell force spectroscopy, we found that SdrF mediates bacterial adhesion to collagen-coated substrates through both weak and strong bonds. Single-molecule force spectroscopy demonstrated that these bonds involve the A and B regions of SdrF, thus revealing that the protein is capable of dual ligand-binding activity. Both weak and strong bonds showed high dissociation rates, indicating they are much less stable than those formed by the well-characterized 'dock, lock and latch' mechanism. Collectively, our results show that CWA proteins can bind to ligands by novel mechanisms. We anticipate that AFM will greatly contribute to the identification of novel binding partners and binding mechanisms in staphylococcal CWA proteins.

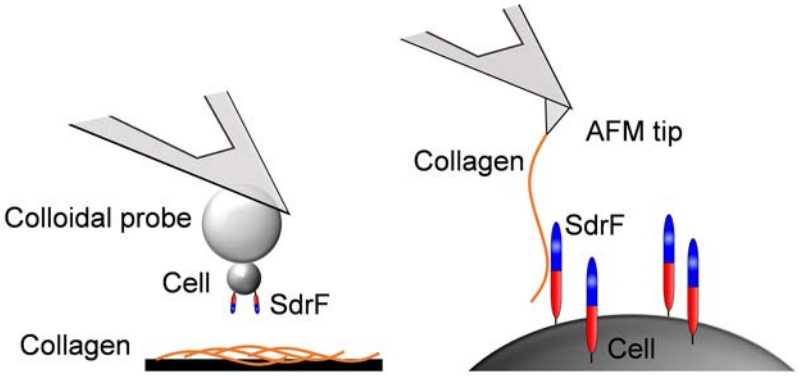

Introduction

Staphylococcus epidermidis is an important nosocomial pathogen which is a leading cause of infections associated with indwelling medical devices (Vuong & Otto, 2002, Otto, 2009). These infections involve adhesion of the bacteria to the implanted materials that have been conditioned with host proteins such as albumin, fibronectin, fibrinogen (Fg) and collagen (Cn). Adhesion to these target proteins is mediated by a family of cell-wall-anchored (CWA) proteins, the Microbial Surface Components Recognizing Adhesive Matrix Molecules (MSCRAMMs) (Otto, 2009, Foster *et al.*, 2014). Despite the vast amount of molecular biology data available on staphylococcal MSCRAMMs, we know little about the molecular forces by which these proteins drive bacterial adhesion.

The serine-aspartate repeat protein F (SdrF), which belongs to Sdr subclass of MSCRAMMs (McCrea *et al.*, 2000, Bowden *et al.*, 2005), is known to bind Cn (Arrecubieta *et al.*, 2007), thus helping to explain how *S. epidermidis* is able to attach to transcutaneous drivelines from explanted ventricular assist devices from patients with congestive heart failure (Arrecubieta *et al.*, 2009). SdrF is composed of a secretion signal sequence, followed by the A region containing the three separately folded subdomains N1, N2 and N3 (**Figure 1A**). Next to the A region is the B region, followed by serine-aspartate repeats sequences and the C-terminus region that anchors the protein to the cell wall (Bowden *et al.*, 2005). Sequence similarity analysis and secondary structure prediction have suggested that the A region is the ligand binding domain, while the B region would help projecting the A region on the cell surface (Bowden *et al.*, 2005). However, recent work using *Lactococcus lactis* expressing SdrF, a protein-protein interaction assay and Western ligand blot analysis revealed that Cn binding involves the B region (Arrecubieta *et al.*, 2007). So the relative contributions of the A and B regions in Cn binding are not completely clear. Also, the specific forces engaged in ligand binding are not known.

Classical bioassays have provided valuable information about the molecular details of staphylococcal adhesion. These approaches probe large ensembles of cells and molecules, and they are not capable of measuring the molecular forces that govern cell adhesion. Recently, atomic force microscopy (AFM) has been increasingly used to address this issue, both at the single-cell and single-molecule levels (Dufrêne, 2014, Dufrêne, 2015). Single-molecule force spectroscopy (SMFS) enables researchers to map the localization of individual proteins on the surface of staphylococci and to probe their binding strength (Lower *et al.*, 2010, Xu *et al.*, 2012). In parallel, single-cell force spectroscopy

(SCFS) can measure the forces involved in cell-substrate and cell-cell interactions (Emerson *et al.*, 2006, Beaussart *et al.*, 2013a, Herman *et al.*, 2014, Herman-Bausier *et al.*, 2015, Vanzieleghem *et al.*, 2015). Here, we combine SCFS and SMFS to investigate the ligand-binding activity of SdrF. To study the protein in its fully functional cellular context and in the absence of other staphylococcal adhesive molecules, we used recombinant *L. lactis* strains expressing SdrF (Arrecubieta *et al.*, 2007). Comparative analysis of strains producing either full-length proteins or only the A or B regions enables us to assess the relative roles of these regions in type I Cn binding. The results show that SdrF mediates ligand binding by strong and weak bonds involving both the A and B regions of the protein, thus highlighting an unanticipated dual collagen-binding activity for this protein.

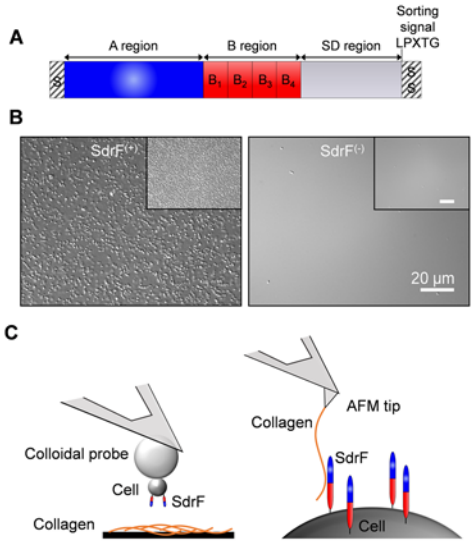

Figure 1: Collagen-binding activity of SdrF: from the microscale to the nanoscale.
A. Schematic representation of the *S. epidermidis* SdrF protein: S, secretory signal sequence; A region comprising N1 N2 and N3 subdomains; B region containing binding subdomains; SD region comprising repetition of Ser-Asp dipeptide repeats and C-terminus region containing a sorting signal comprising the LPXTG motif. While the subdomains of the A region do not have any amino acid sequence similarity, the B subdomains share an average identity of 55 % (Arrecubieta *et al.*, 2007).
B. SdrF mediates microscopic bacterial adhesion to Cn surfaces. Optical (DIC) images showing the adhesion behavior of *L. lactis* SdrF$^{(+)}$ cells (left) and *L. lactis* SdrF$^{(-)}$ cells (right), after 2 h incubation on type I Cn-coated substrates. Insets are representative images from duplicate experiments.
C. Force nanoscopy of the SdrF-Cn interaction. To study single-cell adhesion forces by SCFS (left), living bacteria were attached on polydopamine-coated colloidal cantilevers and force curves were obtained between cellular probes and type I Cn-substrates. To probe the distribution and binding forces of single SdrF proteins on living bacteria with SMFS (right), bacterial cell surfaces were scanned using AFM tips functionalized with type I Cn. The cartoons are not to scale.

Results and discussion

Bacterial adhesion to collagen-coated substrates

Microscopic adhesion assays were used to confirm that SdrF was expressed on the surface of *L. lactis* producing the full-length protein (hereafter SdrF$^{(+)}$ cells), and that the proteins were functional, thus capable of binding to Cn. Optical microscopy images revealed that SdrF$^{(+)}$ cells adhered strongly to type I Cn-coated substrates, while no adhesion was observed with wild-type *L. lactis* cells (SdrF$^{(-)}$ cells, **Figure 1B**). This indicates that SdrF is produced appropriately by *L. lactis* SdrF$^{(+)}$ cells and that the protein shows strong Cn-binding activity.

Force nanoscopy of the SdrF-collagen interaction

We used SCFS (Helenius *et al.*, 2008, Müller *et al.*, 2009, Beaussart *et al.*, 2013b, Beaussart *et al.*, 2014, Herman *et al.*, 2014) to measure the SdrF-Cn binding forces at the whole cell level. Single SdrF$^{(+)}$ cells were attached onto colloidal cantilevers coated with polydopamine, a bioinspired polydopamine wet adhesive, and force-distance curves were then recorded between the cell probes and Cn substrates (**Figure 1C**, left). Labelling of the cell probe with the *Bac*light LIVE/DEAD stain showed that the bacterial cell membrane was still intact and that the method is non-destructive (**Figure 2A**, inset, green color). SMFS (Dupres *et al.*, 2005, Hinterdorfer & Dufrêne, 2006, Dupres *et al.*, 2009, Alsteens *et al.*, 2010, Andre *et al.*, 2010, El-Kirat-Chatel *et al.*, 2014, Herman *et al.*, 2014) with AFM tips functionalized with Cn enabled us to map and manipulate single SdrF proteins on living bacteria (**Figure 1C**, right). The tip was functionalized with a PEG-benzaldehyde linker to favor single-molecule detection (Ebner *et al.*, 2007).

Specific adhesive forces between single bacteria and collagen

By means of SCFS, we measured the forces between single bacterial cells and Cn-substrates. Fluorescence images revealed that most cells on the AFM probes were actually dividing cells (**Figure 2A**, inset image). **Figure 2** shows the adhesion forces, rupture lengths, and representative retraction force curves, obtained at 1 s contact time for three different *L. lactis* SdrF$^{(+)}$ cells from independent cultures (similar data were obtained in a total of 21 SdrF$^{(+)}$ cells). The main features of the force curves did not substantially change when recording consecutive curves on different spots of the substrate, meaning that the measurements did not alter the adhesive response of the cells. Cells from different cultures generally yielded similar results, indicating homogeneity and reproducibility of the cell populations. Essentially all force profiles showed adhesion events of ~100-3000 pN magnitude and ~25-1000 nm rupture length (range from a total of 1290 curves). As these forces were not observed on

SdrF$^{(-)}$ cells (**Figure 2B**) and were decreased upon injection of soluble Cn, they represent specific interactions between single (or a few) SdrF and Cn molecules. The long ruptures (up to 1000 nm) are consistent with the structure of Cn, known to form 300 nm-long filaments that tend to self-associate.

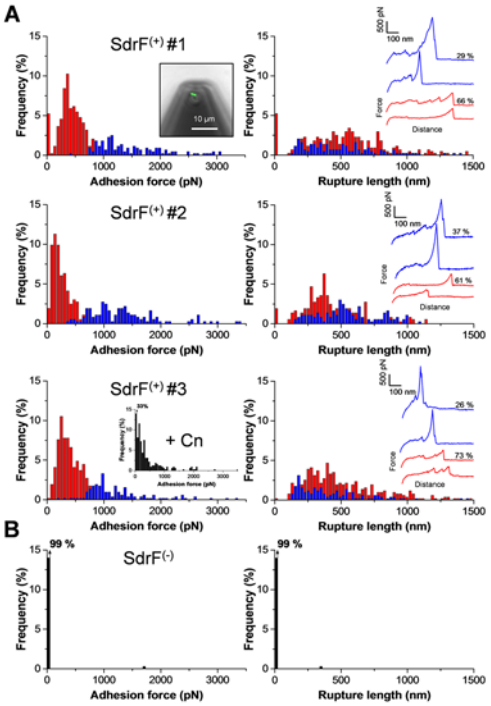

Figure 2: Specific adhesion forces between single *L. lactis* SdrF$^{(+)}$ cells and collagen-coated substrates.
A. Adhesion force histograms (left) and rupture length histograms (right) with representative force signatures (insets), obtained by recording multiple force-distance curves (n > 370 curves for each cell) in PBS buffer between three different SdrF$^{(+)}$ cells and type I Cn-substrates. The inset in the upper left panel is an optical microscope image of a living bacterial cell attached to the colloidal cantilever probe (green color). The inset in the lower left panel shows an adhesion force histogram obtained after injection of free Cn (0.1 mg ml^{-1}). All curves were obtained using a contact time of 1 s, a maximum applied force of 250 pN, and approach and retraction speeds of 1000 nm s^{-1}. Similar data were obtained in a total of 21 different SdrF$^{(+)}$ cells.
B. Force data obtained in the same conditions for a SdrF$^{(-)}$ cell. Similar data were obtained in a total of 5 different SdrF$^{(-)}$ cells.

Close examination of the binding forces revealed two types of signatures: weak forces of 362 ± 200 pN magnitude (n = 844 curves from 3 cells; frequency ~70%) and strong forces of 1264 ± 423 pN magnitude (n = 351 curves; frequency ~30%). Because these events were reproducibly observed on different cells, we suggest they represent two distinct binding processes, involving different regions of SdrF. The measured adhesion forces are larger than values typically observed for single bacterial adhesins, implying that either multiple bonds are probed in parallel and/or that the SdrF-Cn bonds are strong.

We then asked whether SdrF shows similar binding behaviour in its natural staphylococcal environment? We therefore investigated the *S. epidermidis* 9142 strain (McCrea *et al.*, 2000), which shows a strong capacity to bind collagen (**Figure 3A**, inset). **Figure 3** presents the force data obtained between single *S. epidermidis* cells and Cn-substrates. Remarkably, the adhesion frequencies, adhesion forces and rupture lengths were similar to those of the *L. lactis* SdrF$^{(+)}$ strain, both weak and strong binding forces being also observed. This finding leads us to believe that the SdrF-Cn binding forces measured in *L.*

lactis are relevant to those occurring in *S. epidermidis*, and that the use of *L. lactis* as a surface display model to study SdrF is appropriate.

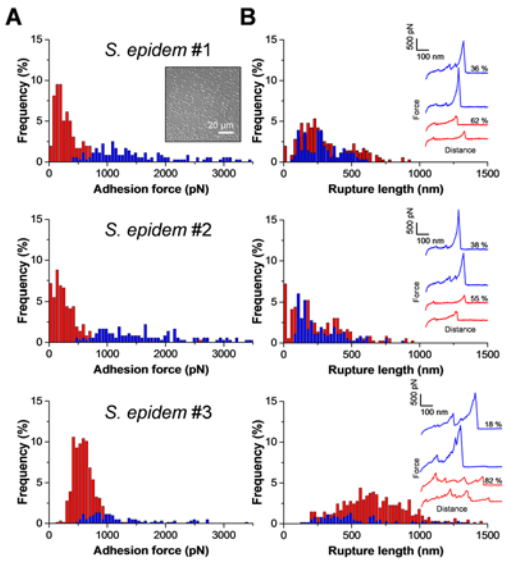

Figure 3: Adhesion forces between single *S. epidermidis* cells and collagen-coated substrates. **A, B.** Adhesion force histograms (**A**) and rupture length histograms (**B**) with representative force signatures (insets), obtained by recording multiple force-distance curves (n > 350 curves for each cell) in PBS buffer between three different cells from the *S. epidermidis* 9142 strain and type I Cn-substrates. The inset in the upper left panel shows that this strain displays a strong ability to bind collagen. All curves were obtained using a contact time of 1 s, a maximum applied force of 250 pN, and approach and retraction speeds of 1000 nm s^{-1}. Similar data were obtained in a total of 6 different cells.

Single-molecule analysis documents a dual collagen-binding activity for SdrF

To gain a molecular view of the SdrF-Cn binding forces, spatially-resolved SMFS with AFM tips labelled with type I Cn was used to localize single SdrF proteins on living bacteria and to quantify the strength of single SdrF-Cn bonds (**Figure 4**). A large fraction (~40 %) of the force profiles recorded across the surface of *L. lactis* $SdrF^{(+)}$ cells featured single adhesion peaks with either weak force, 132 ± 48 pN, or strong force, 520 ± 140 pN (from a total of 3072 curves obtained on 3 cells; similar data were obtained in a total of 12 $SdrF^{(+)}$ cells). As these binding events were not seen in $SdrF^{(-)}$ cells (**Figure 4B**), they can be attributed to SdrF. Adhesion maps (**Figure 4A**, left insets) revealed that SdrF was largely exposed on the cell surface, and that weak and strong forces were randomly distributed. Considering the average detection frequency, 43 %, and the size of adhesion maps, 1024 curves across 0.25 µm² areas, this yields a minimum surface density of ~1760 proteins/µm².

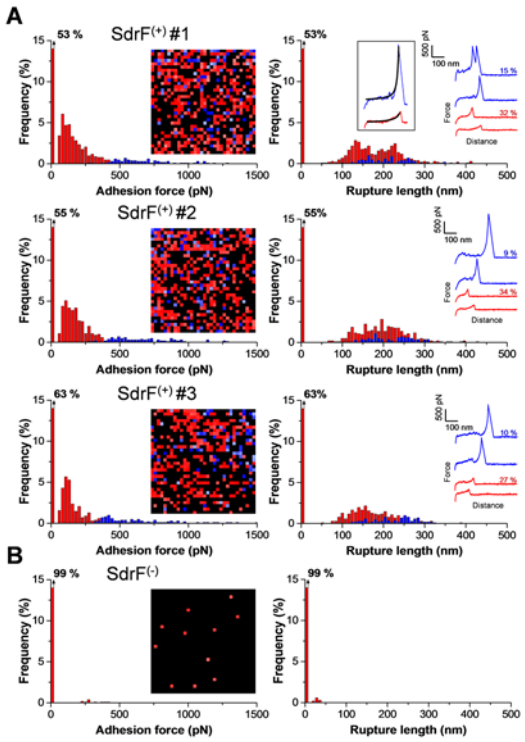

Figure 4: Localization and binding strength of single SdrF proteins on *L. lactis* SdrF$^{(+)}$ cells.
A. Adhesion force histograms with adhesion force maps (insets, 500 nm x 500 nm, color scale: 1000 pN) (left) and rupture length histograms with representative force curves (right) obtained by recording force curves in PBS across the surface of three SdrF$^{(+)}$ cells using tips labelled with type I Cn. The red and blue colors highlight dual detection of weak and strong binding events. The curves in the upper right inset (box) show that adhesion forces were well-fitted with the worm-like-chain model (WLC) using a persistence length of 0.4 nm. All curves were obtained using a contact time of 100 ms, a maximum applied force of 250 pN, and approach and retraction speeds of 1000 nm s^{-1}. Similar data were obtained in a total of 12 different SdrF$^{(+)}$ cells.
B. Force data obtained in the same conditions for a SdrF$^{(-)}$ cell. Similar data were obtained in a total of 3 different SdrF$^{(-)}$ cells.

Despite the long, filamentous nature of the Cn molecule, we believe that mostly single SdrF-Cn interactions were probed at a time, and that the same adhesins were not detected multiple times as: (i) we used a well-established protocol making use of a PEG-benzaldehyde linker for tip modification (Ebner *et al.*, 2007); with this procedure, a tip of 20 nm radius carries no more than 1 to 5 proteins (Ebner *et al.*, 2007), (ii) similar adhesion force distributions were reproducibly observed from one tip (or one cell) to another; if multiple bonds were probed in parallel, we would expect to see variations in the force values when comparing different tips, reflecting variations in the number of bonds, which was not observed here. Accordingly, as Cn was attached at low density on the tip, and as the weak and strong binding events were reproducibly observed on different cells, we believe they originate from two different types of SdrF-Cn bonds. Comparison with the SCFS data suggests that the forces measured at the whole-cell level originate, on average, from double weak and strong SdrF-Cn bonds that are probed in parallel. Thus, our work shows that single-cell and single-molecule AFM methods are capable of dual detection, therefore enabling us to unravel simultaneously two different types of molecular bonds in living bacteria.

Low and high force peaks were well-described by the worm-like-chain model (WLC), suggesting they reflect the force-induced unfolding of protein

secondary structures (**Figure 4A**, right inset; black lines). The high force (~500 pN) is larger than the unfolding force of strong -folds domains (<300 pN; Oberhauser *et al.*, 1998, Rief *et al.*, 1997), suggesting that it involves mechanically-strong protein domains. We speculate that this mechanical strength is important for the protein's adhesive function, enabling adhering bacteria to withstand physiological shear forces while retaining the SdrF functional activity.

Do the ligand-binding forces of SdrF compare with those of the structurally-related SdrG protein? Using AFM (Herman *et al.*, 2014), the strength of the SdrG-Fg bond was shown to be remarkably strong, ~2 nN, consistent with the "dock, lock and latch (DLL)" mechanism in which dynamic conformational changes of the N2 and N3 subdomains of the A region of the protein result in a greatly stabilized adhesin-ligand complex (Ponnuraj *et al.*, 2003, Bowden *et al.*, 2008, Foster *et al.*, 2014). The ~500 pN force seen with SdrF binding to collagen is weaker than the ~2 nN force of the SdrG-Fg bond (Herman *et al.*, 2014), suggesting strongly that the SdrF-Cn bond does not involve a DLL mechanism. This is consistent with the notion that in the DLL mechanism, the ligand binding trench only accepts linear peptides. Another prominent feature is that some of the 500 pN forces showed double force peaks separated by only 29 ± 5 nm ($n = 64$ curves; top curve in **Figure 4A**). Similar signatures were seen for the SdrG-Fg bond, yet with a peak-to-peak separation of 38 nm (Herman *et al.*, 2014). As these double force peaks are always separated by the same distance, we suggest they reflect an intrinsic property of the protein subdomains. In summary, in view of the structural and biophysical similarities of SdrF and SdrG, we suggest that the N1, N2 and/or N3 subdomains of the A region of SdrF promote the strong Cn-binding forces of SdrF and that this involves a novel mechanism. As for the SdrG-Fg interaction (Ponnuraj *et al.*, 2003), it is likely that the SdrF-Cn interaction involves a combination of both hydrophobic forces and hydrogen bonds between the amino-acids implicated in ligand recognition.

In light of our single-cell and single-molecule data, we postulated that the low and high Cn-binding forces originate from weak and strong bonds involving both the A and B domains of SdrF. To test this hypothesis, we analyzed *L. lactis* bacteria expressing only one of the two domains (hereafter called $SdrF_A^{(+)}$ and $SdrF_B^{(+)}$ cells). As can be seen in **Figure 5A**, SMFS data for $SdrF_A^{(+)}$ cells were quite similar to those for $SdrF^{(+)}$ cells. By contrast, $SdrF_B^{(+)}$ cells showed strongly decreased adhesion frequency and only low force peaks (**Figure 5B**). So both the A and B regions exhibit Cn-binding activity, the A region being involved in both strong and weak adhesion, and the B region only in weak adhesion.

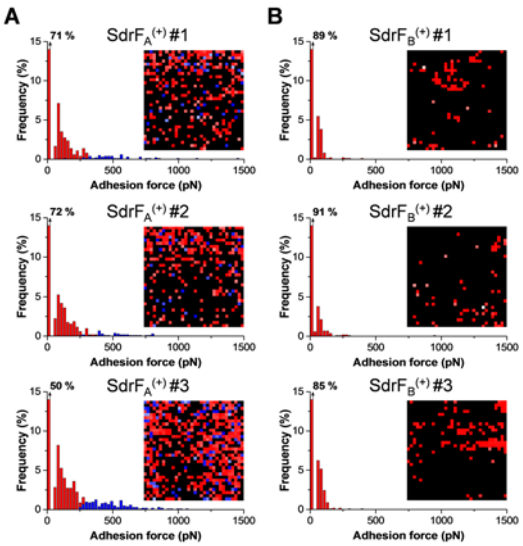

Figure 5: Both the A and B regions of SdrF are involved in collagen-binding.
A. Adhesion force histograms and maps obtained by recording force curves in PBS across the surface of three *L. lactis* $SdrF_A^{(+)}$ cells using tips labelled with Cn.
B. Adhesion force histograms and maps obtained by recording force curves in PBS across the surface of

We then assessed the dissociation rate of the bonds involving full-length proteins ($SdrF^{(+)}$ cells), by studying the dependence of the binding forces on the loading rate, *i.e.* the rate at which the force is applied to the complex (Fritz *et al.*, 1998, Baumgartner *et al.*, 2000) (**Figure 6A and B**). Both the weak and strong binding forces (F) increased linearly with the logarithm of the loading rate (r), as observed for other receptor-ligand bonds (Hinterdorfer & Dufrêne, 2006). The length scale of the energy barrier, x, was assessed from the slope f of the F *versus* $\ln(r)$ plot, and extrapolation to zero forces yielded the kinetic off-rate constant of dissociation at zero force, $k_{off} = r_{F=0}\, x \,/\, k_BT$. Dissociation rates of 4.2 and 0.1 s^{-1} were obtained for the weak and strong binding forces. These off-rates are much faster than that of the SdrG-Fg bond, confirming that the SdrF-Cn bonds do not involve highly stabilized complexes formed by variants of the DLL mechanism. The fast dissociation rate, that is similar to that of homophilic bonds formed by cadherins (Baumgartner *et al.*, 2000) and by the *Staphylococcus aureus* fibronectin-binding protein A

(Herman-Bausier *et al.*, 2015), could be important for biofilm dynamics. In other words, short duration of adhesion to Cn may help the bacteria detach and to colonize new sites. Such a trait could be important for biomaterial-associated infections but also for the colonization of the skin, the natural habitat of *S. epidermidis*.

We also found that the interaction time profoundly affects the adhesion frequency (*i.e.* total number of curves with adhesion events; **Figure 6C**). The binding frequency increased to reach a plateau corresponding to about 60 % binding probability after 2 s, suggesting that the probability of forming SdrF-Cn bonds increases with interaction time. In fact, the time-dependency may result from an increased number of SdrF-Cn bonds, as observed for other receptor-ligand bonds, but may also reflect the time necessary for conformational changes within the SdrF molecule.

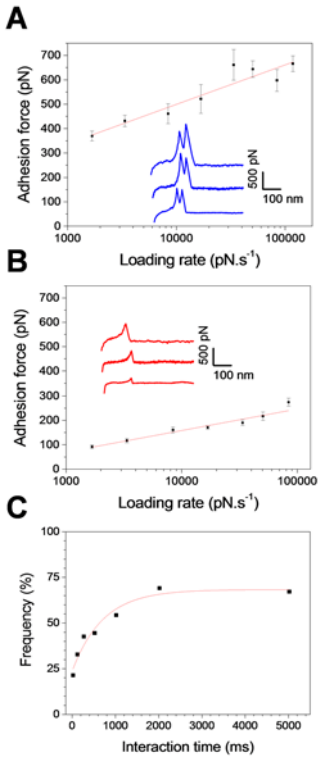

Figure 6: SdrF-collagen interactions show fast dissociation and time-dependency.
A, B. Dependence of the weak (A) and strong (B) Cn-binding forces on the loading rate applied during retraction, using a contact time of 100 ms, an approach speed of 1000 nm/s and increasing retraction speed (mean ± s.e.m; $n > 1000$ force curves for each data point). The mean adhesion forces of full-length SdrF proteins (*L. lactis* SdrF$^{(+)}$ cells) (F) increased linearly with the logarithm of the loading rate in both cases, for the weak binding forces (r): $F = 3.8\ 10^{-11} \ln(r) + 8{,}6\ 10^{-10}$ and for the strong binding forces (r): $F = 7.0\ 10^{-11} \ln(r) + 1{,}8\ 10^{-9}$. From these plots, we obtained k_{off} values indicating that Cn-binding forces show fast dissociation rates (see text for details). R^2 values obtained for the linear fits were 0.94 and 0.95, respectively. Shown in the insets are representative force curves. Similar loading rate plots were obtained in multiple experiments using different tips.
C. Dependence of the adhesion frequency of full-length SdrF proteins (including both weak and strong adhesion forces) on the interaction time, measured at a constant approach and retraction speed of 1000 nm s^{-1}. Similar interaction time plots were obtained in multiple experiments using different tips.

Conclusions

Recent AFM experiments have shed new light into the mechanisms of bacterial adhesion and biofilm formation (Dufrêne, 2014, Dufrêne, 2015). We have used advanced SCFS and SMFS techniques to gain insight into the mechanical strength and binding mechanisms of SdrF. We have shown that these methods are capable of dual detection, *i.e.* of analyzing simultaneously two different

types of biomolecular bonds in living bacteria. Our main discoveries are that: i) SdrF shows dual Cn-binding activity; ii) ligand-binding occurs via both strong (~500 pN) and weak (~100 pN) bonds involving the A and B regions, with the A region playing the major role; iii) compared to the stable SdrG-Fg DLL bond, SdrF-Cn bonds show weaker binding strength and much faster dissociation, which could be of relevance for biofilm dynamics.

Collectively, these results show that MSCRAMMs can bind to ligands by mechanisms other that the well-established DLL mechanism. Staphylococci have the capacity to express a limited repertoire of CWA surface proteins (Foster *et al.*, 2014). *S. aureus* can express up to 24 CWA proteins but in *S. epidermidis* this is much less (~8). These proteins are exposed to the host and are under strong pressure to support adhesion to the extracellular matrix and to host cells, as well as to help evade innate immune responses. Therefore a single protein may have evolved to bind to more than one ligand and to have more than one function. Different binding mechanisms are also likely. Thus FnBPA and FnBPB A domains can bind to fibrinogen and elastin by the DLL mechanism (Keane *et al.*, 2007). In addition, the A domains can form dimers by homophilic interactions that do not involve DLL. Mutants of FnBPA that lacked the ability to bind Fg by DLL could still form biofilm. Similarly the A domain of SdrC can form dimers and promote biofilm aggregation (Barbu *et al.*, 2014). Two short peptides within the N2 subdomain of the A region of SdrC were identified by phage display. Modelling the peptide subdomains within SdrC indicated that they were outside the region predicted to participate in DLL. So we conclude that SdrF A region binds collagen by a novel mechanism. In the future, it would be interesting to complement AFM analyses with alternative approaches like surface plasmon resonance. Also, AFM could be used to study the relative contributions, and possible cooperativity, of the A and B subdomains in Cn-binding. More broadly, we anticipate that detailed and exhaustive AFM analyses of other CWA surface proteins will undoubtedly identify new binding partners and binding mechanisms.

Experimental procedures

Bacterial strains and growth conditions

L. lactis strains used for surface expression of *S. epidermidis* SdrF proteins were obtained as previously described (Arrecubieta *et al.*, 2007). *L lactis* strain MG1363 ($SdrF^{(-)}$) was grown at 30°C in M17 medium (BD Biosciences) supplemented with 0.5 % glucose (GM17) and *L. lactis* MG1363 $SdrF^{(+)}$,MG1363 $SdrF_A^{(+)}$,MG1363 $SdrF_B^{(+)}$, harbouring plasmids derived from pOri23 were grown in GM17 supplemented with erythromycin (5 µg ml^{-1}). *S. epidermidis* 9142 strain was grown overnight in tryptic soy broth (TSB) or agar (TSA) (Bio-Rad) at 37°C. For AFM experiments, cells from the stationary growth phase (16-18 h) were harvested by centrifugation 3 min at 2500 x *g* and washed 2 times in PBS buffer. AFM analyses were carried out immediately after cell harvesting and lasted up to 8 hrs.

Collagen-coated substrates

To prepare Cn-coated substrates for SCFS experiments, glass coverslips coated with a thin layer of gold were immersed overnight in an ethanol solution containing 1 mM of 10 % 16-mercaptododecahexanoic acid/90 % 1-mercapto-1-undecanol (Sigma), rinsed with ethanol, and dried with N_2. Substrates were then immersed for 30 min into a solution containing 10 mg ml^{-1} N-hydroxysuccinimide (NHS) and 25 mg ml^{-1} 1-ethyl-3-(3-dimethylaminopropyl)-carbodiimide (EDC) (Sigma), rinsed 5 times with Ultrapure water (ELGA LabWater), incubated with 0.1 mg ml^{-1} of collagen type 1 from rat tail (Sigma, 95 % purity) for 1 h, rinsed further with PBS buffer, and then immediately used without de-wetting.

Microscopic adhesion

A microscopic adhesion assay was used to assess bacterial adhesion on Cn substrates. Substrates were incubated during 2 h in 200 µl bacterial suspensions adjusted in PBS to an OD_{600} of 3. After 2 h, the substrates were gently rinsed by 3 consecutives washing in PBS and directly imaged using an inverted optical microscope (Zeiss axio Observer Z1) equipped with a Hamamatsu camera C10600.

Single-cell force spectroscopy

Bacterial cell probes were obtained as previously described (Beaussart *et al.*, 2013b, Beaussart *et al.*, 2014). Briefly, colloidal probes were obtained by attaching single silica microsphere (6.1 µm diameter, Bangs laboratories) with a thin layer of UV-curable glue (NOA 63, Norland Edmund Optics) on triangular shaped tipless cantilevers (NP-O10, Microlevers, Bruker Corporation) and using a Nanoscope VIII Multimode AFM (Bruker corporation, Santa Barbara, CA). The cantilever was then immersed for 1 h

in a 10 mM Tris Buffer + 150 mM NaCl solution (pH 8.5) containing 4 mg ml^{-1} dopamine hydrochloride (99 %, Sigma). The probe was then rinsed in TRIS Buffer + 150 mM NaCl solution (pH 8.5) and used directly for cell probe preparation. The nominal spring constant of the colloidal probe cantilever was ~0.06 N m^{-1} as determined by the thermal noise method (Picoforce, Bruker).
For cell probe preparation, 50 µl of a suspension of *ca.* 1 x 10^6 cells were transferred into a glass petri dish in which Cn-coated substrates were attached. The cells were stained in the dark during 15 min using a *Bac*light viability kit (Invitrogen, kit L7012) following the manufacturer instructions to check viability and positioning of the cell. After staining, 4 ml of PBS were added to immerse bacteria and Cn substrates. The colloidal probe was brought into contact with an isolated bacterium. Single bacteria were attached on the centre of the colloidal probes using a Bioscope Catalyst AFM (Bruker Corporation, Santa Barbara, CA) equipped with a Zeiss Axio Observer Z1 and a Hamamatsu camera C10600. When proper attachment of the cell was confirmed by fluorescence imaging, the cell probe was positioned over the Cn-substrates without de-wetting. Single-cell interaction forces with Cn-substrates were measured at room temperature (20 °C) by recording multiple forces curves on three different spots, using a maximum applied force of 250 pN, contact time of 1 s, and constant approach and retraction speeds of 1000 nm s^{-1}. Force measurements using either stained or non-stained cells gave the same results, suggesting that labelling did not alter the cell surface properties. For blocking experiments, free Cn was added to the sample at a final concentration of 0.1 mg ml^{-1}.

Single-molecule force spectroscopy

SMFS measurements were performed at room temperature (20 °C) in PBS buffer using a Nanoscope VIII Multimode AFM (Bruker corporation, Santa Barbara, CA) and oxide sharpened microfabricated Si_3Ni_4 cantilevers with a nominal spring constant of ~0.01 N m^{-1} (MSCT, Microlevers, Bruker Corporation). The spring constants of the cantilevers were measured using the thermal noise method (Picoforce, Bruker). Bacterial cells were immobilized by mechanical trapping into porous polycarbonate membranes (Millipore, Billerica, MA) with a pore diameter of 0.8 µm (Dufrêne *et al.*, 1999). After filtering a cell suspension, the filter was gently rinsed with PBS, carefully cut (1 cm x 1 cm), attached to a steel sample puck using a small piece of double face adhesive tape, and the mounted sample was transferred into the AFM liquid cell while avoiding de-wetting.
Cn-functionalized tips were obtained using PEG-benzaldehyde linkers (Ebner *et al.*, 2007). Prior to functionalization, cantilevers were washed with chloroform and ethanol, placed in an UV-ozone-cleaner for 30 min, immersed

overnight into an ethanolamine solution (3.3 g ethanolamine into 6 ml of DMSO), then washed 3 times with DMSO and 2 times with ethanol, and dried with N_2. The ethanolamine-coated cantilevers were immersed for two hours in a solution prepared by mixing 1 mg Acetal-PEG-NHS dissolved in 0.5 ml of chloroform with 10 µl triethylamine, then washed with chloroform and dried with N_2. Cantilevers were further immersed for 5 min in a 1 % citric acid solution, washed in Ultrapure water (ELGA LabWater), and then covered with a 200 µl droplet of PBS solution containing 2 µM type I Cn from rat tail (Sigma) to which 2 µl of a 1 M $NaCNBH_3$ solution were added. After 50 min, cantilevers were incubated with 5 µl of a 1 M ethanolamine solution in order to passivate unreacted aldehyde groups and then washed with and stored in buffer.

For single-molecule imaging, bare tips were first used to localize and image individual cells and then replaced by Cn-tips. Adhesion maps were obtained by recording 32 x 32 force-distance curves on areas of 500 x 500 nm, calculating the adhesion force for each force curve and displaying adhesive events as red or blue pixels. Unless specified otherwise, all force curves were recorded at 100 ms contact time, with a maximum applied force of 250 pN and using a constant approach and retraction speed of 1000 nm s^{-1}. For blocking experiments, 0.1 mg ml^{-1} of free Cn were added.

Acknowledgements

Work at the Université catholique de Louvain was supported by the National Fund for Scientific Research (FNRS), the FNRS-WELBIO under Grant n°WELBIO-CR-2015A-05, the Université catholique de Louvain (Fonds Spéciaux de Recherche), the Federal Office for Scientific, Technical and Cultural Affairs (Interuniversity Poles of Attraction Programme), and the Research Department of the Communauté française de Belgique (Concerted Research Action). Y.F.D. is a Research Director of the FNRS. We thank F. Lowy (Columbia University) and T. Foster (Trinity College Dublin) for providing us with bacterial strains used in this study, and T. Foster and J. Geoghegan (Trinity College Dublin) for fruitful discussion.

References

Alsteens, D., Garcia, M.C., Lipke, P.N. & Dufrêne, Y.F., (2010) Force-induced formation and propagation of adhesion nanodomains in living fungal cells. *Proc Natl Acad Sci USA* **107**: 20744-20749.

Andre, G., Kulakauskas, S., Chapot-Chartier, M.P., Navet, B., Deghorain, M., Bernard, E.*, et al.* (2010) Imaging the nanoscale organization of peptidoglycan in living *Lactococcus lactis* cells. *Nat Commun* **1**: 27.

Arrecubieta, C., Lee, M.H., Macey, A., Foster, T.J. & Lowy, F.D. (2007) SdrF, a *Staphylococcus epidermidis* surface protein, binds type I collagen. *J Biol Chem* **282**: 18767-18776.

Arrecubieta, C., Toba, F.A., von Bayern, M., Akashi, H., Deng, M.C., Naka, Y. & Lowy, F.D. (2009) SdrF, a *Staphylococcus epidermidis* surface protein, contributes to the initiation of ventricular assist device driveline-related infections. *PLoS Pathog* **5**: e1000411.

Barbu, E.M., Mackenzie, C., Foster, T.J. & Hook, M., (2014) SdrC induces staphylococcal biofilm formation through a homophilic interaction. *Molecular Microbiol.* **94**: 172-185.

Baumgartner, W., Hinterdorfer, P., Ness, W., Raab, A., Vestweber, D., Schindler, H. & Drenckhahn, D. (2000) Cadherin interaction probed by atomic force microscopy. *Proc. Natl. Acad. Sci. USA.* **97**: 4005-4010.

Beaussart, A., Herman, P., El-Kirat-Chatel, S., Lipke, P.N., Kucharikova, S., Van Dijck, P. & Dufrêne, Y.F. (2013a) Single-cell force spectroscopy of the medically important *Staphylococcus epidermidis-Candida albicans* interaction. *Nanoscale* **5**: 10894-10900.

Beaussart, A., El-Kirat-Chatel, S., Herman, P., Alsteens, D., Mahillon, J., Hols, P. & Dufrêne, Y.F. (2013b) Single-cell force spectroscopy of probiotic bacteria. *Biophys J* **104**: 1886-1892.

Beaussart, A., El-Kirat-Chatel, S., Sullan, R.M., Alsteens, D., Herman, P., Derclaye, S. & Dufrêne, Y.F., (2014) Quantifying the forces guiding microbial cell adhesion using single-cell force spectroscopy. *Nat Protoc* **9**: 1049-1055.

Bowden, M.G., Chen, W., Singvall, J., Xu, Y., Peacock, S.J., Valtulina, V.*, et al.* (2005) Identification and preliminary characterization of cell-wall-anchored proteins of *Staphylococcus epidermidis*. *Microbiology* **151**: 1453-1464.

Bowden, M.G., Heuck, A.P., Ponnuraj, K., Kolosova, E., Choe, D., Gurusiddappa, S.*, et al.* (2008) Evidence for the "dock, lock, and latch" ligand binding mechanism of the staphylococcal microbial surface

component recognizing adhesive matrix molecules (MSCRAMM) SdrG. *J Biol Chem* **283**: 638-647.

Dufrêne, Y.F. (2014) Atomic force microscopy in microbiology: new structural and functional insights into the microbial cell surface. *mBio* **5**: e01363-01314.

Dufrêne, Y.F. (2015) Sticky microbes: forces in microbial cell adhesion. *Trends Microbiol* **23**: 376-382.

Dufrêne, Y.F., Boonaert, C.J., Gerin, P.A., Asther, M. & Rouxhet, P.G. (1999) Direct probing of the surface ultrastructure and molecular interactions of dormant and germinating spores of *Phanerochaete chrysosporium*. *J Bacteriol* **181**: 5350-5354.

Dupres, V., Alsteens, D., Wilk, S., Hansen, B., Heinisch, J.J. & Dufrêne, Y.F. (2009) The yeast Wsc1 cell surface sensor behaves like a nanospring *in vivo*. *Nat Chem Biol* **5**: 857-862.

Dupres, V., Menozzi, F.D., Locht, C., Clare, B.H., Abbott, N.L., Cuenot, S., *et al.* (2005) Nanoscale mapping and functional analysis of individual adhesins on living bacteria. *Nat Methods* **2**: 515-520.

Ebner, A., Wildling, L., Kamruzzahan, A.S., Rankl, C., Wruss, J., Hahn, C.D., *et al.* (2007) A new, simple method for linking of antibodies to atomic force microscopy tips. *Bioconjug Chem* **18**: 1176-1184.

El-Kirat-Chatel, S., Boyd, C.D., O'Toole, G.A. & Dufrêne, Y.F. (2014) Single-molecule analysis of *Pseudomonas fluorescens* footprints. *ACS Nano* **8**: 1690-1698.

Emerson, R.J.t., Bergstrom, T.S., Liu, Y., Soto, E.R., Brown, C.A., McGimpsey, W.G. & Camesano, T.A. (2006) Microscale correlation between surface chemistry, texture, and the adhesive strength of *Staphylococcus epidermidis*. *Langmuir* **22**: 11311-11321.

Foster, T.J., Geoghegan, J.A., Ganesh, V.K. & Hook, M. (2014) Adhesion, invasion and evasion: the many functions of the surface proteins of *Staphylococcus aureus*. *Nat Rev Microbiol* **12**: 49-62.

Fritz, J., Katopodis, A.G., Kolbinger, F. & Anselmetti, D. (1998) Force-mediated kinetics of single P-selectin/ligand complexes observed by atomic force microscopy. *Proc Natl Acad. Sci USA.* **95**: 12283-12288.

Helenius, J., Heisenberg, C.P., Gaub, H.E. & Müller, D.J. (2008) Single-cell force spectroscopy. *J Cell Sci* **121**: 1785-1791.

Herman-Bausier, P., El-Kirat-Chatel, S., Foster, T.J., Geoghegan, J.A. & Dufrêne, Y.F. (2015) *Staphylococcus aureus* Fibronectin-Binding

Protein A Mediates Cell-Cell Adhesion through Low-Affinity Homophilic Bonds. *mBio* **6**: e00413-00415.

Herman, P., El-Kirat-Chatel, S., Beaussart, A., Geoghegan, J.A., Foster, T.J. & Dufrêne, Y.F. (2014) The binding force of the staphylococcal adhesin SdrG is remarkably strong. *Mol Microbiol* **93**: 356-368.

Hinterdorfer, P. & Dufrêne, Y.F. (2006) Detection and localization of single molecular recognition events using atomic force microscopy. *Nat Methods* **3**: 347-355.

Keane, F.M., Loughman, A., Valtulina, V., Brennan, M., Speziale, P. & Foster, T.J., (2007) Fibrinogen and elastin bind to the same region within the A domain of fibronectin binding protein A, an MSCRAMM of *Staphylococcus aureus*. *Mol Microbiol* **63**: 711-723.

Lower, S.K., Yongsunthon, R., Casillas-Ituarte, N.N., Taylor, E.S., DiBartola, A.C., Lower, B.H., *et al.* (2010) A tactile response in *Staphylococcus aureus*. *Biophys J* **99**: 2803-2811.

McCrea, K.W., Hartford, O., Davis, S., Eidhin, D.N., Lina, G., Speziale, P., *et al.* (2000) The serine-aspartate repeat (Sdr) protein family in *Staphylococcus epidermidis*. *Microbiology* **146 (Pt 7)**: 1535-1546.

Müller, D.J., Helenius, J., Alsteens, D. & Dufrêne, Y.F. (2009) Force probing surfaces of living cells to molecular resolution. *Nat Chem Biol* **5**: 383-390.

Oberhauser, A.F., Marszalek, P.E., Erickson, H.P. & Fernandez, J.M. (1998) The molecular elasticity of the extracellular matrix protein tenascin. *Nature* **393**: 181-185.

Otto, M. (2009) *Staphylococcus epidermidis*-the 'accidental' pathogen. *Nat Rev Microbiol* **7**: 555-567.

Ponnuraj, K., Bowden, M.G., Davis, S., Gurusiddappa, S., Moore, D., Choe, D., *et al.* (2003) A "dock, lock, and latch" structural model for a staphylococcal adhesin binding to fibrinogen. *Cell* **115**: 217-228.

Rief, M., Gautel, M., Oesterhelt, F., Fernandez, J.M. & Gaub, H.E. (1997) Reversible unfolding of individual titin immunoglobulin domains by AFM. *Science* **276**: 1109-1112.

Vanzieleghem, T., Herman-Bausier, P., Dufrêne, Y.F. & Mahillon, J. (2015) *Staphylococcus epidermidis* Affinity for Fibrinogen-Coated Surfaces Correlates with the Abundance of the SdrG Adhesin on the Cell Surface. *Langmuir* **31**: 4713-4721.

Vuong, C. & Otto, M. (2002) *Staphylococcus epidermidis* infections. *Microbes Infect* **4**: 481-489.

Xu, L. C., & Siedlecki C.A. (2012) Effects of plasma proteins on *Staphylococcus epidermidis* RP62A adhesion and interaction with platelets on polyurethane biomaterial surfaces. *J Biomater Biotechnol* **3**:487-498.

Chapter IV

Staphylococcus aureus fibronectin-binding protein A mediates cell-cell adhesion through low affinity homophilic bonds

Philippe Herman-Bausier, Sofiane El-Kirat-Chatel, Timothy J. Foster, Joan A. Geoghegan, and Yves F. Dufrêne
P.H-B and S.E-K-C. contributed equally to this article

In *mBio*, **2015**, 6 (3), e00413

I performed the research and wrote the paper.
S.E-K-C. helped me with some of the experiments and biological interpretation.

Abstract

Staphylococcus aureus is an important opportunistic pathogen which is a leading cause of biofilm-associated infections on indwelling medical devices. The cell surface-located fibronectin-binding protein A (FnBPA) plays an important role in the accumulation phase of biofilm formation by methicillin-resistant *S. aureus* (MRSA), but the underlying molecular interactions are not yet established. Here, we use single-cell and single-molecule atomic force microscopy to unravel the mechanism by which FnBPA mediates intercellular adhesion. We show that FnBPA is responsible for specific cell-cell interactions that involve the FnBPA A domain and cause microscale cell aggregation. We demonstrate that the strength of FnBPA-mediated adhesion originates from multiple low-affinity homophilic interactions between FnBPA A domains on neighbouring cells. Low affinity binding by means of FnBPA may be important for biofilm dynamics. These results provide a molecular basis for the ability of FnBPA to promote cell accumulation during *S. aureus* biofilm formation. We speculate that homophilic interactions may represent a generic strategy among staphylococcal cell surface proteins for guiding intercellular adhesion. As biofilm formation by MRSA strains depends on proteins rather than polysaccharides, our approach offers exciting prospects for the design of drugs or vaccines to inhibit protein-dependent intercellular interactions in MRSA biofilms.

Importance

Staphylococcus aureus is a human pathogen that forms biofilms on indwelling medical devices, such as central venous catheters and prosthetic joints. This leads to biofilm infections that are difficult to treat with antibiotics because many cells within the biofilm matrix are dormant. The fibronectin-binding proteins FnBPA and FnBPB promote biofilm formation by clinically-relevant methicillin-resistant *S. aureus* (MRSA) strains, but the molecular mechanisms involved remain poorly understood. We used atomic force microscopy techniques to demonstrate that FnBPA mediates cell-cell adhesion *via* multiple, low affinity homophilic bonds between FnBPA A domains on adjacent cells. Therefore, FnBP-mediated homophilic interactions represent an interesting target to prevent MRSA biofilms. We propose that such homophilic mechanism may be widespread among staphylococcal cell surface proteins, providing a means to guide intercellular adhesion and biofilm accumulation.

Staphylococcus aureus is a human commensal and opportunistic pathogen that causes both superficial and invasive infections (1, 2). This species is a major cause of infections associated with indwelling medical devices such as central venous catheters and prosthetic joints (1, 2). The ability to form biofilms on implanted devices results in infections that are difficult to treat with antibiotics because many cells within the biofilm matrix are dormant. This is compounded by the prevalence of strains that are resistant to multiple antibiotics (methicillin-resistant *S. aureus*; MRSA) (3, 4). Consequently, understanding the molecular mechanisms leading to the formation of staphylococcal biofilms may contribute to the development of novel therapeutic approaches for combating biofilm-related infections.

Until recently the accumulation phase of *S. aureus* biofilms was attributed solely to the elaboration of polysaccharide intercellular adhesin PIA, also known as poly-N-acetyl-glucosamine (PNAG) (1, 2, 5). However it is now clear that proteins that are covalently anchored to the cell wall by sortase (cell wall-anchored proteins) can also promote biofilm accumulation. In the cases of SraP, SdrC and SasG, cell-cell interactions have been shown to be due to specific homophilic binding between protein molecules located on adjacent cells (2, 5).

The fibronectin (Fn)-binding proteins FnBPA and FnBPB promote biofilm formation by clinically-relevant MRSA, both community-associated and hospital-associated strains (6-8). Both FnBPA and FnBPB have N-terminal A domains that are structurally and functionally-related to clumping factor A (ClfA) and the *S. epidermidis* SdrG protein and bind to fibrinogen by a variation of the dock, lock and latch (DLL) mechanism whereby conformational changes in subdomains N2N3 within the A region result in highly stabilized complexes (9-11). The C-terminal fibronectin binding domain comprises tandem repeats that are intrinsically disordered resulting in an extended flexible "stalk" that projects the A domain from the cell surface (**Figure 1A**). The biofilm forming region of FnBPA was localized to subdomains N2N3 of the N-terminal A region but accumulation was shown not to involve a DLL mechanism (6, 7). FnBP-promoted biofilms could involve direct homophilic interactions or binding of the proteins to surface-located receptors on adjacent cells (**Figure 1B**) (2).

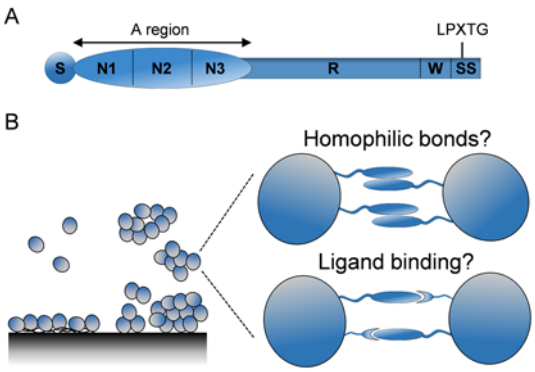

Figure 1: FnBPA-dependent biofilm formation.
A. Schematic representation of the *S. aureus* FnBPA protein: S, secretory signal sequence; A region comprising N1 N2 and N3 subdomains involved in fibrinogen and elastin binding and cell-cell aggregation during biofilm formation; R, tandem repeats of fibronectin binding domains; W, proline-rich cell wall-spanning region; SS, sorting signal comprising the LPXTG motif, membrane-spanning domain and positively charged tail.
B. Role of FnBPA in biofilm formation. In a first stage, FnBPA proteins promote attachment to host plasma proteins on biomaterial surfaces (left part of the left cartoon). Then, FnBPA mediates cell aggregation and biofilm accumulation (right part of the left cartoon). Whether this is achieved by homophilic protein-protein interactions or by binding to other ligands on adjacent cells is not yet established (right cartoons).

Atomic force microscopy (AFM) has provided valuable insights into the molecular basis of staphylococcal adhesion. Force spectroscopy with biospecific probes has been used to probe the localization and binding strength of adhesins, including FnBPs, down to the single-molecule level (12-16). Furthermore, the use of bacterial cell probes has enabled the quantification of cell-substrate and cell-cell adhesive forces at the whole cell level (17-19). In this study, we explore the molecular mechanism of FnBPA-dependent cell-cell adhesion using these AFM techniques (20, 21). Specifically, we address the following questions: how strong are intercellular bonds, how many FnBPA proteins do they involve, and is FnBPA-mediated intercellular adhesion achieved by means of homophilic interactions or ligand binding? We analyze the binding mechanism of full-length FnBPA expressed from a plasmid in *S. aureus* strain SH1000 defective in clumping factors (Clfs) A and B, and in FnBPA and B (hereafter *S. aureus* FnBPA$^+$ cells), as well as of the recombinant FnBPA A domain immobilized on model surfaces. The results demonstrate that FnBPA mediates specific cell-cell adhesion *via* multiple, low affinity homophilic bonds that depend on Zn^{2+} ions and involve the A domain.

Results

FnBPA is involved in fibronectin binding and in cell aggregation. We first confirmed that FnBPA adhesins were expressed on FnBPA$^+$ bacteria by analyzing their ability to adhere to Fn-coated substrates at the microscopic scale. Optical microscopy showed that FnBPA$^+$ cells adhered strongly to Fn-coated surfaces unlike FnBPA$^-$ cells which hardly adhered at all (**Figure 2**). Consistent with published data, this shows that FnBPA promotes bacterial adhesion to Fn and that the adhesin is expressed appropriately on FnBPA$^+$ cells described here.

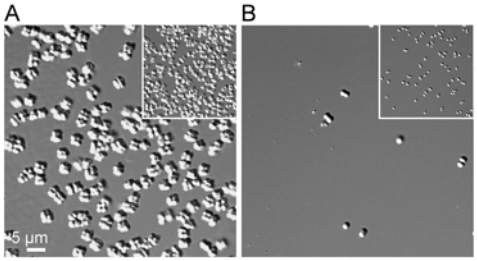

Figure 2: FnBPA-mediated adhesion to fibronectin. Optical (DIC) images showing the microscopic adhesion behaviour of two staphylococcal strains.
A. FnBPA$^+$ cells, after 2 h incubation on Fn-coated surfaces.
B. FnBPA$^-$ cells, after 2 h incubation on Fn-coated surfaces.
Insets are representative images from a duplicate experiment.

We then studied the involvement of FnBPA in cell-cell adhesion (**Figure 3**). **Figure 3A-C** shows that FnBPA$^+$ cells re-suspended in buffer were isolated, without any evidence for aggregation. Addition of 1 mM Zn^{2+} induced the formation of large aggregates, 5 µm to 5 mm in size (**Figure 3D-F**). Cell aggregates were disrupted in the presence of 1 mM EDTA (ethylenediaminetetraacetic acid) (**Figure 3G-I**), but restored upon further addition of Zn^{2+} (**Figure 3J-L**). Aggregation was much less pronounced in *S. aureus* cells expressing no FnBPA (FnBPA$^-$ cells; **Figure 3M-O**). These results show that FnBPA mediates cell-cell adhesion *via* Zn^{2+}-dependent interactions.

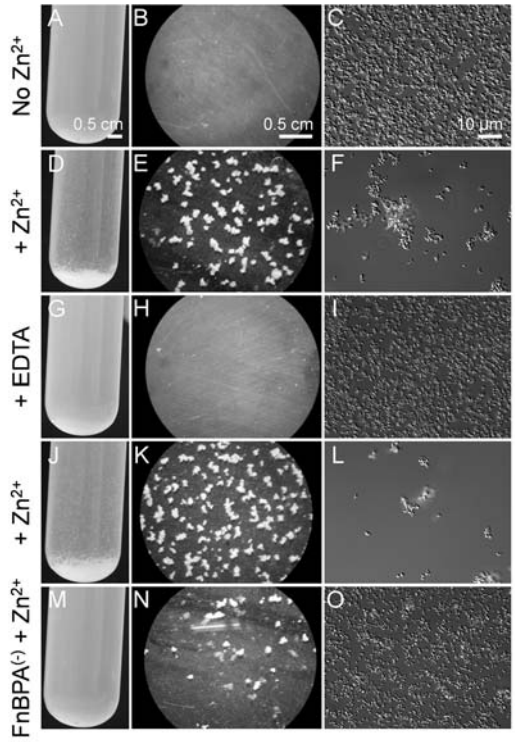

Figure 3: A to L. Role of FnBPA in cell aggregation.
Stereomicrographs (**A, D G and J)**, low (**B, E H and K**) and high (**C, F, I and L)** resolution optical microscopy images of *S. aureus* cells expressing FnBPA (FnBPA$^+$ cells).
A to C. After resuspension in TBS buffer.
D to F. Resuspension in TBS buffer containing 1 mM Zn^{2+}.
G to I. Addition of 1 mM EDTA.
J to L. Addition of 1 mM Zn^{2+}.
M to O. Control experiment using a *S. aureus* strain expressing no FnBPA (FnBPA$^-$ cells), in TBS with 1 mM Zn^{2+}.

Force spectroscopy of FnBPA interactions. AFM-based force spectroscopy was applied to living bacteria and to purified proteins to investigate the forces driving FnBPA-mediated cell-cell adhesion (**Figure 4**). We used single-cell force spectroscopy (SCFS) (22, 23) to quantify the adhesion forces between single *S. aureus* cells. Single FnBPA$^+$ cells were attached on colloidal cantilevers coated with polydopamine, allowing us to record force-distance curves between the cellular probes and the edges of small cell aggregates adhering on solid substrates (**Figure 4A**). Single-molecule force spectroscopy (SMFS) was employed to probe single FnBPA bonds on live cells (**Figure 4B**). Recent work showed that the region required for biofilm formation by FnBPA localizes to residues 166 to 498 of the A domain (7). Recombinant full-length FnBPA A domain was covalently bound to AFM tips in a random orientation, and the modified tips were used to record force-distance curves on FnBPA$^+$ cells immobilized in porous membranes. To probe single FnBPA-FnBPA bonds in the absence of any other interactions, forces were also measured between tips and substrates both functionalized with fully-oriented recombinant A domains (**Figure 4C**).

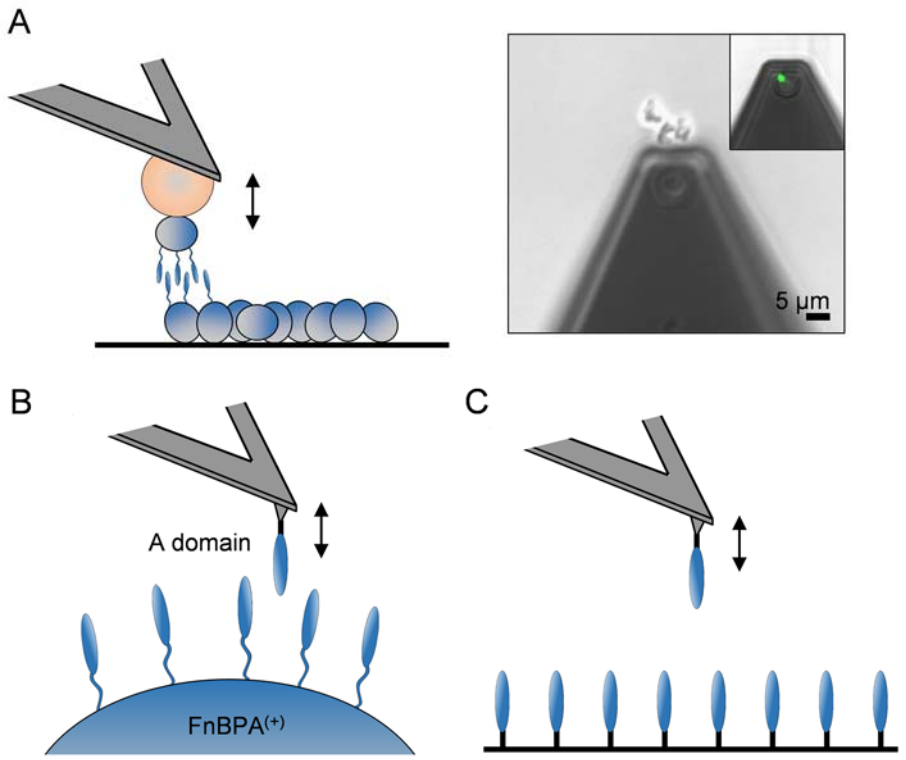

Figure 4: Force spectroscopy of FnBPA interactions.
A.To investigate cell-cell adhesion forces with SCFS, living bacteria were attached on polydopamine-coated colloidal cantilevers and force curves were obtained between cellular probes and small bacterial aggregates. The right micrograph shows a cell probe cantilever approaching a cell aggregate. The inset is a fluorescence image of a single bacterium attached to the colloidal probe.
B. To analyze single FnBPA bonds on living bacteria with SMFS, bacterial cell surfaces were probed using AFM tips labelled with the recombinant A domain.
C. To study single FnBPA homophilic bonds by SMFS, force curves were recorded between AFM tips and substrates functionalized with the recombinant A domain.

FnBPA promotes specific cell-cell adhesion forces. We measured the adhesion forces between two individual *S. aureus* cells. Adhesion forces, rupture lengths and typical force signatures obtained for three representative pairs of FnBPA$^+$ cells are shown in **Figure 5A,B** (see also **Figure S1** for data obtained on more cells). Many curves featured large adhesion force peaks of 250-3000 pN magnitude and 150-500 nm rupture length (cell #1: 1966 ± 470 pN, 351 ± 83 nm, mean ± s.d. on $n = 98$ adhesive curves; cell #2: 834 ± 424 pN, 294 ± 68 nm, $n = 470$; cell #3: 1640 ± 514 pN, 327 ± 73 nm, $n = 223$). There were some variations from one cell pair to another (see also **Figure S1**), which may reflect cellular heterogeneity as well as small variations in cell-cell contact area. Discrete rupture steps were often seen before rupture of the main adhesion peak, suggesting multiple bonds were involved. However, adhesion peaks generally showed sharp ruptures, implying that, upon stretching, the different bonds detached simultaneously.

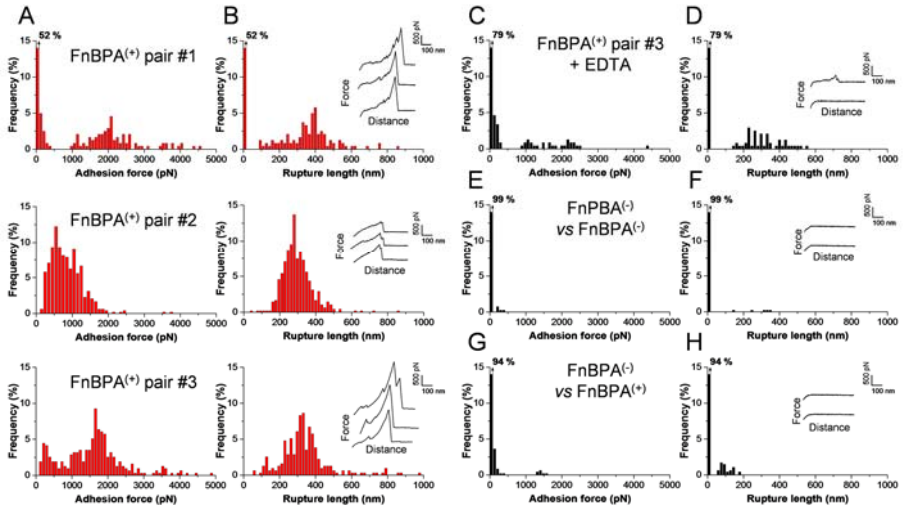

Figure 5: Cell-cell force spectroscopy of FnBPA bonds.
A and B. Adhesion force histograms (**A**) and rupture length histograms (**B**) with representative force signatures (insets), obtained by recording multiple force-distance curves in TBS supplemented with 1 mM Zn^{2+} between three pairs of interacting FnBPA$^+$ cells.
C and D. Force data obtained in the same conditions (cell 3) following addition of 1 mM EDTA.
E to H. Force data obtained in the same conditions for the interaction between two *S. aureus* FnBPA$^-$ cells (**E and F**), and between FnBPA$^+$ and FnBPA$^-$ cells (**G and H**). All curves were obtained using a contact time of 1 s, a maximum applied force of 250 pN, and approach and retraction speeds of 1,000 nm s^{-1}.

Do cell adhesion forces involve FnBPA proteins? We found that EDTA dramatically decreased the adhesion probability (**Figure 5C,D**; **Figure S2**), consistent with the notion that FnBPA interactions require Zn^{2+} ions (7). As can be seen in **Figure 5E,F** (see also **Figure S2**), we also measured the forces between *S. aureus* FnBPA$^-$ cells that lack FnBPA. Most adhesion events were abolished, indicating that the large adhesion forces on FnBPA$^+$ cells involve FnBPA proteins. Intriguingly, the same effect was observed for the interaction between FnBPA$^+$ and FnBPA$^-$ cells (**Figure 5G,H**; **Figure S2**). This suggests that interaction between two FnBPA$^+$ cells involves FnBPA proteins located on the two cell surfaces. So, our single-cell experiments show that FnBPA proteins on the *S. aureus* cell surface mediate specific, zinc-dependent, cell-cell interactions.

Binding strength of single FnBPA proteins on living bacteria. How strong is a single FnBPA bond? To address this question we analyzed the forces between recombinant FnBPA A domains attached to AFM tips and full length FnBPA proteins on FnBPA$^+$ cells (**Figure 6** and **Figure S3**). **Figure 6A-C** (see **Figure S3** for more cells) shows that a large fraction (~50%) of the force curves recorded across three different cells featured single adhesion peaks with a moderate force of 125 ± 65 pN (mean ± s.d. from a total of 3072 curves obtained on 3 cells). We believe these forces originate from single FnBPA bonds as: (i) adhesion was strongly decreased upon addition of EDTA (**Figure 6D-F** and **Figure S3**), when using *S. aureus* FnBPA$^-$ cells (**Figure 6G-I** and **Figure S3**), or bare tips (**Figure S3**); (ii) the A domains were attached at low density on the tip, and (iii) the measured forces are in the range of the binding force typically reported for single cell adhesion proteins (24, 25). Presumably, the larger adhesion forces sometimes detected (200-300 pN) are due to multiple FnBPA bonds. How does the measured bond strength compare with that reported for Fn-FnBP bonds? Our ~125 pN force is stronger than the ~60 pN force measured for single Fn-FnBP bonds at similar loading rate (12, 15), suggesting that different mechanisms are involved. Strikingly, several groups have reported much larger adhesion forces for Fn-FnBP interactions, up to 6 nN depending on the strain investigated (13, 14, 16). However, the authors attached Fn at high density on the tip, meaning many Fn-FnBPs bonds were probed in parallel (up to 80). This is an important difference with the present work in which FnBPA A domains were covalently attached at low density on the tip to favor single bond detection.

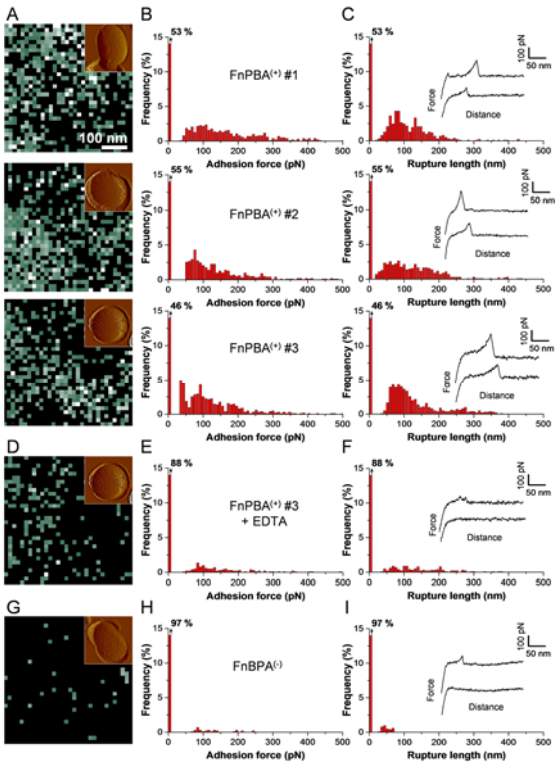

Figure 6: Single-molecule force spectroscopy of FnBPA bonds on living bacteria.
A. Adhesion force maps (500 nm x 500 nm, grey scale: 500 pN).
B. Adhesion force histograms.
C. Rupture length histograms together with representative force curves obtained by recording force curves in TBS with 1 mM Zn^{2+} across the surface of three *S. aureus* $FnBPA^{+}$ cells using tips labelled with the FnBPA A domain. Shown in the insets in **A** are deflection images of the cells.
D to I. Force data obtained for a $FnBPA^{+}$ cell (cell 3) in the presence of 1 mM EDTA (**D to F**), and for a *S. aureus* $FnBPA^{(-)}$ cell (**G to I**). All curves were obtained using a contact time of 100 ms, a maximum applied force of 250 pN, and approach and retraction speeds of 1000 nm s^{-1}.

Adhesion force maps indicate that the adhesins were largely exposed on the cell surface. Assuming that each adhesion event in the maps represents the detection of a single FnBPA, we find that the protein is exposed at a surface density of ~2000 proteins/μm². In earlier work, the distribution of adhesins was mapped on the surface of staphylococcal cells. Immunogold electron microscopy was used to study the distribution of SssF and UafB adhesins on *Staphylococcus saprophyticus* (26, 27). While the authors claimed there was abundant labelling, the density was lower than here, an effect that may reflect actual differences between species, or variations in the sensitivity of the techniques. AFM force mapping was also used to map FnBPs on staphylococcal cells (15, 28). Lower *et al.* (15) revealed the spatial localization of putative FnBP proteins on *S. aureus* bacteria deposited on different substrates. Results suggested that the production and localization of FnBP proteins may be induced by an external stimulus, such as the presence of Fn on a surface.

Do the observed rupture lengths, 98 ± 44 nm (mean ± s.d.; 3 different cells), compare with the lengths of the probed molecules? As the full-length FnBPA protein and its His-tagged A domain are 948 and 481 amino acids in length (6, 7), respectively, and assuming that each amino acid contributes 0.36 nm to

the contour length of a fully-extended polypeptide chain (29), the length of fully extended proteins and A domains are expected to be 341 nm and 173 nm, respectively. Full extension of the A domain-FnBPA complex should therefore lead to a length of about 500 nm, which is much longer than what we observed. This means that the bond ruptures before complete unfolding of the proteins, hence that the latter are mechanically stable. This observation agrees well with earlier single-molecule results showing that SdrG, which share strong structural similarities with FnBP, is not completely unfolded when subjected to large forces (30). We note that longer extensions were observed for cell-cell bonds (**Figure 5**), supporting the notion that they involve pairs of full-length FnBPA proteins.

How many FnBPA bonds are involved in a cell-cell bond? As a rough estimate, this number may be inferred by comparing our single-molecule (**Figure 6**) and single-cell (**Figure 5**) forces, and by considering the interaction area between two cells. The contact zone of two deformable spheres pressed on each other may be described by the Hertz model (31): $A = (3FR/4E^*)^{1/3}$, in which A is the radius of the contact area, R the effective radius ($1/R = 2/r$, where r is the cell radius), F the applied load (here, 250 pN), and E^* the effective Young modulus ($1/E^* = (2\text{-}2\nu^2)/E$, in which E is the elastic moduli and ν the Poisson's ratio associated with the cell). Assuming that the *S. aureus* cell radius r is 0.5 μm, the Young modulus 1.8 MPa (32), and the Poisson's ratio 0.3, we found an area radius of ~36 nm, thus yielding a contact area of ~0.004 μm². What is the number of interacting molecules in this area? Considering a surface density of ~2000 FnBPA/μm², as determined above from the force maps, the adhesion forces measured between two cells would involve about 8 FnBPA proteins in parallel on each cell. Given the variability of the data and the assumptions made in the model, this is in the range of the value obtained by comparing the adhesion forces measured for single molecules and single cells (~125 *vs* 800-2000 pN). This leads us to believe that FnBPA-dependent cell-cell adhesion involves about 10 cumulative bonds, as also indicated by the sharp peak ruptures.

FnBPA mediates low affinity homophilic bonds. To explain how FnBPA mediates cell-cell adhesion, two possible mechanisms were recently postulated, *i.e.* homophilic interactions or receptor-ligand binding (7) (**Figure 1B**). Although our single-cell results are in favor of homophilic bonds, a direct demonstration for these was still lacking. We therefore measured the forces and dynamics of the interaction between purified FnBPA A domains in the absence of any other cell wall components (**Figure 4C**). Force measurements between A domains revealed adhesion events with a mean adhesion force of 182 ± 78 pN (**Figure 7A**, inset), that we attribute to single FnBPA-FnBPA bonds as A domains were uniformly oriented at low density on the two interacting surfaces. The measured strength is slightly larger than that between the A domain and full-length FnBPA on cells, an effect that could reflect differences in the orientation and accessibility of the molecules. The ~180 pN force is much weaker than the 2 nN force measured for SdrG-Fg bonds (30), indicating that FnBPA-mediated cell-cell adhesion does not involve a DLL binding mechanism. FnBPA-FnBPA bonds showed extensions (~50 nm) that were much shorter than on live cells, suggesting that the A domains were hardly unfolded.

We then explored the dynamics of the FnBPA-FnBPA interaction, with the aim to assess the affinity of the bond. The forces needed to rupture homophilic bonds have been shown to depend on the loading rate, *i.e.* the rate at which the force is applied to the complex (24, 25, 33, 34). In agreement with this, we found that the mean adhesion force (F) between two A domains increases linearly with the logarithm of the loading rate (r), as illustrated in **Figure 7A**. The length scale of the energy barrier, x, was assessed from the slope f of the F *versus* $\ln(r)$ plot and found to be 0.2 nm, *i.e.* in the range of values (0.2-1 nm) typically measured by single-molecule AFM. Extrapolation to zero forces yielded the kinetic off-rate constant of dissociation at zero force: $k_{off} = r_{F=0}\, x \,/\, k\,T = 0.11\ s^{-1}$. This fast dissociation rate, similar to that of homophilic bonds in cadherins (33) and in bacterial trimeric autotransporter adhesins (24), suggests that FnBPA homophilic bonds are highly dynamic. This short duration of adhesion may contribute to biofilm dissemination, by helping the bacteria to rapidly detach and colonize new sites.

We also studied how the adhesion frequency (*i.e.* number of curves with adhesion events) vary with interaction time, while keeping the loading rate constant (**Figure 7B**). The binding frequency increased to reach a plateau corresponding to almost 100% binding probability after only 0.5 s, indicating that bond formation is fast. Similar fast bond formation was also observed with cadherins (33). Considering the interaction time needed for half-maximal probability of binding, $t_{0.5} = 168$ ms, we assessed the association rate constant,

$k_{on} = t_{0.5}^{-1} N_A V_{eff} = 7.5\ M^{-1}\ s^{-1}$, where V_{eff} is the effective volume explored by the tip-tethered protein (approximated here to a half-sphere of 1 nm radius) (35). We then estimated the equilibrium dissociation constant: $K_D = k_{off}/k_{on} =$ 15 mM. The obtained K_D value is much higher than that for FnBPA binding to fibrinogen (~1 µM) (11) but in the range of that of homophilic interactions by trimeric autotransporter adhesins (24), thus indicating that homophilic FnBPA bonds have low affinity. This finding may have important biological implications. Low affinity binding by means of FnBPA may represent the primary step in biofilm accumulation, enabling dynamic cell behaviors to occur, while subsequent higher affinity binding would lead to firm cell-cell adhesion. In particular, the positively charged PIA polysaccharide, also known as poly-N-acetyl-glucosamine (PNAG), may enhance intercellular interactions by high affinity multivalent binding with the negatively charged cell surfaces.

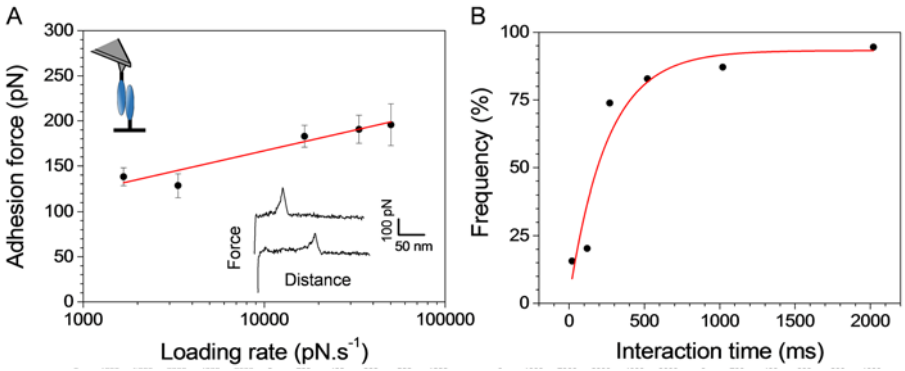

Figure 7: Force and dynamics of FnBPA homophilic interactions.
A. Dependence of the adhesion force on the loading rate applied during retraction, measured in TBS with 1 mM Zn^{2+} between a tip and a substrate both functionalized with FnBPA A domains, using a contact time of 100 ms and an approach speed of 1000 nm/s (mean ± s.e.m). The mean adhesion force (F) increased linearly with the logarithm of the loading rate (r): $F = 5.3\ 10^{-11} \ln(r) + 2.0\ 10^{-11}$. The R^2 value obtained for the linear fit was 0.85. Shown in the lower inset are representative force curves.
B. Dependence of the adhesion frequency on the interaction time, measured at a constant approach and retraction speed of 1000 nm s^{-1}. Similar loading rate and interaction time plots were obtained in multiple experiments using different tips and substrates.

Discussion

There is now considerable evidence that FnBPs participate in biofilm accumulation by *S. aureus* (6-8, 36), but the underlying molecular mechanisms are poorly understood. This study demonstrates that FnBPA mediates strong cell-cell adhesion *via* multiple, low affinity homophilic bonds between A domains on adjacent cells. We speculate that homophilic interactions may be widespread among staphylococcal cell surface proteins, providing a means to promote intercellular adhesion and biofilm accumulation. Our methodology

offers exciting prospects for the design of drugs or vaccines to inhibit protein-dependent intercellular interactions in MRSA biofilms.

The N2N3 subdomains of SdrC (37) have also been shown to promote cell-cell interactions, suggesting homophilic interactions by these domains could be a general mechanism to promote the accumulation phase in *S. aureus* biofilms. Although the structural details of FnBPA homophilic interactions are unclear, we speculate that they occur between residues on the surface of the N2 or N3 subdomains. In the case of SdrC, two amino acid sequences located within the N2 subdomain were found to act cooperatively to promote SdrC dimerization and, as a result, intercellular interactions (37). Whether a similar mechanism applies to FnBPA remains to be determined.

The occurrence of FnBPA homophilic bonds correlated with the cell aggregation behavior, leading us to believe that these interactions represent an important driving force for biofilm formation. Unlike the very strong and stable DLL bonds, homophilic bonds show moderate strength and fast dissociation, a trait which may be important for biofilm dissemination. Several factors can lead to biofilm detachment, including mechanical stress like fluid flow, and detachment agents like enzymes or surfactants (1, 38). Together with these factors, the fast dissociation of the FnBPA bonds may contribute to cell detachment (isolated cells or cell clusters) therefore favoring colonization of new sites.

Our finding that zinc is required to form homophilic bonds is consistent with earlier reports showing that FnBPA (7), but also other staphylococcal adhesins like SasG (39) and Aap (40, 41) promote zinc-dependent biofilm accumulation. It is therefore tempting to speculate that *S. aureus* has evolved these subdomains to promote homophilic cellular interactions, thus providing a general mechanism to favor biofilm accumulation. The biological significance of the Zn^{2+} dependent cell-cell interactions promoted by FnBPA can be called into question if the cation is limiting *in vivo*. The mammalian host restricts access to cations such as Zn and Mn that bacteria need for growth and proliferation *in vivo*, a phenomenon called nutritional immunity (42). An important host factor that contributes to this phenomenon is calprotectin, a Zn^{2+}-binding protein that can reach high levels in infected tissue (43). However, successful pathogens such as *S. aureus* produce dedicated uptake machinery for cations (42). It should be noted that Zn^{2+} is present in the cytosol of mammalian cells and bacteria (44). *S. aureus* lyses host cells by secreting cytolytic toxins which releases cytoplasmic contents. In addition during biofilm development some of the bacterial cells undergo autolysis to release DNA which is an important component of the biofilm matrix (45). This altruistic action will also release bacterial cytoplasmic contents including Zn^{2+}.

More than 3% of *E. coli* proteins contain Zn^{2+} (46). The extracellular zinc-dependent metalloprotease aureolysin of *S. aureus* contributes to virulence in mice indicating that it is active *in vivo* and presumably acquires its Zn^{2+} co-factor following secretion (47). We thus argue that the local concentration of Zn^{2+} at the early stages of biofilm development will be sufficient to support FnBP-mediated aggregation. Finally, the expression of FnBPs has been shown to support biofilm formation on subcutaneous catheters during an experimental infections of mice, arguing that adequate Zn^{2+} is likely to be present *in vivo* (36).

Materials and methods

Bacterial strains and growth conditions. *S. aureus* FnBPA$^-$ (strain SH1000 *clfA clfB fnbA fnbB*) is defective in clumping factors A and B and fibronectin binding proteins A and B (6). FnBPA$^-$ cells were grown overnight in TSB, washed once with TSB, subcultured into TSB at a 1:100 dilution and allowed to grow to an OD_{600} of 0.4. The *S. aureus* strain FnBPA+ is a derivative of strain SH1000 *clfA clfB fnbA fnbB* carrying plasmid pFNBA4 expressing fibronectin binding protein A from strain 8325-4 (7). For expression of FnBPA, FnBPA$^+$ cells were grown overnight in TSB with chloramphenicol (10 µg/ml), washed once in TSB, subcultured into TSB at a 1:100 dilution and allowed to grow to an OD_{600} of 0.4 in TSB + chloramphenicol.

Recombinant proteins. Plasmid pQE30::FnBPA$_{37–511}$ (10) was used as template for inverse PCR with the phosphorylated primers 5'-TCA GAA CAA AAG ACA ACT ACA G-3' and 5'-TTA ATT TTT CTC ATT TCC GTT CG-3' to eliminate DNA encoding the N-terminal His-tag and to introduce an in-frame fusion with DNA encoding a C-terminal His-tag. The PCR product was treated with DpnI to eliminate template DNA and, following blunt-end ligation, the plasmid was transformed into *E. coli* XL-1 Blue. The C-terminally hexahistidine-tagged FnBPA A domain protein (residues 37-511) was expressed and purified by Ni^{2+} affinity chromatography as previously described (39).

Adhesion assay. To assess the adhesion phenotype of the bacterial strains, bacteria were incubated with Fn-coated substrates prepared as follows. Glass coverslips coated with a thin layer of gold were immersed overnight in an ethanol solution containing 1 mM of 10 % 16-mercaptododecahexanoic acid/90% 1-mercapto-1-undecanol (Sigma), rinsed with ethanol, and dried with N_2. Substrates were then immersed for 30 min into a solution containing 10 mg ml^{-1} N-hydroxysuccinimide (NHS) and 25 mg ml^{-1} 1-ethyl-3-(3-dimethylaminopropyl)-carbodiimide (EDC) (Sigma), rinsed 5 times with

Ultrapure water (ELGA LabWater), incubated with 0.1 mg ml^{-1} of Fn from bovine plasma (Sigma) for 1 h, rinsed further with PBS buffer. Fn-substrates were incubated at 37°C in 200 µl bacterial suspensions adjusted in TBS buffer supplemented with 1 mM $ZnCl_2$ to an OD_{600} of 0.3-0.4. After 2 h, the substrates were gently rinsed by 3 consecutives washing in TBS buffer supplemented with 1 mM $ZnCl_2$ and directly imaged using an inverted optical microscope (Zeiss axio Observer Z1) equipped with a Hamamatsu camera C10600.

Aggregation assays. Aggregation phenotypes were directly observed after cell resuspension in TBS buffer (pH 7.4), TBS buffer supplemented with 1 mM $ZnCl_2$, addition of 1 mM of EDTA (ethylenediaminetetraacetic acid), and further addition of 1 mM of $ZnCl_2$. Aggregation levels were observed in test tubes, by optical microscopy at low magnification (Zeiss Stemi DV4 Stereo Microscope, Oberkochen, Germany) and at high magnification (Zeiss Axio Observer Z1 equipped with Hamamatsu camera C10600, Oberkochen, Germany).

Cell-cell force spectroscopy. To probe bacterial aggregates with single-cell probes, hydrophobic substrates were prepared by coating glass coverslips with a thin layer of gold, immersion overnight in a solution of 1 mM 1-dodecanethiol (Sigma-Aldrich), and rinsing with ethanol and dried under N_2. Cells resuspended in TBS buffer + 1 mM $ZnCl_2$ were deposited and let to adhere on hydrophobic substrates for 2 h. Non-adhering cells were removed by gentle rinsing and the cell coated substrates were attached, while avoiding dewetting, to the bottom of a glass Petri dish. Bacterial cell probes were obtained as previously described (22, 23). Briefly, colloidal probes were prepared by attaching single silica microsphere (6.1 µm diameter, Bangs laboratories) with a thin layer of UV-curable glue (NOA 63, Norland Edmund Optics) on triangular shaped tipless cantilevers (NP-O10, Microlevers, Veeco Metrology Group) and using a Nanoscope VIII Multimode AFM (Bruker corporation, Santa Barbara, CA). Cantilevers were then immersed for 1 h in a 10 mM Tris buffer + 150 mM NaCl solution (pH 8.5) containing 4 mg/ml dopamine hydrochloride (99%, Sigma), rinsed in Tris buffer + 150mM NaCl solution (pH 8.5) and used directly for cell probe preparation. The nominal spring constant of the colloidal probe cantilever was ~0.06 N/m as determined by the thermal noise method (Picoforce, Bruker). For cell probe preparation, 50 µl of a concentrated cell suspension were transferred into the glass Petri dish containing the cell coated hydrophobic substrates, after which 4 ml of TBS + 1 mM $ZnCl_2$ were added to the system. The colloidal probe was brought into contact with an isolated bacterium, using a Bioscope Catalyst AFM (Bruker Corporation, Santa Barbara, CA) equipped with a Zeiss Axio Observer Z1 and a Hamamatsu camera C10600. Optical microscopy was used to check for

proper attachment of the cell, and the cell probe was positioned over the edge of a cell aggregate lying on the hydrophobic substrates. Cell probes were used to measure cell-cell interaction forces at room temperature (20 °C), by recording multiple forces curves, using a maximum applied force of 250 pN, 1 s contact time, and constant approach and retraction speeds of 1000 nm s^{-1}. Adhesion force and rupture length histograms were obtained by calculating the maximum adhesion force and the last rupture distance for each curve. In total, 24 different cell probes were used to measure cell adhesion forces in standard and control conditions.

Single-molecule force spectroscopy on live cells. For SMFS on live cells, gold coated AFM cantilevers with a nominal spring constant of ~0.02 N m^{-1} (OMCL-TR4, Olympus Ltd., Tokyo, Japan) were functionalized with FnBPA A domains at low density and with a random orientation (48). Cleaned gold cantilevers were immersed overnight in a 1 mM solution 10% of $HS(CH_2)_{16}COOH$ (Sigma-Aldrich) and 90% of $HS(CH_2)_{11}OH$ (Sigma-Aldrich), rinsed with ethanol, immersed for 30 min in a solution containing 10 mg ml^{-1} N-hydroxysuccinimide (NHS) (Sigma-Aldrich) and 25 mg ml^{-1} 1-ethyl-3-(3-dimethylaminopropyl)-carbodiimide (EDC) (Sigma-Aldrich), and rinsed with water. The activated cantilevers were then incubated with 0.2 mg ml^{-1} of recombinant FnBPA A domains in PBS for 2 h, followed by rinsing and storage in PBS. All probes were freshly prepared and used the same day. The spring constants of the cantilevers were measured using the thermal noise method (Picoforce, Bruker).

SMFS measurements were performed at room temperature (20 °C) in TBS buffer + 1 mM $ZnCl_2$ using a Nanoscope VIII Multimode AFM (Bruker corporation, Santa Barbara, CA). Bacterial cells were immobilized by mechanical trapping into porous polycarbonate membranes (Millipore, Billerica, MA) with a pore size similar to the cell size. After filtering a cell suspension, the filter was gently rinsed with TBS + 1 mM $ZnCl_2$, carefully cut (1 cm x 1 cm), attached to a steel sample puck using a small piece of double face adhesive tape, and the mounted sample was transferred into the AFM liquid cell while avoiding de-wetting. First, bare probes were used to localized and image individual cells, and then replaced by A domain probes. Adhesion force maps were obtained by recording 32 x 32 force-distance curves on areas of 500 x 500 nm, calculating the adhesion force for each force curve and displaying the adhesive events as grey pixels. All force curves were recorded at 100 ms contact time, with a maximum applied force of 250 pN, and using a constant approach and retraction speed of 1000 nm/s.

Single-molecule force spectroscopy on model surfaces. SMFS measurements using tips and substrates functionalized with FnBPA A domains

were performed at room temperature (20 °C) in TBS buffer + 1 mM $ZnCl_2$ using a Nanoscope VIII Multimode AFM (Bruker corporation, Santa Barbara, CA). Recombinant FnBPA A domain with a C-terminal His-tag was immobilized onto cantilevers and substrates as follows. Silicon substrates were coated by thermal evaporation with a thin layer of Cr (5 nm) followed by a thin layer of gold (30 nm). Gold substrates and gold cantilevers (see above) were rinsed in ethanol, cleaned for 10 min by UV-ozone treatment, rinsed in ethanol and dried with N_2. They were immersed overnight in a 0.1 mM solution of 99% HS-C_{11}-$(EG)_3$-OH thiols (ProChimia) and 1% HS-C_{11}-$(EG)_3$-NTA thiols (ProChimia), rinsed with ethanol, dried with N_2, and immersed in a 40 mM aqueous solution of $NiSO_4$ (pH 7.2) for 30 min. Cantilevers and substrates were then incubated in a 200 µl droplet of a 200 µg/ml solution of FnBPA A domains for 1 h, rinsed and stored in PBS. Unless stated otherwise, multiple force curves were recorded at 100 ms contact time, with a maximum applied force of 250 pN, and using a constant approach and retraction speed of 1000 nm/s.

Supplemental material

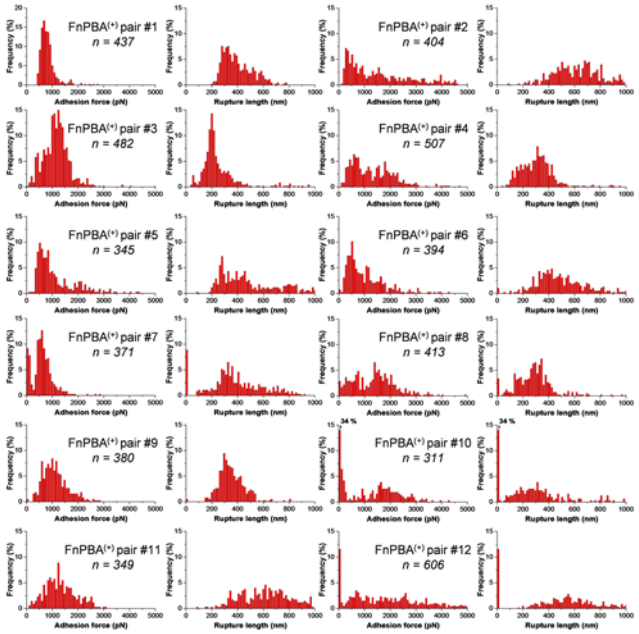

Figure S1. Cell-cell force spectroscopy of FnBPA$^{(+)}$ cells. Adhesion force histograms (left) and rupture length histograms (right) obtained by recording multiple force-distance curves in TBS supplemented with 1 mM Zn^{2+} between 12 pairs of interacting FnBPA$^{(+)}$ cells. All curves were obtained using a contact time of 1 s, a maximum applied force of 250 pN, and approach and retraction speeds of 1000 nm s^{-1}. n values represent the total number of force curves for each experiment.

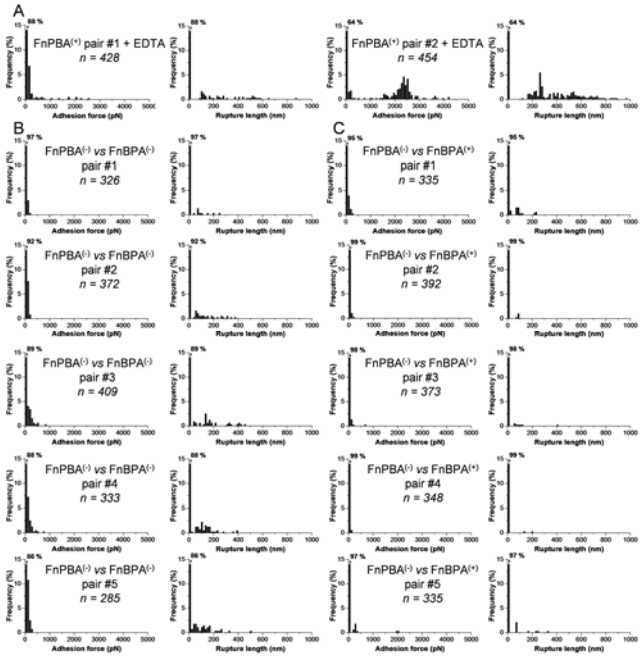

Figure S2. Cell-cell force spectroscopy: control experiments.
A. Force data obtained for cell pairs #1 and #2 following addition of 1 mM EDTA.
B,C. Force data obtained in TBS supplemented with 1 mM Zn^{2+} for the interaction between 5 pairs of *S. aureus* FnBPA$^{(-)}$ cells (**B**), and between 5 pairs of FnBPA$^{(+)}$ and FnBPA$^{(-)}$ cells (**C**).

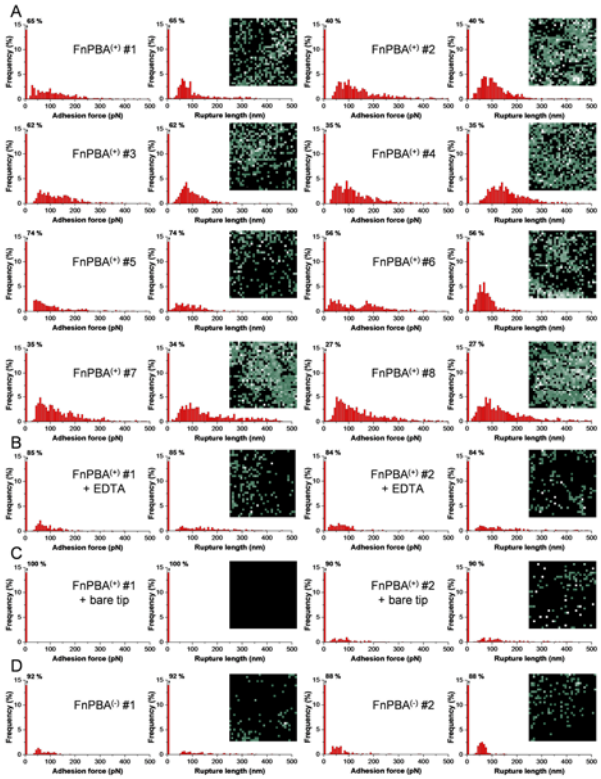

Figure S3. Single-molecule force spectroscopy on living bacteria.
A. Adhesion force maps (500 nm x 500 nm, grey scale: 500 pN), adhesion force histograms, and rupture length histograms obtained by recording force curves in TBS with 1 mM Zn^{2+} across the surface of 8 *S. aureus* FnBPA$^{(+)}$ cells using tips labelled with the FnBPA A domain.
B,C. Force data obtained with labelled tips for 2 FnBPA$^{(+)}$ cells (cells #1, 2) in the presence of 1 mM EDTA (B), and with bare tips on 2 FnBPA$^{(+)}$ cells (**C**).
D. Force data obtained for 2 *S. aureus* FnBPA$^{(-)}$ cells. All curves were obtained using a contact time of 100 ms, a maximum applied force of 250 pN, and approach and retraction speeds of 1000 nm s^{-1}. *n* values represent the total number of force curves for each experiment.

Acknowledgements

Work at the Université catholique de Louvain was supported by the National Fund for Scientific Research (FNRS), the Université catholique de Louvain (Fonds Spéciaux de Recherche), the Région Wallonne, the Federal Office for Scientific, Technical and Cultural Affairs (Interuniversity Poles of Attraction Programme), and the Research Department of the Communauté française de Belgique (Concerted Research Action). Y.F.D. is a Research Director of the FNRS.

References

1. Otto, M. 2008. Staphylococcal biofilms. Curr. Top. Microbiol. Immunol. 322:207-228. http://dx.doi.org/10.1007/978-3-540-75418-3_10.
2. Foster, T. J., J. A. Geoghegan, V. K. Ganesh, and M. Hook. 2014. Adhesion, invasion and evasion: the many functions of the surface proteins of *Staphylococcus aureus*. Nat. Rev. Microbiol. 12:49-62. http://dx.doi.org/10.1038/nrmicro3161.
3. Chambers, H. F., and F. R. Deleo. 2009. Waves of resistance: *Staphylococcus aureus* in the antibiotic era. Nat. Rev. Microbiol. 7:629-641. http://dx.doi.org/10.1038/nrmicro2200.
4. DeLeo, F. R., M. Otto, B. N. Kreiswirth, and H. F. Chambers. 2010. Community-associated meticillin-resistant *Staphylococcus aureus*. Lancet. 375:1557-1568. http://dx.doi.org/10.1016/S0140-6736(09)61999-1.
5. Speziale, P., Pietrocola, G., Foster T. J., Geoghegan, J. A. 2014. Protein-based biofilm matrices in Staphylococci. Front. Cell. Infec. Microbiol. 4:1-10. http://dx.doi.org/10.3389/fcimb.2014.00171.
6. O'Neill, E., C. Pozzi, P. Houston, H. Humphreys, D. A. Robinson, A. Loughman, T. J. Foster, and J. P. O'Gara. 2008. A novel *Staphylococcus aureus* biofilm phenotype mediated by the fibronectin-binding proteins, FnBPA and FnBPB. J. Bacteriol. 190:3835-3850. http://dx.doi.org/10.1128/JB.00167-08.
7. Geoghegan, J. A., I. R. Monk, J. P. O'Gara, and T. J. Foster. 2013. Subdomains N2N3 of fibronectin binding protein A mediate *Staphylococcus aureus* biofilm formation and adherence to fibrinogen using distinct mechanisms. J. Bacteriol. 195:2675-2683. http://dx.doi.org/10.1128/JB.02128-12.
8. McCourt, J., D. P. O'Halloran, H. McCarthy, J. P. O'Gara, and J. A. Geoghegan. 2014. Fibronectin-binding proteins are required for biofilm formation by community-associated methicillin-resistant *Staphylococcus aureus* strain LAC. FEMS Microbiol. Lett. 353:157-164. http://dx.doi.org/10.1111/1574-6968.12424.
9. Ponnuraj, K., M. G. Bowden, S. Davis, S. Gurusiddappa, D. Moore, D. Choe, Y. Xu, M. Hook, and S. V. Narayana. 2003. A "dock, lock, and latch" structural model for a staphylococcal adhesin binding to fibrinogen. Cell. 115:217-228. http://dx.doi.org/10.1016/S0092-8674(03)00809-2.
10. Keane, F. M., A. Loughman, V. Valtulina, M. Brennan, P. Speziale, and T. J. Foster. 2007. Fibrinogen and elastin bind to the same region within

the A domain of fibronectin binding protein A, an MSCRAMM of *Staphylococcus aureus*. Mol. Microbiol. 63:711-723. http://dx.doi.org/10.1111/j.1365-2958.2006.05552.x.

11. Stemberk, V., R. P. Jones, O. Moroz, K. E. Atkin, A. M. Edwards, J. P. Turkenburg, A. P. Leech, R. C. Massey, and J. R. Potts. 2014. Evidence for steric regulation of fibrinogen binding to *Staphylococcus aureus* fibronectin-binding protein A (FnBPA). J. Biol. Chem. 289:12842-12851. http://dx.doi.org/10.1074/jbc.M113.543546.
12. Bustanji, Y., C. R. Arciola, M. Conti, E. Mandello, L. Montanaro, and B. Samori. 2003. Dynamics of the interaction between a fibronectin molecule and a living bacterium under mechanical force. Proc. Natl. Acad. Sci. U.S.A. 100:13292-13297. http://dx.doi.org/10.1073/pnas.1735343100.
13. Xu, C. P., N. P. Boks, J. de Vries, H. J. Kaper, W. Norde, H. J. Busscher, and H. C. van der Mei. 2008. *Staphylococcus aureus*-fibronectin interactions with and without fibronectin-binding proteins and their role in adhesion and desorption. Appl. Environ. Microbiol. 74:7522-7528. http://dx.doi.org/10.1128/AEM.00948-08.
14. Buck, A. W., V. G. Fowler, Jr., R. Yongsunthon, J. Liu, A. C. DiBartola, Y. A. Que, P. Moreillon, and S. K. Lower. 2010. Bonds between fibronectin and fibronectin-binding proteins on *Staphylococcus aureus* and *Lactococcus lactis*. Langmuir. 26:10764-10770. http://dx.doi.org/10.1021/la100549u.
15. Lower, S. K., R. Yongsunthon, N. N. Casillas-Ituarte, E. S. Taylor, A. C. DiBartola, B. H. Lower, T. J. Beveridge, A. W. Buck, and V. G. Fowler, Jr. 2010. A tactile response in *Staphylococcus aureus*. Biophys. J. 99:2803-2811. http://dx.doi.org/10.1016/j.bpj.2010.08.063.
16. Casillas-Ituarte, N. N., B. H. Lower, S. Lamlertthon, V. G. Fowler, Jr., and S. K. Lower. 2012. Dissociation rate constants of human fibronectin binding to fibronectin-binding proteins on living *Staphylococcus aureus* isolated from clinical patients. J. Biol. Chem. 287:6693-6701. http://dx.doi.org/10.1074/jbc.M111.285692.
17. Emerson, R. J. t., T. S. Bergstrom, Y. Liu, E. R. Soto, C. A. Brown, W. G. McGimpsey, and T. A. Camesano. 2006. Microscale correlation between surface chemistry, texture, and the adhesive strength of *Staphylococcus epidermidis*. Langmuir. 22:11311-11321. http://dx.doi.org/10.1021/la061984u.
18. Peters, B. M., E. S. Ovchinnikova, B. P. Krom, L. M. Schlecht, H. Zhou, L. L. Hoyer, H. J. Busscher, H. C. van der Mei, M. A. Jabra-Rizk, and M. E. Shirtliff. 2012. *Staphylococcus aureus* adherence to *Candida*

albicans hyphae is mediated by the hyphal adhesin Als3p. Microbiology. 158:2975-2986. http://dx.doi.org/10.1099/mic.0.062109-0.

19. Zeng, G., T. Müller, and R. L. Meyer. 2014. Single-cell force spectroscopy of bacteria enabled by naturally derived proteins. Langmuir. 30:4019-4025. http://dx.doi.org/10.1021/la404673q.
20. Alsteens, D., A. Beaussart, S. El-Kirat-Chatel, R. M. Sullan, and Y. F. Dufrêne. 2013. Atomic force microscopy: a new look at pathogens. PLoS Pathog. 9:e1003516. http://dx.doi.org/10.1371/journal.ppat.1003516.
21. Dufrêne, Y. F. 2014. Atomic force microscopy in microbiology: new structural and functional insights into the microbial cell surface. mBio. 5:e01363-01314. http://dx.doi.org/10.1128/mBio.01363-14.
22. Beaussart, A., S. El-Kirat-Chatel, P. Herman, D. Alsteens, J. Mahillon, P. Hols, and Y. F. Dufrêne. 2013. Single-cell force spectroscopy of probiotic bacteria. Biophys. J. 104:1886-1892. http://dx.doi.org/10.1016/j.bpj.2013.03.046.
23. Beaussart, A., S. El-Kirat-Chatel, R. M. Sullan, D. Alsteens, P. Herman, S. Derclaye, and Y. F. Dufrêne. 2014. Quantifying the forces guiding microbial cell adhesion using single-cell force spectroscopy. Nat. Protoc. 9:1049-1055. http://dx.doi.org/10.1038/nprot.2014.066.
24. El-Kirat-Chatel, S., D. Mil-Homens, A. Beaussart, A. M. Fialho, and Y. F. Dufrêne. 2013. Single-molecule atomic force microscopy unravels the binding mechanism of a *Burkholderia cenocepacia* trimeric autotransporter adhesin. Mol. Microbiol. 89:649-659. http://dx.doi.org/10.1111/mmi.12301.
25. Fritz, J., A. G. Katopodis, F. Kolbinger, and D. Anselmetti. 1998. Force-mediated kinetics of single P-selectin/ligand complexes observed by atomic force microscopy. Proc. Natl. Acad. Sci. U.S.A. 95:12283-12288. http://dx.doi.org/10.1073/pnas.95.21.12283.
26. King, N. P., S. A. Beatson, M. Totsika, G. C. Ulett, R. A. Alm, P. A. Manning, and M. A. Schembri. 2011. UafB is a serine-rich repeat adhesin of *Staphylococcus saprophyticus* that mediates binding to fibronectin, fibrinogen and human uroepithelial cells. Microbiology 157:1161-1175. http://dx.doi.org/10.1099/mic.0.047639-0.
27. King, N. P., T. Sakinc, N. L. Ben Zakour, M. Totsika, B. Heras, P. Simerska, M. Shepherd, S. G. Gatermann, S. A. Beatson, and M. A. Schembri. 2012. Characterisation of a cell wall-anchored protein of *Staphylococcus saprophyticus* associated with linoleic acid resistance. BMC Microbiol. 12:8. http://dx.doi.org/10.1186/1471-2180-12-8.
28. Xu, L. C., and C. A. Siedlecki. 2012. Effects of plasma proteins on *Staphylococcus epidermidis* RP62A adhesion and interaction with

platelets on polyurethane biomaterial surfaces. J. Biomater. Biotechnol. 3:487-498. http://dx.doi.org/10.4236/jbnb.2012.324050.

29. Oesterhelt, F., D. Oesterhelt, M. Pfeiffer, A. Engel, H. E. Gaub, and D. J. Müller. 2000. Unfolding pathways of individual bacteriorhodopsins. Science 288:143-146. http://dx.doi.org/10.1126/science.288.5463.143.
30. Herman, P., S. El-Kirat-Chatel, A. Beaussart, J. A. Geoghegan, T. J. Foster, and Y. F. Dufrêne. 2014. The binding force of the staphylococcal adhesin SdrG is remarkably strong. Mol. Microbiol. 93:356-368. http://dx.doi.org/10.1111/mmi.12663.
31. Alsteens, D., P. Van Dijck, P. N. Lipke, and Y. F. Dufrêne. 2013. Quantifying the forces driving cell-cell adhesion in a fungal pathogen. Langmuir. 29:13473-13480. http://dx.doi.org/10.1021/la403237f.
32. Francius, G., O. Domenech, M. P. Mingeot-Leclercq, and Y. F. Dufrêne. 2008. Direct observation of *Staphylococcus aureus* cell wall digestion by lysostaphin. J. Bacteriol. 190:7904-7909. http://dx.doi.org/10.1128/JB.01116-08.
33. Baumgartner, W., P. Hinterdorfer, W. Ness, A. Raab, D. Vestweber, H. Schindler, and D. Drenckhahn. 2000. Cadherin interaction probed by atomic force microscopy. Proc. Natl. Acad. Sci. U.S.A. 97:4005-4010. http://dx.doi.org/10.1073/pnas.070052697.
34. Verbelen, C., D. Raze, F. Dewitte, C. Locht, and Y. F. Dufrêne. 2007. Single-molecule force spectroscopy of mycobacterial adhesin-adhesin interactions. J. Bacteriol. 189:8801-8806. http://dx.doi.org/10.1128/JB.01299-07.
35. Hinterdorfer, P., W. Baumgartner, H. J. Gruber, K. Schilcher, and H. Schindler. 1996. Detection and localization of individual antibody-antigen recognition events by atomic force microscopy. Proc. Natl. Acad. Sci. U.S.A. 93:3477-3481. http://www.ncbi.nlm.nih.gov/pmc/articles/PMC39634/.
36. Vergara-Irigaray, M., J. Valle, N. Merino, C. Latasa, B. Garcia, I. Ruiz de Los Mozos, C. Solano, A. Toledo-Arana, J. R. Penades, and I. Lasa. 2009. Relevant role of fibronectin-binding proteins in *Staphylococcus aureus* biofilm-associated foreign-body infections. Infec. Immun. 77:3978-3991. http://dx.doi.org/10.1128/IAI.00616-09.
37. Barbu, E. M., C. Mackenzie, T. J. Foster, and M. Hook. 2014. SdrC induces staphylococcal biofilm formation through a homophilic

interaction. Mol. Microbiol. 94:172-185. http://dx.doi.org/10.1111/mmi.12750.

38. Otto, M. 2014. Physical stress and bacterial colonization. FEMS Microbiol. Rev. 38:1250-1270. http://dx.doi.org/10.1111/1574-6976.12088.
39. Geoghegan, J. A., R. M. Corrigan, D. T. Gruszka, P. Speziale, J. P. O'Gara, J. R. Potts, and T. J. Foster. 2010. Role of surface protein SasG in biofilm formation by *Staphylococcus aureus*. J. Bacteriol. 192:5663-5673. http://dx.doi.org/10.1128/JB.00628-10.
40. Conrady, D. G., C. C. Brescia, K. Horii, A. A. Weiss, D. J. Hassett, and A. B. Herr. 2008. A zinc-dependent adhesion module is responsible for intercellular adhesion in staphylococcal biofilms. Proc. Natl. Acad. Sci. U.S.A. 105:19456-19461. http://dx.doi.org/10.1073/pnas.0807717105.
41. Conrady, D. G., J. J. Wilson, and A. B. Herr. 2013. Structural basis for Zn2+-dependent intercellular adhesion in staphylococcal biofilms. Proc. Natl. Acad. Sci. U.S.A. 110:E202-211. http://dx.doi.org/10.1073/pnas.1208134110.
42. Becker, K. W., and E. P. Skaar. 2014. Metal limitation and toxicity at the interface between host and pathogen. FEMS Microbiol. Rev. 38:1235-1249. http://dx.doi.org/10.1111/1574-6976.12087.
43. Kehl-Fie, T. E., and E. P. Skaar. 2010. Nutritional immunity beyond iron: a role for manganese and zinc. Curr. Op. Chem. Biol. 14:218-224. http://dx.doi.org/10.1016/j.cbpa.2009.11.008.
44. Zalewski, P., A. Truong-Tran, S. Lincoln, D. Ward, A. Shankar, P. Coyle, L. Jayaram, A. Copley, D. Grosser, C. Murgia, C. Lang, and R. Ruffin. 2006. Use of a zinc fluorophore to measure labile pools of zinc in body fluids and cell-conditioned media. BioTechniques 40:509-520. http://www.ncbi.nlm.nih.gov/pubmed/16629398
45. Rice, K. C., E. E. Mann, J. L. Endres, E. C. Weiss, J. E. Cassat, M. S. Smeltzer, and K. W. Bayles. 2007. The cidA murein hydrolase regulator contributes to DNA release and biofilm development in *Staphylococcus aureus*. Proc. Natl. Acad. Sci. U.S.A. 104:8113-8118. http://dx.doi.org/10.1073/pnas.0610226104.
46. Katayama, A., A. Tsujii, A. Wada, T. Nishino, and A. Ishihama. 2002. Systematic search for zinc-binding proteins in *Escherichia coli*. FEBS J. 269:2403-2413. http://dx.doi.org/10.1046/j.1432-1033.2002.02900.x.
47. Cassat, J. E., N. D. Hammer, J. P. Campbell, M. A. Benson, D. S. Perrien, L. N. Mrak, M. S. Smeltzer, V. J. Torres, and E. P. Skaar. 2013. A secreted bacterial protease tailors the *Staphylococcus aureus* virulence

repertoire to modulate bone remodeling during osteomyelitis. Cell Host Microbe 13:759-772. http://dx.doi.org/10.1016/j.chom.2013.05.003.

48. Berquand, A., N. Xia, D. G. Castner, B. H. Clare, N. L. Abbott, V. Dupres, Y. Adriaensen, and Y. F. Dufrêne. 2005. Antigen binding forces of single antilysozyme Fv fragments explored by atomic force microscopy. Langmuir. 21:5517-5523. http://dx.doi.org/10.1021/la050162e.

Chapter V

Single-cell force spectroscopy of the medically important *Staphylococcus epidermidis*-*Candida albicans* interaction

Audrey Beaussart, Philippe Herman, Sofiane El-Kirat-Chatel, Peter N. Lipke, Soňa Kucharíková, Patrick Van Dijck and Yves F. Dufrêne

In *Nanoscale*, **2013**, 3, 10894

I contributed by doing some AFM analyses, and by helping to write the paper.

Abstract

Despite the clinical importance of bacterial-fungal interactions, their molecular details are poorly understood. A hallmark of such medically-important interspecies associations is the interaction between the two nosocomial pathogens *Staphylococcus aureus* and *Candida albicans*, which can lead to mixed biofilm-associated infections with enhanced antibiotic resistance. Here, we use single-cell force spectroscopy (SCFS) to quantify the forces engaged in bacterial-fungal co-adhesion, focusing on the poorly investigated *S. epidermidis*-*C. albicans* interaction. Force curves recorded between single bacterial and fungal germ tubes showed large adhesion forces (~5 nN) with extended rupture lengths (up to 500 nm). By contrast, bacteria poorly adhered to yeast cells, emphasizing the important role of the yeast-to-hyphae transition in mediating adhesion to bacterial cells. Analysis of mutant strains altered in cell wall composition allowed us to distinguish the main fungal components involved in adhesion, *i.e.* Als proteins and *O*-mannosylations. We suggest that the measured co-adhesion forces are involved in the formation of mixed biofilms, thus possibly as well in promoting polymicrobial infections. In the future, we anticipate that this SCFS platform will be used in nanomedicine to decipher the molecular mechanisms of a wide variety of pathogen-pathogen interactions and may help designing novel anti-adhesion agents.

Introduction

The interactions between bacterial and fungal pathogens are of high clinical importance as they may lead to higher morbidity and mortality.[1-4] Polymicrobial infections generally involve the formation of mixed biofilms, *i.e.* attachment of various microbial species to a substrate and to each other.[5-8] Therefore, knowledge of the molecular mechanisms behind bacterial-fungal co-adhesion is critical to our understanding of mixed infections and may aid in the development of novel anti-biofilm molecules.

A widely investigated example of such association is the interaction between *Staphylococcus aureus* and *Candida albicans*.[9-11] It has been shown that co-inoculation of *C. albicans* and *Staphylococcus aureus* leads to mortality increases.[2, 3, 12] *In vivo*, the synergistic effect of the two microorganisms has been observed in mice.[12] When grown in mixed biofilms, *S. aureus* has been shown to attach primarily to *C. albicans* hyphae.[9, 10] Recent biochemical and microscopy studies have shown that the *C. albicans* adhesion proteins Als mediate fungal-bacterial interactions,[13] in particular Als3 which is primarily expressed on germ tubes and is directly involved in the adhesion to *Streptococcus gordonii*[14] and *Staphylococcus aureus*.[15] Whether the other nosocomial *Staphylococcus* species *S. epidermidis* also interacts with *C. albicans* and can lead to mixed infections has been much less investigated. Both species showed extensive interactions when grown in mixed fungal-bacterial biofilms.[16] In addition, it appeared that the two species could modulate the action of antibiotics and antifungals in mixed biofilms.[16] So far, however, the adhesion forces engaged in the *S. epidermidis* - *C. albicans* interaction have never been investigated.

Single-cell microbiology is a fast-growing field that uses emerging technologies for single-cell analysis, thereby revealing population and cell heterogeneity, as well as rare events that were otherwise not accessible.[17, 18] In cell adhesion and biofilm research, single-cell force spectroscopy (SCFS) offers unprecedented possibilities to quantify cell-cell and cell-solid interactions at the single-cell and single-molecule levels.[19, 20] In this report, we used SCFS to quantify the forces engaged in the *S. epidermidis*-*C. albicans* interaction. As the yeast-to-hyphae transition is important for *C. albicans* adhesion and biofilm formation,[4, 21] we measured the forces between single bacterial cells and fungal hyphae. The

results emphasize the important role of cellular morphogenesis, Als proteins and *O*-mannosylations in controlling *S. epidermidis*-*C. albicans* co-adhesion.

Results and discussion

Experimental set-up

To probe bacterial-fungal interaction forces by SCFS, we used a recently developed protocol which combines the use of colloidal probe cantilevers and of a bioinspired polydopamine wet adhesive.[22] Single *S. epidermidis* cells were picked up with a polydopamine-coated colloidal probe and approached towards a fungal cell immobilized on a hydrophobic substrate (**Figure 1a**). Using an integrated AFM-inverted optical microscope, the bacterial probe was positioned on top of random spots across the fungal cell (**Figure 1b**). Fluorescence imaging confirmed that single bacterial cells attached on the probe were alive (*Bac*light LIVE/DEAD stain; green color). Note that in **Figure 1b** *C. albicans* was stained in blue (Calcofluor White) for better visualization, but as this dye alters cell surface properties it was not used in force experiments.

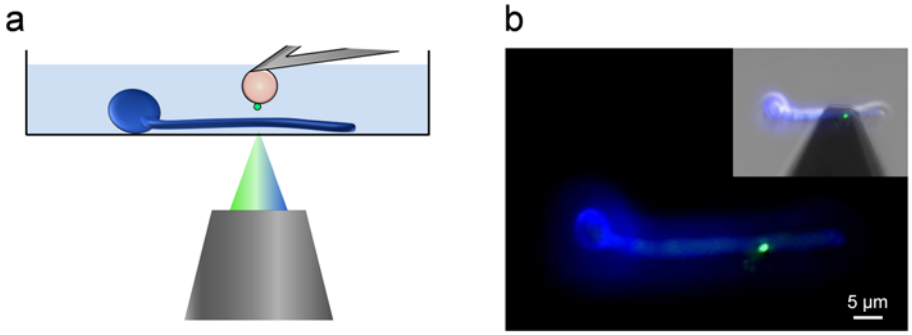

Figure 1: Single-cell force spectroscopy of bacterial-fungal interactions.
a. Schematic of the experimental set-up.
b. Using an integrated AFM-inverted optical microscope, the *S. epidermidis* probe (green) is approached towards a *C. albicans* hyphae (blue). The image was obtained using epifluorescence microscopy while the inset shows a merged phase/epifluorescence image.

Bacterial-fungal adhesion: germ tube *vs.* yeast region

In *C. albicans*, the yeast-to-hyphae transition is associated with changes in cell wall composition that play important roles in promoting biofilm formation.[4] Consistent with this, single-molecule analyses recently showed that cellular morphogenesis leads to a major increase in the distribution and biophysical properties (stickiness, extension) of Als adhesins on the fungal cell surface.[23] With this in mind, we measured the adhesion between single *S. epidermidis* cells and *C. albicans* hyphae (**Figure 2a**). **Figure 2b** shows a set of representative force-distance curves recorded between individual bacteria and germ tubes. All curves showed large adhesion forces (4.6 nN ± 1.5 nN; n =

975 force curves corresponding to cell pair #1 in **Figures 2c and d**) with multiple, sequential peaks and extended rupture lengths (419 ± 137 nm). The general features of the curves did not substantially change when recording consecutive force curves (up to several hundreds) on the same spot, indicating that force measurements did not alter the interacting cell surfaces. Also, similar force signatures were observed when probing different regions of the germ tubes (*e.g.* apex *vs.* center of the tube), suggesting that the adhesion properties of the tube were homogeneous. **Figures 2c and d** show that probing bacterial-fungal interactions using cells from independent cultures generally revealed adhesion properties that were in the same range (pairs #1 and #2); however, in some cases weaker adhesion was observed (1.9 nN ± 1.0 nN, pair #3), an effect that we believe could reflect heterogeneity in the bacterial and/or fungal cell populations.

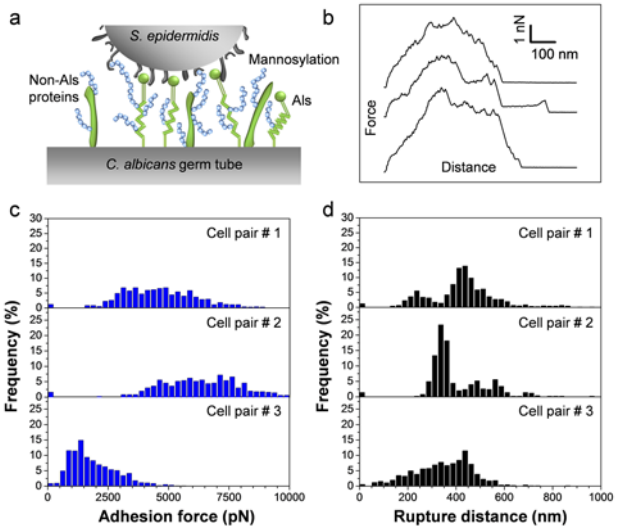

Figure 2: SCFS quantifies the adhesion forces between *S. epidermidis* and *C. albicans* germ tubes.
a. Key cell wall components that are involved in *C. albicans* surface interactions are cell-surface glycoproteins (in green) and mannose-rich glycoconjugates (in blue).
b. Typical force-distance curves recorded in Tris NaCl buffer between *S. epidermidis* and *C. albicans* hyphae.
c and d. Adhesion force (**c**) and rupture length (**d**) histograms obtained by recording force curves between 3 cell pairs from different cell cultures, and representative of a total of 7 cell pairs (n > 500 force-distances curves for each pair).

To determine whether the measured forces are specific to the *C. albicans* germ tube, we then probed the yeast region of the germinating cell (**Figure 3a**). As can be seen in **Figure 3**, a drop in adhesion frequency was observed (from 99 % on germ tube to 84 % on yeast; cell pair #1), together with a decrease in adhesion forces (from 4.6 nN ± 1.5 nN to 0.6 nN ± 0.5 nN). Sometimes, these effects were even more pronounced (cell pair #3). On close examination, a number of force curves showed sawtooth patterns with multiple large force peaks rupturing at around 500 pN and in the 300-600 nm range. In the light of earlier single-molecule work,[23-25] we suggest these features reflect the sequential unfolding of the tandem repeat (TR) domains of Als proteins on the yeast surface. As the average forces measured on germ tubes (4.6 nN) are much larger than those associated with single protein unfolding, it is likely

that the strongly adhesive signatures result from multiple Als unfolding interactions, thus explaining why they consist of multiple poorly defined peaks.

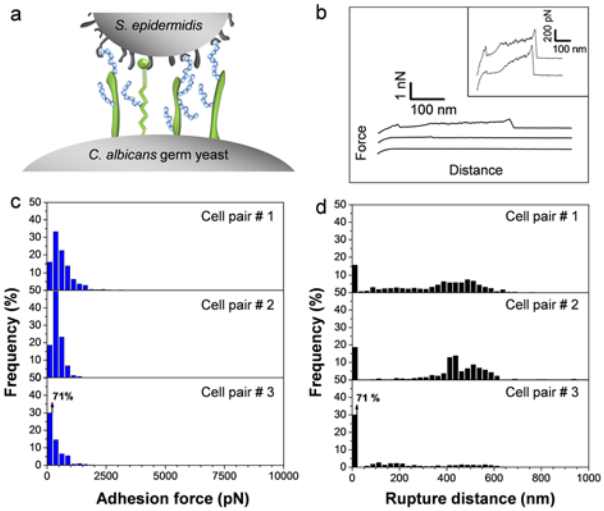

Figure 3: *C. albicans* germinating yeasts show much weaker adhesion than germ tubes.
a. Germinating yeasts express fewer Als proteins than germ tubes.
b. Typical force-distance curves recorded in Tris NaCl buffer between *S. epidermidis* and *C. albicans* germinating yeasts.
c, d. Adhesion force (**c**) and rupture length (**d**) histograms obtained by recording force curves between 3 cell pairs from different cell cultures, and representative of a total of 6 cell pairs (n > 500 force-distances curves for each pair).

Biological specificity of adhesion forces

To determine the specificity of the measured adhesion forces and rule out the possibility of artifacts associated with the cell probe preparation, two control experiments were performed, *i.e.* use of polydopamine-coated probes or silica probes instead of bacterial probes. As can be seen in **Figure 4**, use of these non-cellular probes led to a major reduction of adhesion frequency (down to 1 % between polydopamine and the germinating yeast, **Figure 4a**) and mean adhesion force, indicating that the strong adhesion forces measured earlier indeed reflect bacterial-fungal interactions. These data also confirm that the polydopamine adhesive does not interfere with the measurements, *e.g.* through contamination of the bacterial probe.

Als proteins and *O*-mannosylations on the *C. albicans* surface are required for bacterial adhesion

Cell-surface glycoproteins and mannose-rich glycoconjugates play key roles in *C. albicans* surface interactions.[26] Specifically, Als adhesins mediate cell adhesion and biofilm formation, and mannose-rich polymers are recognized by a variety of lectin receptors on immune cells. We therefore reasoned that both compounds may be involved in bacterial-fungal adhesion. To test this hypothesis, we measured the forces between single *S. epidermidis* cells and *C. albicans* mutant strains altered in cell wall components. **Figures 5a and b** show the curves obtained on germ tubes from the double mutant *als3Δ/als3Δ als1Δ/als1Δ,* in which the genes coding for the expression of Als1 and Als3 proteins have been deleted. Adhesion forces and rupture distances that were much smaller than those on the WT were observed, thus demonstrating that

Als3 and/or Als1 proteins, primarily expressed on germ tubes, are required for bacterial-fungal association. Similar observations have recently been reported for the interaction between *S. aureus* and *C. albicans*.[15, 27] We suggest that N-terminal immunoglobulin-like regions of Als proteins specifically binds peptide ligands on the bacterial surface, *i.e.* peptide sequences containing the "τϕ+" motif.[28]

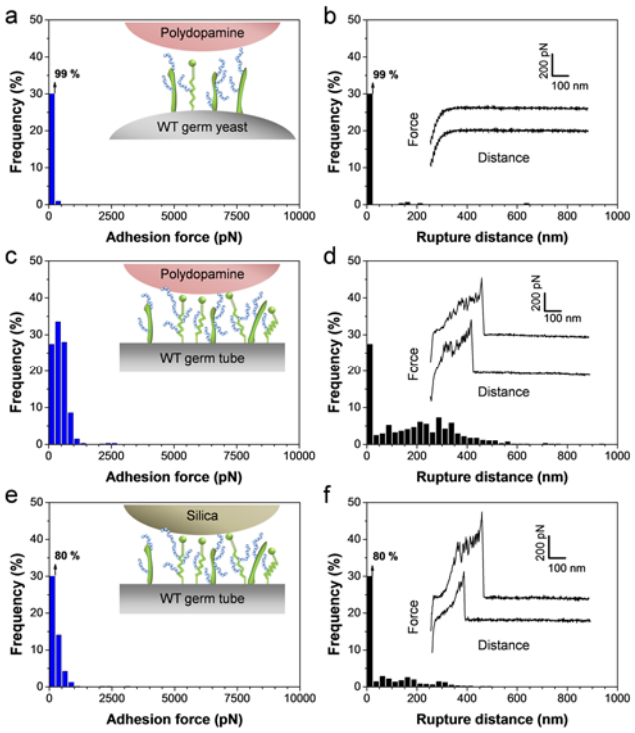

Figure 4: Control experiments using polydopamine and silica probes. **a to f.** Adhesion force (**a, c, e**) and rupture length (**b, d, f**) histograms, together with representative force curves, obtained by recording force curves between polydopamine-coated probes and *C. albicans* germinating yeasts (**a, b**) or germ tubes (**c, d**), and between silica probes and *C. albicans* germ tubes (**e, f**). For each probe, similar data were obtained in 3 independent experiments.

Can the measured adhesion forces be converted into a surface density of interacting molecules? As the specific binding force of single Als proteins was previously measured to be ~330 pN,[23] we estimate that the 4.6 nN forces would correspond to ~14 Als bonds. The obtained values may be converted into protein surface densities, considering the cell-cell contact area. As a rough approximation, the contact zone of a deformable sphere (the bacterium) pressed on a more rigid flat surface (the fungus) may be estimated by the following equation[29, 30] $A = R\,\delta$, in which A is the contact area, R the radius of the cell, and δ the cell deformation. Considering a cell radius of 0.5 µm and a deformation of 30 nm (estimated from indentation curves), we found a contact area of ~0.05 µm², thus yielding a protein surface density of around 280 proteins/µm². Note that this value is an upper estimate as we expect that the curvature of the fungal germ tube will lower the cell-cell contact area. Nevertheless, this density is roughly consistent with the value expected for

fungal adhesins, and with numbers estimated from single-molecule imaging experiments.[23]

Another important finding is that the *C. albicans* double mutant strain *mnt1Δ/mnt1Δ mnt2Δ/mnt2Δ* defective in *O*-linked mannosylations[31] showed similar reduction in adhesion probability and adhesion strength (**Figures 5c and d**), suggesting strongly that fungal mannosylations are recognized by lectins on the bacterial surface. In addition, smaller rupture distances were observed, consistent with the notion that mannosylations in the mutant are shorter. That *O*-linked mannosylations are important for bacterial-fungal adhesion agrees well with earlier reports showing their involvement in adhesion to host cells[31] and to *Pseudomonas aeruginosa* bacteria.[32] This result is also consistent with the notion that adhesion of bacterial pathogens, such as *Pseudomonas aeruginosa*, involves mannose-binding lectins on the bacterial surface.[33]

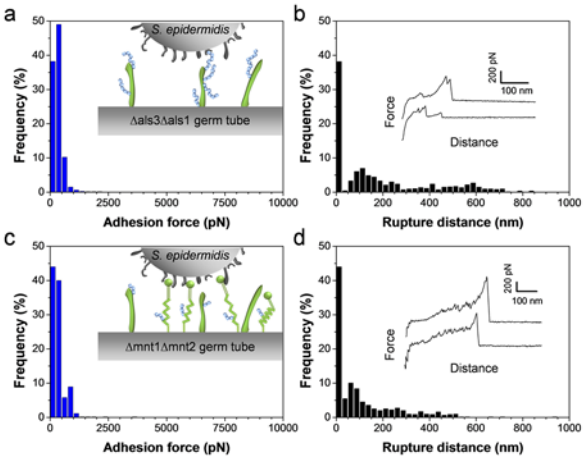

Figure 5: Als proteins and *O*-mannosylations on the *C. albicans* surface are required for bacterial adhesion.
a to d. Adhesion force (**a, c**) and rupture length (**b, d**) histograms, together with representative force curves, obtained by recording force curves in Tris NaCl buffer between a single *S. epidermidis* bacterium and a *C. albicans* germ tube from the mutant *als3Δ/als3Δ als1Δ/als1Δ* (Δals3Δals1) (**a, b**) or a *C. albicans* germ tube from the mutant *mnt1Δ/mnt1Δ mnt2Δ/mnt2Δ* (Δmnt1Δmnt2) (**c, d**). For each mutant, similar data were obtained in 3 independent experiments using 3 different cell pairs.

Conclusions

In recent years, there have been several attempts to apply AFM force spectroscopy to probe the adhesion forces engaged in bacterial-fungal interactions, including the important *S. aureus* – *C. albicans* interaction.[15, 27] These results are difficult to interpret at the molecular level because of a poorly-controlled methodology: cells are attached on the cantilever using protocols that may lead to cell surface denaturation or cell death, multiple cells are attached and probed together, cell positioning and cell-substrate contact area are poorly controlled. We have shown that SCFS with polydopamine-coated colloidal probes is a valuable approach for quantifying the adhesion forces of medically-important bacterial-fungal interactions. Unlike most other protocols used in microbiology, this method is non-destructive (living cells are probed), guarantees true single-cell measurements and affords precise positioning of the interacting cells, thereby ensuring true and reliable single-bacterial cell analysis. **Figure 6** summarizes our main findings, that is: (i) *S. epidermidis* strongly binds to *C. albicans* germ tubes but poorly adheres to yeast cells, emphasizing the important role of the yeast-to-hyphae transition in mediating adhesion to bacterial cells; (ii) co-adhesion primarily involves two types of highly adhesive and extended macromolecules, *i.e.* Als proteins and O-mannosylations, that we believe bind to Als ligands and lectins on the bacterial surface. When subjected to mechanical force, the interacting cell surfaces will detach but the cells will remain bridged through these extended polymers. Our finding of strong *S. epidermidis*-*C. albicans* adhesion forces is reminiscent of the well-known *S. aureus*-*C. albicans* interaction[3, 9, 15, 27, 34] thus suggesting that the *S. epidermidis*-*C. albicans* co-adhesion quantified here will favor the formation of mixed biofilms, and in turn promote polymicrobial infections.

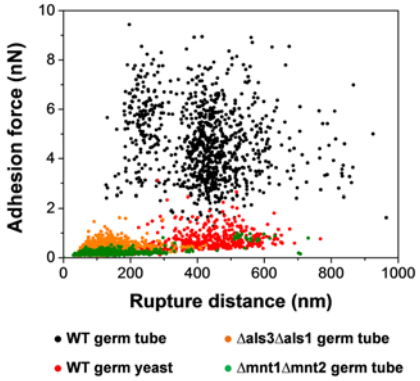

Figure 6: Role of cellular morphogenesis, Als proteins and *O*-mannosylations in *S. epidermidis*-*C. albicans* adhesion. Plots of the adhesion forces versus rupture distances measured between *S. epidermidis* and WT germ tubes (black symbols), WT germinated yeasts (red symbols), *als3Δ/als3Δ als1Δ/als1Δ* (Δals3Δals1) germ tubes (orange symbols) and *mnt1Δ/mnt1Δ mnt2Δ/mnt2Δ* (Δmnt1Δmnt2) germ tubes (green symbols). Strong co-adhesion is only observed on germ tubes and involves two types of highly adhesive and extended macromolecules, *i.e.* Als proteins and *O*-mannosylations.

Methods

Microorganisms and cultures

C. albicans SC5314[35] was cultivated in YPD medium (1% yeast extract, 2% Bacto-peptone, 2% D-glucose, supplemented with 2% agar) at 30°C. A few colonies were inoculated in YPD liquid medium and incubated overnight (30°C, 200 rpm). For hyphae formation, germination was induced by inoculating 250 µL of cell suspension in 8 mL of RPMI 1640 medium buffered with MOPS (Sigma) at pH 7, and incubated at 37°C, 200 rpm, for 90 min unless otherwise stated.[36] We used two *C. albicans* mutant strains, *i.e. als3Δ/als3Δ als1Δ/als1Δ* (designated as △als3△als1) with deletions of both alleles of *ALS* genes (kindly provided by Aaron Mitchell, Carnegie Mellon University, Pittsburgh, PA)[37] and *mnt1*△/*mnt1*△ *mnt2*△/*mnt2*△ (designated as △mnt1△mnt2) yielding defective *O*-linked mannosylations (kindly provided by Neil Gow, University of Aberdeen, UK).[31] *S. epidermidis* ATCC 35984 cells were grown in Trypto-Caseine-Soy (Bio-rad) at 37°C, 150 rpm. Overnight cultures were diluted in fresh media to an $OD_{600\ nm}$ of 0.1. The cells were harvested in the exponential growth phase (5 hours at 37°C, 150 rpm), and washed 3 times in 50 mM Tris-NaCl buffer. For cell probe preparation, 50 µL of a 100-fold diluted solution were transferred in a glass petri dish and the bacteria were let to settle for 15 min.

Immobilization of *C. albicans*

Germinating yeast cells of *C. albicans* were immobilized through hydrophobic attachment on solid substrata. To this end, glass coverslips coated with a thin layer of gold were immersed overnight in a 1 mM solution of 1-dodecanethiol (Sigma), rinsed with ethanol and dried under N_2. After induction of germ tube formation in RPMI, the cells were harvested and rinsed three times in Tris-NaCl buffer, pH 7.5. Drops (200 µL) of the concentrated suspension were deposited on the hydrophobic substrates and let stand for 3 h. The substrate was then rinsed to remove unattached yeast and fixed on a glass-bottom petri dish using double-sided tape. A droplet of buffer was then deposited on the substrate to avoid drying of the immobilized yeast.

Bacterial cell probes

Using a Nanoscope VIII Multimode AFM (Bruker corporation, Santa Barbara, CA), triangular shaped tipless cantilevers (NP-O10, Microlevers, Veeco Metrology Group) were slowly immersed in a very thin layer of UV-curable glue (NOA 63, Norland Edmund Optics) spread on a glass slide, and slowly brought into contact with a silica microsphere (6.1 µm diameter, bangs laboratories). After 3 min of contact, the colloidal probe was cured for 10 min under a UV-lamp. The cantilever was then immersed for 1 hr in a 10 mM Tris

Buffer solution (pH 8.5) containing 4 mg/mL dopamine hydrochloride (99%, Sigma). The probe was then washed and dried under N_2.

Proper attachment and positioning of bacteria on the colloidal probe were achieved using a Bioscope Catalyst (Bruker Corporation, Santa Barbara, CA) equipped with a Zeiss Axio Observer Z1 and a Hamamatsu camera C10600. To check the viability of the bacteria, a Live-dead Bac*light* viability kit (Invitrogen, kit L7012) was used. Prior to attachment, 2 µL of a 1:1 Syto 9 (green fluorescent nucleic acid stain)/Propidium iodide (red-fluorescent nuclear and chromosome counterstain) mixture at 1.5 mM were added to a drop of 50 µL bacteria suspension and mixed thoroughly. The suspension was deposited in the glass petri dish where the substrate covered with *C. albicans* had been previously attached, and the bacteria were let to incubate with the dyes for 15 min in the dark. 4mL of buffer were then added to the petri dish, immerging both the bacteria deposited at the bottom of the petri dish and the *C. albicans* substrate. The colloidal probe was then mounted into the AFM and brought into contact with an isolated bacterium. When proper attachment of the bacterium was achieved, the probe was positioned over the *C. albicans* surface without dewetting. Using this protocol, we never (rarely) observed floating bacteria interacting with *C. albicans.*

Force measurements

AFM measurements were performed at room temperature (20 °C) in Tris-NaCl buffer at pH 7.5 using a Bioscope Catalyst AFM (Bruker AXS Corporation, Santa Barbara, CA). Using the inverted optical microscope, the bacterial probe was approached towards a fungal cell. Multiple forces curves were recorded on various spots using a maximum applied force of 250 pN, a contact time of 50 ms, and constant approach and retraction speeds of 1000 $nm.s^{-1}$. For each condition, the interaction forces between at least 3 pairs of bacterial-fungal cells from independent cultures were measured.

Acknowledgements

Work at the Université catholique de Louvain was supported by the National Foundation for Scientific Research (FNRS), the Université catholique de Louvain (Fonds Spéciaux de Recherche), the Région Wallonne, the Federal Office for Scientific, Technical and Cultural Affairs (Interuniversity Poles of Attraction Programme), and the Research Department of the Communauté française de Belgique (Concerted Research Action). Work at VIB, KU Leuven was supported by Flemish Science Foundation (FWO), the KU Leuven and by the Interuniversity Attraction Poles Programme, initiated by the Belgian Science Policy Office (IAP; P7/28). Work at Brooklyn College was supported

by NIH grant R01 GM 098616. Y.F.D. is Senior Research Associate of the FNRS.

References

1. A. Y. Peleg, D. A. Hogan and E. Mylonakis, *Nat. Rev. Microbiol.*, 2010, **8**, 340-349.
2. D. K. Morales and D. A. Hogan, *PLoS Pathog.*, 2010, **6**, 1-4.
3. M. E. Shirtliff, B. M. Peters and M. A. Jabra-Rizk, *FEMS Microbiol. Lett.*, 2009, **299**, 1-8.
4. L. J. Douglas, *Trends Microbiol.*, 2003, **11**, 30-36.
5. S. Elias and E. Banin, *FEMS Microbiol. Rev.*, 2012, **36**, 990-1004.
6. A. S. Lynch and G. T. Robertson, 2008, vol. **59**, pp. 415-428.
7. M. M. Harriott and M. C. Noverr, *Trends Microbiol.*, 2011, **19**, 557-563.
8. D. A. Hogan and R. Kolter, *Science*, 2002, **296**, 2229-2232.
9. B. M. Peters, M. A. Jabra-Rizk, M. A. Scheper, J. G. Leid, J. W. Costerton and M. E. Shirtliff, *FEMS Immunol. Med. Mic.*, 2010, **59**, 493-503.
10. M. M. Harriott and M. C. Noverr, *Antimicrob. agents ch.*, 2009, **53**, 3914-3922.
11. M. M. Harriott and M. C. *Noverr, Antimicrob. agents ch.*, 2010, **54**, 3746-3755.
12. E. Carlson, *Infect. Immun.*, 1983, **42**, 285-292.
13. S. A. Klotz, N. K. Gaur, R. De Armond, D. Sheppard, N. Khardori, J. E. Edwards, P. N. Lipke and M. El-Azizi, *Med. Mycol.*, 2007, **45**, 363-370.
14. R. J. Silverman, A. H. Nobbs, M. M. Vickerman, M. E. Barbour and H. F. Jenkinson*, Infect. Immun.*, 2010, **78**, 4644-4652.
15. B. M. Peters, E. S. Ovchinnikova, B. P. Krom, L. M. Schlecht, H. Zhou, L. L. Hoyer, H. J. Busscher, H. C. van der Mei, M. A. Jabra-Rizk and M. E. Shirtliff, *Microbiology*, 2012, **158**, 2975-2986.
16. B. Adam, G. S. Baillie and L. J. Douglas, *J. Med. Microbiol.*, 2002, **51**, 344-349.
17. M. E. Lidstrom and M. C. Konopka, *Nat. Chem. Biol.*, 2010, **6**, 705-712.
18. B. F. Brehm-Stecher and E. A. Johnson, *Microbiol. Mol. Biol.* R., 2004, **68**, 538-559.
19. D. J. Müller, J. Helenius, D. Alsteens and Y. F. Dufrêne, *Nat. Chem. Biol.*, 2009, **5**, 383-390.

20. M. Benoit, D. Gabriel, G. Gerisch and H. E. Gaub, *Nat. Cell Biol.*, 2000, **2**, 313-317.
21. J. S. Finkel and A. P. Mitchell, *Nat. Rev. Microbiol.*, 2011, **9**, 109-118.
22. A. Beaussart, S. El-Kirat-Chatel, P. Herman, D. Alsteens, J. Mahillon, P. Hols and Y. F. Dufrêne, *Biophys. J.*, 2013, **104**, 1886-1892.
23. A. Beaussart, D. Alsteens, S. El-Kirat-Chatel, P. N. Lipke, S. Kucharíková, P. Van Dijck and Y. F. Dufrêne, *ACS Nano*, 2012, **6**, 10950-10964.
24. D. Alsteens, V. Dupres, S. A. Klotz, N. K. Gaur, P. N. Lipke and Y. F. Dufrêne, *ACS Nano*, 2009, **3**, 1677-1682.
25. D. Alsteens, M. C. Garcia, P. N. Lipke and Y. F. Dufrêne, *Proc. Natl. Acad. Sci. U.S.A.*, 2010, **107**, 20744-20749.
26. N. A. R. Gow, F. L. Van De Veerdonk, A. J. P. Brown and M. G. Netea, *Nat. Rev. Microbiol.*, 2012, **10**, 112-122.
27. E. S. Ovchinnikova, B. P. Krom, H. J. Busscher and H. C. Van Der Mei, BMC *Microbiol.*, 2012, **12**.
28. S. A. Klotz, N. K. Gaur, D. F. Lake, V. Chan, J. Rauceo and P. N. Lipke, *Infect. Immun.*, 2004, **72**, 2029-2034.
29. B. Chatterjee and P. Sahoo, *Tribol. Ind.*, 2011, **33**, 164-172.
30. L. Kogut and I. Etsion, *J. appl. Mech.*, 2002, **69**, 657-662.
31. C. A. Munro, S. Bates, E. T. Buurman, H. B. Hughes, D. M. MacCallum, G. Bertram, A. Atrih, M. A. J. Ferguson, J. M. Bain, A. Brand, S. Hamilton, C. Westwater, L. M. Thomson, A. J. P. Brown, F. C. Odds and N. A. R. Gow, *J. Biol. Chem.*, 2005, **280**, 1051-1060.
32. A. Brand, J. D. Barnes, K. S. Mackenzie, F. C. Odds and N. A. R. Gow, *FEMS Microbiol. Lett.*, 2008, **287**, 48-55.
33. D. Hauck, I. Joachim, B. Frommeyer, A. Varrot, B. Philipp, H. M. Möller, A. Imberty, T. E. Exner and A. Titz, *ACS Chem. Biol.*, 2013, **8**, 1775-1784.
34. E. S. Ovchinnikova, H. C. Van der Mei, B. P. Krom and H. J. Busscher, *Colloid Surf. B*, 2013, **110**, 45-50.
35. A. M. Gillum, E. Y. H. Tsay and D. R. Kirsch, *Mol Gen. Genet.*, 1984, **198**, 179-182.
36. S. Kucharíková, H. Tournu, K. Lagrou, P. van Dijck and H. Bujdáková, *J. Med. Microbiol.*, 2011, **60**, 1261-1269.
37. C. J. Nobile, H. A. Schneider, J. E. Nett, D. C. Sheppard, S. G. Filler, D. R. Andes and A. P. Mitchell, *Curr. Biol.*, 2008, **18**, 1017-1024.

Chapter VI

Forces guiding staphylococcal adhesion

Philippe Herman-Bausier, Cécile Formosa-Dague, Cécile Feuillie, Claire Valotteau, and Yves F. Dufrêne

In *Journal of Structural Biology*, **2015**, DOI:10.1016/j.jsb.2015.12.009

I wrote this Minireview, with the help of the other authors.

Abstract

Staphylococcus epidermidis and *Staphylococcus aureus* are two important nosocomial pathogens that form biofilms on indwelling medical devices. Biofilm infections are difficult to fight as cells within the biofilm show increased resistance to antibiotics. Our understanding of the molecular interactions driving bacterial adhesion, the first stage of biofilm formation, has long been hampered by the paucity of appropriate force-measuring techniques. In this minireview, we discuss how atomic force microscopy techniques have enabled to shed light into the molecular forces at play during staphylococcal adhesion. Specific highlights include the study of the binding mechanisms of adhesion molecules by means of single-molecule force spectroscopy, the measurement of the forces involved in whole cell interactions using single-cell force spectroscopy, and the probing of the nanobiophysical properties of living bacteria *via* multiparametric imaging. Collectively, these findings emphasize the notion that force and function are tightly connected in staphylococcal adhesion.

1. Introduction

Many microbial pathogens attach to host tissues and implanted devices, leading to the formation of surface-associated communities called biofilms (Costerton *et al.*, 1999; Kolter and Greenberg, 2006). Cells in the biofilm are protected from host defences and are resistant to antibiotics, making biofilm-associated infections difficult to eradicate. As biofilms are estimated to be involved in more than 65% of nosocomial infections, they represent a tremendous burden on our healthcare system.

The development of a biofilm is a multistep process (**Figure 1**), starting with the adhesion of the microbial cells to host surfaces, polymer substrates, and protein-coated biomaterials, followed by cell aggregation and cell multiplication to form a mature biofilm in which the cells are trapped in a matrix of extracellular polymers. For most species, the complex set of molecular interactions at play during biofilm formation is poorly understood. Hence, there is a growing need for biophysical methods that can quantify the forces leading to cell adhesion and biofilm formation, with high force sensitivity and high spatial resolution.

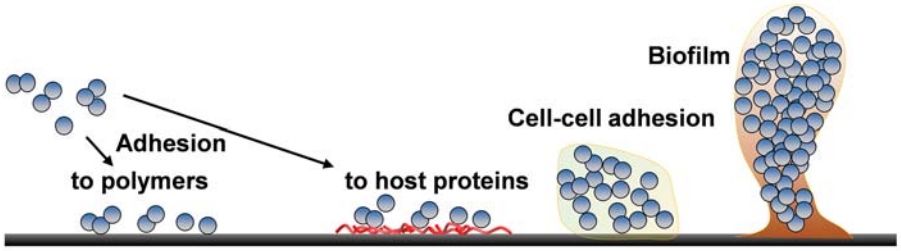

Figure 1: Biofilm formation, a multistep process.

Staphylococcus epidermidis and *Staphylococcus aureus* are nosocomial pathogens that represent a leading cause of biofilm-associated infections (Otto, 2008; Otto, 2009; Foster *et al.*, 2014). Major players in staphylococcal biofilms are the Microbial Surface Components Recognizing Adhesive Matrix Molecules (MSCRAMMs), a family of cell surface adhesins that target host extracellular proteins such as albumin, fibronectin and fibrinogen (Otto, 2009; Foster *et al.*, 2014). While the biology of staphylococcal adhesins has been extensively investigated, little attention has been paid to their molecular forces.

Traditionally, biofilms are studied using molecular biology and genetic approaches, optical and electron microscopy, and microscopic adhesion or biofilm assays (Donelli, 2014; Ghannoum *et al.*, 2015). These methods generally probe large ensembles of cells and molecules, and do not provide information on molecular interaction forces. By contrast, several force-

measuring techniques have been developed to measure molecular forces on cell surfaces, including optical and magnetic tweezers, and atomic force microscopy (AFM) (Tanase *et al.*, 2007; Moffitt *et al.*, 2008; Neuman and Nagy, 2008). Among these tools, AFM is the only method that can simultaneously quantify and localize specific forces on cells, at a resolution of a few nanometers. This is an important asset as biomolecular interactions are linked to structure in living cells. In microbiology, AFM has opened up new avenues for studying the forces involved in cell adhesion and biofilm formation, down to molecular resolution (Dufrêne, 2014; Dufrêne, 2015). In single-molecule force spectroscopy (SMFS), force-distance curves are acquired between AFM tips labelled with ligands and cell surfaces in order to detect, localize, and force probe individual receptors (Grandbois *et al.*, 2000; Dupres *et al.*, 2005; Hinterdorfer and Dufrêne, 2006). These analyses have provided molecular insights into the binding strength, affinity and specificity of staphylococcal adhesins. In single-cell force spectroscopy (SCFS), a living cell is attached on the AFM probe and force curves are obtained between the cell probe and a solid substrate or another cell (Helenius *et al.*, 2008; Müller *et al.*, 2009). A non-destructive SCFS assay was recently implemented, enabling the reliable and reproducible analysis of single-microbial cell adhesion forces (Beaussart *et al.*, 2013a; Beaussart *et al.*, 2014). A colloidal silica particle is attached to the end of a tip-less cantilever and coated with a bioinspired polydopamine wet adhesive. The sticky colloidal probe is used to pick up a single live cell. Fluorescence microscopy is used to check that the cell is properly positioned and alive. This SCFS assay has enabled the quantification of cell-substrate and cell-cell adhesive forces of staphylococci at the whole cell level. Lastly, the structural and biophysical properties of living cells have been mapped at unprecedented resolution, using newly developed multiparametric imaging (Alsteens *et al.*, 2012; Heu *et al.*, 2012; Alsteens *et al.*, 2013; Chopinet *et al.*, 2013; Dufrêne *et al.*, 2013; Formosa *et al.*, 2015). Force curves are recorded across the cell surface at high frequency, enabling to acquire correlated images of the structure, adhesion and mechanics of cells, including staphylococci, at much higher speed and spatial resolution than before. Here, we provide a survey of recent breakthroughs made in staphylococcal research using these modalities.

2. Fibronectin-binding proteins

There has been much progress in our use of AFM for studying the binding mechanisms of staphylococcal adhesins. Among these, fibronectin-binding proteins (FnBPs) have been the most widely investigated (Bustanji *et al.*, 2003;

Xu *et al.*, 2008; Buck *et al.*, 2010; Lower *et al.*, 2010; Casillas-Ituarte *et al.*, 2012). In early work, Bustanji and co-workers used SMFS to study the strength and dynamics of the interaction between single fibronectin (Fn) molecules and living *S. epidermidis* cells (Bustanji *et al.*, 2003). The strength of single Fn-FnBP bonds was found to be ~100 pN and varied with the loading rate, as expected for specific receptor-ligand bonds. Dynamic SMFS data were consistent with macroscopic observations showing that Fn-dependent bacterial infections are influenced by the blood velocity. Surprisingly, several studies have reported much larger adhesion forces for Fn-FnBP interactions, up to 6 nN depending on the strain investigated (Xu *et al.*, 2008; Buck *et al.*, 2010; Casillas-Ituarte *et al.*, 2012). This can be explained by the fact that Fn was attached at high density on the tip, meaning multiple Fn-FnBPs bonds were probed in parallel. It is therefore important to control the tip chemistry for proper interpretation of SMFS data. In a clinical context, the activity of the transcription factor SigB was shown to promote strong Fn-*S. aureus* bonds, an effect suggested to help host tissue colonization by small-colony variants isolated from cystic fibrosis patients (Mitchell *et al.*, 2008). Fn-FnBP adhesion forces for *S. aureus* clinical isolates were consistent with a multivalent bond consisting of multiple proteins in parallel, and the bond lifetime was longer for bloodstream isolates from patients with an infected device (Casillas-Ituarte *et al.*, 2012). These isolates showed a distinct force signature and had specific single amino acid polymorphisms in FnBP proteins (Lower *et al.*, 2011). Molecular dynamics simulations revealed that three residues in the protein form extra hydrogen bonds with Fn.

Another important role of FnBPs is the promotion of cell-cell adhesion during biofilm formation, particularly in clinically-relevant methicillin-resistant *S. aureus* (MRSA) strains. Until recently, an unsolved question was whether intercellular adhesion involves direct homophilic interactions or recognition of receptors on adjacent cells. By combining SMFS and SCFS, Herman-Bausier *et al.* (2015) showed that low-affinity homophilic bonds between FnBPA A domains on neighbouring cells mediate cell-cell adhesion. Homophilic binding required the presence of zinc, in agreement with earlier studies showing that FnBPs and other staphylococcal adhesins mediate zinc-dependent adhesion. Low-affinity binding may be of biological significance, providing a means to the bacteria to detach and colonize new sites during biofilm formation. Such homophilic cell-cell interactions could represent a widespread strategy among staphylococci to favor biofilm accumulation.

Besides providing novel insights into the FnBP binding forces, spatially-resolved force spectroscopy has revealed the distribution of single FnBPs on staphylococcal cells. In a first study, the localization of putative FnBP proteins

was studied on *S. aureus* bacteria deposited on different substrates (Lower *et al.*, 2010). The authors suggested that the production of FnBPs may be triggered by external stimuli, such as the presence of Fn on a surface. More recently, SMFS with tips functionalized with recombinant FnBP domains was used to explore the distribution of FnBPA proteins on *S. aureus* cells, showing that the adhesin was largely exposed on the cell surface, *i.e.* with a surface density of ~2000 proteins/µm² (Herman-Bausier *et al.*, 2015).

3. Serine-aspartate proteins

The serine-aspartate repeat (Sdr) proteins have also received considerable attention. A hallmark of such adhesins is the *S. epidermidis* SdrG protein which binds with high affinity to the blood plasma protein fibrinogen (Fg) *via* the "dock, lock, and latch" (DLL) mechanism involving dynamic conformational changes (Ponnuraj *et al.*, 2003; Bowden *et al.*, 2008). Because this interaction promotes bacterial attachment to Fg-coated biomaterials, it is thought to play an important role in infections. SCFS revealed that SdrG mediates time-dependent attachment to Fg-coated surfaces, suggesting that stable cell adhesion requires conformational changes (Herman *et al.*, 2014; **Figure 2**). The strength of single SdrG-Fg bonds measured by SMFS was ~2 nN, thus much larger than that of other cell adhesion proteins, which is typically in the 50-400 pN range depending on the protein and on the loading rate (**Figure 2**). Dynamic SMFS revealed a low dissociation rate and suggested that the SdrG-Fg bond is stable. These findings favour a dynamic, multistep DLL binding mechanism in which SdrG undergoes conformational changes to form greatly stabilized complexes. The strong binding and slow dissociation of SdrG rationalize the ability of *S. epidermidis* to colonize protein-coated biomaterials and to withstand physiological shear forces.

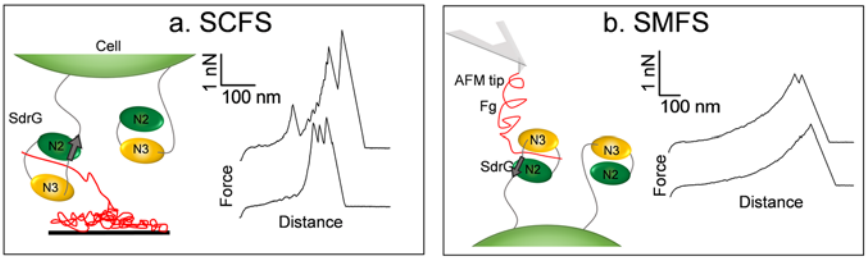

Figure 2: The binding force of the staphylococcal adhesin SdrG is equivalent to the strength of a covalent bond.
a. SCFS unravels adhesion forces between single *S. epidermidis* bacteria and fibrinogen (Fg) on solid substrates.
b. SMFS quantifies the binding strength of single SdrG adhesins on living bacteria. The left panels are cartoons of the experimental set-ups and the right panels show representative force profiles. Adapted from (Herman *et al.*, 2014).

In addition, spatially-resolved force spectroscopy with Fg-coated tips captured the localization of single SdrG proteins, demonstrating that they form nanoscale domains on the *S. epidermidis* cell surface (Herman *et al.*, 2014). Similar to multivalency, a ligand that dissociates from a cluster of adhesins is much more likely to rebind, thus largely contributing to stabilize adhesive interactions. Using a combination of AFM and macroscopic assays, the surface density of SdrG was shown to control the ability of various *S. epidermidis* clinical strains to bind to Fg-coated surfaces (Vanzieleghem *et al.*, 2015). Strains that showed enhanced adhesion towards Fg displayed increased amounts of SdrG adhesins, meaning that the abundance of SdrG on the cell surface dramatically improves the ability of the cells to bind to Fg-coated implanted medical devices.

SdrF is another Sdr protein from *S. epidermidis* that binds collagen, thereby helping the bacteria to attach to transcutaneous drivelines from explanted ventricular assist devices from patients. Single-cell analysis showed that SdrF mediates bacterial adhesion to collagen-coated substrates through both weak and strong bonds (Herman-Bausier and Dufrêne, 2015). Single-molecule assays further demonstrated that these bonds involve two distinct regions of SdrF, thus revealing that the protein is capable of dual ligand-binding activity. So AFM was capable of dual detection, enabling researchers to simultaneously detect two different types of molecular bonds in living bacteria. Both weak and strong bonds displayed high dissociation rates, meaning they are less stable than those formed by the well-characterized DLL mechanism. This study shows that AFM can discover novel and unanticipated binding mechanisms in staphylococcal adhesins

4. *S. aureus* surface protein G

During biofilm formation, staphylococcal cells produce a matrix of extracellular polymeric substances that hold the cells together. Among these, the *S. aureus* surface protein SasG plays a key role in mediating cell-cell adhesion, but how this is achieved at the molecular level is not known. AFM was recently used to demonstrate that SasG exhibits remarkable mechanical properties that are critical for its adhesive function (Gruszka *et al.*, 2015; Formosa-Dague *et al.*, 2015; **Figure 3**). Nanoscale multiparametric imaging of living bacteria revealed that Zn^{2+} strongly alters the structural, mechanical and adhesive properties of the cell surface, in that the surface morphology was much smoother, stiffer and stickier when this cation was present (**Figure 3**). Using SCFS, SasG was shown to be engaged in specific Zn^{2+}-dependent homophilic bonds, rather than in receptor-ligand bonds. The force required to

unfold individual SasG domains was remarkably strong, up to ~500 pN (**Figure 3**). This mechanical strength results from tandemly arrayed mechanical clamps involving long stretches of hydrogen bonds and associated side-chain packing interactions along the β-strands (Gruszka *et al.*, 2015). Owing to its mechanical strength, SasG will resist physiological shear forces and maintain cell-cell contacts. Under high mechanical force, the sequential unfolding of SasG repeats may expose extended conformations in which previously masked adhesive residues may become available for interaction. SasG was also found to form homophilic bonds with the structurally-related accumulation-associated protein of *S. epidermidis*, which could be relevant for the formation of multi-species biofilms during infection. All together, these findings favored a new model for the zinc-dependent activation of SasG-mediated adhesion: adsorption of zinc ions to cell wall components increases the cohesion of the cell surface, thus promoting the extension of SasG proteins beyond other surface components and making them fully available for zinc-dependent homophilic interactions.

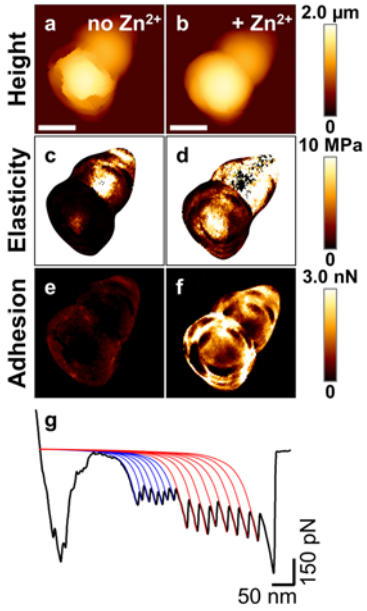

Figure 3: An unexpected relationship between mechanics and adhesion in the staphylococcal adhesin SasG.
a to f. Nanoscale multiparametric imaging of living bacteria: (**a, b**) height images of two dividing *S. aureus* cells expressing SasG in TBS buffer in the absence (**a**) or presence (**b**) of zinc ions, and simultaneous elasticity (**c, d**) and adhesion (**e, f**) images. Scale bars: 1 µm.
g. Nanomechanics of SasG bonds in living bacteria: representative force curve displaying low (blue) and high (red) force peaks that represent the sequential unfolding of E and G5 protein domains. Adapted from (Formosa-Dague *et al.* 2015).

5. Multispecies co –adhesion

Co-adhesion between different species is of medical relevance as this leads to mixed biofilm infections with increased antibiotic resistance. SCFS was used to quantify the forces driving the co-adhesion between *S. epidermidis* and the fungal pathogen *Candida albicans* (Peters *et al.*, 2012; Beaussart *et al.*, 2013b). Using an integrated AFM-inverted optical microscope, a bacterial probe was

positioned on top of a fungal cell (Beaussart *et al.*, 2013b). Bacterial-fungal adhesion involved two types of highly adhesive fungal macromolecules, *i.e.*, Als adhesins and O-mannosylations, which presumably recognize Als ligands and lectins on the bacterial surface. Adhesion was always stronger on germ tubes than on yeast cells, and was primarily mediated by the hyphal adhesin Als3, confirming the important role of the yeast-to-hyphae transition in co-adhesion. Along the same line, the forces between *Pseudomonas aeruginosa* and *C. albicans* were stronger on hyphae (Ovchinnikova *et al.*, 2012). In the bacterial co-adhesion context, strong adhesion forces were demonstrated between lactobacilli and virulent *S. aureus* strains, explaining how co-aggregation could eliminate these pathogens (Younes *et al.*, 2012). These reports indicate that AFM may become an important tool to understand the molecular bases of polymicrobial interactions.

6. Conclusions

Studying the fundamental interactions involved in biofilm formation is an important challenge in current microbiological and medical research. In recent years, AFM has provided fundamental insights into the molecular bases of bacterial and fungal adhesion, the first stage of biofilm formation, including deciphering the binding force and specificity of cell surface adhesins, understanding the contribution of hydrophobic forces in cell-substrate interactions, unravelling the mechanical properties of bacterial pili, and measuring the forces involved in microbe–microbe and microbe–host interactions (Dufrêne, 2014).

The studies surveyed here indicate that the forces of cell surface molecules play a central role in guiding cell adhesive functions in staphylococci. Key breakthroughs include unravelling the binding mechanisms (binding strength, binding specificity, molecular elasticity) of adhesins, including FnBPs, SdrG, SdrF and SasG, uncovering the forces involved in cell-cell and cell-substrate interactions, and deciphering the nanoscale surface properties of single bacteria. In the future, AFM should contribute to the identification of novel binding partners and binding mechanisms in staphylococcal adhesins. It should be noted that while the present review focused primarily on the specific interactions of cell adhesion proteins, bacterial adhesion may also involve non-specific forces, including hydrogen bonding, hydrophobic, van der Waals, electrostatic, and macromolecular forces (Busscher *et al.*, 2008). An important

challenge is therefore to establish the relative contribution of specific and non-specific forces in staphylococcal adhesion.
An important technical issue is the low throughput of current SCFS assays, which severely limits their widespread use in microbiology. This problem could be solved using the FluidFM technology, where pressures applied through hollow AFM probes enable the fast manipulation of individual cells (Meister *et al.*, 2009; Guillaume-Gentil *et al.*, 2014). Finally, it is hoped that AFM will help design new anti-adhesion drugs to treat microbial infections, including those caused by multidrug-resistant organisms. In an effort towards this goal, the adhesion force between P-fimbriated *Escherichia coli* and human uroepithelial cells was shown to be inhibited upon exposure to cranberry juice (Liu *et al.*, 2010). Also, cranberry juice consumption was shown to lower the forces between *E. coli* or *S. aureus* and an AFM tip (Abu-Lail et al, 2012).

Acknowledgements

Work at the Université catholique de Louvain was supported by the National Fund for Scientific Research (FNRS), the FNRS-WELBIO under Grant n°WELBIO-CR-2015A-05, the Federal Office for Scientific, Technical and Cultural Affairs (Interuniversity Poles of Attraction Programme), and the Research Department of the Communauté française de Belgique (Concerted Research Action). Y.F.D. and C. F-D are respectively Research Director and Postdoctoral Researcher at the FNRS.

References

Abu-Lail, L., Yuanyuan, T., Pinzón-Arango, P. A., Howell, A., Camesano, T., A., 2012. Using atomic force microscopy to measure anti-adhesion effects on uropathogenic bacteria, observed in urine after cranberry juice consumption. J. Biomater. Nanobiotechnol. 3, 533-540.

Alsteens, D., Trabelsi, H., Soumillion, P., Dufrêne, Y.F., 2013. Multiparametric atomic force microscopy imaging of single bacteriophages extruding from living bacteria. Nat. Commun. 4, 2926.

Alsteens, D., Dupres, V., Yunus, S., Latge, J.P., Heinisch, J.J., Dufrêne, Y.F., 2012. High-resolution imaging of chemical and biological sites on living cells using peak force tapping atomic force microscopy. *Langmuir* 28, 16738-16744.

Beaussart, A., El-Kirat-Chatel, S., Herman, P., Alsteens, D., Mahillon, J., Hols, P., Dufrêne, Y.F., 2013a. Single-cell force spectroscopy of probiotic bacteria. Biophy. J. 104, 1886-1892.

Beaussart, A., Herman, P., El-Kirat-Chatel, S., Lipke, P.N., Kucharikova, S., Van Dijck, P., Dufrêne, Y.F., 2013b. Single-cell force spectroscopy of the medically important *Staphylococcus epidermidis-Candida albicans* interaction. Nanoscale 5, 10894-10900.

Beaussart, A., El-Kirat-Chatel, S., Sullan, R.M., Alsteens, D., Herman, P., Derclaye, S., Dufrêne, Y.F., 2014. Quantifying the forces guiding microbial cell adhesion using single-cell force spectroscopy. Nat. Protoc. 9, 1049-1055.

Bowden, M.G., Heuck, A.P., Ponnuraj, K., Kolosova, E., Choe, D., Gurusiddappa, S., Narayana, S.V., Johnson, A.E., Hook, M., 2008. Evidence for the "dock, lock, and latch" ligand binding mechanism of the staphylococcal microbial surface component recognizing adhesive matrix molecules (MSCRAMM) SdrG. J. Biol. Chem. 283, 638-647.

Buck, A.W., Fowler, V.G., Jr., Yongsunthon, R., Liu, J., DiBartola, A.C., Que, Y.A., Moreillon, P., Lower, S.K., 2010. Bonds between fibronectin and fibronectin-binding proteins on *Staphylococcus aureus* and *Lactococcus lactis*. *Langmuir* 26, 10764-10770.

Busscher, H.J., Norde, W., van der Mei, H.C., 2008. Specific molecular recognition and nonspecific contributions to bacterial interaction forces. Appl. Environ. Microbiol. 74, 2559-2564.

Bustanji, Y., Arciola, C.R., Conti, M., Mandello, E., Montanaro, L., Samori, B., 2003. Dynamics of the interaction between a fibronectin molecule

and a living bacterium under mechanical force. Proc. Natl. Acad. Sci. U.S.A. 100, 13292-13297.

Casillas-Ituarte, N.N., Lower, B.H., Lamlertthon, S., Fowler, V.G., Jr., Lower, S.K., 2012. Dissociation rate constants of human fibronectin binding to fibronectin-binding proteins on living *Staphylococcus aureus* isolated from clinical patients. J. Biol. Chem. 287, 6693-6701.

Chopinet, L., Formosa, C., Rols, M.P., Duval, R.E., Dague, E., 2013. Imaging living cells surface and quantifying its properties at high resolution using AFM in QI™ mode. Micron 48, 26-33.

Costerton, J.W., Stewart, P.S., Greenberg, E.P., 1999. Bacterial biofilms: a common cause of persistent infections. Science 284, 1318-1322.

Donelli, G. (Ed.), 2014. Microbial Biofilms: Methods and protocols, Human Press, New York.

Dufrêne, Y.F., 2014. Atomic force microscopy in microbiology: new structural and functional insights into the microbial cell surface. mBio 5, e01363-01314.

Dufrêne, Y.F., 2015. Sticky microbes: forces in microbial cell adhesion. Trends Microbiol 23, 376-382.

Dufrêne, Y.F., Martinez-Martin, D., Medalsy, I., Alsteens, D., Müller, D.J., 2013. Multiparametric imaging of biological systems by force-distance curve-based AFM. Nat. Methods 10, 847-854.

Dupres, V., Menozzi, F.D., Locht, C., Clare, B.H., Abbott, N.L., Cuenot, S., Bompard, C., Raze, D., Dufrêne, Y.F., 2005. Nanoscale mapping and functional analysis of individual adhesins on living bacteria. Nat. Methods 2, 515-520.

Formosa, C., Schiavone, M., Boisrame, A., Richard, M.L., Duval, R.E., Dague, E., 2015. Multiparametric imaging of adhesive nanodomains at the surface of *Candida albicans* by atomic force microscopy. Nanomedicine 11, 57-65.

Formosa-Dague, C., Speziale, P., Foster, T.J., Geoghegan, J.A., Dufrêne, Y.F., 2015. Zinc-dependent mechanical properties of *Staphylococcus aureus* biofilm-forming protein SasG. Proc. Natl. Acad. Sci. U.S.A., in press.

Foster, T.J., Geoghegan, J.A., Ganesh, V.K., Hook, M., 2014. Adhesion, invasion and evasion: the many functions of the surface proteins of *Staphylococcus aureus*. Nat. Rev. Microbiol. 12, 49-62.

Ghannoum, M., Parsek, M., Whiteley, M., Mukherjee, P. K. (Eds.), 2015. Microbial biofilms, 2nd ed. Amercian Society for Microbiology, Washington.

Guillaume-Gentil, O., Potthoff, E., Ossola, D., Franz, C.M., Zambelli, T., Vorholt, J.A., 2014. Force-controlled manipulation of single cells: from AFM to FluidFM. Trends Biotechnol 32, 381-388.

Grandbois, M., Dettmann, W., Benoit, M., Gaub, H.E., 2000. Affinity imaging of red blood cells using an atomic force microscope. J. Histochem. Cytochem. 48, 719-724.

Gruszka, D.T., Whelan, F., Farrance, O.E., Fung, H.K., Paci, E., Jeffries, C.M., Svergun, D.I., Baldock, C., Baumann, C.G., Brockwell, D.J., Potts, J.R., Clarke, J. 2015. Cooperative folding of intrinsically disordered domains drives assembly of a strong elongated protein. Nat. Commun. 6:7271.

Helenius, J., Heisenberg, C.P., Gaub, H.E., Müller, D.J., 2008. Single-cell force spectroscopy. Journal of cell science 121, 1785-1791.

Herman-Bausier, P., Dufrêne, Y.F., 2015. Atomic force microscopy reveals a dual collagen-binding activity for the staphylococcal surface protein SdrF. Mol. Microbiol.

Herman, P., El-Kirat-Chatel, S., Beaussart, A., Geoghegan, J.A., Foster, T.J., Dufrêne, Y.F., 2014. The binding force of the staphylococcal adhesin SdrG is remarkably strong. Mol. Microbiol. 93, 356-368.

Herman-Bausier, P., El-Kirat-Chatel, S., Foster, T.J., Geoghegan, J.A., Dufrêne, Y.F., 2015. *Staphylococcus aureus* Fibronectin-Binding Protein A Mediates Cell-Cell Adhesion through Low-Affinity Homophilic Bonds. mBio 6, e00413-00415.

Heu, C., Berquand, A., Elie-Caille, C., Nicod, L., 2012. Glyphosate-induced stiffening of HaCaT keratinocytes, a Peak Force Tapping study on living cells. J. Struct. Biol. 178, 1-7.

Hinterdorfer, P., Dufrêne, Y.F., 2006. Detection and localization of single molecular recognition events using atomic force microscopy. Nat. Methods 3, 347-355.

Kolter, R., Greenberg, E.P., 2006. Microbial sciences: the superficial life of microbes. Nature 441, 300-302.

Liu, Y., Pinzon-Arango, P.A., Gallardo-Moreno, A.M., Camesano, T.A., 2010. Direct adhesion force measurements between *E. coli* and human uroepithelial cells in cranberry juice cocktail. Mol. Nutr. Food. Res. 54, 1744-1752.

Lower, S.K., Yongsunthon, R., Casillas-Ituarte, N.N., Taylor, E.S., DiBartola, A.C., Lower, B.H., Beveridge, T.J., Buck, A.W., Fowler, V.G., Jr., 2010. A tactile response in *Staphylococcus aureus*. Biophys. J. 99, 2803-2811.

Lower, S.K., Lamlertthon, S., Casillas-Ituarte, N.N., Lins, R.D., Yongsunthon, R., Taylor, E.S., DiBartola, A.C., Edmonson, C., McIntyre, L.M.,

Reller, L.B., Que, Y.A., Ros, R., Lower, B.H., Fowler, V.G., Jr., 2011. Polymorphisms in fibronectin binding protein A of *Staphylococcus aureus* are associated with infection of cardiovascular devices. Proc. Natl. Acad. Sci. U.S.A. 108, 18372-18377.

Meister, A., Gabi, M., Behr, P., Studer, P., Voros, J., Niedermann, P., Bitterli, J., Polesel-Maris, J., Liley, M., Heinzelmann, H., Zambelli, T., 2009. FluidFM: combining atomic force microscopy and nanofluidics in a universal liquid delivery system for single cell applications and beyond. Nano. Lett. 9, 2501-2507.

Mitchell, G., Lamontagne, C.A., Brouillette, E., Grondin, G., Talbot, B.G., Grandbois, M., Malouin, F., 2008. *Staphylococcus aureus* SigB activity promotes a strong fibronectin-bacterium interaction which may sustain host tissue colonization by small-colony variants isolated from cystic fibrosis patients. Mol.Microbiol. 70, 1540-1555.

Moffitt, J.R., Chemla, Y.R., Smith, S.B., Bustamante, C., 2008. Recent advances in optical tweezers. Annu. Rev. Biochem. 77, 205-228.

Müller, D.J., Helenius, J., Alsteens, D., Dufrêne, Y.F., 2009. Force probing surfaces of living cells to molecular resolution. Nat. Chem. Biol. 5, 383-390.

Neuman, K.C., Nagy, A., 2008. Single-molecule force spectroscopy: optical tweezers, magnetic tweezers and atomic force microscopy. Nat. Methods 5, 491-505.

Otto, M., 2008. Staphylococcal biofilms. Curr. Top. Microbiol. Immunol. 322, 207-228.

Otto, M., 2009. *Staphylococcus epidermidis*--the 'accidental' pathogen. Nat. Rev. Microbiol. 7, 555-567.

Ovchinnikova, E.S., Krom, B.P., Busscher, H.J., van der Mei, H.C., 2012. Evaluation of adhesion forces of *Staphylococcus aureus* along the length of *Candida albicans* hyphae. BMC Microbiol. 12, 281.

Peters, B.M., Ovchinnikova, E.S., Krom, B.P., Schlecht, L.M., Zhou, H., Hoyer, L.L., Busscher, H.J., van der Mei, H.C., Jabra-Rizk, M.A., Shirtliff, M.E., 2012. *Staphylococcus aureus* adherence to *Candida albicans* hyphae is mediated by the hyphal adhesin Als3p. Microbiology 158, 2975-2986.

Ponnuraj, K., Bowden, M.G., Davis, S., Gurusiddappa, S., Moore, D., Choe, D., Xu, Y., Hook, M., Narayana, S.V., 2003. A "dock, lock, and latch"

structural model for a staphylococcal adhesin binding to fibrinogen. Cell 115, 217-228.

Tanase, M., Biais, N., Sheetz, M., 2007. Magnetic tweezers in cell biology. Methods Cell Biol. 83, 473-493.

Vanzieleghem, T., Herman-Bausier, P., Dufrêne, Y.F., Mahillon, J., 2015. *Staphylococcus epidermidis* Affinity for Fibrinogen-Coated Surfaces Correlates with the Abundance of the SdrG Adhesin on the Cell Surface. *Langmuir* 31, 4713-4721.

Xu, C.P., Boks, N.P., de Vries, J., Kaper, H.J., Norde, W., Busscher, H.J., van der Mei, H.C., 2008. *Staphylococcus aureus*-fibronectin interactions with and without fibronectin-binding proteins and their role in adhesion and desorption. Appl. Environ. Microbiol. 74, 7522-7528.

Younes, J.A., van der Mei, H.C., van den Heuvel, E., Busscher, H.J., Reid, G., 2012. Adhesion forces and coaggregation between vaginal staphylococci and lactobacilli. PloS ONE 7, e36917.

Part III

Appendices

Appendix I

Single-cell force spectroscopy of probiotic bacteria

Audrey Beaussart, Sofiane El-Kirat-Chatel, Philippe Herman, David Alsteens, Jacques Mahillon, Pascal Hols and Yves F. Dufrêne

In *Biophysical Journal*, **2013**, 104, 1886

I contributed by doing some AFM analyses, and by helping to write the paper.

Abstract

Single-cell force spectroscopy is a powerful atomic force microscopy modality in which a single living cell is attached to the atomic force microscopy cantilever to quantify the forces that drive cell-cell and cell-substrate interactions. Although various single-cell force spectroscopy protocols are well established for animal cells, application of the method to individual bacterial cells remains challenging, mainly owing to the lack of appropriate methods for the controlled attachment of single live cells on cantilevers. We present a non-destructive protocol for single-bacterial cell force spectroscopy, which combines the use of colloidal probe cantilevers and of a bioinspired polydopamine wet adhesive. Living cells from the probiotic species *Lactobacillus plantarum* are picked up with a polydopamine-coated colloidal probe, enabling us to quantify the adhesion forces between single bacteria and biotic (lectin monolayer) or abiotic (hydrophobic monolayer) surfaces. These minimally invasive single-cell experiments provide novel, to our knowledge, insight into the specific and nonspecific forces driving the adhesion of *L. plantarum*, and represent a generic platform for studying the molecular mechanisms of cell adhesion in probiotic and pathogenic bacteria.

1886 Biophysical Journal Volume 104 May 2013 1886–1892

Single-Cell Force Spectroscopy of Probiotic Bacteria

Audrey Beaussart,[†] Sofiane El-Kirat-Chatel,[†] Philippe Herman,[†] David Alsteens,[†] Jacques Mahillon,[‡] Pascal Hols,[§] and Yves F. Dufrêne[†*]

[†]Université catholique de Louvain, Institute of Life Sciences, Louvain-la-Neuve, Belgium; [‡]Université catholique de Louvain, Laboratory of Food and Environmental Microbiology, Earth and Life Institute, Louvain-la-Neuve, Belgium; and [§]Université catholique de Louvain, Institute of Life Sciences, Biochemistry and Molecular Genetics of Bacteria, Louvain-la-Neuve, Belgium

ABSTRACT Single-cell force spectroscopy is a powerful atomic force microscopy modality in which a single living cell is attached to the atomic force microscopy cantilever to quantify the forces that drive cell-cell and cell-substrate interactions. Although various single-cell force spectroscopy protocols are well established for animal cells, application of the method to individual bacterial cells remains challenging, mainly owing to the lack of appropriate methods for the controlled attachment of single live cells on cantilevers. We present a nondestructive protocol for single-bacterial cell force spectroscopy, which combines the use of colloidal probe cantilevers and of a bioinspired polydopamine wet adhesive. Living cells from the probiotic species *Lactobacillus plantarum* are picked up with a polydopamine-coated colloidal probe, enabling us to quantify the adhesion forces between single bacteria and biotic (lectin monolayer) or abiotic (hydrophobic monolayer) surfaces. These minimally invasive single-cell experiments provide novel, to our knowledge, insight into the specific and nonspecific forces driving the adhesion of *L. plantarum*, and represent a generic platform for studying the molecular mechanisms of cell adhesion in probiotic and pathogenic bacteria.

INTRODUCTION

Studying the molecular mechanisms of bacterial adhesion is critical to our understanding of bacterial-host interactions. Bacterial adhesion results from a complex interplay of physicochemical forces, that can be either specific (receptor-ligand interactions) or nonspecific (hydrophobic and electrostatic interactions) (1). Although various macroscopic assays are available to investigate microbial adhesion, these approaches probe large ensembles of cells and do not provide information on the fundamental forces driving cell adhesion. Consequently, there is a growing need for methods that can quantify bacterial adhesion forces on a single-cell basis (2,3). Such single-cell techniques would be of great help to refine our perception of cellular heterogeneity, and to reveal otherwise invisible adhesive mechanisms (4).

Probiotic bacteria, which mostly belong to the Gram-positive lactic acid bacteria group, offer exciting prospects in medicine owing to their ability to induce various beneficial health effects (5,6). Among these, *Lactobacillus plantarum* is a promising candidate in view of its ability to survive several days in the human gastrointestinal tract (7), and to adhere to human mucosa in vitro (8). Positive health effects of probiotics are thought to be related to their ability to attach to epithelial cells and mucus. Therefore, the efficient use of probiotics requires a detailed understanding of their adhesive interactions toward inert and living surfaces. These interactions are determined by the main macromolecules that constitute the bacterial cell wall, i.e., peptidoglycan, proteins, and glycopolymers such as polysaccharides and teichoic acids (5,9). Although much is known about the structure and synthesis of these constituents in *L. plantarum*, the extent to which they contribute to bacterial adhesion, particularly host interactions, is poorly understood. Accordingly, there is much interest in measuring the molecular forces driving the adhesion of *L. plantarum* to biotic and abiotic surfaces. In probiotic research, such experiments have great promise for the screening of strains exhibiting enhanced adhesive properties and health effects.

In addition to being used as an imaging tool, atomic force microscopy (AFM) is being increasingly applied to quantify the interactions of biological systems, over scales ranging from single molecules to whole cells (10–13). In the past years, there has been considerable progress in the use of single-cell force spectroscopy (SCFS) to quantify cell-cell and cell-solid interactions (10–15). The general idea is to replace the tip of the AFM cantilever by a living cell that is then used to measure interactions toward other cells or substrates (14,15). Several techniques have been developed to attach cells onto cantilevers, including the use of specific receptor-ligand interactions (16), electrostatic (17,18) or hydrophobic (19) interactions, glue (20), or chemical fixation (21). However, none of these methods enable true, reliable single-bacterial cell analysis for at least one of the following reasons: i), the cell-cantilever bond is too weak, leading to cell detachment; ii), the use of chemicals or drying leads to cell surface denaturation and/or cell death; iii), multiple cells are often attached and probed together, meaning reliable single-cell analysis is not accessible. An interesting approach to solve these problems is the use of cantilevers modified with colloids or beads. For instance,

Submitted February 26, 2013, and accepted for publication March 28, 2013.

*Correspondence: Yves.Dufrene@uclouvain.be

Editor: Daniel Muller.

0006-3495/13/05/1886/7 $2.00

http://dx.doi.org/10.1016/j.bpj.2013.03.046

Lower and co-workers (22,23) attached bacteria-coated beads to cantilevers to measure the forces between living *Shewanella oneidensis* bacteria and goethite. In this method, the bead is covered with multiple bacteria, meaning single-cell analysis is difficult to guarantee. Also exciting is the recently developed fluidFM, which uses hollow cantilevers for local liquid dispensing and manipulation of single living cells under physiological conditions (24). FluidFM is currently able to manipulate bacterial cells (25), but its application to bacterial force measurements is not yet fully established.

In this work, we report a noninvasive method for the SCFS analysis of individual bacteria, which combines colloidal probes cantilevers (26) and bioinspired polydopamine adhesive (27). We show that the use of polydopamine-coated colloidal probes is a simple, versatile platform for the controlled attachment of single bacterial cells on AFM cantilevers, and for quantifying their adhesive interactions toward various surfaces (alkanethiol monolayers, lectin monolayers). The results emphasize the important roles of nonspecific (hydrophobic) and specific (glycopolymer-lectin) interactions in mediating the adhesion of *L. plantarum*. We expect that this SCFS method will be a valuable tool in biomedical research for understanding the molecular interactions between bacteria (probiotics, pathogens) and host cells.

MATERIALS AND METHODS

Microorganisms and cultures

L. plantarum NZ7100 cells were grown in Mann-Rogosa-Shape broth (Difco) at 30°C without agitation. Overnight cultures were diluted in fresh media to an $OD_{600\ nm}$ of 0.1. The cells were harvested in the exponential growth phase (4 h at 30°C), and washed 3 times in acetate buffer. For cell probe preparation, 50 μL of a 100-fold diluted solution were transferred to a glass petri dish.

Preparation of cell probes

Using a Nanoscope VIII Multimode AFM (Bruker, Santa Barbara, CA), triangular shaped tipless cantilevers (NP-O10, Microlevers, Veeco Metrology Group) were slowly immersed in a very thin layer of ultraviolet (UV)-curable glue (NOA 63, Norland Edmund Optics) spread on a glass slide, and slowly brought into contact with a silica microsphere (6.1 μm diameter, Bangs Laboratories). After 3 min of contact, the colloidal probe was cured for 10 min under a UV lamp. The cantilever was then immersed for 1 h in a 10 mM Tris Buffer solution (pH 8.5) containing 4 mg/mL dopamine hydrochloride (99%, Sigma). The probe was then washed and dried under N_2. Using a Bioscope Catalyst (Bruker), the colloidal probe was brought into contact with an isolated cell for 3 min, and the obtained cell probe was then transferred without dewetting over a solid substrate for further force measurements.

Viability of attached bacteria was tested using a LIVE/DEAD *Bac*light Viablility Kit (Invitrogen, kit L7012). Prior attachment, 2 μL of a 1:1 Syto 9/IP mixture at 1.5 mM were added to a 50 μL cell suspension, mixed thoroughly, and incubated for 15 min in the dark. The labeled cells were then attached to polydopamine colloidal probes or substrates, and their viability checked using a Zeiss Axio Observer Z1 equipped with a Hamamatsu camera C10600. Dead bacteria attached onto polydopamine substrates were obtained by immersing them for 1 h in isopropanol.

Substrate preparation

To prepare hydrophobic and hydrophilic substrates, clean glass coverslips coated with a thin layer of gold were immersed overnight in a 1 mM solution of 1-dodecanethiol or 11-mercapto-1-undecanol (Sigma), rinsed with ethanol, and dried under N_2. Lectin-coated substrates were obtained by immersing gold-coated coverslips overnight in an ethanol solution containing 1 mM of 10% mercaptododecahexanoic acid/90% 11-mercapto-1-undecanol (Sigma), rinsed with ethanol, and dried with N_2. Substrates were then immersed for 30 min into a solution containing 20 g/L *N*-hydroxysuccinimide (NHS) and 50 g/L 1-ethyl-3-(3-dimethylaminopropyl)-carbodiimide (EDC) (Sigma), rinsed 5 times with MilliQ water (Millipore), incubated with 0.2 mg/mL of Concanavalin A (ConA) for 1 h, rinsed further with acetate, and then immediately used.

AFM

AFM measurements were performed at room temperature (20°C) in sodium acetate buffer—supplemented with Ca^{2+} and Mn^{2+} at 1 mM for experiments with ConA lectins—using a Bioscope Catalyst AFM (Bruker AXS, Santa Barbara, CA). Force-distance curves were obtained by recording multiple force curves in different locations, using a maximum applied force of 250 pN and a constant approach and retraction speed of 1000 $nm.s^{-1}$. For mannoside blocking experiments, a concentrated methyl α-D-mannopyranoside solution (Sigma) was injected into the AFM chamber to reach a final concentration of 200 mM.

RESULTS AND DISCUSSION

Cell probe preparation

Marine mussels produce adhesive proteins that strongly bind to solid surfaces in aqueous environments, owing to the presence of the unusual amino acid 3,4-dihydroxy-L-phenylalanine (dopa) (27,28). Mussel-inspired polydopamine films have recently attracted much interest for the design of adhesive interfaces and materials (29,30). In the AFM context, Kang and Elimelech (31) used polydopamine for attaching bacterial cells onto AFM cantilevers for SCFS experiments. Although this approach is an important improvement to earlier methods, it does not offer a precise control of the cell-substrate contact area. Given the small size of bacteria and the tilted orientation of the cantilever, the controlled immobilization of single cells on the same given area of the cantilever ends is difficult; this leads to a lack of control of the interacting area, and sometimes even to a direct contact between the cantilever and the substrate.

We therefore combined the polydopamine method with the use of colloidal probes of large, well-defined geometry (26) (Fig. 1). Colloidal probe cantilevers were produced by attaching silica microspheres (~6 μm) to tipless cantilevers using a UV-curable glue (Fig. 1, *step 1*). Colloidal probes were coated with a thin polydopamine film. Using an integrated AFM-inverted optical microscope, polydopamine probes were then approached toward single bacterial

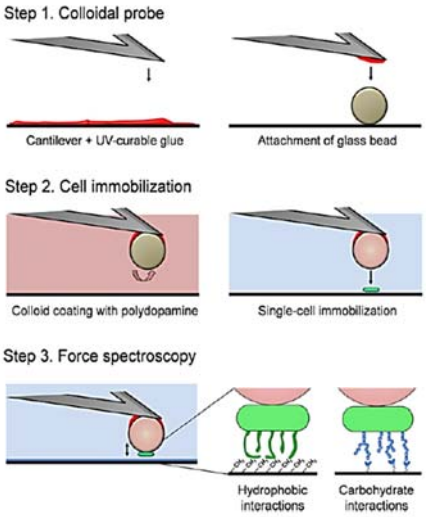

FIGURE 1 Single-bacterial cell force spectroscopy using colloidal probe cantilevers combined with bioinspired polydopamine polymers. The method involves three main steps, i.e., preparation of the colloidal probe, controlled immobilization of a single cell, and force-distance curve measurements (see text for details).

cells deposited on a glass petri dish in buffer, kept in contact for 3 min, and withdrawn (Fig. 1, *step 2*). The obtained cell probes were directly used for SCFS measurements (Fig. 1, *step 3*), although avoiding dewetting as this may cause cell detachment or cell surface denaturation. Because single cells are precisely attached in the center of the colloids, this method guarantees reliable and reproducible single-cell force measurements.

To confirm that the polydopamine-colloidal probe method is nondestructive, cells were labeled with the *Bac*light LIVE/DEAD stain, in which living bacteria exhibit green fluorescence, whereas dead bacteria are red. Fig. 2 *a* shows that most bacteria attached onto a polydopamine-coated substrate were alive (*green*), whereas bacteria attached onto the same polydopamine substrate but treated with isopropanol were dead (*red*). Fig. 2 *b* (*left*) reveals that single-bacterial cells attached onto polydopamine-colloidal probes were alive even after 60 min measurements, whereas bacteria attached directly onto tipless cantilevers were generally killed (Fig. 2 *b*, *right*). Although the reason for this difference is not known yet, a possible explanation is that bacteria in direct contact with the cantilever may be more subject to heating by the laser beam of the AFM optical detection system. Hence, besides affording much better control of the cell-substrate interaction area, the polydopamine-colloidal probe method guarantees that the cells remain alive during the course of the experiment.

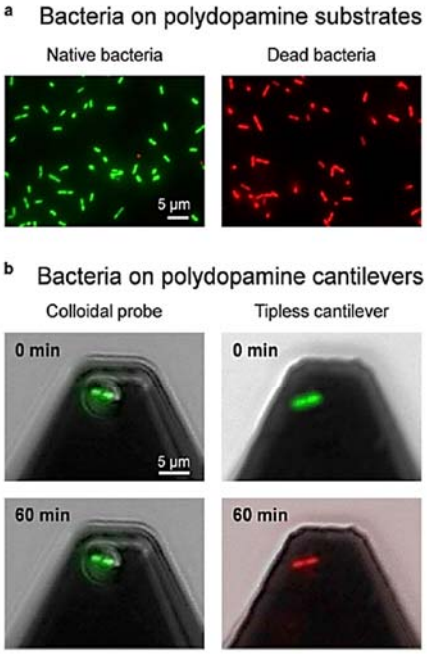

FIGURE 2 Use of polydopamine-colloidal probe guarantees reliable, single-live cell experiments. (*a*) Fluorescence images of *Lactobacillus plantarum* bacteria labeled with the *Bac*light LIVE/DEAD stain and attached onto polydopamine-coated substrates: comparison of native cells (*left*) and of cells killed with isopropanol (*right*). (*b*) Fluorescence images of bacterial cells labeled with the *Bac*light LIVE/DEAD stain, attached onto polydopamine-coated cantilevers and imaged either immediately (0 min, *top*) or after 60 min of force measurements (*bottom*): comparison of the colloidal probe cantilever method developed here (*left*) and of the conventional tipless cantilever approach (*right*).

Quantifying hydrophobic forces

Hydrophobic forces represent one of the driving forces for the adhesion of bacteria to surfaces and tissues (32). To assess whether this indeed applies to *L. plantarum*, multiple force curves were recorded between bacterial cells and hydrophobic surfaces. Fig. 3, *a* and *b*, show the adhesion force histogram with representative force curves, and the rupture length histogram recorded at a short contact time (<100 ms) between single *L. plantarum* cells and methyl-terminated self-assembled monolayers (SAMs). All curves showed large adhesion forces (from 250 to 2500 pN) with multiple,

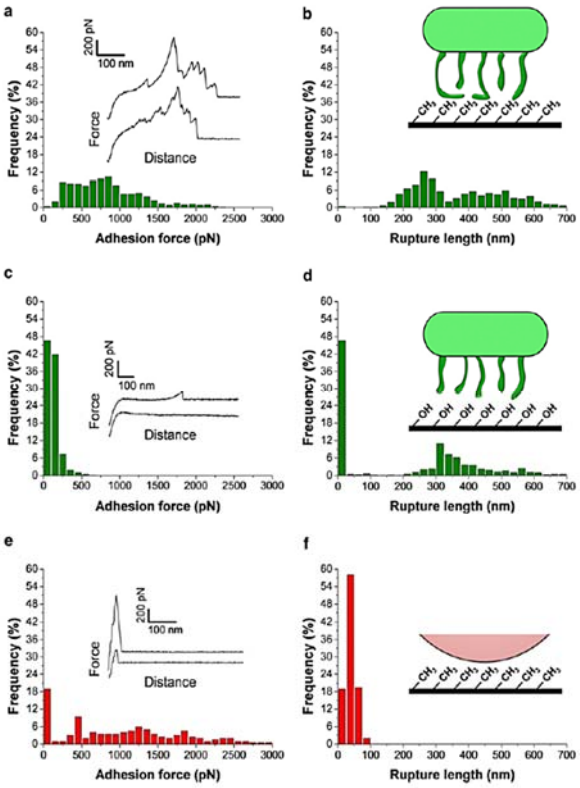

FIGURE 3 SCFS quantifies hydrophobic interactions between *Lactobacillus plantarum* and solid surfaces. (*a*) Adhesion force histogram with representative force curves and (*b*) histogram of rupture distances recorded in buffer at a short contact time (<100 ms) between single bacterial cells and hydrophobic, methyl-terminated monolayers. The data shown correspond to a total of 1000 force curves obtained from three independent experiments (different cell probes and different substrates). (*c*) Adhesion force histogram with representative force curves and (*d*) histogram of rupture distances recorded in buffer between single bacterial cells and hydrophilic, hydroxyl-terminated monolayers. The data shown correspond to a total of 1000 force curves obtained from three independent experiments. (*e*) Adhesion force histogram with representative force curves and (*f*) histogram of rupture distances recorded in buffer between polydopamine-coated colloidal probes and Hydrophobic, methyl-terminated monolayers.

sequential peaks and extended rupture lengths (from 150 to 600 nm). The general features of the curves did not substantially change when recording consecutive force curves (up to several hundred), or when probing different cells or substrates, supporting the notion that force measurements did not lead to cell surface alteration. These cell-adhesion signatures are reminiscent of those observed on animal cells (15) and indicate that bonds that have been formed between the substrate and the cell break sequentially until the cell has completely separated from the surface. The maximum downward force exerted on the cantilever is referred to as the adhesion force (measured relative to the base line) and used to build the adhesion force histogram, whereas the last rupture peak is used to generate the rupture length histogram.

We believe that the measured adhesion forces reflect hydrophobic interactions between the substrate and cell surface proteins for the following reasons: i), the extended rupture lengths and multiple force peaks are consistent with the stretching and unfolding of cell surface proteins; by contrast, peptidoglycan that forms fairly compact, stiff structures is not expected to show such extensions (33); ii), unlike proteins, glycopolymers are hydrophilic in nature, thus not expected to strongly bind to hydrophobic surfaces; iii), large, multipeak force signatures were never observed on hydrophilic hydroxyl-terminated SAMs (Fig. 3, *c* and *d*); rather, force curves recorded on hydrophilic substrates showed single, well-defined force peaks of ~200 pN magnitude and 250–500 nm rupture length that we attribute to glycopolymer stretching; iv), control experiments between polydopamine-coated beads and hydrophobic SAMs (Fig. 3, *e* and *f*), never exhibited multipeaks typically observed with stretched proteins, but only single, sharp adhesive events with very short extensions. Similar

polydopamine signatures were observed when the cells were not well centered on the probe or weakly immobilized. In light of these observations, we suggest that the large adhesion force profiles are associated with the binding and unfolding of hydrophobic domains from cell surface-associated proteins. As observed for the pathogen *Candida albicans* (34), the force-induced unfolding of protein domains may lead to extended conformations in which hydrophobic groups are freshly exposed and favor hydrophobic interactions toward biotic and abiotic surfaces. In view of the large cell-substrate contact area and of the force magnitude, it is likely that the complex adhesion profiles reflect the simultaneous stretching of multiple proteins.

Measuring glycopolymer interactions

Glycopolymers (teichoic acids, polysaccharides) on the surface of probiotic bacteria play important physiological roles, including controlling cell morphogenesis, and mediating cellular recognition and adhesion, e.g., via lectin binding (3,4). To probe the glycopolymer properties (adhesion, extension) of *L. plantarum*, we recorded force curves between single bacterial cells and substrates coated with ConA, a lectin that specifically binds the glucose (or mannose) residues contained in glycopolymers (35). As shown in Fig. 4, *a* and *b*, most curves (92%) recorded at a short contact time (<100 ms) showed no adhesion. At first sight this seems surprising as i), glucose-rich glycopolymers that decorate the bacterial cell surface are expected to bind to ConA, and ii), SMFS with ConA tips detected substantial amounts of glucose (or mannose) residues on the *L. plantarum* surface (35). However, this discrepancy can easily be explained by the contact time, which in SCFS experiments dramatically enhances specific interactions (15). For animal cells, the idea is that single receptor-ligand pairs initially anchor the cell to a substrate or another cell, after which these molecular bonds generally increase with time and undergo modifications to greatly increase the total

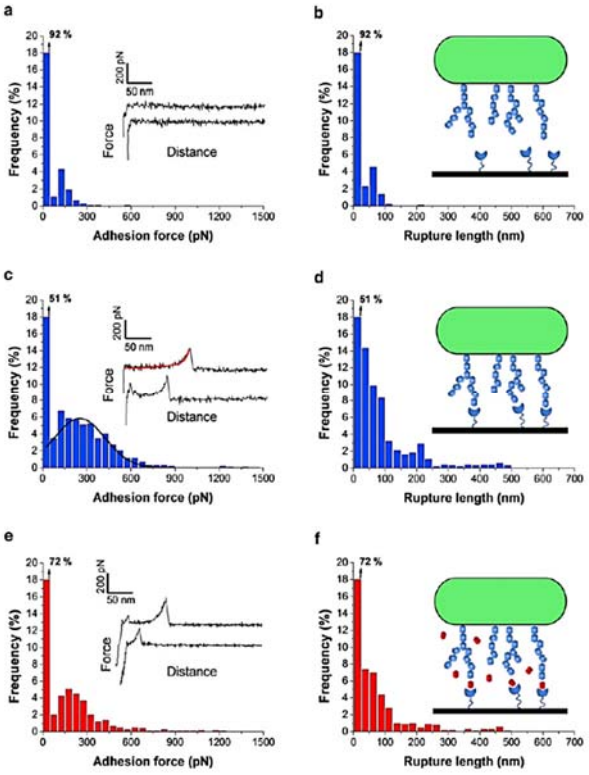

FIGURE 4 SCFS measures the specific interactions between *Lactobacillus plantarum* cell surface glycopolymers and lectin surfaces. (*a* and *c*) Adhesion force histograms with representative force curves and (*b* and *d*) histograms of rupture distances recorded in buffer between single bacterial cells and lectin monolayers, using a contact time of either <100 ms (*a* and *b*) or 1 s (*c* and *d*). The fit on the top curve of panel *c* shows that elongation forces were well described by an extended freely jointed chain model with a Kuhn length of 0.4 nm and a segment elasticity of 1 N/m: $x(F) = L_c$ [coth (Fl_k/k_bT)- k_bT/Fl_k] [1 + nFl/k_sL_c], where L_c and l_k are the contour length and Kuhn length of the molecule, n and k_s the number of segments and their elasticity, k_b is the Boltzmann constant, and T the absolute temperature. The line on the histogram of panel *c* is a Gaussian fit to the data. (*e* and *f*) Same measurements performed with a contact time of 1 s, following blocking with 200 mM methyl α-D-mannopyranoside. The data shown for every condition (*a* and *b*, *c* and *d*, *e* and *f*) correspond to a total of 1000 force curves obtained from three independent experiments (different cell probes and different substrates).

strength of adhesion (15). Consistent with this behavior, Fig. 4, *c* and *d*, show that increasing the contact time to 1 s dramatically changed the force profiles: a large fraction (49%) of the curves displayed single or multiple adhesion forces, of 251 ± 146 pN mean magnitude (mean ± SD; total number of force curves = 1000 from three different cell probes and substrates), along with elongation forces and rupture lengths ranging essentially from 25 to 250 nm. The force signatures did not substantially change when recording consecutive force curves, or when probing different cells or substrates. The observed time-dependency suggests that formation of lectin bonds is much slower than hydrophobic bonds, for which full binding was achieved within <100 ms (Fig. 3 *a*). Earlier SMFS studies have shown that lectin-sugar complexes rupture at forces around 30–60 pN at fairly similar loading rates (36–38). Therefore, we attribute the ~250 pN forces to the simultaneous detection of multiple ConA-glucose interactions. Finally, we assessed the specificity of the recognition events by blocking the cell surface with free α-methyl mannoside. Fig. 4, *e* and *f*, show that treatment of the cells with mannoside led to a much lower frequency of adhesion events (from 49% to 28%), confirming they are associated with specific glucose/mannose binding events.

The glycopolymers detected here are likely to consist of cell surface polysaccharides because i), elongation forces were well described by an extended freely jointed chain model (Fig. 4 *c*); ii), the extended rupture lengths are in the range of those observed by SMFS on bacterial cell surface polysaccharides, including those from the probiotic bacterium *Lactobacillus rhamnosus* GG (37); iii), compared to polysaccharides, teichoic acids give rise to much shorter rupture lengths (35). Our results therefore suggest that glucose-based polysaccharides on the *L. plantarum* cell surface mediate strong adhesion toward lectin-coated surfaces. Because of their long, flexible nature, polysaccharide chains may strengthen adhesion through long-range polymer bridging interactions. This finding may be of biological significance as lectins on intestinal epithelial and dendritic cells may act as host receptors for probiotic molecules (5).

CONCLUSIONS

In conclusion, our experiments have shown that SCFS with polydopamine-coated colloidal probes provide a powerful platform for quantifying bacterial cell adhesion forces on a single-cell basis. Unlike other existing protocols, our methodology is simple, versatile, nondestructive (even after 1 h measurements), and affords much better control of the cell positioning of the cell-substrate contact area. These assets guarantee true and reliable single-bacterial cell analysis. Using this approach, we found that *L. plantarum* cells show strong adhesive properties toward biotic and abiotic surfaces. Binding to hydrophobic surfaces does not depend on interaction time and gives rise to multiple force peaks and extended rupture lengths that may be attributed to the stretching and unfolding of cell surface proteins. Binding to lectin surfaces is strongly time-dependent and is associated with the stretching of long, flexible glucose (mannose)-based macromolecules, most likely cell-bound polysaccharides. The measured specific and nonspecific adhesive forces are of biological relevance as they are likely to play important roles in mediating *L. plantarum* adhesive interactions toward inert and living surfaces.

Work at the Université catholique de Louvain was supported by the National Foundation for Scientific Research (FNRS), the Université catholique de Louvain (Fonds Spéciaux de Recherche), the Région Wallonne, the Federal Office for Scientific, Technical and Cultural Affairs (Interuniversity Poles of Attraction Programme), and the Research Department of the Communauté française de Belgique (Concerted Research Action). Y.F.D., P.H., and D.A. are Senior Research Associate, Research Associate, and Postdoctoral Researcher of the FNRS.

REFERENCES

1. Busscher, H. J., W. Norde, and H. C. van der Mei. 2008. Specific molecular recognition and nonspecific contributions to bacterial interaction forces. *Appl. Environ. Microbiol.* 74:2559–2564.
2. Camesano, T. A., Y. Liu, and M. Datta. 2007. Measuring bacterial adhesion at environmental interfaces with single-cell and single-molecule techniques. *Adv. Water Resour.* 30:1470–1491.
3. Busscher, H. J., and H. C. van der Mei. 2012. How do bacteria know they are on a surface and regulate their response to an adhering state? *PLoS Pathog.* 8:e1002440.
4. Brehm-Stecher, B. F., and E. A. Johnson. 2004. Single-cell microbiology: tools, technologies, and applications. *Microbiol. Mol. Biol. Rev.* 68:538–559.
5. Lebeer, S., J. Vanderleyden, and S. C. J. De Keersmaecker. 2010. Host interactions of probiotic bacterial surface molecules: comparison with commensals and pathogens. *Nat. Rev. Microbiol.* 8:171–184.
6. Bron, P. A., P. van Baarlen, and M. Kleerebezem. 2012. Emerging molecular insights into the interaction between probiotics and the host intestinal mucosa. *Nat. Rev. Microbiol.* 10:66–78.
7. Vesa, T., P. Pochart, and P. Marteau. 2000. Pharmacokinetics of *Lactobacillus plantarum* NCIMB 8826, *Lactobacillus fermentum* KLD, and *Lactococcus lactis* MG 1363 in the human gastrointestinal tract. *Aliment. Pharmacol. Ther.* 14:823–828.
8. Adlerberth, I., S. Ahrne, …, A. E. Wold. 1996. A mannose-specific adherence mechanism in *Lactobacillus plantarum* conferring binding to the human colonic cell line HT-29. *Appl. Environ. Microbiol.* 62:2244–2251.
9. Delcour, J., T. Ferain, …, P. Hols. 1999. The biosynthesis and functionality of the cell-wall of lactic acid bacteria. *Antonie van Leeuwenhoek.* 76:159–184.
10. Müller, D. J., and Y. F. Dufrêne. 2008. Atomic force microscopy as a multifunctional molecular toolbox in nanobiotechnology. *Nat. Nanotechnol.* 3:261–269.
11. Müller, D. J., and Y. F. Dufrêne. 2011. Atomic force microscopy: a nanoscopic window on the cell surface. *Trends Cell Biol.* 21:461–469.
12. Müller, D. J., and Y. F. Dufrêne. 2011. Force nanoscopy of living cells. *Curr. Biol.* 21:R212–R216.
13. Müller, D. J., J. Helenius, …, Y. F. Dufrêne. 2009. Force probing surfaces of living cells to molecular resolution. *Nat. Chem. Biol.* 5:383–390.
14. Benoit, M., and H. E. Gaub. 2002. Measuring cell adhesion forces with the atomic force microscope at the molecular level. *Cells Tissues Organs (Print).* 172:174–189.

15. Helenius, J., C. P. Heisenberg, ..., D. J. Muller. 2008. Single-cell force spectroscopy. *J. Cell Sci.* 121:1785–1791.

16. Benoit, M., D. Gabriel, ..., H. E. Gaub. 2000. Discrete interactions in cell adhesion measured by single-molecule force spectroscopy. *Nat. Cell Biol.* 2:313–317.

17. Le, D. T. L., Y. Guérardel, ..., E. Dague. 2011. Measuring kinetic dissociation/association constants between *Lactococcus lactis* bacteria and mucins using living cell probes. *Biophys. J.* 101:2843–2853.

18. Ovchinnikova, E. S., B. P. Krom, ..., H. J. Busscher. 2012. Force microscopic and thermodynamic analysis of the adhesion between *Pseudomonas aeruginosa* and *Candida albicans*. *Soft Matter.* 8:6454–6461.

19. Emerson, 4th, R. J., T. S. Bergstrom, ..., T. A. Camesano. 2006. Microscale correlation between surface chemistry, texture, and the adhesive strength of *Staphylococcus epidermidis*. *Langmuir.* 22:11311–11321.

20. Bowen, W. R., R. W. Lovitt, and C. J. Wright. 2001. Atomic force microscopy study of the adhesion of *Saccharomyces cerevisiae*. *J. Colloid Interface Sci.* 237:54–61.

21. Razatos, A., Y. L. Ong, ..., G. Georgiou. 1998. Molecular determinants of bacterial adhesion monitored by atomic force microscopy. *Proc. Natl. Acad. Sci. USA.* 95:11059–11064.

22. Lower, S. K., M. F. Hochella, Jr., and T. J. Beveridge. 2001. Bacterial recognition of mineral surfaces: nanoscale interactions between *Shewanella* and α-FeOOH. *Science.* 292:1360–1363.

23. Yongsunthon, R., and S. K. Lower. 2005. Force measurements between a bacterium and another surface In Situ. *Adv. Appl. Microbiol.* 58C: 97–124.

24. Meister, A., M. Gabi, ..., T. Zambelli. 2009. FluidFM: combining atomic force microscopy and nanofluidics in a universal liquid delivery system for single cell applications and beyond. *Nano Lett.* 9:2501–2507.

25. Dorig, P., P. Stiefel, ..., T. Zambelli. 2010. Force-controlled spatial manipulation of viable mammalian cells and micro-organisms by means of FluidFM technology. *Appl. Phys. Lett.* 97:023701.

26. Ducker, W. A., T. J. Senden, and R. M. Pashley. 1991. Direct measurement of colloidal forces using an atomic force microscope. *Nature.* 353:239–241.

27. Lee, H., B. P. Lee, and P. B. Messersmith. 2007. A reversible wet/dry adhesive inspired by mussels and geckos. *Nature.* 448:338–341.

28. Lee, H., N. F. Scherer, and P. B. Messersmith. 2006. Single-molecule mechanics of mussel adhesion. *Proc. Natl. Acad. Sci. USA.* 103: 12999–13003.

29. Brubaker, C. E., and P. B. Messersmith. 2012. The present and future of biologically inspired adhesive interfaces and materials. *Langmuir.* 28:2200–2205.

30. Lee, H., S. M. Dellatore, ..., P. B. Messersmith. 2007. Mussel-inspired surface chemistry for multifunctional coatings. *Science.* 318:426–430.

31. Kang, S., and M. Elimelech. 2009. Bioinspired single bacterial cell force spectroscopy. *Langmuir.* 25:9656–9659.

32. Doyle, R. J. 2000. Contribution of the hydrophobic effect to microbial infection. *Microbes Infect.* 2:391–400.

33. Andre, G., S. Kulakauskas, ..., Y. F. Dufrêne. 2010. Imaging the nanoscale organization of peptidoglycan in living *Lactococcus lactis* cells. *Nat. Commun.* 1:27.

34. Beaussart, A., D. Alsteens, ..., Y. F. Dufrêne. 2012. Single-molecule imaging and functional analysis of Als adhesins and mannans during *Candida albicans* morphogenesis. *ACS Nano.* 6:10950–10964.

35. Andre, G., M. Deghorain, ..., Y. F. Dufrene. 2011. Fluorescence and atomic force microscopy imaging of wall teichoic acids in *Lactobacillus plantarum*. *ACS Chem. Biol.* 6:366–376.

36. Alsteens, D., V. Dupres, ..., Y. F. Dufrêne. 2008. Structure, cell wall elasticity and polysaccharide properties of living yeast cells, as probed by AFM. *Nanotechnology.* 19:384005.

37. Francius, G., S. Lebeer, ..., Y. F. Dufrêne. 2008. Detection, localization, and conformational analysis of single polysaccharide molecules on live bacteria. *ACS Nano.* 2:1921–1929.

38. Dettmann, W., M. Grandbois, ..., H. E. Gaub. 2000. Differences in zero-force and force-driven kinetics of ligand dissociation from beta-galactoside-specific proteins (plant and animal lectins, immunoglobulin G) monitored by plasmon resonance and dynamic single molecule force microscopy. *Arch. Biochem. Biophys.* 383:157–170.

Appendix II

Quantifying the forces guiding microbial cell adhesion using single-cell force spectroscopy

Audrey Beaussart, Sofiane El-Kirat-Chatel, Ruby May A Sullan, David Alsteens, Philippe Herman, Sylvie Derclaye & Yves F Dufrêne

In *Nature Protocols*, **2014**, 9, 1049

I contributed by doing some AFM analyses, and by helping to write the paper.

Abstract

During the past decades, several methods (e.g., electron microscopy, flow chamber experiments, surface chemical analysis, surface charge and surface hydrophobicity measurements) have been developed to investigate the mechanisms controlling the adhesion of microbial cells to other cells and to various other substrates. However, none of the traditional approaches are capable of looking at adhesion forces at the single-cell level. In recent years, atomic force microscopy (AFM) has been instrumental in measuring the forces driving microbial adhesion on a single-cell basis. The method, known as single-cell force spectroscopy (SCFS), consists of immobilizing a single living cell on an AFM cantilever and measuring the interaction forces between the cellular probe and a solid substrate or another cell. Here we present SCFSprotocols that we have developed for quantifying the cell adhesion forces of medically important microbes. Although we focus mainly on the probiotic bacterium *Lactobacillus plantarum*, we also show that our procedures are applicable to pathogens, such as the bacterium *Staphylococcus epidermidis* and the yeast *Candida albicans*. For well-trained microscopists, the entire protocol can be mastered in 1 week.

PROTOCOL

Quantifying the forces guiding microbial cell adhesion using single-cell force spectroscopy

Audrey Beaussart, Sofiane El-Kirat-Chatel, Ruby May A Sullan, David Alsteens, Philippe Herman, Sylvie Derclaye & Yves F Dufrêne

Université Catholique de Louvain, Institute of Life Sciences, Louvain-la-Neuve, Belgium. Correspondence should be addressed to Y.F.D. (Yves.Dufrene@uclouvain.be).

Published online 10 April 2014; doi:10.1038/nprot.2014.066

During the past decades, several methods (e.g., electron microscopy, flow chamber experiments, surface chemical analysis, surface charge and surface hydrophobicity measurements) have been developed to investigate the mechanisms controlling the adhesion of microbial cells to other cells and to various other substrates. However, none of the traditional approaches are capable of looking at adhesion forces at the single-cell level. In recent years, atomic force microscopy (AFM) has been instrumental in measuring the forces driving microbial adhesion on a single-cell basis. The method, known as single-cell force spectroscopy (SCFS), consists of immobilizing a single living cell on an AFM cantilever and measuring the interaction forces between the cellular probe and a solid substrate or another cell. Here we present SCFS protocols that we have developed for quantifying the cell adhesion forces of medically important microbes. Although we focus mainly on the probiotic bacterium *Lactobacillus plantarum*, we also show that our procedures are applicable to pathogens, such as the bacterium *Staphylococcus epidermidis* and the yeast *Candida albicans*. For well-trained microscopists, the entire protocol can be mastered in 1 week.

INTRODUCTION

An understanding of how microbial cells attach to each other, to solid substrates and to host cells is a crucial challenge in microbiology, and it is key in medicine for controlling microbial interactions. Microbial adhesion involves a complex interplay of physico-chemical forces, including specific receptor-ligand forces and nonspecific hydrophobic and electrostatic forces[1,2]. Macroscopic assays that are traditionally used to investigate the adhesion behavior of microbial cells provide average information obtained on large populations of cells and do not measure the forces driving cell adhesion. Therefore, there is an urgent need for novel methods for the reliable analysis of single-cell adhesion[3,4].

The field of single-cell microbiology uses novel technologies for single-cell analysis, thereby revealing cellular properties, interactions and behaviors that are otherwise inaccessible with traditional tools[4,5]. Examples of single-cell technologies include fluorescence assays, flow cytometry techniques, micro-spectroscopic methods, mechanical, optical and electrokinetic micromanipulations, microcapillary electrophoresis, biological microelectromechanical systems and scanning probe microscopies[4,5]. Among scanning probe microscopy methods, AFM is increasingly being used to probe the interactions of single live cells to molecular resolution[6,7]. Specifically, SCFS is a valuable AFM modality for measuring the forces that drive cell-cell and cell-substrate interactions[8–10].

Attaching cells to cantilevers

Regardless of the cell type investigated, the key step of the SCFS procedure is the proper attachment of the cell to the cantilever. Protocols to attach animal cells on cantilevers are generally based on the use of specific receptor-ligand interactions[8–10]. Yet for most microbes the cell-cantilever bond is too weak, leading to cell detachment. Therefore, alternative approaches have been developed, including the use of electrostatic interactions (e.g., poly(ethyleneimine) (PEI)[11], poly-L-lysine[12] or charged silanes[13]), hydrophobic interactions[14], glue[15], chemical fixation[16] or bioinspired wet adhesives[17,18]. The latter approach will be described in the procedure of this protocol; the relative merits and limitations of other approaches are discussed below.

In the chemical fixation protocol, PEI is adsorbed from a 1% (wt/vol) aqueous solution onto the AFM probe[19]. After rinsing the probe with deionized water, a cell pellet is transferred onto the PEI-coated probe by using a micromanipulator. The coated probe is then treated with a drop of 2.5% (vol/vol) glutaraldehyde at 4 °C for 1–2 h, and it is finally rinsed with water. Although this method has been used to measure the forces of a variety of systems, such as those between *Escherichia coli* and surfaces with different surface hydrophobicities[19], the use of chemicals leads to cell surface denaturation and cell death.

This problem can be avoided by coating probes with native living cells by using electrostatic interactions[13]. Glass beads are incubated in a solution of 3-aminopropyltriethoxysilane (5–10% in acetone) for 6 h, and the cells are then linked to the amino-functionalized beads by spinning a cell-bead mixture at 7,000*g* for 2 min. A single bacteria-coated bead is then attached to a cantilever with epoxy. By using this approach, the forces between living *Shewanella oneidensis* bacteria and goethite were measured quantitatively[13]. Although it is of interest, the method implies that multiple cells are generally attached on the bead, meaning single-cell analysis is not possible. 'FluidFM' is a recent method that uses hollow cantilevers for local liquid dispensing and manipulation of single living cells under physiological conditions[20,21]. This method has a strong potential for use in single-cell force measurements, but it requires more sophisticated instrumentation than classical commercial instruments.

Overview of the procedure

SCFS of bacterial cell adhesion involves functionalization of AFM cantilevers with single live bacteria, preparation of the target substrates and recording of force-distance curves between the

PROTOCOL

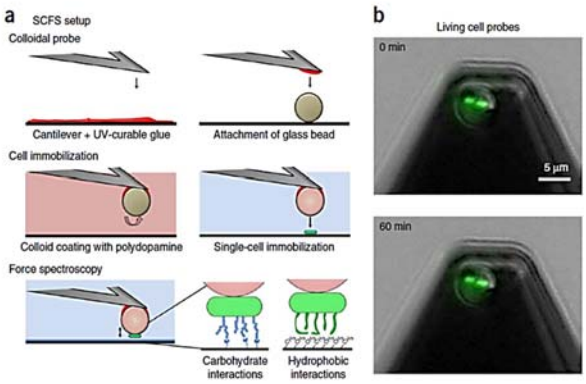

Figure 1 | Principles of SCFS. (**a**) The SCFS protocol involves the use of colloidal probe cantilevers combined with bioinspired polydopamine polymers, and it consists of three steps: preparation of the colloidal probe, controlled attachment of single cells and force-distance curve measurements. (**b**) Checking that the probed cells are still alive by using fluorescence stains: fluorescence images of bacterial cells labeled with the *Bac*light LIVE/DEAD stain, attached on polydopamine-coated cantilevers and imaged either immediately (0 min, top) or after 60 min of force measurements (bottom). Adapted with permission from *Biophys. J.*, vol. 104, Single-cell force spectroscopy of probiotic bacteria, 1886–1892, Beaussart, A. *et al.*, Copyright 2013, with permission from Elsevier (ref. 18).

cellular probes and the substrates (**Fig. 1a**). For well-trained microscopists, the entire protocol can be mastered in 1 week. Our approach involves attaching a colloidal particle to the end of a cantilever and coating it with wet adhesive polymers. The sticky colloidal probe is then used to pick up single live cells. Once a cell is attached, it is essential to check its proper positioning and viability under a fluorescence microscope (**Fig. 1b**). In case of poor positioning, the probe should be discarded and the procedure should be repeated. It is recommended to check that the immobilized cells are alive by using fluorescent stains that probe the membrane integrity (e.g., LIVE/DEAD *Bac*light viability kit). Then, researchers should record several hundred force curves on different areas of the substrate with the same cellular probe. To get statistically meaningful results, they should record at least two or three other sets of curves by using different substrates and different cellular probes prepared with cells from independent cultures. An important feature for reliable SCFS measurements is to demonstrate the specificity of the measured forces. In the case of receptor-ligand interactions, this can be readily achieved by blocking the cell surface (or substrate) receptor sites by injecting a solution of free ligands into the AFM chamber. An alternative control is to show that the obtained curves differ markedly fro those obtained with a polydopamine probe without a bacteriu attached.

Here we describe procedures (i) for preparing single bacteri probes by using colloidal probe cantilevers and a bioinspire polydopamine wet adhesive, and (ii) for quantifying bacteri cell adhesion forces on a single-cell basis[18]. As a prototype, v focus on probiotic bacteria from the species *L. plantarum*[1] Quantification of cell adhesion forces in this organism is cruci as the ability of probiotics to attach to epithelial cells and muc is believed to have an important role in inducing beneficial heal effects. We have also shown that the protocol is applicable to oth microbial species, including the pathogens *S. epidermidis*[22,23] ar *C. albicans*[24,25]. We anticipate that the approach will be usef to researchers interested in understanding the molecular bas of cell adhesion in a broad range of microorganisms. Advance SCFS technologies could also contribute to the development ar screening of anti-adhesion molecules that are capable of inhibi ing the adhesion of pathogens.

MATERIALS

REAGENTS

- *L. plantarum* strain NZ7100
- Mann-Rogosa-Sharpe (MRS) broth (Difco)
- Sodium acetate (Sigma-Aldrich)
- Acetic acid (Sigma-Aldrich)
- UV-curable glue NOA 63 (Norland, Edmund Optics)
- LIVE/DEAD *Bac*light viability kit (Invitrogen, kit no. L7012)
- Dopamine hydrochloride, 99% (Sigma-Aldrich)
- Isopropyl alcohol, >99.7% (Sigma-Aldrich)
- PureLab ultrapure water (ELGA LabWater)
- 1-Dodecanethiol (Sigma-Aldrich)
- 11-Mercapto-1-undecanol (Sigma-Aldrich)
- 16-Mercaptohexadecanoic acid (Sigma-Aldrich)
- *N*-Hydroxysuccinimide (Sigma-Aldrich)
- *N*-(3-dimethylaminopropyl)-*N*′-ethylcarbodiimide hydrochloride (Sigma-Aldrich)
- Concanavalin A (Sigma-Aldrich)
- $CaCl_2$; $MnCl_2$ (Sigma-Aldrich)
- Methyl α-D-mannopyranoside (Sigma-Aldrich)
- Ethanol, absolute (VWR International)

EQUIPMENT

- Nanoscope VIII multimode atomic force microscope (Bruker)
- Bioscope Catalyst atomic force microscope (Bruker) mounted on an invert optical microscope (Zeiss Axio Observer Z1) equipped with a Hamamatsu C10600 camera with a 40× objective and a 100× oil-immersion objective
- Triangular-shaped tipless cantilevers (NP-O10, Microlevers, Veeco Metrology Group) with a nominal spring constant of 0.06 N m^{-1}
- Steel sample pucks (Bruker)
- Glass-bottomed Petri dishes (WillCo-dish)
- Tips and gold surface cleaning: UV/ozone treatment (Jetlight)
- UV lamp, 365 nm, 6 W (handheld UV lamp UVL-56; UVP)
- Centrifuge (Multifuge X1, Thermo Scientific)
- Autoclave (Presto)
- For gold coating, electron beam thermal evaporator (Auto 306, Boc Edwards)
- MATLAB software v.7.0 (R14), (MathWorks)

- Nanoscope 8.10 software (Bruker)
- AxioVision rel. 4.8.2 software (Zeiss)
- Silica microspheres, 6.1-µm diameter (Bangs Laboratories)
- Round cover glasses, 10-mm diameter (VWR International)
- Double-sided tape
- Precision wipes (Kimwipes, Kimberly-Clark)

REAGENT SETUP

Cell culture and cell treatments From freshly plated cells, grow *L. plantarum* bacterial cells in MRS broth at 30 °C without agitation for 12 h. Dilute the cell culture in fresh MRS broth to an OD_{600nm} of 0.1. Collect the cells in the exponential growth phase (~4 h at 30 °C) by centrifugation at 7,500*g*, and rinse them three times in acetate buffer. We note that cell culture and cell treatments vary according to the kind of microbial species being probed.

Dopamine solution For cell probe preparation, prepare a dopamine solution at 4 mg ml^{-1} concentration in 10 mM Tris-HCl buffer, pH 8.5 (this solution should be used immediately).

Sodium acetate buffer For force measurements, prepare a sodium acetate buffer solution (pH 4.75) containing 10 mM acetic acid and 10 mM sodium acetate. For lectin experiments, this buffer should be supplemented with Ca^{2+} and Mn^{2+} at 1 mM. These solutions can be autoclaved and stored for 2 weeks at 4 °C.

PROCEDURE

Preparation of cell probes ● TIMING ~8 h

1| Stick a round cover glass on a magnetic steel puck with double-sided tape, and then deposit a small amount of UV-curable glue on the cover glass and spread it to form a very thin layer.

2| Use an atomic force microscope equipped with an optical microscope (for instance, a Nanoscope VIII Multimode) to immerse triangular-shaped tip-less cantilevers one by one in the very thin layer of glue.

▲ CRITICAL STEP To avoid excess glue on the cantilever, use another glass slide or a pointed tweezer to generate isolated glue droplets on the glass slide. Use the optical microscope of the atomic force microscope to manually engage the cantilever onto a very small droplet or on the edge of a drop of glue.

3| Stick another round cover glass on a magnetic steel puck with double-sided tape, and then deposit a small amount of silica microspheres on the cover glass.

4| Use the atomic force microscope to slowly bring the cantilever into contact with a single silica microsphere.

▲ CRITICAL STEP Only use a small amount of microspheres to spread onto the glass slide to maximize the chances of attaching a single bead on the cantilever. This can be achieved by using either a spatula or an unused pipette tip. To prevent any unwanted contact between the cantilever and the surface during force measurements, make sure to attach the silica bead at the very end of the cantilever (**Fig. 1b**).

5| After ~30 s of contact, put the colloidal probe under a UV lamp for 10 min to cure the glue.

6| Repeat Steps 1–5 ten times to obtain ten colloidal cantilevers for each experiment.

■ PAUSE POINT Colloidal probes can be kept for up to 1 week in a desiccator.

7| Immerse a colloidal cantilever for 1 h in a 10 mM Tris-HCl buffer solution (pH 8.5) containing 4 mg ml^{-1} dopamine hydrochloride. Next, wash the probe briefly with water and gently dry it under a nitrogen flow.

▲ CRITICAL STEP Polydopamine is a wet adhesive that has a great potential for the design of adhesive interfaces[26], and it can be used to immobilize living bacteria[17]. As it quickly polymerizes, it is important to immerse the cantilever directly after preparing the dopamine solution. To slow down the polymerization process, protect the solution from light during colloidal cantilever preparation.

8| Measure the cantilever sensitivity on a hard substrate (e.g., clean glass) and calibrate the cantilever spring constant by using, for instance, the thermal noise method available on most commercial instruments.

9| Use an atomic force microscope mounted on an inverted fluorescence microscope (such as a Bioscope Catalyst) to attach and position single bacterial cells on the colloidal probe. To this end, first incubate a 50-µl diluted bacterial suspension on a glass-bottomed Petri dish for 15 min. Bring the colloidal probe into contact with an isolated bacterial cell for 3 min.

▲ CRITICAL STEP Proper positioning of the cell on the colloidal particle is crucial for reliable force measurements. As this can be difficult to achieve, a good suggestion is to create grids on the glass substrate with a diamond pen to facilitate trapping of the bacteria and to prevent them from rolling. For biologically relevant measurements, it is also essential to make sure that the cells are still alive.

? TROUBLESHOOTING

PROTOCOL

Preparation of the substrates ● TIMING ~24 h

10| In SCFS, researchers measure the interaction forces between a cell probe and either biotic (e.g., lectin monolayer, Step 11A) or abiotic (e.g., hydrophobic monolayer, Step 11B) substrates. These substrates are coated onto a gold surface. To prepare the gold surface, place clean glass coverslips in an electron-beam thermal evaporator and coat them with a 5-nm-thick chromium layer followed by a 30-nm-thick layer of gold.

▲ CRITICAL STEP A thin adhesion layer of chromium is required in order to provide stability to the gold coatings.

■ PAUSE POINT The obtained gold substrates can be stored for several months. Before use, clean the gold surfaces with ethanol, dry them with nitrogen and place them in a UV/ozone cleaner for 15 min. Rinse them with ethanol and dry with nitrogen.

11| We provide steps for functionalizing the gold surfaces with a lectin or a hydrophobic monolayer (options A or B).

(A) Functionalization with a lectin monolayer ● TIMING ~15 h

(i) Immerse the substrates for 12 h in an ethanol solution containing 10% of 1 mM 16-mercaptohexadecanoic acid/90% of 1 mM 11-mercapto-1-undecanol.

(ii) Wash the substrates with ethanol, dry them with nitrogen, immerse them in a solution containing 10 g per liter *N*-hydroxysuccinimide and 25 g per liter *N*-(3-dimethylaminopropyl)-*N'*-ethylcarbodiimide hydrochloride for 30 min, and then rinse them five times with water (avoid de-wetting).

(iii) Dip the surfaces into a 0.2 g per liter solution of the lectin concanavalin A, incubate them for 1 h, rinse with sodium acetate buffer solution supplemented with Ca^{2+} and Mn^{2+} (1 mM) and use them immediately.

▲ CRITICAL STEP The buffer for AFM measurements should contain Ca^{2+} and Mn^{2+}, as many lectins need these ions for binding.

(B) Functionalization with a hydrophobic monolayer ● TIMING ~12 h

(i) To obtain hydrophobic substrates, immerse clean gold substrates in ethanol solution containing 1 mM 1-dodecanethiol for 12 h, rinse them with ethanol and dry them with nitrogen. To minimize surface contamination, use the functionalized surfaces immediately after they are prepared.

Force spectroscopy ● TIMING ~2 d

12| Engage the cell probe on the substrate of interest (e.g., lectin or hydrophobic monolayers) while maintaining the maximum applied force at a small value (typically, 250 pN).

13| Record 50 consecutive force-distance curves at a single location (**Fig. 2**), and then move to another spot ~10 µm away to record another set of curves. Repeat this multiple times.

▲ CRITICAL STEP It is crucial to record force curves at multiple locations on the substrates to confirm that the results do not vary from one spot to another. In addition, make sure that only the cell surface is being probed by checking whether the shape of consecutive force curves is reproducible and consistent with the stretching and rupturing of cellular bonds (**Fig. 2a–d**).

? TROUBLESHOOTING

14| Vary the contact time (e.g., from 100 ms to 5 s) and the applied force (from 100 pN to 1,000 pN), as these two parameters may markedly influence the probed cellular bonds and thus affect the shape of the force curves[10].

15| For statistics, the measurements should be repeated using different substrates and different cells, including cells from independent cultures (restart procedure from Step 7). The total number of cell-substrate combinations will depend on the reliability and reproducibility of the adhesion force data.

Demonstrating the specificity of the measured forces ● TIMING ~4 h

16| To confirm the specificity of the measured glycopolymer interactions, disengage the probe, inject a 200 mM solution of methyl α-D-mannopyranoside and restart from Step 12 with the same probe.

17| As another control, change the cell probe for a polydopamine probe (prepared as described in Steps 1–8) and restart from Step 12 (**Fig. 2e,f**).

Data treatment ● TIMING ~2 d

18| To generate adhesion-force and rupture-length histograms (**Fig. 2**), use the AFM software to convert the raw 'voltage-displacement' curves into 'force-distance' curves, as well as to calculate the maximum adhesion force and the rupture distance for each curve (more details can be found in ref. 27).

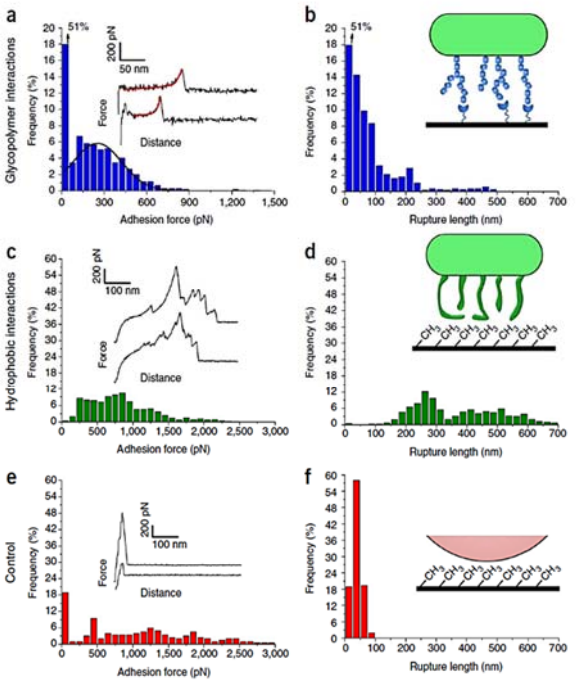

Figure 2 | Measurement of the specific (glycopolymer) and nonspecific (hydrophobic) interactions of probiotic bacteria. (**a**–**d**) Adhesion force histograms with representative force curves (**a**,**c**), and histograms of rupture distances (**b**,**d**) recorded in buffer between single *L. plantarum* bacteria and lectin (**a**,**b**) or hydrophobic (**c**,**d**) substrates. (**e**,**f**) Control experiment: the same data obtained between polydopamine-coated colloidal probes and hydrophobic substrates. Adapted with permission from *Biophys. J.*, vol. 104, Single-cell force spectroscopy of probiotic bacteria, 1886–1892, Beaussart, A. *et al.*, Copyright 2013, with permission from Elsevier (ref. 18).

▲ **CRITICAL STEP** Although current microscope software enables automatic detection of different parameters from multiple-force curves, we highly recommend manually checking the values of the detected forces to eliminate systematic errors.

19| Assess the elasticity of cell surface macromolecules. The worm-like chain (WLC) and the freely jointed chain (FJC) models are often used to quantitatively describe the elasticity of flexible macromolecules[27]. When pulling on polysaccharides, as described here in lectin substrates, the adhesion force peaks should be well described with an FJC model[28,29] (**Fig. 2a**). In contrast, the stretching of proteins is best described with a WLC model[30,31].

? TROUBLESHOOTING

Is the probed cell still alive during the analysis? (Step 9)

A key asset of the current procedure is that it allows researchers to perform force measurements directly on single live cells. However, for a given set of analyses, we highly recommend checking that the immobilized cells are alive by using a LIVE/DEAD *Bac*light viability kit (i.e., fluorescent stains that probe the membrane integrity (**Fig. 1b**)). Before Step 9, add 2 µl of a 1:1 Syto 9 (green-fluorescent nucleic acid stain; 0.25 mM)/propidium iodide (red-fluorescent nuclear and chromosome counterstain; 1.5 mM) to a 50-µl drop of bacterial suspension and mix thoroughly. Allow the bacteria to incubate with the dyes for 15 min in the dark, and then add 4 ml of buffer to the Petri dish. After attaching the cell on the cantilever (Step 9) or at the end of the force measurements, visualize the attached cell with the inverted fluorescence microscope coupled to the AFM instrument. Green color means that the membrane is intact, hence that the cell is still alive (**Fig. 1b**), whereas red color means that the membrane is damaged.

Checking the shape of the force curves (Step 13)

During the analysis, the cellular probe may be altered because the cell is not well positioned on or well attached to the cantilever. A convenient method for confirming that the probe is fully functional is to check whether the curves show single or multiple well-defined adhesion events with extended rupture lengths, consistent with the pulling of cell surface macromolecules. If sharp adhesion forces are measured at very short rupture distances (**Fig. 2e**,**f**), this could mean that the polydopamine-coated colloid is being probed because the cell rolls, detaches or is poorly positioned. Restart the whole procedure with a fresh cell probe (prepared as for Steps 1–6). Another important point to avoid probe alteration is to trigger the maximum contact force to 100–1,000 pN.

PROTOCOL

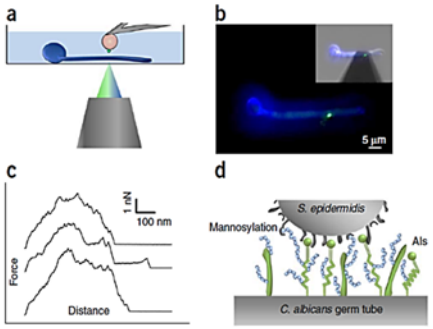

Figure 3 | Quantification of the specific forces engaged in bacterial-fungal interactions. (**a**,**b**) Principle of the SCFS experiment: schematic of the setup (**a**); by using an integrated AFM-inverted optical microscope (**b**), a single *S. epidermidis* cell attached on a colloidal cantilever (*Bac*light LIVE/DEAD stain; green color) is approached toward a single *C. albicans* hyphae immobilized on a hydrophobic substrate (Calcofluor White stain; blue color). (**c**) Typical force-distance curves recorded in the buffer between *S. epidermidis* and *C. albicans* hyphae. (**d**) Key players in the adhesion process are the *C. albicans* cell-surface glycoproteins (green) and mannose-rich glycoconjugates (blue). Adapted from ref. 22 with permission from The Royal Society of Chemistry.

● TIMING

Steps 1–9, preparation of cell probes: ~8 h
Step 10, preparation of the substrates: ~24 h
Step 11A, functionalization with a lectin monolayer: ~15 h
Step 11B, functionalization with a hydrophobic monolayer: ~12 h
Steps 12–15, force spectroscopy: ~2 d
Steps 16 and 17, demonstrating the specificity of the measured forces: ~4 h
Steps 18 and 19, data treatment: ~2 d

ANTICIPATED RESULTS

The SCFS protocol described here (**Fig. 1**) represents a versatile and nondestructive method for measuring bacterial cell adhesion forces on a true single-cell basis. A key asset of the procedure described here is that it provides excellent control of the cell positioning, and thus of the cell-substrate contact area, meaning that reliable single-cell analysis is guaranteed.

Figure 2 shows how we used this protocol to measure the adhesion strength between probiotic bacteria from *L. plantarum* and biotic (lectin monolayer) or abiotic (hydrophobic monolayer) surfaces[18]. These data demonstrate that the experiment can give some clue to the nature of the interaction. Binding to lectins, for example, was specific, time-dependent and involved long, flexible glucose (mannose)-based polysaccharides (**Fig. 2a**,**b**). Notice that apart from the 51% null adhesion, the distribution of the frequency of the adhesion force measured is Gaussian (**Fig. 2a**). The null adhesion relates to the fact that specific interactions depend on different parameters including the surface density of biomolecules, their proper orientation, the contact time or the affinity between the ligand and its receptor; not all the curves, therefore, will result in adhesion. In contrast, binding to hydrophobic surfaces did not depend on interaction time and gave rise to multiple force peaks and extended rupture lengths attributed to the unfolding of hydrophobic domains from cell surface proteins (**Fig. 2c**,**d**). The null adhesion peak was not seen for the hydrophobic interactions, as these do not require specific orientation of the molecules or a specific contact time. The importance of using a polydopamine control probe is demonstrated; we were assured of the biological specificity because the signatures were never observed when using a polydopamine-coated colloidal probe instead of a cellular probe (**Fig. 2e**,**f**).

We also showed the power of the method to measure cell-cell adhesion forces in the context of mixed biofilm-associated infections (**Fig. 3**)[22]. The study of the interactions between bacterial and fungal pathogens is important to understand the molecular bases of polymicrobial infections. With this in mind, we used the above protocol (**Fig. 3a**,**b**) to quantify the forces driving the co-adhesion between *S. epidermidis* and *C. albicans*[22]. Germinated *C. albicans* cells were obtained as described[22] and immobilized via hydrophobic interactions on gold surfaces coated with hydrophobic monolayers (prepared as in Step 11B; a concentrated suspension of hyphae was incubated for 3 h before the AFM experiment[22]). *S. epidermidis* was found to strongly bind to *C. albicans* germ tubes (**Fig. 3c**,**d**) but to poorly adhere to yeast cells, indicating the important role of the yeast-to-hyphae transition in mediating adhesion to bacterial cells. Co-adhesion primarily involved two types of highly adhesive fungal macromolecules, i.e., cell adhesion proteins (Als proteins) and O-mannosylations, which presumably recognize Als ligands and lectins on the bacterial surface. In a related study, SCFS provided quantitative information on the fundamental forces driving the adhesion of *S. epidermidis* to blood plasma proteins[23].

ACKNOWLEDGMENTS Work at the Université Catholique de Louvain was supported by the National Foundation for Scientific Research (FNRS), the Université Catholique de Louvain (Fondation Louvain-Prix De Merre), the Federal Office for Scientific, Technical and Cultural Affairs (Interuniversity Poles of Attraction Programme) and the Research Department of the Communauté Française de Belgique (Concerted Research Action). Y.F.D. and D.A. are Research Director and Postdoctoral Researcher of the Fonds de la Recherche Scientifique (FRS)-FNRS, respectively.

AUTHOR CONTRIBUTIONS A.B., S.E.-K.-C., R.M.A.S., D.A., P.H., S.D. and Y.F.D. designed the research; A.B., S.E.-K.-C., R.M.A.S., D.A., P.H. and S.D. performed the research; A.B., S.E.-K.-C., R.M.A.S., D.A., P.H., S.D. and Y.F.D. analyzed the data and wrote the paper.

COMPETING FINANCIAL INTERESTS The authors declare no competing financial interests.

1. Busscher, H.J., Norde, W. & van der Mei, H.C. Specific molecular recognition and nonspecific contributions to bacterial interaction forces. *Appl. Environ. Microb.* **74**, 2559–2564 (2008).
2. Busscher, H.J. & van der Mei, H.C. How do bacteria know they are on a surface and regulate their response to an adhering state? *PLoS Pathog.* **8**, e1002440 (2012).
3. Camesano, T.A., Liu, Y. & Datta, M. Measuring bacterial adhesion at environmental interfaces with single-cell and single-molecule techniques. *Adv. Water. Resour.* **30**, 1470–1491 (2007).
4. Brehm-Stecher, B.F. & Johnson, E.A. Single-cell microbiology: tools, technologies, and applications. *Microbiol. Mol. Biol. R.* **68**, 538–559 (2004).
5. Lidstrom, M.E. & Konopka, M.C. The role of physiological heterogeneity in microbial population behavior. *Nat. Chem. Biol.* **6**, 705–712 (2010).
6. Müller, D.J. & Dufrêne, Y.F. Atomic force microscopy as a multifunctional molecular toolbox in nanobiotechnology. *Nat. Nanotechnol.* **3**, 261–269 (2008).
7. Müller, D.J., Helenius, J., Alsteens, D. & Dufrêne, Y.F. Force probing surfaces of living cells to molecular resolution. *Nat. Chem. Biol.* **5**, 383–390 (2009).
8. Benoit, M., Gabriel, D., Gerisch, G. & Gaub, H.E. Discrete interactions in cell adhesion measured by single-molecule force spectroscopy. *Nat. Cell Biol.* **2**, 313–317 (2000).
9. Benoit, M. & Gaub, H.E. Measuring cell adhesion forces with the atomic force microscope at the molecular level. *Cells Tissues Organs* **172**, 174–189 (2002).
10. Helenius, J., Heisenberg, C.P., Gaub, H.E. & Muller, D.J. Single-cell force spectroscopy. *J. Cell. Sci.* **121**, 1785–1791 (2008).
11. Le, D.T.L., Guérardel, Y., Loubière, P., Mercier-Bonin, M. & Dague, E. Measuring kinetic dissociation/association constants between *Lactococcus lactis* bacteria and mucins using living cell probes. *Biophys. J.* **101**, 2843–2853 (2011).
12. Ovchinnikova, E.S., Krom, B.P., van der Mei, H.C. & Busscher, H.J. Force microscopic and thermodynamic analysis of the adhesion between *Pseudomonas aeruginosa* and *Candida albicans*. *Soft Matter* **8**, 6454–6461 (2012).
13. Lower, S.K., Hochella, M.F. Jr & Beveridge, T.J. Bacterial recognition of mineral surfaces: nanoscale interactions between *Shewanella* and α-FeOOH. *Science* **292**, 1360–1363 (2001).
14. Emerson, R.J. IV *et al.* Microscale correlation between surface chemistry, texture, and the adhesive strength of *Staphylococcus epidermidis*. *Langmuir* **22**, 11311–11321 (2006).
15. Bowen, W.R., Lovitt, R.W. & Wright, C.J. Atomic force microscopy study of the adhesion of *Saccharomyces cerevisiae*. *J. Colloid Inter. Sci.* **237**, 54–61 (2001).
16. Razatos, A., Ong, Y.L., Sharma, M.M. & Georgiou, G. Molecular determinants of bacterial adhesion monitored by atomic force microscopy. *Proc. Natl. Acad. Sci. USA* **95**, 11059–11064 (1998).
17. Kang, S. & Elimelech, M. Bioinspired single bacterial cell force spectroscopy. *Langmuir* **25**, 9656–9659 (2009).
18. Beaussart, A. *et al.* Single-cell force spectroscopy of probiotic bacteria. *Biophys. J.* **104**, 1886–1892 (2013).
19. Ong, Y.L., Razatos, A., Georgiou, G. & Sharma, M.M. Adhesion forces between *E. coli* bacteria and biomaterial surfaces. *Langmuir* **15**, 2719–2725 (1999).
20. Meister, A. *et al.* FluidFM: combining atomic force microscopy and nanofluidics in a universal liquid delivery system for single cell applications and beyond. *Nano Lett.* **9**, 2501–2507 (2009).
21. Dörig, P. *et al.* Force-controlled spatial manipulation of viable mammalian cells and micro-organisms by means of FluidFM technology. *Appl. Phys. Lett.* **97**, 023701 (2010).
22. Beaussart, A. *et al.* Single-cell force spectroscopy of the medically important *Staphylococcus epidermidis–Candida albicans* interaction. *Nanoscale* **5**, 10894–10900 (2013).
23. Herman, P. *et al.* Forces driving the attachment of *Staphylococcus epidermidis* to fibrinogen-coated surfaces. *Langmuir* **29**, 13018–13022 (2013).
24. Alsteens, D., van Dijck, P., Lipke, P.N. & Dufrêne, Y.F. Quantifying the forces driving cell-cell adhesion in a fungal pathogen. *Langmuir* **29**, 13473–13480 (2013).
25. Alsteens, D. *et al.* Single-cell force spectroscopy of Als-mediated fungal adhesion. *Anal. Methods* **5**, 3657–3662 (2013).
26. Lee, H., Dellatore, S.M., Miller, W.M. & Messersmith, P.B. Mussel-inspired surface chemistry for multifunctional coatings. *Science* **318**, 426–430 (2007).
27. Francius, G. *et al.* Stretching polysaccharides on live cells using single molecule force spectroscopy. *Nat. Protoc.* **4**, 939–946 (2009).
28. Rief, M., Oesterhelt, F., Heymann, B. & Gaub, H.E. Single molecule force spectroscopy on polysaccharides by atomic force microscopy. *Science* **275**, 1295–1297 (1997).
29. Marszalek, P.E., Oberhauser, A.F., Pang, Y.P. & Fernandez, J.M. Polysaccharide elasticity governed by chair-boat transitions of the glucopyranose ring. *Nature* **396**, 661–664 (1998).
30. Rief, M., Gautel, M., Oesterhelt, F., Fernandez, J.M. & Gaub, H.E. Reversible unfolding of individual titin immunoglobulin domains by AFM. *Science* **276**, 1109–1112 (1997).
31. Oberhauser, A.F., Hansma, P.K., Carrion-Vazquez, M. & Fernandez, J.M. Stepwise unfolding of titin under force-clamp atomic force microscopy. *Proc. Natl. Acad. Sci. USA* **98**, 468–472 (2001).

Appendix III

Forces driving the attachment of *Staphylococcus epidermidis* to fibrinogen-coated surfaces

Philippe Herman, Sofiane El-Kirat-Chatel, Audrey Beaussart, Joan A. Geoghegan, Thomas Vanzieleghem, Timothy J. Foster, Pascal Hols, Jacques Mahillon, and Yves F. Dufrêne

In *Langmuir*, **2013**, 29, 13018

I performed the research and wrote the paper.

Abstract

Cell surface proteins of bacteria play essential roles in mediating the attachment of pathogens to host tissues and, therefore, represent key targets for anti-adhesion therapy. In the opportunistic pathogen *Staphylococcus epidermidis*, the adhesion protein SdrG mediates attachment of bacteria to the blood plasma protein fibrinogen (Fg) through a binding mechanism that is not yet fully understood. We report the direct measurement of the forces driving the adhesion of *S. epidermidis* to Fg-coated substrates using single-cell force spectroscopy. We found that the *S. epidermidis*—Fg adhesion force is of ~150 pN magnitude and that the adhesion strength and adhesion probability strongly increase with the interaction time, suggesting that the adhesion process involves time-dependent conformational changes. Control experiments with mutant bacteria lacking SdrG and substrates coated with the Fg β_{6-20} peptide, instead of the full Fg protein, demonstrate that these force signatures originate from the rupture of specific bonds between SdrG and its peptide ligand. Collectively, our results are consistent with a dynamic, multi-step ligand-binding mechanism called "dock, lock, and latch".

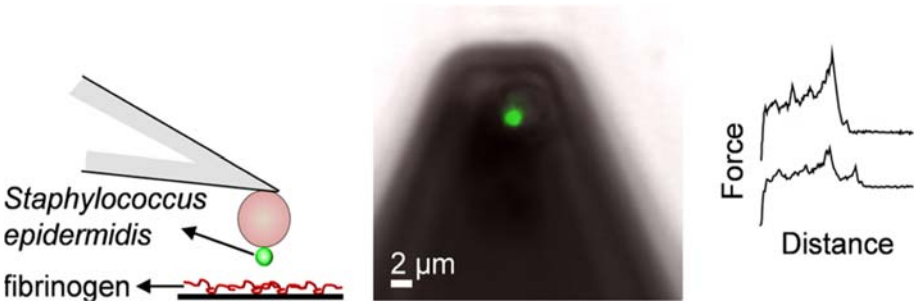

Langmuir

Article

pubs.acs.org/Langmuir

Forces Driving the Attachment of *Staphylococcus epidermidis* to Fibrinogen-Coated Surfaces

Philippe Herman,[†] Sofiane El-Kirat-Chatel,[†] Audrey Beaussart,[†] Joan A. Geoghegan,[‡] Thomas Vanzieleghem,[§] Timothy J. Foster,[‡] Pascal Hols,[∥] Jacques Mahillon,[§] and Yves F. Dufrêne*[,†]

[†]Institute of Life Sciences, Université catholique de Louvain, Croix du Sud 1, bte L7.04.01, B-1348 Louvain-la-Neuve, Belgium

[‡]Microbiology Department, Trinity College, Dublin 2, Ireland

[§]Laboratory of Food and Environmental Microbiology, Earth, and Life Institute, Université catholique de Louvain, Croix du Sud 2, bte L7.05.12, B-1348 Louvain-la-Neuve, Belgium

[∥]Institute of Life Sciences, Biochemistry, and Molecular Genetics of Bacteria, Université catholique de Louvain, Croix du Sud 5/6, B-1348 Louvain-la-Neuve, Belgium

ABSTRACT: Cell surface proteins of bacteria play essential roles in mediating the attachment of pathogens to host tissues and, therefore, represent key targets for anti-adhesion therapy. In the opportunistic pathogen *Staphylococcus epidermidis*, the adhesion protein SdrG mediates attachment of bacteria to the blood plasma protein fibrinogen (Fg) through a binding mechanism that is not yet fully understood. We report the direct measurement of the forces driving the adhesion of *S. epidermidis* to Fg-coated substrates using single-cell force spectroscopy. We found that the *S. epidermidis*−Fg adhesion force is of ∼150 pN magnitude and that the adhesion strength and adhesion probability strongly increase with the interaction time, suggesting that the adhesion process involves time-dependent conformational changes. Control experiments with mutant bacteria lacking SdrG and substrates coated with the Fg β_{6-20} peptide, instead of the full Fg protein, demonstrate that these force signatures originate from the rupture of specific bonds between SdrG and its peptide ligand. Collectively, our results are consistent with a dynamic, multi-step ligand-binding mechanism called "dock, lock, and latch".

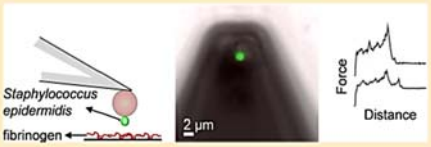

■ INTRODUCTION

Staphylococcus epidermidis is a bacterial commensal of humans that colonizes the skin. It is a common cause of infections associated with indwelling medical devices.[1−3] Survival in the infected host is promoted by the ability of bacteria to attach to the surface of indwelling devices that have been conditioned with host plasma proteins, such as fibrinogen (Fg) and fibronectin. *S. epidermidis* expresses on its surface a protein of the microbial surface component recognizing adhesive matrix molecule (MSCRAMM) family called SdrG,[4,5] which binds to the β-chain of Fg by the "dock, lock, and latch" mechanism.[6,7] The N-terminal ligand-binding A region is linked to the bacterial cell by a flexible stalk comprising a variable number of repeats of the dipeptide Ser-Asp. At the C terminus, a sorting signal promotes covalent attachment of the SdrG protein to cell-wall peptidoglycan. SdrG binds to a short, unfolded peptide near the N terminus of the Fg β-chain (residues 6−20).[7] The peptide docks into a trench located between the separately folded subdomains N2 and N3 of region A. Once docked and stabilized by hydrophobic interactions and hydrogen bonds, a C-terminal extension of subdomain N3 undergoes a conformational change and folds over the inserted Fg peptide to lock it in place and finally complements a β-sheet in subdomain N2, forming the latch. Despite a detailed molecular understanding of ligand binding by SdrG and other staphylococcal MSCRAMMs gained from *in vitro* experiments with purified proteins, little is known about the forces that govern attachment to and detachment from ligand-coated surfaces.

While classical microbiological assays probe large ensembles of cells, single-cell microbiology uses advanced technologies to analyze single-cell heterogeneity and to reveal rare events and properties that were otherwise not accessible.[8−10] Among these new tools, atomic force microscopy (AFM) makes it possible to measure cell surface interactions at the single-molecule and single-cell levels.[10−16] Several protocols have been developed to attach bacterial cells onto AFM cantilevers to measure bacterial adhesion forces, including the use of chemical fixation,[17] electrostatic interactions,[18] and polydopamine adhesives.[19] Here, we combine the use of colloidal probes and polydopamine as a new AFM-based single-cell force spectroscopy (SCFS) approach, enabling us to quantify the specific forces driving the adhesion of *S. epidermidis* to Fg-coated substrates. The results show that the interaction between *S. epidermidis* and Fg involves essentially specific bonds between SdrG and its β_{6-20} peptide ligand and that the interaction force strengthens

Received: July 29, 2013
Revised: September 24, 2013
Published: October 10, 2013

with time, consistent with the "dock, lock, and latch" mechanism.

MATERIALS AND METHODS

Bacterial Cultures. We used *S. epidermidis* ATCC 12228 cells grown at 37 °C and 150 rpm in trypto-caseine-soy (TCS) broth, unless otherwise stated. Control experiments were performed with *S. epidermidis* HB strain, in which SdrG expression was impaired by gene disruption after pG'Host9'*fbe* plasmid integration in the *fbe* (SdrG) gene (SdrG$^{(-)}$).[4] This strain was cultivated in TCS broth supplemented with 10 μg mL^{-1} erythromycin (Sigma, E5389). The cells were harvested in the stationary phase (16−18 h) by centrifugation for 10 min at 7500 × *g* and washed 3 times in phosphate-buffered saline (PBS) buffer. For cell probe preparation, 50 μL of a suspension of ca. 1 × 10^6 cells was transferred into a glass Petri dish.

Bacterial Cell Probes. Using a Nanoscope VIII Multimode atomic force microscope (Bruker Corporation, Santa Barbara, CA), triangular-shaped tipless cantilevers (NP-O10, Microlevers, Veeco Metrology Group) were slowly immersed in a very thin layer of ultraviolet (UV)-curable glue (NOA 63, Norland Edmund Optics) spread on a glass slide and slowly brought into contact with a silica microsphere (6.1 μm diameter, Bangs Laboratories). After 3 min of contact, the colloidal probe was cured for 10 min under a UV lamp. The cantilever was then immersed for 1 h in a 10 mM Tris buffer +150 mM NaCl solution (pH 8.5) containing 4 mg mL^{-1} dopamine hydrochloride (99%, Sigma). The probe was then washed and dried under N_2.

Proper attachment and positioning of bacteria on the colloidal probe were achieved using a BioScope Catalyst (Bruker Corporation, Santa Barbara, CA) equipped with a Zeiss Axio Observer Z1 and a Hamamatsu camera C10600. To check the viability of the bacteria, a LIVE/DEAD BacLight Bacterial Viability Kit (Invitrogen, Kit L7012) was used. Prior to attachment, 2 μL of a 1:1 Syto 9 (green-fluorescent nucleic acid stain)/propidium iodide (red-fluorescent nuclear and chromosome counterstain) mixture at 1.5 mM was added to a drop of 50 μL of bacteria suspension and mixed thoroughly. The suspension was deposited in the glass bottom Petri dish, where the protein model surfaces were previously attached, and the bacteria were left to incubate with the dyes for 15 min in the dark. Sedimented bacteria and Fg substrates were immersed by the addition of 4 mL of PBS buffer in the Petri dish. The colloidal probe was then mounted into the atomic force microscope and brought into contact with an isolated bacterium. After confirmation of proper attachment of the cell by fluorescence imaging, the cell probe was positioned over the Fg substrates without dewetting.

Fg and β_{6-20} Peptide Substrates. To prepare Fg-coated substrates, clean glass coverslips coated with a thin layer of gold were immersed overnight in an ethanol solution containing 1 mM 10% 16-mercaptododecahexanoic acid/90% 1-mercapto-1-undecanol (Sigma), rinsed with ethanol, and dried with N_2. Substrates were then immersed for 30 min into a solution containing 10 mg mL^{-1} *N*-hydroxysuccinimide (NHS) and 25 mg mL^{-1} 1-ethyl-3-(3-dimethylaminopropyl)-carbodiimide (EDC) (Sigma), rinsed 5 times with Ultrapure water (ELGA LabWater), incubated with 0.2 mg mL^{-1} of Fg for 1 h, rinsed further with PBS buffer, and then immediately used. In a control experiment, β_{6-20} peptide substrates were prepared using the same protocol, except that Fg was replaced by the β_{6-20} peptide NEEGFFSARGHRPLD (Eurogentec).

Force Measurements. AFM measurements were performed at room temperature (20 °C) in PBS buffer at pH 7.4 using a BioScope Catalyst AFM (Bruker AXS Corporation, Santa Barbara, CA). Using the inverted optical microscope, the bacterial probe was engaged onto the substrates. Multiple force curves were recorded on three different spots using a maximum applied force of 250 pN, a contact time of 50 ms or 1 s, and constant approach and retraction speeds of 1000 nm s^{-1}. For each condition, at least three bacteria from independent cultures were probed. Optical imaging was used during the measurements to ensure that the cells remained properly positioned on the cantilever.

RESULTS AND DISCUSSION

SCFS Setup. To probe the SdrG−Fg interaction on a single-cell basis, we combined the use of colloidal probe cantilevers and a bioinspired polydopamine wet adhesive (Figure 1a).[20]

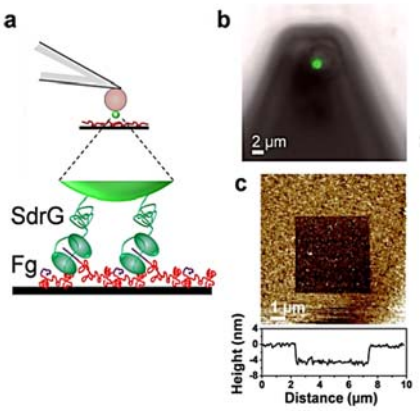

Figure 1. Single-bacterial cell force spectroscopy. (a) Living cells from the pathogen *S. epidermidis* are picked up with a polydopamine-coated colloidal probe, and the forces between individual bacteria and Fg-coated substrates are measured. The enlarged view (bottom) emphasizes specific bonds between the cell adhesion protein SdrG (green) and Fg (red). Two IgG-like subdomains of the SdrG molecule bind to a peptide sequence of 14 amino acids found in the N-terminal β chain of Fg (violet), through a putative dynamic multi-step ligand-binding mechanism. (b) Use of an integrated AFM-inverted optical microscope shows that single *S. epidermidis* bacteria attached to the cantilever probes are properly located and alive (green color). (c) AFM height image (*z* scale = 10 nm; a vertical cross-section taken in the center of the image is shown beneath the image) recorded with a silicon nitride tip documenting the presence of a smooth, homogeneous layer of Fg molecules covalently attached to carboxyl-terminated surfaces. To determine the layer thickness (~4 nm), a small square area was first scanned at large forces (>10 nN), followed by recording a larger image of the same area under smaller forces.

The polydopamine-coated colloidal probes enabled us to attach single bacterial cells on AFM cantilevers without altering their viability (Figure 1b). Using these cellular probes, we measured the forces between single *S. epidermidis* cells and Fg surfaces. Topographic imaging showed that the morphology of Fg-coated substrata was homogeneous and stable upon repeated scanning, indicating strong attachment of the macromolecules (Figure 1c). Imaging a small area at a large force removed the Fg layer and enabled us to assess its thickness, ~4 nm (Figure 1c; see square in the center of the image).

Measuring the Adhesion Forces between *S. epidermidis* and Fg. Multiple force−distance curves were recorded between single bacterial cells and Fg substrates. Figure 2 shows the adhesion force and rupture length histograms, together with representative force curves, obtained at short contact time (50 ms) for three different cells from independent cultures. About 35% of the curves showed well-defined force peaks of 145 ± 27 pN magnitude and 25−250 nm rupture length (cells 1 and 2). The general features of the curves did not substantially change

dx.doi.org/10.1021/la4029172 | *Langmuir* 2013, 29, 13018−13022

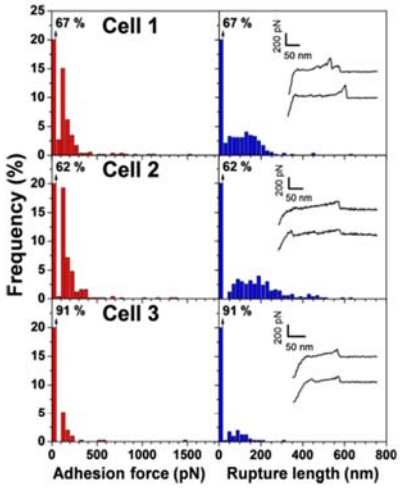

Figure 2. Measuring the adhesion forces between *S. epidermidis* and Fg. Adhesion force (red) and rupture length (blue) histograms, as well as representative retraction force curves (insets), obtained by recording multiple force curves in buffer at short contact time (50 ms) between single *S. epidermidis* cells and Fg substrates. Numbers listed in the top left corners of the graphs represent the percentages of zero adhesion forces. Results from three cells from independent cultures are shown (n > 400 force−distance curves for each cell).

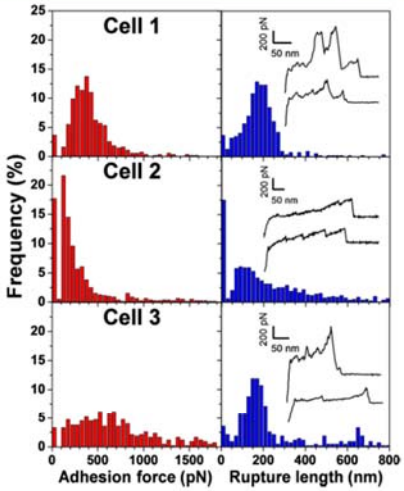

Figure 3. Adhesion forces depend upon contact time. Adhesion force (red) and rupture length (blue) histograms, as well as representative retraction force curves (insets), obtained by recording multiple force curves in buffer at prolonged contact time (1 s) between single *S. epidermidis* cells and Fg substrates. Results from three cells from independent cultures are shown (n > 400 force−distance curves for each cell). Cells 1−3 are the same as those probed at short contact time (Figure 2).

when recording consecutive force curves (up to several hundreds) on different spots, indicating that force measurements did not alter the interacting surfaces. While cells from independent cultures generally yielded adhesion properties that were in the same range (cells 1 and 2), some cells featured lower adhesion frequency (cell 3), an effect that we attribute to heterogeneity of the bacterial population.

In the light of several independent controls (see Figure 4 and text below), we suggest that the measured force signatures reflect the rupture of single (or few) SdrG−Fg complexes. The ~150 pN binding force is larger than the value obtained at fairly comparable loading rates (~60 000 pN s^{-1}) for other cell adhesion molecules, such as cadherins[21] and other bacterial adhesins,[22,23] including staphylococcal adhesins,[24] which suggests that multiple receptor−ligand complexes are probed in parallel or that the SdrG−Fg bond is particularly strong. Adhesion force peaks could not be fitted with the worm-like-chain (WLC) model, which usually describes the unfolding of protein secondary structures.[25,26] This, together with the fact that multiple peaks were rarely observed, could mean that the adjacent subdomains containing IgG-like folds of SdrG are too stable to be unravelled one by one.

Notably, we found that increasing the contact time to 1 s (Figure 3) substantially changed the characteristics of the force profiles. First, a dramatic increase in adhesion frequency was noted (from ~35 to 97%), suggesting that the probability to form SdrG−Fg bonds increases with the interaction time as observed for other receptor−ligand bonds.[21,22] Second, the mean adhesion force generally increased from ~145 to ~250−1500 pN (cells 1 and 3). Some cells (cell 2) however did not show such a large increase in adhesion, suggesting again that the cell population was heterogeneous. Nevertheless, the observed time dependency may reflect the time necessary for conformational changes within the SdrG and Fg molecules to achieve optimal fitting. Specifically, the increased adhesion force is consistent with the "dock, lock, and latch" mechanism, which is thought to stabilize the SdrG−Fg bond. This model involves docking of the ligand in a pocket formed between two SdrG subdomains followed by the movement of a C-terminal extension of one subdomain to cover the ligand and to insert and complement a β-sheet in a neighboring subdomain.[6] Hence, our results suggest that the increased adhesion may originate from an increased number of SdrG−Fg bonds, as observed with animal cells[27] and/or from enhanced stability of the bonds.

Interaction Forces Originate from the Specific Adhesion between SdrG and Its Fg β_{6-20} Peptide Ligand. To determine the specificity of the measured adhesion forces and rule out the possibility of artifacts associated with the cell probe preparation, several control experiments were performed using a 1 s contact time (Figure 4). First, use of polydopamine-coated probes instead of bacterial probes led to a major reduction of adhesion frequency (down to 60%; Figure 4a), indicating that the adhesive events measured above were associated with the *S. epidermidis* surface and not the polydopamine adhesive. Second, treatment of the cells with free Fg molecules led to a lower adhesion frequency (from 90 to 76%), suggesting that blocking of the SdrG molecules inhibits specific SdrG−Fg bonds. However, the observed inhibition was moderate, which could mean that Fg molecules

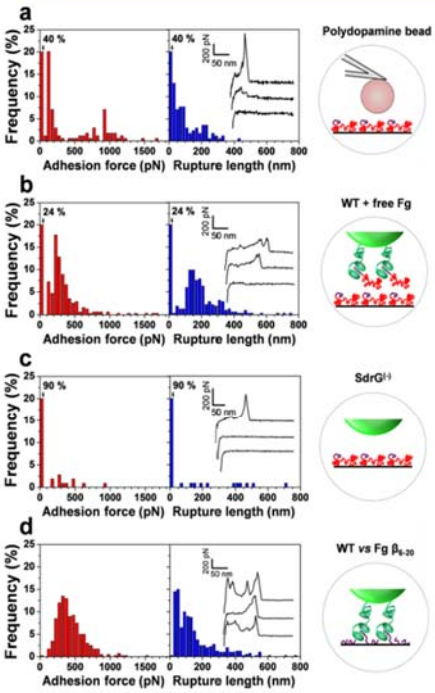

Figure 4. *S. epidermidis*–Fg adhesion forces involve specific bonds between SdrG and its peptide ligand. (a–d) Adhesion force and rupture length histograms, together with representative force curves, obtained by recording force curves at prolonged contact time (1 s) (a) between polydopamine-coated probes and Fg substrates, (b) between WT *S. epidermidis* cells and Fg substrates in the presence of free Fg (0.1 mg mL^{-1}) after 1 h of incubation, (c) between *S. epidermidis* mutant cells impaired in SdrG expression and Fg substrates, and (d) between WT *S. epidermidis* cells and substrates covered with the Fg β_{6-20} peptide. For each condition, similar data were obtained in duplicate experiments.

on the cell surface may bind Fg on the substrate or that other cell surface molecules mediate adhesion (Figure 4b). Third, use of a mutant *S. epidermidis* impaired in SdrG production ($SdrG^{(-)}$) abolished most adhesion events (adhesion frequency of only 10%), providing a direct demonstration that the measured adhesion forces are indeed associated with specific SdrG–Fg bonds (Figure 4c). Fourth, instead of the full Fg molecule, we tested a short synthetic peptide (β_{6-20}) corresponding to the SdrG binding site in Fg.[6] Force curves recorded between WT *S. epidermidis* and a substrate covered with β_{6-20} peptides featured force signatures that were similar to those obtained with the full proteins, thus confirming the specific nature of the probed interactions (Figure 4d). Accordingly, these observations demonstrate that the *S. epidermidis*–Fg interaction forces measured here originate from the specific adhesion between SdrG and its Fg β_{6-20} peptide ligand.

■ CONCLUSION

Knowledge of the fundamental forces driving the adhesion of staphylococci to host cells and matrix components is critical to our understanding of the molecular bases of staphylococcal infections. In recent years, AFM techniques have provided quantitative information on the fundamental forces driving the adhesion of bacterial pathogens, including staphylococci. In particular, the use of force spectroscopy with cell probe cantilevers has enabled researchers to measure the adhesion forces of *Pseudomonas aeruginosa* pili,[15] to probe the interaction forces of *Candida parapsilosis* and *P. aeruginosa* to surfaces,[12] to investigate the effect of cranberry on *Escherichia coli* adhesion,[14] to study the influence of substrate properties on the adhesion of *S. epidermidis*,[11] and to quantify the adhesion forces between *S. epidermidis*[13] or *Staphylococcus aureus*[16,28] and fibronectin. These results however are generally difficult to interpret at the molecular level for several reasons: cells were attached on the cantilever using protocols that lead to cell surface denaturation or cell death; multiple cells were attached and probed together; and cell positioning and cell–substrate contact area were poorly controlled.

We have shown that the use of colloidal probe cantilevers and a bioinspired polydopamine wet adhesive provides a versatile and non-invasive method to quantify the interaction forces between *S. epidermidis* and extracellular matrix proteins on a single-cell basis. As opposed to other protocols, the methodology is non-destructive and affords much better control of single-cell positioning, thus guaranteeing true and reliable single-bacterial cell analysis. Our main findings are that the interaction between *S. epidermidis* and Fg involves specific bonds between SdrG and its β_{6-20} peptide ligand and that the interaction force strengthens with time, consistent with a dynamic "dock, lock, and latch" model. Because SdrG expression may vary with culture age, it would be interesting in future research to compare the behavior of cells harvested in the exponential and stationary phases. Also, we expect that our single-cell experiments will prove useful to investigate the binding mechanisms of a variety of other MSCRAMMs.

■ AUTHOR INFORMATION

Corresponding Author

*Telephone: 32-10-47-36-00. Fax: 32-10-47-20-05. E-mail: yves.dufrene@uclouvain.be.

Notes

The authors declare no competing financial interest.

■ ACKNOWLEDGMENTS

Work at the Université catholique de Louvain was supported by the National Fund for Scientific Research (FNRS), the Université catholique de Louvain (Fonds Spéciaux de Recherche), the Région Wallonne, the Federal Office for Scientific, Technical, and Cultural Affairs (Interuniversity Poles of Attraction Programme), and the Research Department of the Communauté française de Belgique (Concerted Research Action). Yves F. Dufrêne and Pascal Hols are Research Director and Senior Research Associate of the FNRS.

■ REFERENCES

(1) Otto, M. *Staphylococcus epidermidis*—The 'accidental' pathogen. *Nat. Rev. Microbiol.* 2009, 7 (8), 555–567.

(2) Uckay, I.; Pittet, D.; Vaudaux, P.; Sax, H.; Lew, D.; Waldvogel, F. Foreign body infections due to *Staphylococcus epidermidis*. *Ann. Med.* **2009**, *41* (2), 109−119.
(3) Vuong, C.; Otto, M. *Staphylococcus epidermidis* infections. *Microbes Infect.* **2002**, *4* (4), 481−489.
(4) Hartford, O.; O'Brien, L.; Schofield, K.; Wells, J.; Foster, T. J. The Fbe (SdrG) protein of *Staphylococcus epidermidis* HB promotes bacterial adherence to fibrinogen. *Microbiology* **2001**, *147* (9), 2545−2552.
(5) Nilsson, M.; Frykberg, L.; Flock, J. I.; Pei, L.; Lindberg, M.; Guss, B. A fibrinogen-binding protein of *Staphylococcus epidermidis*. *Infect. Immun.* **1998**, *66* (6), 2666−2673.
(6) Bowden, M. G.; Heuck, A. P.; Ponnuraj, K.; Kolosova, E.; Choe, D.; Gurusiddappa, S.; Narayana, S. V.; Johnson, A. E.; Hook, M. Evidence for the "dock, lock, and latch" ligand binding mechanism of the staphylococcal microbial surface component recognizing adhesive matrix molecules (MSCRAMM) SdrG. *J. Biol. Chem.* **2008**, *283* (1), 638−647.
(7) Ponnuraj, K.; Bowden, M. G.; Davis, S.; Gurusiddappa, S.; Moore, D.; Choe, D.; Xu, Y.; Hook, M.; Narayana, S. V. A "dock, lock, and latch" structural model for a staphylococcal adhesin binding to fibrinogen. *Cell* **2003**, *115* (2), 217−228.
(8) Brehm-Stecher, B. F.; Johnson, E. A. Single-cell microbiology: Tools, technologies, and applications. *Microbiol. Mol. Biol. Rev.* **2004**, *68* (3), 538−559.
(9) Lidstrom, M. E.; Konopka, M. C. The role of physiological heterogeneity in microbial population behavior. *Nat. Chem. Biol.* **2010**, *6* (10), 705−712.
(10) Dufrene, Y. F. Towards nanomicrobiology using atomic force microscopy. *Nat. Rev. Microbiol.* **2008**, *6* (9), 674−680.
(11) Emerson, R. J.; Bergstrom, T. S.; Liu, Y.; Soto, E. R.; Brown, C. A.; McGimpsey, W. G.; Camesano, T. A. Microscale correlation between surface chemistry, texture, and the adhesive strength of *Staphylococcus epidermidis*. *Langmuir* **2006**, *22* (26), 11311−11321.
(12) Emerson, R. J.; Camesano, T. A. Nanoscale investigation of pathogenic microbial adhesion to a biomaterial. *Appl. Environ. Microbiol.* **2004**, *70* (10), 6012−6022.
(13) Liu, Y.; Strauss, J.; Camesano, T. A. Adhesion forces between *Staphylococcus epidermidis* and surfaces bearing self-assembled monolayers in the presence of model proteins. *Biomaterials* **2008**, *29* (33), 4374−4382.
(14) Pinzon-Arango, P. A.; Liu, Y.; Camesano, T. A. Role of cranberry on bacterial adhesion forces and implications for *Escherichia coli*−uroepithelial cell attachment. *J. Med. Food* **2009**, *12* (2), 259−270.
(15) Touhami, A.; Jericho, M. H.; Boyd, J. M.; Beveridge, T. J. Nanoscale characterization and determination of adhesion forces of *Pseudomonas aeruginosa* pili by using atomic force microscopy. *J. Bacteriol.* **2006**, *188* (2), 370−377.
(16) Yongsunthon, R.; Fowler, V. G.; Lower, B. H.; Vellano, F. P.; Alexander, E.; Reller, L. B.; Corey, G. R.; Lower, S. K. Correlation between fundamental binding forces and clinical prognosis of *Staphylococcus aureus* infections of medical implants. *Langmuir* **2007**, *23* (5), 2289−2292.
(17) Razatos, A.; Ong, Y.-L.; Sharma, M.; Georgiou, G. Molecular determinants of bacterial adhesion monitored by atomic force microscopy. *Proc. Natl. Acad. Sci. U. S. A.* **1998**, *95*, 11059−11064.
(18) Lower, S. K.; Hochella, M. F.; Beveridge, T. J. Bacterial recognition of mineral surfaces: Nanoscale interactions between *Shewanella* and α-FeOOH. *Science* **2001**, *292* (5520), 1360−1363.
(19) Kang, S.; Elimelech, M. Bioinspired single bacterial cell force spectroscopy. *Langmuir* **2009**, *25* (17), 9656−9659.
(20) Beaussart, A.; El-Kirat-Chatel, S.; Herman, P.; Alsteens, D.; Mahillon, J.; Hols, P.; Dufrene, Y. F. Single-cell force spectroscopy of probiotic bacteria. *Biophys. J.* **2013**, *104* (9), 1886−1892.
(21) Baumgartner, W.; Hinterdorfer, P.; Ness, W.; Raab, A.; Vestweber, D.; Schindler, H.; Drenckhahn, D. Cadherin interaction probed by atomic force microscopy. *Proc. Natl. Acad. Sci. U. S. A.* **2000**, *97* (8), 4005−4010.
(22) Dupres, V.; Menozzi, F. D.; Locht, C.; Clare, B. H.; Abbott, N. L.; Cuenot, S.; Bompard, C.; Raze, D.; Dufrene, Y. F. Nanoscale mapping and functional analysis of individual adhesins on living bacteria. *Nat. Methods* **2005**, *2* (7), 515−520.
(23) Verbelen, C.; Dufrene, Y. F. Direct measurement of *Mycobacterium*−fibronectin interactions. *Integr. Biol.* **2009**, *1* (4), 296−300.
(24) Bustanji, Y.; Arciola, C. R.; Conti, M.; Mandello, E.; Montanaro, L.; Samori, B. Dynamics of the interaction between a fibronectin molecule and a living bacterium under mechanical force. *Proc. Natl. Acad. Sci. U. S. A.* **2003**, *100* (23), 13292−13297.
(25) Oberhauser, A. F.; Marszalek, P. E.; Erickson, H. P.; Fernandez, J. M. The molecular elasticity of the extracellular matrix protein tenascin. *Nature* **1998**, *393* (6681), 181−185.
(26) Rief, M.; Gautel, M.; Oesterhelt, F.; Fernandez, J. M.; Gaub, H. E. Reversible unfolding of individual titin immunoglobulin domains by AFM. *Science* **1997**, *276* (5315), 1109−1112.
(27) Helenius, J.; Heisenberg, C. P.; Gaub, H. E.; Muller, D. J. Single-cell force spectroscopy. *J. Cell Sci.* **2008**, *121* (11), 1785−1791.
(28) Ovchinnikova, E. S.; van der Mei, H. C.; Krom, B. P.; Busscher, H. J. Exchange of adsorbed serum proteins during adhesion of *Staphylococcus aureus* to an abiotic surface and *Candida albicans* hyphae—An AFM study. *Colloids Surf. B* **2013**, *110*, 45−50.